# BIOACTIVE SESQUITERPENOIDS FROM *DICOMA ANOMALA* SUBSP. *GERRARDII*

by

MARINA MIKHAILOVNA VAN DER MERWE

Submitted in fulfilment of the
academic requirements of the degree
of
Master of Science in the
Discipline Chemistry,
School of Chemistry
University of KwaZulu-Natal

Pietermaritzburg
2008

In memory of my dearly beloved mother Nataly Grigor'evna Muranova
(1952-2006)

В память о моей любимой маме Наталии Григорьевне Мурановой
(1952-2006)

# Declaration

I hereby certify that this work is a result of my own investigation, which has not already been accepted in substance for any degree and is not being submitted in candidature for any other degree.

Signed……
Marina M. van der Merwe
Candidate

I hereby certify that this statement is correct

Signed……..
Professor F. R. van Heerden
Supervisor

School of Chemistry
University of KwaZulu-Natal
Pietermaritzburg

Signed……
Doctor C. Parkinson
Co-supervisor

Biosciences, CSIR
Modderfontein

December 2008

# Abstract

Through South Africa's first collaborative project between a large scientific organisation, the Council for Scientific and Industrial Research (CSIR), and the Traditional Healer's Committee, *Dicoma anomala* was identified as a plant containing potent anticancer and antimalarial compounds. In the process of evaluation, extracted plant material with reported or anecdotal use for the treatment of respiratory problems was found to have significant anticancer activity *in vitro* in a 3-cell line preliminary screen. The extract was further shown to have potent anticancer activity against the 60-cell line panel at the National Cancer Institute (NCI) in the USA. Bioassay-guided fractionation, initially utilising an *in vitro* anticancer assay, and structural elucidation resulted in two potent compounds with sesquiterpenoid skeletons (C-15 and C-30). The crystal structure of the C-15 compound, not published previously, was obtained. Both compounds were further screened in an antiplasmodial assay during the course of the National Drug Development Platform (RSA: CSIR, MRC and UCT) project, and were found to have potent activity against *Plasmodium falciparum* (a malaria protozoon). Although the C-15 compound had a selectivity index (SI) of 10, suggesting that it was suitable for subsequent development, the dimer was highly toxic (SI index of 1), limiting opportunities for future development. A further study of the structure-activity relationship (SAR), which was initiated for the C-15 compound, showed that removal of each unsaturated structural component decreased activity 10–fold in both bioassays. Additional investigations were carried out into amino-acid Michael adducts with the exocyclic double bond of the C-15 sesquiterpenoids, and the products were characterised by NMR spectroscopy and mass spectrometry. A similar investigation, involving the conjugate addition of simple amines, was undertaken in an attempt to enhance the bioavailability of the parent sesquiterpenoid. Three diethylamine derivatives were prepared and characterised. A general 10-fold drop in the bioactivity of these "pro-drug" derivatives in both assays was observed. Finally, the C-15 compound was tested *in vivo* in the *Plasmodium berghei* murine malaria model and was found to have some effect on the survival rates of the laboratory animals when compared with the control. A possible mode of action is suggested based on the experimental and published bioactivity data. Further studies to improve the bioactivity and alternative design of future *in vivo* studies are also proposed.

## Acknowledgements

First and foremost, I would like to thank my principal supervisor, Prof. Fanie van Heerden, for her enormous contribution, valued advice and assistance with the writing of this thesis, and my co-supervisor, Dr Chris Parkinson, for his continuous encouragement, support and wisdom throughout the years. The work was funded by full-time employment at CSIR Biosciences; additional funding was received from NDDP and academic funding from the National Research Foundation, for which I will be eternally grateful.

Throughout this project, I was honoured to receive expert advice from highly regarded scientists Dr Gordon Cragg (NCI), Dr Gerda Fouche (CSIR), Prof. Peter Folb (MRC) and Prof. Peter Smith (UCT). My thanks for the technical support go to Dr Paul Steenkamp, Nial Harding, Mutshinyalo Nwamadi, Natasha Kolesnikova and Jerry Senabe, all of the CSIR, to Nothulando Netnou (SANBI), and to Andries Seolwane and Oscar Marumong (CSIR) for their help with large-scale extraction and general laboratory support.

Many thanks to my colleagues at the CSIR for their care and support during some trying times. A special word of appreciation is due to my former research group leader, Dr Vinesh Maharaj, for his advice, tremendous faith in my abilities and the opportunity granted during an ongoing project, part of which I was able to present in this thesis.

I would also like to express my special thanks to Dr Melanie Rademeyer for the work towards my crystal structure and preparation of the publication, to Dr Edwin Mmutlane for providing compounds for the SAR study; to Dr Heinrich Hoppe for his help with understanding of the biochemical nuances of the malarial parasite cycle, and to Jean Meyer for his efforts with the collection of plant material and his fabulous field photographs.

In addition, I would like to extend a general word of gratitude to the research teams of SANBI, NDDP (RSA) and the Division of Cancer Research, NCI (USA).

Finally, I would like to thank my family, my sister Alexandra Chevrier, my darling husband Callie van der Merwe and my grandparents for their unconditional love, encouragement and support. I could not have done it without you!

## Abbreviations

| | |
|---|---|
| 1D | One-dimensional |
| 2D | Two-dimensional |
| $[\alpha]_D$ | Specific optical rotation |
| A | Absorbance |
| Ac | Acetyl |
| Acetone-$d_6$ | Deuterated acetone |
| AcOH | Acetic acid |
| ACN | Acetonitrile |
| Acetyl-CoA | Acetyl coenzyme A |
| amu | Atomic mass units |
| APAD | 3-Acetylpyridine adenine dinucleotide |
| APADH | Reduced APAD |
| br | Broad resonance |
| br s | Broad singlet |
| *c* | Concentration |
| CC | Column chromatography |
| calc. | Calculated |
| CHO | Chinese Hamster Ovarian cell line |
| COSY | Correlated spectroscopy |
| COLO320 | Colorectal cancer cell line |
| conc. | Concentrated |
| CSIR | Council for Scientific and Industrial Research |
| CQ | Chloroquine |
| CQS | Chloroquine sensitive |
| CQR | Chloroquine resistant |
| CYS | Cysteine |
| d | Doublet |
| dd | Doublet of doublets |
| ddd | Doublet of doublets of doublets |
| dddd | Doublet of doublets of doublets of doublets |
| ddq | Doublet of doublets of quartets |
| ddt | Doublet of doublets of triplets |

| | |
|---|---|
| DCM | Dichloromethane |
| DEA | Diethylamine |
| DEAP | Diethylaminparthenolide |
| DI | Deionised |
| DEPT | Distortionless Enhancement by Polarisation Transfer |
| DHB | Dehydrobrachylaenolide |
| DMAP | Dimethylaminparthenolide |
| DMSO | Dimethyl Sulfoxide |
| DMEM | Dulbecos Modified Eagles Medium |
| DNA | Deoxyribonucleic acid |
| dq | Doublet of quartets (NMR) |
| dt | Doublet of triplets (NMR) |
| DU-145 | Prostate tumour cell line |
| EI | Electron Impact |
| EIMS | Electron Impact Mass Spectrometry |
| Eds. | Editors |
| eV | Electron volts |
| ex | According to (botany) |
| EtOH | Ethanol |
| EtOAc | Ethyl acetate |
| ESI | Electrospray ionisation |
| $Et_2NH$ | Diethylamine |
| $Et_3N$ | Triethylamine |
| FA | Formic acid |
| FC | Flash chromatography |
| FBS | Fetal bovine serum |
| FPP | Farnesyl pyrophosphate |
| gCOSY | Gradient Correlated spectroscopy |
| gHMBC | Gradient Heteronuclear Multiple Bond Coherence |
| gHMQC | Gradient Heteronuclear Multiple Quantum Coherence |
| gHSQC | Gradient Heteronuclear Single Quantum Coherence |
| $GLC_4$ | Human lung carcinoma cell line |
| GSH | Reduced form of glutathione |

| | |
|---|---|
| $GI_{50}$ | Drug concentration at which 50% of growth inhibition is achieved |
| h | Hour |
| HEPES | N-[2-hydroxyethyl]-piperazine-N'-[2-ethansulphonic acid] |
| HMBC | Heteronuclear Multiple Bond Correlation |
| HPLC | High-Performance Liquid Chromatography |
| HREI-MS | High-Resolution Electron Ionisation – Mass Spectrometry |
| HRMS | High-Resolution Mass Spectrometry |
| HSQC | Heteronuclear Single Quantum Coherence |
| Hz | Hertz |
| $IC_{50}$ | Inhibitory concentration at which 50% inhibition is achieved |
| ICAM-1 | Intracellular adhesion molecule – 1 |
| IPP | Isopentenyl pyrophosphate |
| J | Spin-spin coupling constant |
| kV | Kilovolts |
| KZN | KwaZulu-Natal |
| LC | Liquid chromatography |
| $LC_{50}$ | 50% lethal concentration, indicative of the cytotoxic effect of the test agent |
| LDH | Lactate dehydrogenase |
| pLDH | Parasite LDH |
| lit. | Literature |
| m | Multiplet (NMR) |
| mm | Millimetre |
| m.p. | Melting point |
| m/z | Mass-to-charge ratio |
| Me | Methyl |
| MeOH | Methanol |
| MCF-7 | Malignant breast cell line |
| MDA-MB-231 | Malignant breast cell line |
| MCF-12A | Non-malignant breast cell line |
| MIC | Minimum Inhibitory Concentration |
| MRC | Medical Research Council |

| | |
|---|---|
| MRA | Michael Reaction Acceptor |
| MTPA | *α*-Methoxy-*α*-trifluoromethylphenyl acetic acid |
| MTT | 3-(4,5-dimethylthiazol-2-yl)-2,5-diphenyltetrazolium bromide |
| Mult. | Multiplicity (NMR) |
| MW | Molecular weight |
| NAC | *N*-acetyl-*L*-cysteine |
| NAD | Nicotinamide adenine dinucleotide |
| NADP | Nicotinamide adenine dinucleotide phosphate |
| NADPH | Reduced form of nicotinamide adenine dinucleotide phosphate |
| NBT | Nitroblue tetrazolium |
| NCI | National Cancer Institute, USA |
| NDP or NPP | Nerolidyl diphosphate or pyrophosphate |
| NF-κB | Nuclear factor kappa B |
| NMR | Nuclear Magnetic Resonance Spectroscopy |
| nm | Nanometres |
| NDDP | National Drug Development Platform |
| NOESY | Nuclear Overhauser Effect Spectroscopy |
| PBS | Phosphate-buffered saline |
| PDA | Photodiode array detector |
| PES | Phenazine ethosulphate |
| pLDH | Parasite lactate dehydrogenase |
| PRBC | Packed red blood cells |
| P388 | Murine lymphocytic leukemia cell line |
| PTFE | (exp p 1 filter) |
| q | Quartet (NMR) |
| RBC | Red blood cells |
| ROS | Reactive oxygen species |
| $R_f$ | Retention factor |
| r/min | Revolutions per minute |
| RT | Room temperature |
| RPMI | Roswell Park Memorial Institute medium |
| RSA | Republic of South Africa |
| s | Singlet (NMR) |

| | |
|---|---|
| SANBI | South African National Biodiversity Institute |
| SAR | Structure-activity relationship |
| SI | Selectivity index |
| SRB | Sulforhodamine B |
| STL | Sesquiterpene lactone |
| t | Triplet (NMR) |
| TCA | Trichloroacetic acid |
| TGI | Drug concentration that is indicative of the cytostatic effect of the test agent |
| TLC | Thin-Layer Chromatography |
| TMD | ThermaBeam Mass Detector |
| TMS | Tetramethylsilane |
| TK10 | Renal tumour cell line |
| $t_R$ | Retention time |
| TRIS | Tris(hydroxymethyl)aminomethane |
| UACC62 | Melanoma cell line |
| UCT | University of Cape Town |
| UKZN | University of KwaZulu-Natal |
| U937 | Human promonocytic leukemia cell line |
| UP | University of Pretoria |
| UV | Ultraviolet |
| VLC | Vacuum Liquid Chromatography |

# Contents

**DECLARATION** ..... **I**

**ABSTRACT** ..... **II**

**ACKNOWLEDGEMENTS** ..... **III**

**ABBREVIATIONS** ..... **IV**

**LIST OF FIGURES** ..... **XVI**

**LIST OF TABLES** ..... **XVII**

**LIST OF SCHEMES** ..... **XIX**

**CHAPTER 1: INTRODUCTION AND OBJECTIVES** ..... **1**

**CHAPTER 2: *DICOMA ANOMALA*: AN OVERVIEW OF THE TAXONOMY, ETHNOBOTANY, PHYTOCHEMISTRY AND BIOLOGICAL ACTIVITIES.** ..... **4**

2.1 Introduction ..... 4

2.2 Taxonomy ..... 5

2.2.1 *D. anomala* ..... 6

2.2.2 Distribution of *D. anomala* subsp. *gerrardii* ..... 6

2.2.3 *D. anomala* subsp. *anomala* ..... 7

2.2.4 *D. anomala* subsp. *gerrardii* ..... 7

2.3 Ethnobotany ..... 8

2.3.1 Vernacular names ..... 8

2.3.2 Medicinal uses ..... 9

2.4 Phytochemistry ..... 11

2.4.1 *D. zeyheri* ..... 12

2.4.2 *D. anomala* Sond. ..... 12

2.4.3 *D. capensis* Less. ..... 14

2.4.4 *D. schinzii* O. Hoffm. ..... 14

2.5 Summary of reported biological activities of the phytochemicals isolated from medicinally used *Dicoma* species ..... 15

2.5.1 Phenolic compounds ..... 15

2.5.2 Phytosterols ..... 15

2.5.3 Terpenoids ..... 16

2.5.3.1 Diterpenes and triterpenes....16
2.5.3.2 Sesquiterpenes....16
2.6 Conclusion....17

**CHAPTER 3: EXPERIMENTAL....19**

3.1 General materials and methods....19
3.1.1 Liquid chromatography....19
3.1.1.1 Column chromatography....19
3.1.1.2 Flash chromatography....19
3.1.1.3 Vacuum liquid chromatography....20
3.1.1.4 HPLC-UV/MS....20
3.1.1.5 Preparative-scale liquid chromatography....21
3.1.2 Mass spectrometry (MS)....22
3.1.2.1 Quattro LC Micro mass spectrometer....22
3.1.2.2 HREI-MS....22
3.1.2.3 Waters ThermaBeam (TMD) system....22
3.1.3 NMR spectroscopy....23
3.1.4 Polarimetry....24
3.1.5 Determination of melting points....24
3.1.6 X-ray crystallography....24
3.2 Biological assays....24
3.2.1 *In vitro* antimalarial screen....24
3.2.2 *In vitro* cytotoxicity assay....26
3.2.3 *In vivo* murine malaria model....27
3.2.4 *In vitro* anticancer pre-screen....27
3.2.5 *In vitro* anticancer 60-cell line panel....30
3.3 Bioassay-guided isolation of sesquiterpenoids from *D. anomala* subsp. *gerrardii* (Chapter 4)....30
3.3.1 Collection of plant material....30
3.3.2 General extract preparation....30
3.3.3 Preparation of extracts with various solvents....31
3.3.4 Processing and extraction of bulk plant material....31
3.3.5 Bioassay-guided fractionation and isolation of active compounds from the extract of *D. anomala*....32

3.3.5.1 Solvent partitioning ....32
3.3.5.2 Vacuum liquid chromatography ....33
3.3.5.3 Further bioassay-guided fractionation of semi-crude fractions D-H ....34
3.3.5.4 Data of compound **4.2** ....36
3.3.5.5 Data of compound **4.3** ....37
3.3.5.6 Targeted isolation of compound **4.2** from the organic extract of Brachylaena transvaalensis ....38
3.4 Preparation of sesquiterpene derivatives (Chapter 5) ....38
3.4.1 Data for (6*β*)-3-oxoeudesm-1,4,11-trien-6,12-olide **(5.17)** ....38
3.4.2 General procedure for preparation of amino-acid adducts of compound **5.17** ....39
3.4.2.1 Reactivity of compound **5.17** towards *L*-cysteine at physiological pH ....40
3.4.2.2 Data of compound **5.28a** ....40
3.4.2.3 Data of compound **5.28b** ....41
3.4.2.4 Addition of *N*-acetyl-*L*-cysteine to compound **5.17** at physiological pH ....41
3.4.2.5 Data of NAC adduct **5.32** ....42
3.4.2.6 Addition of glutathione to compound **5.17** at physiological pH ....42
3.4.2.7 Data of glutathione adduct **5.33** ....43
3.4.3 Reactivity of compound **4.2** towards *L*-cysteine using basic conditions ....44
3.4.3.1 Data of compound **5.27** ....44
3.4.4 General procedure for reduction of sesquiterpene lactones with $NaBH_4$ ....45
3.4.4.1 Stereoselective reduction of compound **5.17** ....45
3.4.4.2 Data of reduction product **5.36** ....45
3.4.4.3 Reduction of compound **4.2** ....46
3.5 Preparation of pro-drugs (Chapter 6) ....46
3.5.1 The OSIRIS Property Explorer ....46
3.5.2 General procedure for preparation of Michael adducts of STLs with $Et_2NH$. ....47
3.5.2.1 Data of diethylamine derivative of parthenolide **(6.6)** ....47

3.5.2.2 Data of (11*α*)-diethylamine-3-oxoeudesma-1(2),4(15),11(13)-dien-12-olide **(6.7)**.....48
3.5.2.3 Structure of ethyl (6*α*)-hydoxy-3-oxoeudesma-1(2),4(15),11(13)-trien-12-oate **(6.8)**.....49
3.5.2.4 Data of 11*α*-diethylamine-3-oxoeudesma-1(2),4(5),11(13)-dien-12-olide **(6.9)**.....49
3.5.2.5 Data of ethyl 6*α*-hydroxy-3-oxoeudesma-1(2),4(5),11(13)-trien-12-oate **(6.10)**.....50
3.5.3 Preparation of Michael adducts of STLs in an aprotic solvent.....51

**CHAPTER 4: ISOLATION, STRUCTURAL ELUCIDATION, BIOACTIVITY AND BIOSYNTHESIS OF BIOACTIVE SESQUITERPENOIDS FROM AN EXTRACT OF *DICOMA ANOMALA* SUBSP. *GERRARDII*.....52**

4.1 Introduction.....52
4.2 Plant recollection and processing.....53
4.2.1 *D. anomala* subsp. *gerrardii*.....53
4.2.2 Bulk recollection and processing.....54
4.2.3 Optimisation of the extraction method using anticancer 3-cell lines bioassay.....54
4.3 Bioassay-guided fractionation and isolation of active compounds from extract of *D. anomala*.....55
4.4 Structure elucidation of compounds **4.2** and **4.3**.....55
4.4.1 Structure of compound **4.2**.....56
4.4.1.1 Structure elucidation of compound **4.2** using spectroscopic techniques.....56
4.4.1.2 X-ray crystallographic study of compound **4.2**.....60
4.4.2 Structure elucidation of compound **4.3**.....62
4.5 Summary of the literature study of compounds **4.2** and **4.3**.....69
4.6 Targeted isolation of compound **4.2** from the organic extract of *B. transvaalensis*.....70
4.7 HPLC analysis of root extract of *D. anomala* subsp. *anomala* for the presence of dehydrobrachylaenolide **(4.2)**.....70
4.8 *In vitro* evaluation of compounds **4.2** and **4.3** in the cancer and malaria models.....71

4.8.1 *In vitro* anticancer activity....71
4.8.2 *In vitro* antimalarial activity....72
4.9 *In vivo* evaluation of compound **4.2** in the rodent malaria model....73
4.10 Discussion....74
4.10.1 Isolation of bioactive compounds and their anticancer activity....74
4.10.2 Evaluation of compounds **4.2** and **4.3** for antimalarial activity....75
4.10.3 Structure-activity relationship considerations for dehydrobrachylaenolide **(4.2)** and other eudesmanolides....77
4.10.4 Drug-likeness and the pro-drugs of STLs....79
4.10.5 Biosynthesis....80
4.10.5.1 Biosynthesis of dehydrobrachylaenolide **(4.2)**....82
4.10.5.2 Biosynthesis of the guaianolide dimer **4.3**....86

**CHAPTER 5: REACTIVITY OF SESQUITERPENE LACTONES TOWARDS BIOLOGICAL NUCLEOPHILES – STRUCTURE-ACTIVITY RELATIONSHIPS OF SOME NATURAL AND SYNTHETIC EUDESMANOLIDES....89**

5.1 Literature overview of the biological activities of eudesmanolides....89
5.1.1 Anticancer activity of eudesmane STLs....92
5.1.2 SAR against *P. falciparum*....95
5.1.3 SAR of eudesmane STLs as inhibitors of induction of the intracellular adhesion molecule-1....96
5.1.4 SAR summary....97
5.2 Objectives....97
5.3 NMR assignments for (6*β*)- 3-oxoeudesm-1,4,11-trien-6,12-olide **(5.17)**....98
5.4 Reactivity towards amino acids....99
5.4.1 Reactivity of dehydrobrachylaenolide **(4.2)** towards *L*-cysteine using basic conditions....100
5.4.2 Reactivity of compound **5.17** towards *L*-cysteine at physiological pH....103
5.4.3 Addition of *N*-acetyl-*L*-cysteine to compound **5.17** at physiological pH....108
5.4.4 Addition of glutathione to compound **5.17** at physiological pH....112

5.5 Reduction of compounds **4.2** and **5.17** with $NaBH_4$ .....115
5.5.1 Stereoselective reduction of compound **5.17** .....115
5.5.2 $NaBH_4$ reduction of dehydrobrachylaenolide **(4.2)** .....118
5.6 SAR.....119
5.6.1 *In vitro* anticancer activity.....119
5.6.2 *In vitro* antimalarial activity.....120
5.7 Discussion.....122
5.7.1 Reactivity towards amino acids and product characterisation.....122
5.7.2 Reduction with $NaBH_4$ .....123
5.7.3 SAR .....124

**CHAPTER 6: PREPARATION, STRUCTURES AND BIOACTIVITY OF PRO-DRUGS OF SESQUITERPENE LACTONES.....126**

6.1 Background and objectives .....126
6.2 Selection of the amino side chain based on prediction of OSIRIS molecular properties.....128
6.3 Preparation of Michael adducts with diethylamine .....130
6.3.1 Preparation of diethylamino-parthenolide **(6.6)** .....130
6.3.2 Preparation of diethylamino-dehydrobrachylaenolide **(6.7)** .....132
6.3.2.1 Structure of (5*α*,6*β*,7*α*,10*β*,11*β*)-13-diethylamino-3-oxoeudesma-1(2),4(15)-dien-12-olide **(6.7)** .....133
6.3.2.2 Structure of ethyl (6*α*)-hydroxy-3-oxoeudesma-1(2),4(15),11(13)-trien-12-oate **(6.8)** .....135
6.3.3 Michael adducts of compound **5.17** .....136
6.3.3.1 Structure of (6*β*,7*α*,10*β*,11*β*)-13-diethyamino-3-oxoeudesma-1(2),4(5),-dien-12-olide **(6.9)** .....136
6.3.3.2 Structure of (6*α*)-hydroxy-3-oxoeudesma-1(2),4(5),11(13)-trien-12-oate **(6.10)** .....138
6.4 Attempted preparation of Michael adducts of STLs in an aprotic solvent .....139
6.5 Biological screening of Michael adducts of STLs .....139
6.5.1 *In vitro* anticancer activity.....139
6.5.2 *In vitro* antimalarial screening .....140
6.6 Discussion.....142

**CHAPTER 7: SUMMARY AND CONCLUDING REMARKS .....143**

7.1 General .....143

7.2 Confirmation of the taxonomic identity of the ethnobotanical sample..143

7.3 Bulk recollection and processing.....143

7.4 Bioassay-guided isolation of active compounds.....144

7.5 Structures and stereochemistry of the active compounds.....144

7.6 Bioactivity of the compounds *vs* activity of the crude extract .....145

7.7 Chemotaxonomic remarks .....145

7.8 Identification of sustainable sources of compound **4.2**.....146

7.9 Antimalarial activity of dehydrobrachylaenolide **(4.2)** .....147

7.10 SAR.....149

7.11 Preparation of pro-dugs .....150

**APPENDIX 1: NMR SPECTRA OF SELECTED COMPOUNDS (CHAPTERS 4 TO 6) .....151**

**APPENDIX 2: X-RAY CRYSTALLOGRAPHIC DATA FOR COMPOUND 4.2 (CHAPTER 4).....165**

**APPENDIX 3: SELECTED DOSE RESPONSE CURVES FOR *IN VITRO* ANTIMALARIAL SCREEN (CHAPTER 4).....175**

# List of Figures

Figure 2.1. Photo of *D. anomala* subsp. *gerrardii* in the Nyala Nature Reserve, Brits (left) and the distribution map© in the RSA (right)' ..... 6
Figure 2.2. Phytoconstituents of various parts of *D. zeyheri* .....11
Figure 3.1. Five-dose assay format .....29
Figure 3.2. Solvent partitioning method and $GI_{50}$ values (primary anticancer assay) .....33
Figure 3.3. Bioassay-guided isolation of compounds from extract of *D. anomala* .....35
Figure 4.2. Size distribution of the rhizomes in a batch .....54
Figure 4.3. X-ray structure of compound **4.2** .....60
Figure 4.4. Packing of the molecules in the crystal of compound **4.2**.....61
Figure 4.5. Edge-on projection illustrating ring conformation of compound **4.2**....61
Figure 4.6. Survival rates of mice following infection with *P. bergei* .....73
Figure 4.7. Potential alkylation sites of compound **4.2** .....78
Figure 5.1. STLs evaluated for activity against $GLC_4$ and COLO320 cell lines ....92
Figure 5.2. STLs evaluated for activity against P388 lymphocytic leukaemia .....93
Figure 5.3. STLs evaluated for activity against KB tumour cells.....94
Figure 5.4. Eudesmanolides evaluated for activity against *P. falciparum*.....95
Figure 5.5. Structures evaluated for inhibitory activity of ICAM-1 induction.....96
Figure 5.6. STLs selected for SAR .....98
Figure 5.7. TLC of the addition of cysteine (left) and glutathione (right) .....104
Figure 5.8. gHSQC spectrum of the supernatant of the reaction mixture of compound **5.17** and *L*-cysteine .....105
Figure 5.9. gCOSY spectrum of the supernatant of the reaction mixture of compound **5.17** and cysteine .....106
Figure 5.11. TLC plates: reduction of compounds **5.17** (left) and **4.2** (right) .....115
Figure 5.12. Mechanism of $NaBH_4$ reduction of compound **5.17**.....116
Figure 5.13. Conceivable mechanism of reduction of dehydrobrachylaenolide **(4.2)**.....118
Figure 6.1. TLC of the reaction of STLs with $Et_2NH$ and structures of the products .....132

# List of Tables

Table 2.1. Ethnobotanical uses of *Dicoma anomala* ..... 9
Table 3.1. Gradient conditions for the Waters Alliance 2690 for methods T3.1-1 and T3.1-2 (run time – 90 min) .....20
Table 3.2. Gradient conditions for the Waters Alliance 2690 for methods T3.2-1 and T3.2-2 (run time - 60 min) .....21
Table 3.3. Gradient conditions for the Agilent 1200 for method T3.3 (run time – 40 min) .....21
Table 3.4. Gradient conditions for the Waters 2695. Method T3.4 (run time – 60 min) .....23
Table 3.5. VLC solvent gradient and fractions collected. Bioassay: $LC_{50}$ (melanoma, renal, breast) .....34
Table 4.1. Cytotoxicity of crude extracts against CHO and cancer cell line panels .....55
Table 4.2. $^{1}H$ and $^{13}C$ NMR data for compound **4.2** in $CDCl_3$ .....59
Table 4.3. $^{1}H$ and $^{13}C$ NMR data for compound **4.3** in $CDCl_3$ .....64
Table 4.4. Evaluation of the *in vitro* activity against cancer cell line panels and CHO .....71
Table 4.5. *In vitro* activity against *P. falciparum* .....72
Table 5.1. $^{1}H$ and $^{13}C$ NMR data for compound **5.17** in $CDCl_3$ .....99
Table 5.2. $^{1}H$ and $^{13}C$ NMR data for compound **5.27** in $D_2O$ .....102
Table 5.3. $^{1}H$ and $^{13}C$ NMR data for compound **5.28b** in $D_2O$ .....107
Table 5.4. $^{1}H$ and $^{13}C$ NMR data for compound **5.28a** in $D_2O$ .....108
Table 5.5. $^{13}C$ and $^{1}H$ NMR data for compound **5.29** in $D_2O$ .....110
Table 5.6. $^{1}H$ NMR data for compound **5.33** in $D_2O$ .....113
Table 5.7. $^{1}H$ and $^{13}C$ NMR data for compound **5.36** in $CDCl_3$ .....117
Table 5.8. *In vitro* cytotoxicity of STLs towards CHO and cancer cell lines .....120
Table 5.9. *In vitro* antiplasmodial activity against *P. falciparum* .....121
Table 6.1. Predicted molecular properties for hypothetic DHB derivatives .....129
Table 6.2. $^{1}H$ and $^{13}C$ NMR data for diethylamino -parthenolide in Acetone-$d_6$ **(6.6)** .....131
Table 6.3. $^{1}H$ and $^{13}C$ NMR data for compound **6.7** in acetone-$d_6$ .....134
Table 6.4. $^{1}H$ and $^{13}C$ NMR data for compound **6.9** in $CDCl_3$ .....137

Table 6.5. $^{1}H$ and $^{13}C$ NMR data for compound **6.10** in $CDCl_3$ .....138
Table 6.6. *In vitro* activity against a 3-cancer cell line panel and CHO.....140
Table 6.7. *In vitro* antiplasmodial activity against *P. falciparum*.....141
Table A2.1. Crystal data, data collection and structure refinement parameters for compound **4.2** .....166
Table A2.2. Atomic coordinates and equivalent isotropic displacement parameters (Ueq) for non-hydrogen atoms of compound **4.2**.....168
Table A2.3. Bond lengths for compound **4.2** .....169
Table A2.4. Bond angles [º] for compound **4.2** .....170
Table A2.5. Anisotropic displacement parameters for compound **4.2** .....172
Table A2.6. Hydrogen coordinates and isotropic displacement parameters for compound **(4.2)** .....173
Table A2.6. Torsion angles for compound **(4.2)** .....174

# List of Schemes

Scheme 4.1. Reported pathway for biosynthesis of STLs in chicory .....83
Scheme 4.2. Proposed biosynthetic pathways to the eudesmanolides from (+)-costunolide .....85
Scheme 4.3. Proposed biosynthetic pathways to the eudesmanolides from costunolide *via* albicolide.....86
Scheme 4.4. Proposed precursors of guaianolide dimer **4.3** .....87
Scheme 4.5. Proposed biosynthetic pathways to the guaianolide fragments from (+)-costunolide .....88
Scheme 5.1. Mechanism of Michael addition of amino acids to STLs under basic and acidic conditions (adopted from Schmidt, 1999)[55] .....100
Scheme 6.1. Synthesis of the diethylamino adduct of parthenolide .....130

# Chapter 1: Introduction and Objectives

South Africa is fortunate in having a plant biodiversity of more than 24000 indigenous plant species, representing about 10% of all higher plants on Earth.[1] A large number of South African plants are endemic. The country also boasts a long history of traditional medicinal practices, which by and large employ plants as a basis for the maintenance of good health. These practices are significant throughout the African continent, where up to 80% of the population makes use of traditional medicine.[2]

European botanists began "bioprospecting" to identify economically important plants in Africa from as early as the 19th century. With the development of biotechnology in the 1950s, many herbal preparations and phytochemicals were also tested for efficacy. One of the research highlights of that time, which turned the interest of the international scientific community towards Africa, was the discovery of the anticancer alkaloids vinblastine and vincristine from the Madagascar periwinkle *Catharanthus roseus.* These systemic chemotherapy drugs, which first became available in the 1960s, are still extensively used in clinical practice.

In 1996, the first review of bioprospecting in South Africa found that virtually every research institution in South Africa was involved in bioprospecting activities, some formally and others informally.[3] One of the largest bioprospecting projects to date began in 1997 at the former Division of Food, Biological and Chemical Technologies of the CSIR. The project was based on a collaboration of chemists with traditional healers, with the support of ethnobotanists, botanists, biotechnologists, pharmacologists and even medical doctors. The traditional healers came on board this Bioprospecting Consortium through a formal Traditional Healers Committee as stakeholders. The right of the providers of indigenous knowledge to any future financial benefits that might be derived from

---

[1] Van Wyk B. -E., Gericke N. (2000). *People's Plants.* Pretoria: Briza Publications, p. 7.
[2] *WHO Traditional Medicine Strategy 2002-2005*. Downloaded on 6 December 2008 from World Health Organization website: http://whqlibdoc.who.int/hq/2002/WHO_EDM_TRM_2002.1.
[3] Laird S., Wynberg R. (1996). Biodiversity prospecting in South Africa: Towards the development of equitable partnerships. Land and Agriculture Policy Centre, Johannesburg.

commercial exploitation of the indigenous knowledge-based product was protected by a Memorandum of Understanding (September 1999) and a Benefit Sharing Agreement (February 2003), which were signed between the CSIR and the Traditional Healers Committee. To date more 250 claims for cures have been provided by traditional healers to the CSIR, which have been captured in the "Bioprospecting Database".

This collaboration soon became one of the fundamental modules of the Drug Discovery and Development Consortium at the CSIR. This module employs a so-called "ethnopharmacological approach" to drug discovery. The idea of this approach is that the indigenous use of a plant is taken as a primary indicator of its biological activity, and the ultimate objective is to obtain a bioactive plant constituent/s, which can be further exploited. The high-throughput screening of ethnobotanical extracts (extracts of plants with reported medicinal uses) has a much higher hit rate than the screening of randomly collected plant samples.

The initial selection of an ethnobotanical-based research "lead" in this project was based on the results of a high-throughput biological screening of the extracts prepared from plant samples supplied by traditional healers. The screening of 410 ethnobotanical extracts using the *in vitro* anticancer screening technology at the CSIR resulted in 171 positive extracts. Plants showing potent (18) and moderate (37) activity were selected for further research and development. Following the evaluation of the prior art, several plants were regarded as "hits". One such hit, an extract of *Dicoma anomala* Sond., constitutes the basis of this thesis.

The aims of this study were to:

- Isolate bioactive constituents from the extract of *Dicoma anomala* subsp. *gerrardii* using bioassay-guided the fractionation
- Determine the structure(s) of the bioactive ingredients by chemical and physicochemical methods (e.g. NMR spectroscopy and mass spectrometry)
- Demonstrate the efficacy of the active compounds in appropriate animal model/s (*in vivo*)

- Optimise the extraction methods to achieve the best yields of the active compound(s)
- Investigate the pharmacological properties of bioactive compound(s) through some structure-activity studies
- Prepare several derivatives/analogues with aim to improve selectivity index and oral bioavailability

# Chapter 2: *Dicoma anomala*: an overview of the taxonomy, ethnobotany, phytochemistry and biological activities

## 2.1 Introduction

An extract of the roots of *Dicoma anomala* was found to exhibit strong growth-inhibitory activity towards a three-cancer cell lines panel. The sample of the roots, with anecdotal information on the use of the plant, emerged from the collaboration of the CSIR with traditional healer Dr Solomon Mahlaba in 1999. It was introduced as Kloenya (Sotho) or Nyongwane (Zulu), and was claimed to be effective in the treatment of respiratory disorders and asthma. A botanical specimen was identified by SANBI as *Dicoma anomala* sensu Wild as the genus was under revision at the time. A review of the latest taxonomic interpretation of the genus was required in order to evaluate prior art of the possible use of the plant or its constituents for the treatment of cancer as an initial step in drug discovery following the identification of the "hit" through high-throughput biological screening of plant extracts.

The genus *Dicoma* Cass., first described by Cassini in 1817, belongs to the subtribe Gochnatiinae, the tribe Mutiseae, and the subfamily Cichorioideae of the Asteraceae family. It was previously reported to consist of about 50 to 65 species, and it is now recognised to comprise 35 species, 16 of which occur in southern Africa.[4,5,6,7.] Most species are herbs or small shrubs and even trees. Habitat was considered as embodying the taxonomically important and distinguishing characteristics in the infrageneric treatment of the genus *Dicoma*.[8] From the highly polymorphic species of *D. anomala* Sond., which has the widest geographical distribution within the genus, several subspecies were the subject of

[4] Cassini M. H. (1818). Bulletin des Sciences de la Société Philomatique de Paris, p. 47.
[5] Bremer K. (1994). *Asteraceae. Cladistics and Classification*. Portland, Oregon: Timber Press.
[6] Ortiz S. (2001). Annals of the Missouri Botanical Garden, **87**, 459–481.
[7] Netnou N. C. MSc Thesis, Rand Afrikaans University, Johannesburg, 2001.
[8] Harvey W. H. (1865). In: Harvey W.H., Sonder O.W. (eds.), *Flora Capensis*, Hodges, Smith, Dublin, Vol. **3**, pp. 44–530.

phytochemical studies during the period 1977–1990.[9,10,11.] The investigation was driven by taxonomic considerations with the aim of chemically characterising the genus and establishing a correlation of the proposed sectional classification and phytochemistry. The formal infrageneric taxonomic division of the species recognised three varieties or subspecies of *Dicoma anomala*: var. *α*, *sonderi* Harv.; var. *β*, *cirsioides* Harv. and var. *γ*, *microcephala* Harv. or *D. gerrardii*.[8]

Even though several morphologically distinct forms existed, ethnobotanical use was reported for the taxa *Dicoma anomala* without further specification of the origin or tradition.

One of the latest taxonomic reviews, which followed the revision by Ortiz (2001), was conducted by Ms Netnou in 2001 under the supervision of Prof. Ben-Erik van Wyk.[7,12] This review was aimed at providing descriptions, keys and distribution maps for the ethnomedicinally important species and thus facilitating their correct identification. This would naturally result in more accurate documenting and use of ethnobotanical information in ethnopharmacological research. An overview of the ethnobotany, old and new taxonomy, phytochemistry and pharmacology of *D. anomala* and a few other members of the genus used medicinally are presented in this chapter.

## 2.2 Taxonomy

*Dicoma anomala* Cass. comprises erect, suberect or prostrate herbs, with underground tubers. It grows in grasslands and stony places on sandy soil. The flowering time of *D. anomala* is from January to May, with peak flowering time in February and March. This is a very widespread species, but regional forms can be easily distinguished.[7]

[9] Bohlmann F., Le Van N. (1978). *Phytochemistry*, **17**, 570–571.
[10] Bohlmann F., Singh P., Jakupovic J. (1982). *Phytochemistry*, **21**, 2029–2033.
[11] Zdero C., Bohlmann F. (1990). *Phytochemistry*, **29**, 183–187.
[12] Ortiz S. (2001). *Taxon*, **50**, 733-744.

### 2.2.1 *D. anomala*

*D. anomala* is widely distributed in sub-Saharan Africa, resulting in pronounced morphological variety. In South Africa it is widely distributed in Limpopo, North-West, Gauteng, Mpumalanga, Free State, Northern Cape and KwaZulu-Natal provinces. *D. anomala* does not occur in the winter rainfall areas of the Western Cape. In KwaZulu-Natal it has been mainly recorded in the Tugela Basin on sandy soils.[13] Following the recent taxonomic revision of Southern African taxa, five informal groups of *D. anomala* subsp. anomala and two of *Dicoma anomala* subsp. *gerrardii* are now recognised to accommodate intraspecific variation. *D. anomala* subsp. *gerrardii* also occurs in Namibia and Botswana. Intermediates between the above two taxa are known to occur in the North West province.

### 2.2.2 Distribution of *D. anomala* subsp. *gerrardii*

*D. anomala* subsp. *gerrardii* is found throughout South Africa except in the Eastern Cape and the winter rainfall areas of the Western Cape (Figure 2.1). Currently, two regional forms are recognised for this taxon: the typical form, which occurs throughout the RSA region, and the Barberton form, which is found in the Barberton area of Mpumalanga Province.

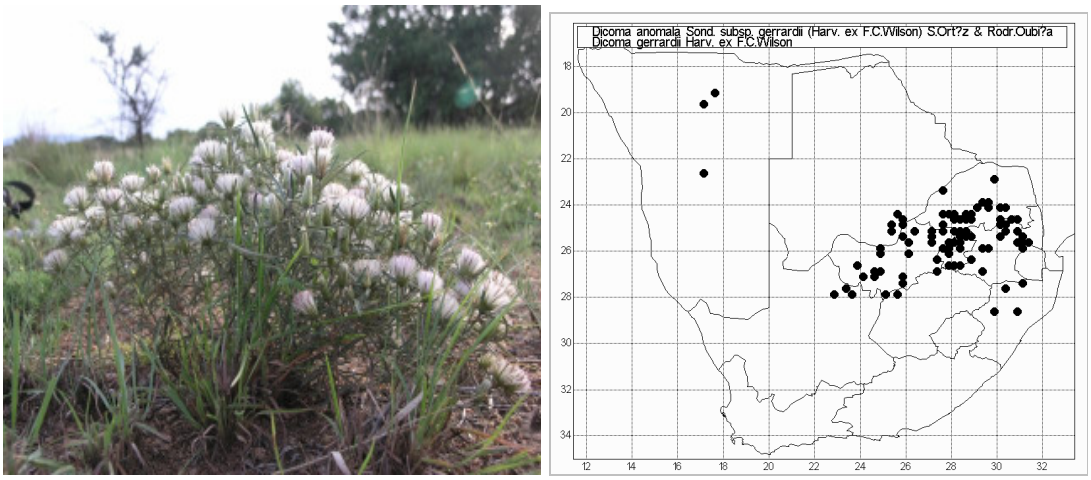


**Figure 2.1. Photo of *D. anomala* subsp. *gerrardii* in the Nyala Nature Reserve, Brits (left) and the distribution map© in the RSA (right)[14,15]**

[13] www.plantzafrica.com/plantcd/dicomanom.htm. Accessed on 10 October 2008.
[14] The photo of *D. anomala* subsp. *gerrardii* was provided by Jean Meyer (SANBI).
[15] Distribution map© (PRECIS) of *D. anomala* subsp. *gerrardii*, curtesy of SANBI.

Several intermediate forms occur between *D. anomala* subsp. *gerrardii* and its close relative *D. anomala* subsp. *anomala.* This could be due to cross-pollination between the two subspecies in the same habitat.

### 2.2.3 *D. anomala* subsp. *anomala*

The plants are prostrate and the leaves are linear to lanceolate-oblong. They have few heads which are solitary, or rarely one to two, at the ends of branches. They are large and wider than they are long, often 30 to 45 mm wide. The involucral bracts, which are nearer to 200 mm, are often recurved. This subspecies has regional forms that are so characteristic that their geographical origin can easily be determined from their appearance. Five forms are recognised at present:[4]

1. Common form (Eastern Cape to Limpopo province, Botswana, Lesotho and Swaziland).
2. Lydenburg form (Lydenburg district, Mpumalanga).
3. Eastern Free State form (north-eastern parts of the Free State and near Barberton).
4. Waterberg form (Waterberg area, Limpopo province).
5. Pretoria form (Pretoria area in Gauteng).

Synonyms: *D. anomala* var. *cirsioides* Harv. and *D. anomala*. *D. anomala* subsp. *cirsioides* (Harv.) with four regional variants. *D. anomala* var. *sonderi* Harv. is a form with narrow leaves.[16]

### 2.2.4 *D. anomala* subsp. *gerrardii*

The plants are erect and the leaves are narrow-linear. The heads are numerous, or arranged three to five subcorymbosely at the ends of branches. They are relatively smaller and longer than they are wide, often 15 – 20 mm in width. The involucral bracts are nearer to 50 than 200. In southern Africa, two forms of *D. anomala* subsp. *gerrardii* are recognised:

---

[16] Hilliard O. M. (1977). *Compositae in Natal*. Pietermaritzburg: University of Natal Press, p. 584.

1 Typical form (throughout the RSA region except for the Western and Eastern Cape.
2 Barberton form (Barberton region, Mpumalanga).

Synonyms: *D. anomala* var. *microcephala* (Harv)., *D. anomala* forma. *microcephala* (Harv.) and *D. gerrardii* Harv. ex F. C. Wilson.

## 2.3 Ethnobotany

Common ethnomedicinally important species of *Dicoma* are the following: *D. capensis*; *D. anomala*; *D. schinzii*, *D. zeyheri*. Species *D. anomala* is used in the primary health care systems of Botswana, Namibia and South Africa.

### 2.3.1 Vernacular names

In Africa several vernacular names for *D. anomala* have been reported: Tihonya in Botswana; umwanzuranya (Kirundi/Kinyarwanda) in Burundi and Democratic Republic of Congo; umwanzuranya (Kinyarwanda) in Rwanda and weya (Hehe) in Tanzania.[17] In South Africa, *D. anomala* is known by the following vernacular names: aambeibos, gryshout,[18] koorsbossie, korsbossie,[19] kalwerbossie,[18] maagwortel, maagbitterwortel,[18] maagbossie, swartstorm,[19,20,21,22] vyfaartjies, wurmbossie (Afrikaans);[18] fever bush, stomach bush (English);[15] chiparurangomo (Manyika);[19] chifumuro (Shona); hlwejane,[19] hloenya, mohasetse (Southern Sotho);[15] thlongati, thlonya (Setswana);[19] inyongwane, inyongana[15] (Swazi, Xhosa); and isihlabamakhondlwane, umuna[18](Zulu).

---

[17] *Prelude Medicinal Plants Database*: http://www.metafro.be/prelude. Accessed on 10 October 2008.
[18] Hutchins A., Scott A. H., Lewis G., Cunningham A. B. (1996). *Zulu Medicinal Plants: An Inventory*. Pietermaritzburg: University of Natal Press, pp. 334-335.
[19] Roberts M. (1990). *Indigenous Healing Plants*. Halfway House: Southern Book Publishers, p. 80.
[20] Van Wyk B. -E., van Oudtshoorn B., Gericke N. (1997). *Medicinal Plants of South Africa*. Pretoria: Briza Publications, pp. 104-105.
[21] The vernacular name "swartstorm" normally refers to another plant, *Cadaba aphylla* (Thunb.) Willd. (Capparaceae); (Ref. 17).
[22] Van Wyk B. -E., de Wet H., van Heerden F. R. (2008). *South African Journal of Botany*, **74**, 696-704.

### 2.3.2 Medicinal uses

The ethnobotanical uses of *D. anomala* are summarised in Table 2.1. These uses could be linked to several pharmacological properties, such as antibacterial, antihelminthic, antiviral, antispasmodic, wound healing, analgesic and antiinflammatory. Other medicinally utilised species of *Dicoma* are used for similar conditions. The roots of *D. zeyheri are* used for coughs and chest ailments, also as a blood strengthener for mothers after long and difficult births, and for lumbago, back pains and stomach problems.[1,23] The leaves and twigs of *D. capensis* Less. are reported to be used for treatment of cancer,[23] high blood pressure, febrile conditions,[24] fever diarrhoea, cough and gastrointestinal complaints.[24] The roots of *D. schinzii* are used to treat *c*oughs, sore throats and febrile convulsions in infants.[23]

**Table 2.1. Ethnobotanical uses of *Dicoma anomala***

| Condition or symptom | Plant part | Geographic reference | Source of information |
|---|---|---|---|
| Circulation | roots | RSA; Namibia | Roberts, 1990; Von Koenen, 2001* |
| Blood disorders | roots | RSA; Zimbabwe | Roberts, 1990; Gelfand, 1985[25)] |
| Cardiovascular disorders | roots | RSA; Namibia | Roberts, 1990; Von Koenen, 2001* |
| Cataracts | roots | Zimbabwe | Gelfand, 1985 |
| Colic | roots | Namibia | Von Koenen, 2001* |
| Constipation | leaves | Rwanda | Prelude |
| Cough | leaves | Botswana; Rwanda; Zimbabwe | Prelude; Gelfand, 1985 |
| Coughs and colds | roots | RSA; Namibia | Roberts, 1990; Von Koenen, 2001* |
| Cutting pain in the stomach | roots | Botswana | Prelude |
| Dermatosis skin eruptions | roots | Burundi; Zimbabwe | Gelfand, 1985; Prelude |
| Diarrhoea | roots | RSA; Zimbabwe; | Roberts, 1990; Gelfand, 1985; Von |

[23] Watt J. M., Breyer-Brandwijk, M. G. (1962). *The Medicinal and Poisonous Plants of Southern and Eastern Africa*, 2nd edition. Edinburgh & London: Livingstone.
[24] Von Koenen E. (2001). *Medicinal, Poisonous and Edible Olants in Namibia.* Windhoek: Klaus Hess, p. 111.
[25] Gelfand M., Mavi S., Drummond R.B., Ndemera B. (1985). *The Traditional Medicinal Practitioner in Zimbabwe*. Gweru (Zimbabwe): Mambo Press.

| | | | |
|---|---|---|---|
| | | Namibia | Koenen, 2001* |
| Dizziness | roots | Zimbabwe | Gelfand, 1985 |
| Dysentery | roots | RSA; Zimbabwe; Namibia | Roberts, 1990; Gelfand, 1985; Koenen, 2001* |
| Fevers | roots | RSA; Zimbabwe | Roberts, 1990; Gelfand, 1985 |
| Gall sickness (animals) | roots | Zimbabwe | Gelfand, 1985 |
| Haemorrhoids (as a purgative) | roots | Zimbabwe; Namibia | Gelfand, 1985; von Koenen, 2001* |
| Infertility | roots | Zimbabwe | Gelfand, 1985 |
| Intestinal parasites | roots | RSA; Zimbabwe; Burundi; Namibia | Roberts, 1990; Gelfand, 1985; Prelude; von Koenen, 2001* |
| Pneumonia | roots | RSA | Van Wyk & Gericke, 2000 |
| Psychosis | roots | Zimbabwe | Gelfand, 1985 |
| Purgative | roots | RSA | Roberts, 1990 |
| Respiratory complaints | roots | Zimbabwe | Gelfand, 1985 |
| Sores and scabs | roots | RSA | Roberts, 1990 |
| Sores and wounds | roots | Zimbabwe | Gelfand, 1985 |
| Stomach upsets | roots | RSA | Roberts, 1990 |
| TB cough | roots | Zimbabwe | Gelfand, 1985 |
| Toothache | roots | RSA; Zimbabwe | Roberts, 1990; Gelfand, 1985 |
| Colic | roots | RSA | Roberts, 1990 |
| Uterine sedative | roots | Zimbabwe | Gelfand, 1985 |
| Varicose veins | roots | RSA | Roberts, 1990 |
| Venereal diseases | roots | RSA | Roberts, 1990 |
| Vertigo | roots | Zimbabwe | Gelfand, 1985 |
| Wounds and ringworm | roots | RSA | Roberts, 1990 |

*Use reported for *D. anomala* subsp. *anomala*

Recently, two studies concerning the scientific evaluation of *D. anomala* and *D. capensis* appeared in the literature. One study reports on the evaluation of the root extract (MeOH and $H_2O$) of *D. anomala* collected in the Johannesburg area for its potential antibacterial and antiinflammatory properties. Both extracts were found to exhibit activity at MIC > 4 mg/mL against all selected bacteria.[26]

[26] Steenkamp V., Mathivha E., Gouws M. C., van Rensburg C. E. J. (2004). *Journal of Ethnopharmacology*, **95**, 353–357.

An aqueous extract of *D. capensis* was evaluated against three cancer cell lines: malignant breast MCF-7 and MDA-MB-231; non-malignant breast cell line MCF-12A; and prostate DU-145. The extract showed pronounced anticancer activity in the range of 30 µg/mL (MCF-7) and 31 µg/mL (MCF-12A) cells.[27] However, no anticancer bioactivity-guided isolation of the active compound of *Dicoma* has been reported to date.

## 2.4 Phytochemistry

All four medicinally used *Dicoma* species were previously investigated from the chemotaxonomic point of view. Several classes of secondary metabolites were isolated and characterised. Apart from *D. zeyheri*, the chemistry of the *Dicoma* species showed much similarity and the compounds commonly occurring in the species could be grouped into several classes: acetylenic compounds (cyclic and acyclic) (Figure 2.2), phenolic acids, flavonoids (cirsimaritin and scutellarein), sesquiterpenes (*β*-farnesene, *α*-humulene), triterpenes (lupeol and lupenone), phytosterols (*β*-sitosterol, stigmasterol, taraxasterol and their acetates) and several others.

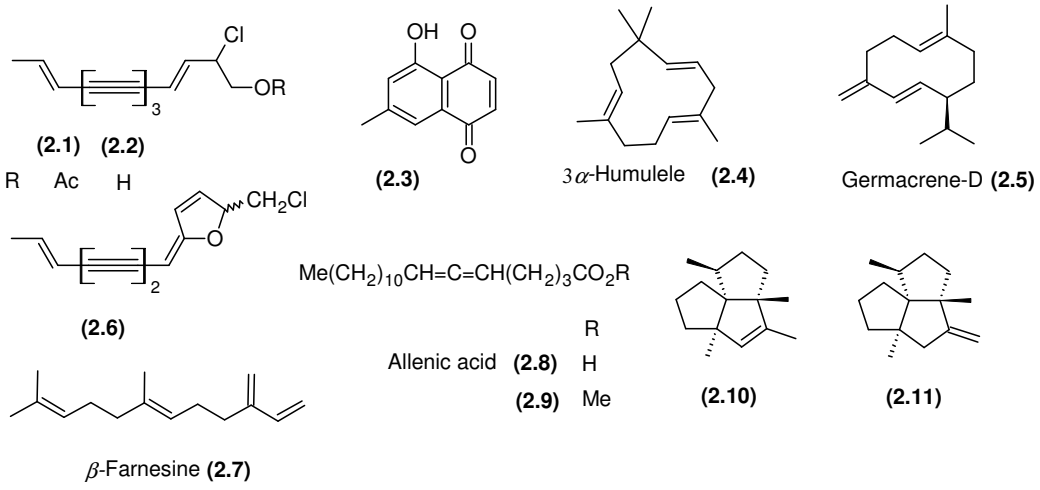


**Figure 2.2. Phytoconstituents of various parts of *D. zeyheri***

[27] Steenkamp V., Gouws M. C. (2006). *South African Journal of Botany*, **72**, 630–633.

### 2.4.1 *D. zeyheri*

Unspecified parts of *D. zeyheri* yielded acetylentic compounds **(2.1** and **2.2)**.[9] The aerial parts contained allenic acid **(2.8)** and its ester but no further characteristic compounds. The roots were reported to contain *β*-farnesine **(2.7)**, *α*-humulene, **(2.4)**, cyclysed acetylenes **(2.6),** allenic acid **(2.8)**, 5*E*- and 5*Z*-zeyherin formed *via* the corresponding chlorohydrine **(2.10**, **2.11** and **2.35)**.[10] Guaianolide *β*-hydroxy dehydrozaluzanin C **(2.33)** was the only compound in common with the other three *Dicoma* species reviewed later in this section.

### 2.4.2 *D. anomala* Sond.

The aerial parts of *D. anomala* subsp. *cirsioides*, collected in KwaZulu-Natal, yielded acetylenic compounds, stigmasterol, *β*-sitosterol, lupeol and some sesquiterpene lactones. The latter group included germacranolides **(2.12** and **2.14),** with a 7,8-lactone function, albicolide **(2.19)** and 14-acetoxydicomanolide **(2.26)**, with 6,7-lactone closure.[9] The roots of *D. anomala* subsp. *cirsoides* (KwaZulu-Natal) yielded mostly the acetylenic compounds (triynediene). The aerial parts of *D. anomala* subsp. *cirsoides,* collected in the former Transvaal region, yielded germacrene D **(2.5)**, lupeol, taraxasterol, and sesquiterpene lactones **(2.23**, **2.27**, **2.31** and **2.32)**. The roots of the Transvaal specimen contained, in addition to sitosterols and lupenone, some guaianolides **(2.33** and **2.34)** and eudesmanolides **(2.39**, **2.41** and **2.42)**.[10] The constituents of the roots of the specimens from the former Natal and Transvaal differed noticeably.[10]

The aerial parts of *D. anomala* subsp. *anomala* collected in the former Transvaal yielded phytol, lupeol and its acetate, germacrene D **(2.5)**, germacranolides **2.23**, **2.31** and **2.32**, while the roots gave no characteristic compounds.[10] Investigation of the aerial parts of the same species, collected in Namibia, resulted in the isolation of melampolides **(2.15** and **2.16)**, germacranolides **(2.20**, **2.21** and **2.23)** and a lactone **(2.36)**, in addition to the lupeol and taraxasterol and their acetates, and two flavonoids, cirsimaritin and scutellarein.[11]

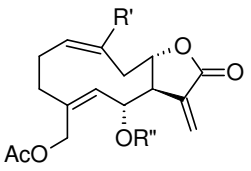

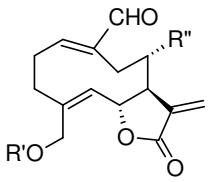

| | (2.12) | (2.13) | (2.14) |
|---|---|---|---|
| R' | $CH_2OAc$ | $CH_2OAc$ | CHO |
| R" | H | Ac | H |

| | (2.15) | (2.16) | (2.17) | (2.18) |
|---|---|---|---|---|
| R' | H | Ac | Ac | Ac |
| R" | OH | OH | H | H |

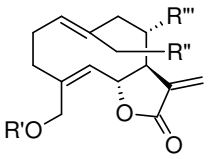

| | (2.19) | (2.20) | (2.21) | (2.22) | (2.23) | (2.24) | (2.25) | (2.26) | (2.27) | (2.28) | (2.29) | (2.30) | (2.31) | (2.32) |
|---|---|---|---|---|---|---|---|---|---|---|---|---|---|---|
| R' | H | H | Ac | Ac | H | Ac | Ac | H | Ac | Ac | Ac | H | H | H |
| R" | OH | OH | OH | OAc | $OR^1$ | H | OH | OAc | OAc | H | OAc | OAc | OAc | OAc |
| R"' | H | OAc | OAc | OAc | OAc | H | H | H | H | OH | OH | OAc | $OR^2$ | $OR^3$ |

$OR^1$ = OCO CH(Me) CH(OH) Me  $OR^2 = OCOC(CH_3)CHCH_3$  $OR^3 = OCOCH(CH_3)CH_2CH_3$

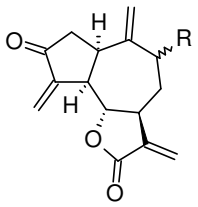

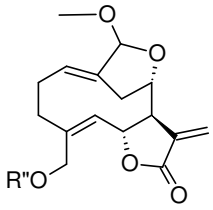

**(2.36)**

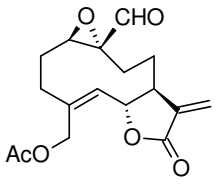

**(2.37)**

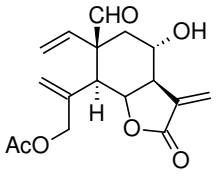

**(2.38)**

| | (2.33) | (2.34) | (2.35) |
|---|---|---|---|
| R | H | a-OH | *B*-OH |

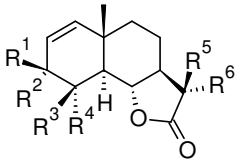

| | $R^1$ | $R^2$ | $R^3$ | $R^4$ | $R^5$ | $R^6$ |
|---|---|---|---|---|---|---|
| **(2.39)** | =O | | H | Me | Me | H |
| **(2.40)** | =O | | H | Me | H | Me |
| **(2.41)** | =O | | H | Me | $=CH_2$ | |
| **(2.42)** | =O | | $=CH_2$ | | $=CH_2$ | |
| **(2.43)** | H | OH | $=CH_2$ | | $=CH_2$ | |
| **(2.44)** | H | OAc | $=CH_2$ | | $=CH_2$ | |

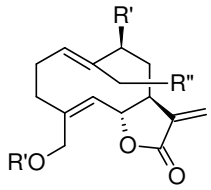

| | (2.45) | (2.46) | (2.47) | (2.48) | (2.49) |
|---|---|---|---|---|---|
| R' | H | i-Bu | H | Ac | H |
| R" | OH | OH | OAc | OAc | H |
| R"' | i-Bu | i-Bu | i-Bu | i-Bu | R* |

R* = $COC(CH_3)CH_2$

**Figure 2.3. Sesquiterpene lactones from *Dicoma* species**

The most recent report is of the phytochemicals isolated through bioassay-guided fractionation of the root extracts of *D. anomala* (subspecies not specified) collected

in Lesotho (Morifi and Mohales' Hoek areas), the Free State (Reitz area), and Limpopo Province (Sekhukhuni area). Roots that were purchased at the “muthi” markets in Durban (KwaZulu-Natal), were also investigated. This investigation resulted in the isolation of the novel guaianolide-type sesquiterpene lactone dimer **2.50** with potent antiplasmodial properties.[28]

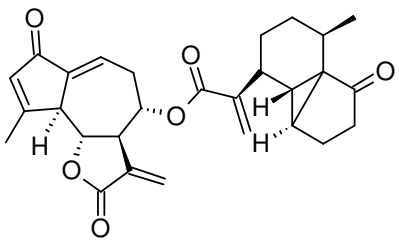

**(2.50)**

Some differences were noticed when comparing the phytochemical profiles of *D. anomala* and its subspecies *D. anomala* subsp. *cirsioides* and *D. anomala* subsp. *anomala*. However, further studies are required to compare five recognised regional forms of *D. anomala* subsp. *anomala* to make a more chemotaxonomically sound conclusion.

### 2.4.3 *D. capensis* Less.

The aerial parts of *D. capensis* harvested in Namibia yielded several structural types of sesquiterpene lactones: melampolides **(2.17**, **2.18** and **2.37)**; germacranolides **(2.19**, **2.24**, **2.25** and **2.28)**; and eudesmanolides **(2.43** and **2.44)**.[11]

### 2.4.4 *D. schinzii* O. Hoffm.

Roots of *D. schinzii* collected in the former Transvaal region yielded taraxasterol, lupeol and its acetate, their $\Delta^{12}$-isomers and eudesmanolides **2.39**, **2.41** and **2.42**, whilst the aerial parts yielded isobutyrates with a germacrane skeleton **(2.45**, **2.46** and **2.47)** with a 9*β*-oxygen function.[10] Investigation of the aerial parts of *D.*

[28] Matsabisa G. M., Campbell W. E., Folb P. I., Smith P. J. (2006). Treatment of parasitic infections in humans and animals (WO/2006/048734).

*schinzii* collected in Namibia resulted in several germacranolides **(2.24**, **2.26** and **2.28)**, which lacked the 9*β*-oxygen function.[11]

## 2.5 Summary of reported biological activities of the phytochemicals isolated from medicinally used *Dicoma* species

### 2.5.1 Phenolic compounds

Caffeic acid, which was isolated from unspecified parts of *D. anomala,* is reported to have potent antioxidant properties.[29] The flavonoids cirsimaritin and scutellarein were isolated from *D. anomala* subsp. *anomala*.[11] Cirsimaritin is used to treat proteinuria (or kidney failure) and was found to have adenosine and benzodiazepine receptor antagonist properties *in vitro*.[30] Scutellarein was shown to have some effects on the pathologic changes of the heart caused by hypertension (uncompetitive protein kinase c inhibitor): it can reverse the ventricular remodelling, improve cardiomuscular stiffness and protect cardiac muscle.[31] The presence of these flavonoids in the aerial parts of *D. capensis* could contribute to its effectiveness in treating high blood pressure, *i.e.* hypertension.

### 2.5.2 Phytosterols

The *β*-sitosterol, which was found in the roots of *D. anomala* subsp. *cirsoides*, is best known for its cholesterol-lowering properties.[32] In addition, *β*-sitosterol exhibited the following therapeutic properties: anticancer (inhibition of growth and metastasis of prostate and skin cancer cells *in vitro*)[33] and antioxidant. It is also used for the treatment of prostate enlargement (possibly through inhibition of 5α–reductase)[34] and heart conditions related to high levels of blood cholesterol. It has also been shown to increase levels of testosterone and 11-ketotestosterone, and

---

[29] Gülçin İ. (2006). *Toxicology*, **217**, 213-220.
[30] Wang J.–P., Chang L.–C., Hsu M.-F., Chen S.–C., Kuo S.–C. (2002). *Naunyn-Schmiedeberg's Archives of Pharmacology*, **366**, 307-314.
[31] Zhou J., Lei H. A., Chen Y., Li F., Ma C. (2002). *Chinese Medical Journal*, **115**, 375–377.
[32] Law M. R., (2000). *The Western Journal of Medicine*, **173**, 43-47.
[33] Awad A. B., Fink C. S., Williams H., Kim U. (2001). *European Journal of Cancer Prevention*, **10**, 507–513.
[34] Cabeza M., Bratoeff E., Heuze I., Ramirez E., Sanchez M., Flores E. (2003). *Proceedings of the Western Pharmacology Society,* **46**,153-155.

to accelerate spermatogenesis.[35] The high concentrations of phytosterols in the roots could be responsible for the reported use of *D. anomala* for the treatment of infertility[35] and "heart problems".

### 2.5.3 Terpenoids

#### *2.5.3.1 Diterpenes and triterpenes*

Phytol (an acyclic diterpene) is reported to possess potent antimycobacterial properties (MIC of 2 µg/mL) in the same concentration range as ethambutol, a clinically useful drug with an MIC in the range 0.95 to 3.8 µg/mL.[36] Lupeol is reported to act as a potent modulator of the NF-kB pathway, which is related to inflammation and shows lipoxygenase inhibitory activity ($IC_{50}$ = 35 µM) and was shown to inhibit skin cancer in mice.[37,38.]

#### *2.5.3.2 Sesquiterpenes*

The compound *α*-humulene **(2.4)**, which was isolated from the roots of *D. zeyheri,* is known for its antitumour activity.[10,39] Costunolide is reported to inhibit various biological and immunological actions. It has shown a preventative effect against carcinogenesis and is known to induce apoptosis in human promonocytic leukaemia U937 cells by depleting intracellular thiols.[40] Furthermore, costunolide has been reported to inhibit the killing activity of cytotoxic T-lymphocytes, which are important in the process of the elimination of virus-infected cells.[41] The presence of costunolide has not been reported in any of the reviewed *Dicoma* species, but the 14-,15-oxygenated costunolide derivatives appeared characteristic and could possess biological properties similar to those of

---

[35] Christianson-Heiska I., Smeds P., Granholm N., Bergelin E., Isomaa B. (2007). *Comparative Biochemistry and Physiology, Part C: Toxicology and Pharmacology,* **145**, 518–527.
[36] Rajab M. S., Cantrell C. L., Franzblau S. G., Fischer N. H. (1998). *Planta Medica*, **58**, 19-21.
[37] Gutierrez-Lugo M. -T., Deschamps J. D., Holman T. R., Suarez E., Timmermann B. N. (2004). *Planta Medica*, **70**, 263–265.
[38] Saleem M., Afaq F., Adhami M. V., Mukhtar H. (2004). *Oncogene*, **23**, 5203-5214.
[39] Pichette A., Legault J., Madelmont J. -C. (2008). Use of Compositions Comprising Sesquiterpene Derivatives for the Treatment of Cancer, EP20020708107.
[40] Choi J. -H., Ha J., Park J. -H., Lee Y. S., Park H. -J., Choi J. -W., Masuda Y., Nakaya K., Lee K.-T. (2002). *Japanese Journal of Cancer Research*, **93**, 1327–1333.
[41] Taniguchi M., Kataoka T., Suzuki H., Uramoto M., Ando M., Arao K., Magae J., Nishimura T., Otake N., Nagai K. (1995). *Biosciences, Biotechnology and Biochemistry*, **59**, 2064–2067.

costunolide. The dehydrozaluzanin C **(2.33)** is reported to possess antiprotozoal[42] and antifungal properties ($GI_{50}$ = 30 μM).[43] For tuberiferin **(2.41)**, an inhibitory action has been shown on the respiratory burst of peritoneal inflammatory polymorphonuclear leukocytes. This implies some potential of tuberiferin as an antiinflammatory agent. It also substantially decreased carrageenan-induced mouse paw oedema. The latter bioactivity could contribute to the wound-healing property of the *Dicoma* plants.

## 2.6 Conclusion

It is apparent that the original sample of the roots of *D. anomala* delivered by a traditional healer and identified as *D. anomala* sensu Wild could probably be further sub-classified into *D. anomala* subsp. *gerrardii* on the basis of the description of the plants as "erect and with small leaves". Previously classified as *D. anomala* var. *microcephala* and as *D. gerrardii*, there was no information in the literature on the results of the phytochemical investigations of *D. anomala* subsp. *gerrardii*. A comprehensive literature review of *Dicoma* ethnobotany did not reveal any anecdotal information on the use of *D. anomala* subsp. *gerrardii* or any of its synonyms. However, many anecdotes described the *D. anomala* plants as erect or prostrate, therefore the information related to the use of the plant is fuzzy and should be treated with caution. Furthermore, *D. anomala* has not been linked directly to cancer as such, unlike *D. capensis*, where the aerial parts are said to be used to treat the pathology associated with cancer.

With regard to the bioactivity of phytochemicals isolated from the extracts of *D. anomala* Sond., lupeol and *β*-sitosterol are reported to have anticancer properties by directly inhibiting the growth of skin cancer in mice[38] and of prostate cancer cell lines in culture.[34] Lupeol was isolated from the aerial parts but not the roots of *D. anomala,* and was found in the roots of *D. schinzii*. The presence of costunolide derivatives with oxygen functions at C-14 and C-15 are characteristic for the genus and may have bioactivity similar to that of costunolide. Furthermore,

---

[42] Fournet A., Munoz V., Roblot F., Hocquemiller R., Cave A., Gantier J.-C. (1993). *Phytotherapy Research*, **7**, 111–115.
[43] Wedge D. E., Galindo J. C. G., Macias F. A. (2000). *Phytochemistry*, **53**, 747–757.

sesquiterpenes such as dehydrozaluzanin C **(2.33)** or tuberiferin **(2.41)** could have contributed to the observed effects.

To date no reports on the phytochemistry of *D. anomala* subsp. *gerrardii* could be found. In the following chapter the work on bioassay-guided fractionation of organic extract of *D. anomala* subsp. *gerrardii* and the isolation of compounds responsible for the anticancer activity of the crude organic extract is presented.

# Chapter 3: Experimental

## 3.1 General materials and methods

### 3.1.1 Liquid chromatography

The purification of the compounds from the extracts was performed using the following chromatographic techniques: vacuum liquid chromatography (VLC), column chromatography (CC), flash chromatography (FC) and semi preparative liquid chromatography (LC).

For detection, identification and estimation of yields, two high performance liquid chromatography (HPLC) instruments were used (Sections 3.1.1.4 and 3.1.2.3).

#### *3.1.1.1 Column chromatography*

In the purifications by column chromatography (CC), packed with Silica gel 60 (0.063 - 0.2 mm), the choice of the column sizes was based mainly on the quantity and the complexity of the crude sample; columns usually ranged from 10-90 cm in length and 1-4 cm in diameter; EtOAc/Hexane/DCM/MeOH – isocratic solvent mixtures were employed for all consecutive purifications (the proportions of the solvents are specified in relevant sections). Fractions were combined based on the similar chemical compositions as determined by thin layer chromatography (TLC). The solvent was removed under vacuum on a rotary evaporator. TLC plates, used throughout the experiments, were pre-coated glass silica gel plates ($F_{254}$; 0.2 mm; Merck or Sigma Aldrich).

#### *3.1.1.2 Flash chromatography*

This method is based on the same principle as for CC, but flash silica gel with particle sizes ranging from 35 – 75 µm, was used as a stationary phase and the fractions were collected by applying vacuum. Smaller columns (25 – 90 cm in length and 1-2 cm in diameter) were used to achieve a separation of compounds with similar $R_f$ values, and fractions of smaller volumes were collected.

*3.1.1.3 Vacuum liquid chromatography*

VLC was utilised mostly for the large-scale purifications of the crude extracts and fractions in batches of 5 – 10 g of extract on 400 – 500 g of $SiO_2$ 60 (0.063 – 0.2 mm) under reduced pressure, using a range of solvents and stepwise gradients. Pooled fractions were combined on the basis of similarity of chemical profiles as determined by TLC. Fractions were concentrated under vacuum on a rotary evaporator and the extracts further dried in the vacuum desiccator.

*3.1.1.4 HPLC-UV/MS*

A HPLC Waters Alliance 2690 system, equipped with a Waters 996 photodiode array detector (UV), and coupled to a Quattro micro mass spectrometer (Section 3.1.3), interfaced with Masslynx software, was utilised to profile, identify and estimate the yields of plant metabolites. Stock solutions of test samples were prepared on the basis of the complexity to concentrations ranging from 5 000 ppm (crude extracts) to 100 ppm (pure compounds). The choice of solvent depended on the solubility of a sample. All stock solutions were filtered though a 0.45 µm PTFE filter (Microsep) prior to injection. HPLC-grade solvents (Romil, Microsep) were used. The calibrations and quantifications were carried out using Waters Millennium 2010 Chromatography manager GPC software version 2.0 (Millipore Corporation, Waters Chromatography Division). A range of analytical columns and two sets of gradient conditions were used for analyses, and are summarised in Tables 3.1 and 3.2. These analyses were performed at CSIR Biosciences.

**Table 3.1. Gradient conditions for the Waters Alliance 2690 for methods T3.1-1 and T3.1-2 (run time – 90 min)**

| Time (min) | Flow (mL/min) | % A (Water) | % B (ACN) | Curve |
|---|---|---|---|---|
| 0.00 | 1.000 | 90 | 10 | 1 |
| 61.00 | 1.000 | 20 | 80 | 6 |
| 64.00 | 1.000 | 0 | 100 | 6 |
| 75.00 | 1.000 | 0 | 100 | 6 |
| 75.10 | 1.000 | 90 | 10 | 6 |
| 90.00 | 1.000 | 90 | 10 | 6 |
| **HPLC Method T3.1-1.** Column: Thermo C8 Hypersil Gold (250 x 4.6 mm, 5 µm ), T = 40 °C | | | | |
| **HPLC Method T3.1-2.** Column: Agilent Tech Zorbax Rx-C8 (250 x 4.6 mm, 5 µm ), T = 40 °C | | | | |
| **HPLC Method T3.1-3.** Column: ODS Hypersil C18 column (250 x 4.6 mm, 5 µm ), T = 40 °C | | | | |

**Table 3.2. Gradient conditions for the Waters Alliance 2690 for methods T3.2-1 and T3.2-2 (run time - 60 min)**

| Time (min) | Flow (mL/min) | % A (Water)* | % B (ACN) | Curve |
|---|---|---|---|---|
| 0.00 | 1.000 | 90 | 10 | 1 |
| 10.00 | 1.000 | 90 | 10 | 5 |
| 35.00 | 1.000 | 0 | 100 | 6 |
| 45.00 | 1.000 | 0 | 100 | 4 |
| 50.10 | 1.000 | 90 | 10 | 5 |
| 60.00 | 1.000 | 90 | 10 | 5 |
| **HPLC Method T3.2-1.** Column: Supelco F5 Discovery® HS F5 (150 x 2.1 mm, 3 µm), T = 50 °C | | | | |
| **HPLC Method T3.2-2.** Column: Waters Atlantis® T3 RP-amide (150 x 2.1 mm, 3 µm), T = 50 °C | | | | |
| **HPLC Method T3.2-3.** Column: Agilent Tech Zorbax Rx-C8 (250 x 4.6 mm, 5 µm ), T = 40 °C | | | | |

*Water containing 0.1% formic acid

*3.1.1.5 Preparative-scale liquid chromatography*

The Semi-prep HPLC System: Agilent 1200 series, fitted with Waters Atlantis C18 T3 (10 x 250 mm, 5 µm) column, was used for purification of water-soluble amino acid adduct **(5.27)**. A stock solution of 5 000 ppm was prepared and was injected onto a preparative scale column (100 µL). The gradient table presented in Table 3.3 was utilised. This work was carried out at CSIR Biosciences.

**Table 3.3. Gradient conditions for the Agilent 1200 for method T3.3 (run time – 40 min)**

| Time (min ) | Flow (mL/min) | %A (Water)* | %B (ACN) |
|---|---|---|---|
| 0.0 | 5.000 | 100 | 0 |
| 3.00 | 5.000 | 100 | 0 |
| 12.50 | 5.000 | 80 | 20 |
| 18.00 | 5.000 | 0 | 100 |
| 22.00 | 5.000 | 0 | 100 |
| 25.00 | 5.000 | 100 | 0 |
| 40.00 | 5.000 | 100 | 0 |
| **HPLC Method T3.3: Column: Waters Atlantis C18 Prep. T3 (250 x 10 mm, 5 µm)** | | | |

*Water containing 0.1% formic acid

### 3.1.2 Mass spectrometry (MS)

#### *3.1.2.1 Quattro LC Micro mass spectrometer*

The mass spectral data were obtained from a hyphenated HPLC-UV/MS instrument (Section 3.1.1.4) equipped with a triple quadrupole Quattro LC Micro mass spectrometer, which was set to operate in both the $ESI^-$ and $ESI^+$ modes (49 – 478 amu) with a gain of 10. The cone voltage was varied between 20 and 70 eV, the desolvation temperature was 450 °C, and the source block temperature was set at 120 °C. Samples were dissolved in ACN/MeOH (2:1 v/v), vortexed until fully dissolved, and volumes between 10 and 50 µL were injected onto the analytical column. This work was carried out at CSIR Biosciences.

#### *3.1.2.2 HREI-MS*

HREI-MS spectral data were obtained from University of the Witwatersrand. A VG 70SEQ HRMS instrument, operated mainly in the EI mode, using 8 kV as the standard ionisation energy was used to generate the spectra.

#### *3.1.2.3 Waters ThermaBeam (TMD) system*

This type of analysis was done on a Waters ThermaBeam (TMD) system comprising a 2695 Solvent Delivery System fitted with analytical column (Phenomenex Gemini C18; 250 x 2 mm, 5 µm; T = 40 °C), a 2996 PDA detector, column heater and ThermaBeam EI-MS detector (TMD). The gradient table is summarised in Table 3.4. The TMD was operated in positive scan mode (50 – 650 amu) with a gain of 10. The nebuliser temperature set at 70 °C, the expansion region temperature at 80 °C and the source temperature at 225 °C. The total volume of post-column eluent was sent to the TMD. The TMD was tuned every day prior to starting an analysis run and caffeine was injected as a test compound to ensure functionality of the total system. The three samples were suspended in ACN/MeOH (2:1 v/v), vortexed until fully dissolved, filtered (0.45 µm) and 10 µL was injected onto the analytical column. This work was carried out at CSIR Biosciences.

**Table 3.4. Gradient conditions for the Waters 2695. Method T3.4 (run time – 60 min)**

| Time (min) | Flow (mL/min) | % C ($H_2O$) | % D (ACN) | Curve |
|---|---|---|---|---|
| 0.0 | 0.2 | 90 | 10 | 6 |
| 1.0 | 0.2 | 90 | 10 | 6 |
| 20 | 0.2 | 30 | 70 | 6 |
| 40.0 | 0.2 | 0 | 100 | 6 |
| 41.0 | 0.25 | 0 | 100 | 6 |
| 45.0 | 0.25 | 0 | 100 | 2 |
| 50.0 | 0.25 | 90 | 10 | 3 |
| 58.0 | 0.2 | 90 | 10 | 6 |
| 59.0 | 0.2 | 90 | 10 | 6 |

### 3.1.3 NMR spectroscopy

NMR analyses were carried out on a Varian 400 MHz Unity spectrometer at the CSIR. TMS was used as an internal reference standard. Routine analysis generally involved the following 1D and 2D core procedures:

- 1D $^{1}H$ analysis (investigation of chemical shifts, signal intensities and scalar (J) couplings between nuclei)
- 1D $^{13}C$ analysis (to establish the chemical shifts and the number of carbons present)
- DEPT sequence (to determine number of proton baring carbons)
- 2D $^{1}H\leftrightarrow$ $^{1}H$ COSY/gCOSY sequence (to establish proton connectivity)
- 2D HMQC/gHMQC and HSQC/gHSQC sequences (to establish $^{1}H\leftrightarrow^{13}C$ correlations)
- 2D HMBC sequence (to identify fragments through long-range $^{1}H\leftrightarrow^{13}C$ correlations due to spin exchange over 2 or 3 bonds or across heteroatoms)
- 2D NOESY experiments (for stereochemical analysis of space interactions though dipole coupling and spin relaxation).

### 3.1.4 Polarimetry

A Perkin Elmer 241 polarimeter at 589 nm with a sodium lamp at 589 nm as a light source and a cell with path length 1 dm was used in all experiments. These experiments were performed with $CHCl_3$ as the solvent.

### 3.1.5 Determination of melting points

Melting points were determined using a Reichert hotstage apparatus and are uncorrected.

### 3.1.6 X-ray crystallography

Crystallography experiments were conducted by Dr Melanie Rademeyer at the University of KwaZulu-Natal on an Oxford Diffraction Excalibur-2 CCD area detector diffractometer, using Mo-K$\alpha$ X-radiation and a graphite-crystal monochromator. Data collection, cell refinement and reduction were conducted using CrysAlis CCD (version 1.171.29.9) and CrysAlis RED (version 1.171.29.9), Oxford Diffraction Ltd., 2006. Structure solution and refinement were performed using the SHELXS97 and SHELXL-97 (Sheldrick, 2008) programs respectively.[44] Mercury was used for molecular graphics.[45]

## 3.2 Biological assays

### 3.2.1 *In vitro* antimalarial screen

In this *in vitro* biological activity assay method, compounds or crude extracts were evaluated for their effect on *Plasmodium falciparum* erythrocytic forms of two strains, namely chloroquine-sensitive (CQS) D10 and chloroquine-resistant (CQR) strains K1. Asexsual erythrocytic stages of *P. falciparum* were continuously maintained in culture following the method of Trager and Jensen.[46] Static cultures were incubated in sterile culture flasks at 37 ℃ in an atmosphere of 93% $N_2$, 4% $CO_2$ and 3% $O_2$. The host cells were human red blood cells. The parasites were maintained at a 5% haematocrit in RPMI 1640 (Biowhittaker) culture medium

[44] Sheldrick G. M. (1997). SHELXL97 and SHELXS97. University of Göttingen, Germany.
[45] Bruno I. J., Cole J. C., Edgington P. R., Kessler M., Macrae C. F., McCabe P., Pearson J., Taylor R. (2002). *Acta Chrystallografica*, **B58**, 389-397.
[46] Trager W., Jensen J. B. (1976). *Science,* **193**, 673–675.

supplemented with 25 g/L of Albumax II (lipid-rich bovine albumin) (GibcoBRL), 44 mg/L of hypoxanthine, and 50 mg/L HEPES (Sigma Aldrich).

All test substances were stored at –20 $^{o}$C prior to testing. Stock solutions of test substances were prepared in 10% methanol or 10% DMSO, depending on the solubility, and diluted in Millipore water to prepare 2 µg/mL solutions, which were stored at –20 $^{o}$C. All solvent systems used for preparation of stock solutions were evaluated prior to the use and had no measurable effect on the host cells or the parasite. Chloroquine diphosphate (Sigma) was used as a reference drug in all experiments. The test substances were evaluated in nine serial two-fold dilutions (0.2 – 100 µg/mL) in medium and tested once, for each concentration, in replicate of two. Test solutions were plated together with the suspension of infected human red blood cells and incubated for 24 h in microtitre plates. The conditions for incubation were the same as described for the routine maintenance of the *P. falciparum* cultures.

Quantitative assessment of *in vitro* antiplasmodial activity was determined *via* a modified parasite pLDH assay of Makler *et al*.[47] This enzyme assay differentiates between pLDH and host LDH activity by using APAD. The pLDH uses APAD as a coenzyme in the conversion of pyruvate to lactate and reduces it to APADH. The formation of APADH can be measured by the subsequent reduction of a yellow NBT salt to a blue formazan product, the absorbance of which is measured with a 7520 microplate reader (Cambridge Technology) at λ 620 nm.

The $IC_{50}$ values, serving as a measure for antiplasmodial activities, were calculated using a non-linear dose-response curve fitting analysis *via* GraphPad Prism v.4.0 software. This work was carried out at the Pharmacology Department of UCT.

[47] Makler M. T., Ries J. M., Williams J. A., Bancroft J. E., Piper R. C., Gibbins B. L., Hinrichs D. J. (1993). *American Journal of Tropical Medicine Hygiene*, **48**, 739–741.

### 3.2.2 *In vitro* cytotoxicity assay

Compounds were tested for *in vitro* cytotoxicity against a CHO cell line using the MTT assay.[48] This colorimetric assay is based on the ability of viable cells to metabolise a yellow water-soluble tetrazolium salt into a water-insoluble purple formazan product. The amount of formazan produced can be measured spectrophotometrically and is proportional to the metabolic activity and number of cells in the test plate. The CHO cells were cultured in DMEM: Hams F-12 medium (1:1) supplemented with 10% heat-inactivated fetal calf serum (FCS) and gentamycin (0.04 µg/mL) (Highveld Biological, RSA).

Samples were dissolved in MeOH/$H_2O$ (1:9 v/v). Stock solutions (2 mg/mL) were prepared and were stored at –20 °C until use. Emetine was used as the positive control. The initial concentration of emetine was 100 µg/mL, which was serially diluted in complete medium with ten-fold dilutions to give six concentrations, the lowest being 0.001 µg/mL. The same dilution technique was applied to all test samples with an initial concentration of 100 µg/mL to give five concentrations, the lowest being 0.01 µg/mL.

In the initial stage of the experiments, the cells were adjusted to a concentration of $10^5$/mL, and 100 µL of this cell suspension was seeded in all wells except in column 1 ("blank") in a 96-well culture plate (Costar). The plates were incubated at 37 °C for 24 h in a humidified 5% $CO_2$-air atmosphere. After the incubation period, the medium was aspirated out of the wells and 100 µL of the test substances (drug stock solutions) was added in quadruplicate to the dedicated wells. A further 100 µL of culture medium was then added to all the wells containing cells and drugs, and 200 µL of medium was added to the "blank" wells and to the "no drug" wells containing only cells. The microplate was then incubated at 37 °C for 48 h.

After the 48 h incubation period, 25 µL of sterile MTT (5 mg/mL in PBS) was added to each well and incubation was continued for 4 h at 37 °C. The plates were then centrifuged at 2 050 r/min for 10 min, and the supernatant was carefully aspirated from the wells to ensure that the formazan crystals were not disturbed. The formazan crystals were then dissolved in DMSO (100 µL) and the plate was

[48] Mosmann T. (1983). *Journal of Immunological Methods*, **65**, 55-63.

gently placed on a shaker for 5 min. The plate was blanked on the wells in column 1 and the absorbance of the crystals was measured at λ 540 nm on a Microtitre Plate Reader (Cambridge Technologies). The cell viability was calculated in each well using the formula:

$$\% \text{ Cell viability} = \frac{A_{\lambda 540} \text{ test well (cells + drug)}}{A_{\lambda 540} \text{ cell control well (cells + no drug)}} \times 100$$

The concentration of drug that inhibits 50% of the cells ($IC_{50}$ values) for these samples was obtained from dose-response curves, using a non-linear dose-response curve fitting analysis *via* GraphPad Prism v.2.01 software. This assay was conducted by the UCT Pharmacology Department.

### 3.2.3 *In vivo* murine malaria model

The *in vivo* protocol was set up by Prof. Peter J. Smith (UCT). Ethical approval for this study was granted by the UCT Animal Ethics Committee. The strain of mice used for the experiment was C57 Black6 (6 – 10 weeks old) with average mass 20-25 g. There were five mice in each tested substance and four mice in each control group. The positive control group was treated with standard drug chloroquine. The negative control group received no treatment. The mice were infected with chloroquine-sensitive *Plasmodium bergei* ANKA. They were infected interperitoneally with 200 µL of $10^6$ cells/mL parasite stock. After 24 h post-infection, the mice were treated once a day for four consecutive days. From the second day post-infection, slides were made from three animals per group to determine the percentage of the parasitaemia in the blood using Giemsa stained smears. Test substances were administered orally or subcutaneously using water or DMSO/water (1:9 v/v). Pure compounds were tested at 100 mg/kg, and CQ was administered at 5 mg/kg to the positive control group. This assay was conducted by the UCT Pharmacology Department.

### 3.2.4 *In vitro* anticancer pre-screen

All extracts, fractions and compounds were assayed in the 3-cell line panel consisting of TK10 (renal), MCF7 (breast), and UACC62 (melanoma). A primary anticancer assay was performed in accordance with the adopted protocol of the

Drug Evaluation Branch of the NCI.[49,50,51] Crude extracts were tested at ½ log serial dilutions of five concentrations ranging from 6.25 to 100 ppm, or at log serial dilutions for molar concentrations ranging from 0.01 to 100 µM. The results were obtained for each cell line as dose-response curves. For selection and prioritization of test substances the biological activities were separated into four categories based on the value of the concentration of the compound needed to totally inhibit growth of the cells (TGI):

| | |
|---|---|
| Inactive: | TGI > 50 ppm |
| Weak: | TGI between 15 and 50 ppm for two or three cell lines |
| Moderate: | TGI between 6.25 and 15 ppm for two or three cell lines |
| Potent: | TGI < 6.25 ppm for two or three cell lines. |

The screening results were reported in terms of the averaged response parameters, $GI_{50}$, TGI, and $LC_{50}$, calculated for all cell lines.

The cell lines were grown in RPMI 1640 medium (Whitehead Scientific), supplemented with 10% heat-inactivated FBS (Adcock Ingram Scientific) and 2 mM of *L*-glutamine (Sigma Aldrich). The cells were inoculated into 96-well flat-bottom polystyrene plates at 100 µL with inoculation densities of 1000 (UACC62), 5000 (MCF7) to 15 000 (TK10) cells/well. The cell lines were plated as per Figure 3.1.

After cell inoculation, the microtitre plates were incubated at 36 ℃, 5% $CO_2$, 95% air and 100% relative humidity for 24 h prior to the addition of the experimental drugs. After 24 h, the time zero ($T_0$) plate was fixed *in situ* with chilled TCA to measure the cell population for each cell line at the time of drug addition.

---

[49] Monks A., Scudiero D., Skehan P., Shoemaker R., Paull K. D., Vistica D., Hose C., Langley J., Cronise P., Vaigro-Wolff A., Gray-Goodrich A., Campbell H., Mayo J., Boyd M. (1991). *Journal of the National Cancer Institute*, **83**, 757–766.

[50] Kuo S. -C., Lee H. -Z., Juang J. -P., Lin Y. -T., Wu T. -S., Chang J. -J., Lednicer D., Paull K. D., Lin C. M., Hamel E., Lee K. -H. (1993). *Journal of Medicinal Chemistry*, **36**, 1146–1156.

[51] Leteurtre F., Kohlhagen G., Paull K. D., Pommier Y. (1994). *Journal of the National Cancer Institute*, **86**, 1239–1244.

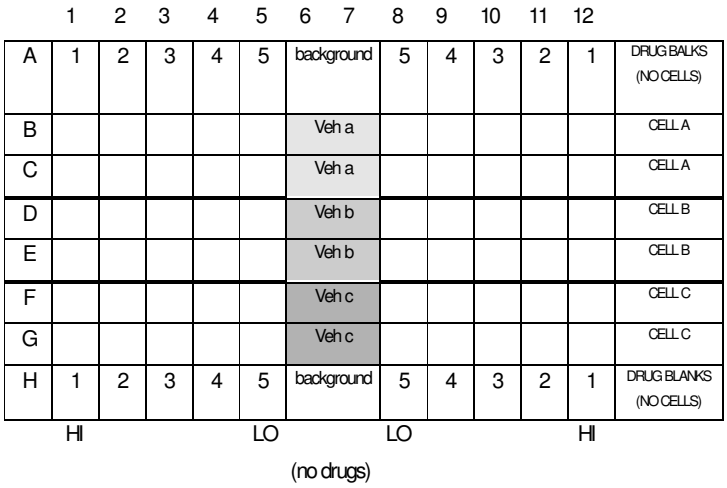


**Figure 3.1. Five-dose assay format**

Stock solutions of experimental drugs were prepared in DMSO at a concentration of 10 000 ppm (or less, with subsequent adjustment of dilution volumes) and stored frozen prior to use. Extracts, fractions or compounds were diluted in complete media with 0.1% gentamycin sulfate and dispensed into the first of five dilution tube. Serial dilutions were made by transferring a set volume (in mL) from one tube to the next. The contents of the dilution tubes consisting of the media with a range of drug concentrations were dispensed into shallow basins prior to plating with a multi-channel pipettor aid. Following addition of the drugs, the plates were incubated for 48 h and then fixed *in situ* by the addition of 50 µL of chilled 50% TCA. After addition of the TCA, the plates were refrigerated for 1 – 3 h at 4 ℃. The supernatant was discarded, the plates were washed five times with tap water to remove excess TCA and media, and air-dried. SRB (Sigma Aldrich), at 0.4% in 1.0% acetic acid (v/v), was added to each well, and the plates were left to stand for 10-20 min at RT to ensure full staining of the cellular protein in the wells. Unbound dye was removed by inversion of the plates. The plates were then rinsed five times with 1.0% acetic acid and tap water to remove excess water, after which they were air-dried. Bound SRB was solubilised in 100 µL of 10 mM trizma base on the shaker for 5 min. The absorbance was measured at λ 540 nm on a microtitre plate reader (Labsystems Multiscan RC). The percentage of cells in each well was calculated using a spreadsheet based on the standard NCI-formula. This work was carried out at CSIR Biosciences.

### 3.2.5 *In vitro* anticancer 60-cell line panel

The cytotoxicity profile of the candidate extracts and compounds was determined against the panels of human cancer cell lines at the NCI (Maryland, USA). The NCI panel of 60 cell lines included leukaemia (L) lines, non-small cell lung cancer (NSCLC) lines, colon cancer (CL) lines, central nervous system cancer (CNSC) lines, melanoma (M) lines, ovarian cancer (OC) lines, renal cancer (RC) lines, prostate cancer (PC) lines, and breast cancer (BC) lines. The results from the NCI were reported as mean log10 functions of the three response parameters, $GI_{50}$, TGI, and $LC_{50}$, calculated for each cell line. Compounds having overall average log10 $GI_{50}$ values of less than 1.1 for all cell lines were selected for further investigation.

## 3.3 Bioassay-guided isolation of sesquiterpenoids from *D. anomala* subsp. *gerrardii* (Chapter 4)

### 3.3.1 Collection of plant material

Plant material of *D. anomala subsp. gerrardii* was collected in February 2006 and identified by Jean Meyer, a botanist from SANBI. Specimen vouchers were deposited at the SANBI Herbarium. All collections were chosen on the basis of plant population to ensure sustainable harvesting. A total of 6 kg of rhizomes was collected from the Brits district in North West province. The plants were sun-dried prior to delivery.

### 3.3.2 General extract preparation

The preparation of plant extracts from the material delivered by a traditional healer depended on the anecdotal information and on the intended route of administration described in the anecdote. In general, plant material was first dried in an oven at 60 ℃ and ground to a fine powder with a hammer mill. Two extraction methods were used. In method A, the plant material was separated into two portions and one portion was immersed in distilled DI $H_2O$ and boiled to produce a hot infusion or “tea”. The infusion was filtered through a cheese cloth followed by filtration through Whatman filter paper, after which the filtrate was lyophilised (extract yield = 2.5% w/w of dry plant material). The second portion of the plant material was extracted for 24 h with a solvent mixture of

methanol/dichloromethane (MeOH/DCM 1:1 v/v) sufficient to fully immerse the plant material. The extract was filtered and concentrated in a vacuum on the rotary vacuum evaporator at 60 °C. The concentrate was further dried in a vacuum desiccator to give a finished organic extract (extract yield = 2.7% w/w of dry plant material).

In method B, a sequential extraction was performed where firstly, a MeOH/DCM (1:1 v/v) extract was prepared, filtered and dried. The plant material was then dried overnight in an oven at 60 °C and then immersed in cold distilled water for 4 h and then extracted. The water extract was filtered and the filtrate was lyophilised.

### 3.3.3 Preparation of extracts with various solvents

Equal parts (5 g) of dried and ground plant material were extracted once with 50 mL of solvent for 24 h with occasional stirring. The following range of solvents was utilised in order of increasing polarity: hexane (A), DCM (B), EtOAc (C), MeOH/DCM (1:1 v/v) (D), MeOH (E), DI water (F). The extracts were filtered and the solvent was removed under vacuum with a rotary evaporator (60 °C). The extracts were further dried in a vacuum desiccator overnight and then stored in the coldroom at –24 °C.

### 3.3.4 Processing and extraction of bulk plant material

A total of 5.6 kg of plant material was oven dried (30 °C) and ground into small particles with hammer mill to give 3.7 kg of processed plant material. Part of the plant material (300 g) was used for optimisation of the extraction method. The remaining portion of the processed material was consecutively extracted with 3 volumes of EtOAc (15 L) over 3 days. The extraction solvent was filtered through a cheese cloth and then through a filter paper. The extract was concentrated under reduced pressure on the rotary evaporator at 60 °C and further dried in a vacuum desiccator for 96 h to remove all traces of solvent. The extraction yielded 48 g of brown gum (1.3% w/w of dry plant material).

### 3.3.5 Bioassay-guided fractionation and isolation of active compounds from the extract of *D. anomala*

A primary 3-cell line anticancer assay was employed in the bioactivity-guided isolation of compounds from the extract of *D. anomala*. In the initial step, the crude extract was separated by polarity by solvent partitioning (Section 3.3.5.1). Fractions showing anticancer activity comparable to that of the crude extract were then subjected to further fractionation by VLC, CC and FC.

#### *3.3.5.1 Solvent partitioning*

Solvent partitioning of the crude extract was used to pool fractions of various polarity ranges (Figure 3.2). The extract (1 g) was dissolved in 100 mL of aqueous methanol (MeOH/$H_2O$ 9:1 v/v) and extracted with hexane (3 x 100 mL). Hexane aliquots were separated with a separating funnel and combined. It was then dried over anhydrous $NaSO_4$, filtered through Whatman filter paper and concentrated under vacuum on a rotary evaporator (60 °C) to give a hexane-soluble fraction **(A)**. Methanol was removed from the remaining aqueous methanol layer under vacuum on a rotary evaporator, and the remaining solution was diluted to 100 mL with DI $H_2O$ and extracted with DCM (3 x 100 mL). The mixture was separated with a separating funnel into organic, aqueous and insoluble phases. The organic layers were combined and dried over anhydrous $Na_2SO_4$, filtered and concentrated under vacuum on a rotary evaporator to give a DCM-soluble fraction **(B)**. Traces of the organic solvent were removed from the remaining aqueous phase under vacuum on a rotary evaporator, after which it was lyophilised to give an $H_2O$-soluble fraction **(C)**. The insoluble phase was dried under vacuum on a rotary evaporator to give a MeOH-soluble fraction **(D)**.

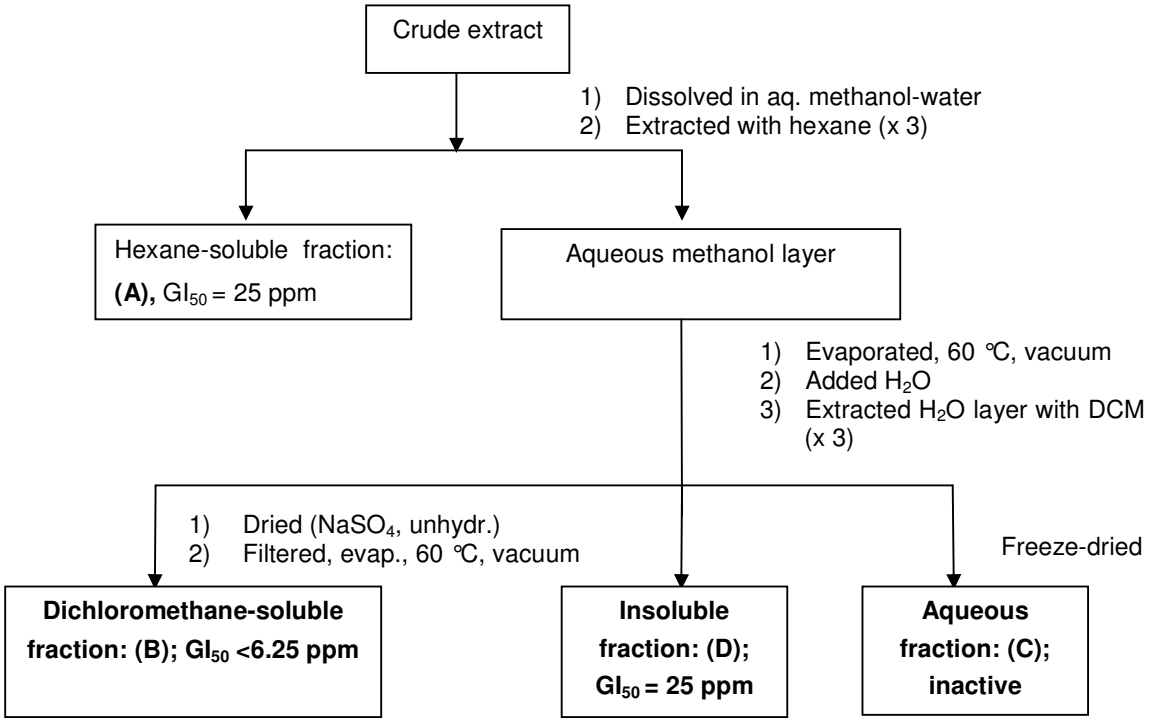


**Figure 3.2. Solvent partitioning method and $GI_{50}$ values (primary anticancer assay)**

*3.3.5.2 Vacuum liquid chromatography*

Large-scale purification of the DCM-soluble fraction **(B)** was done using VLC in batches of 5 – 10 g of extract on 400 – 500 g of $SiO_2$ 60 (0.063 – 0.2 mm) under reduced pressure, using EtoAc/Hexane/DCM/MeOH and Acetone/DCM/MeOH gradients. Pooled fractions were combined on the basis of similarity of chemical profile by TLC. Crude fractions A-L were concentrated in vacuum on the rotary evaporator and further dried in the vacuum desiccator for 48 h prior to bioassaying. The results are summarised in Table 3.5.

**Table 3.5. VLC solvent gradient and fractions collected. Bioassay: $LC_{50}$ (melanoma, renal, breast)**

| | EtOAc (parts) | Acetone (parts) | Hexane (parts) | DCM (parts) | MeOH (parts) | Total V (mL) | $LC_{50}$ (ppm) |
|---|---|---|---|---|---|---|---|
| Fraction A | 5 | - | 47.5 | 47.5 | - | 3 000 | >100 |
| Fraction B | | - | | | - | | >100 |
| Fraction C | 1 | - | 4.5 | 4.5 | - | 6 000 | 100 |
| **Fraction D** | | - | | | - | | 6.25 |
| **Fraction E** | | - | | | - | | <6.25 |
| **Fraction F** | 2 | - | 4 | 4 | - | 3 000 | 6.25 |
| **Fraction G** | 2 | - | - | 8 | - | 1 000 | 12.5 |
| **Fraction H** | - | 2 | - | 8 | - | 1 000 | 25 |
| Fraction I | - | 3 | - | 7 | - | 3 000 | 100 |
| Fraction J | - | 3 | - | 6.5 | 5 | 2 000 | >100 |
| Fraction K | - | 3 | - | 5 | 2 | 2 000 | >100 |
| Fraction L (wash) | - | 3 | - | 3 | 4 | 2 000 | 50 |

Fractions D-H, which showed $LC_{50}$ values of less than 25 ppm, were combined on the basis of similarity of the TLC profile and subjected to further column chromatography and bioassay-guided fractionation.

*3.3.5.3 Further bioassay-guided fractionation of semi-crude fractions D-H*

Fractions D-H were subjected to further CC and FC (Figure 3.3). The first, fractionation was performed using a 90 cm column packed with $SiO_2$60 and eluted with an EtOAc/Hexane/DCM/MeOH isocratic solvent mixture (9:45:45:1 v/v) to give fractions 3.3.5.4 A-N, which were tested for bioactivity. Final purification of the major compounds from the two most active fractions 3.3.5.3 ***F1*** and 3.3.5.3 ***H2*** was achieved by means of FC, using a 40 cm flash column, packed with flash silica gel and eluted with a Hexane/DCM/EtOAc/MeOH isocratic solvent mixture (45:45:9:1 v/v). The fractions were combined on the basis of similarity of the chemical composition determined by TLC analysis. Fractions 3.3.5.3 ***F1*** and 3.3.5.3 ***H2*** yielded pure compounds **2.14** and **4.3,** which exhibited increased biological activity in the primary anticancer bioassay. Detection: TLC plates ($SiO_2$ $F_{254}$, Merck) were developed in EtOAc/Hexane/DCM, 15:42.5:42.5 v/v, UV $\lambda_{max}$ = 352 nm, $R_f$ **(4.2)** = 0.38 and $R_f$ **(4.3)** = 0.64; HPLC-MS/UV, Method T3.2-3: $t_R$ **(4.2)**

= 15.55 min; UV $\lambda_{max}$ = 211, 242 nm; *m/z* 245.2 $[M+H]^+$ and $t_R$ **(4.3)** = 23.2 min; UV $\lambda_{max}$ = 215, 313 nm; *m/z* 485.2 $[M+H]^+$. Compound **4.2** was recrystallised from 2-propanol, to yield 400 mg of white orthorhombic crystals. Compound **4.3** was recrystallised from cold MeOH to yield 150 mg of yellow needle-like crystals.

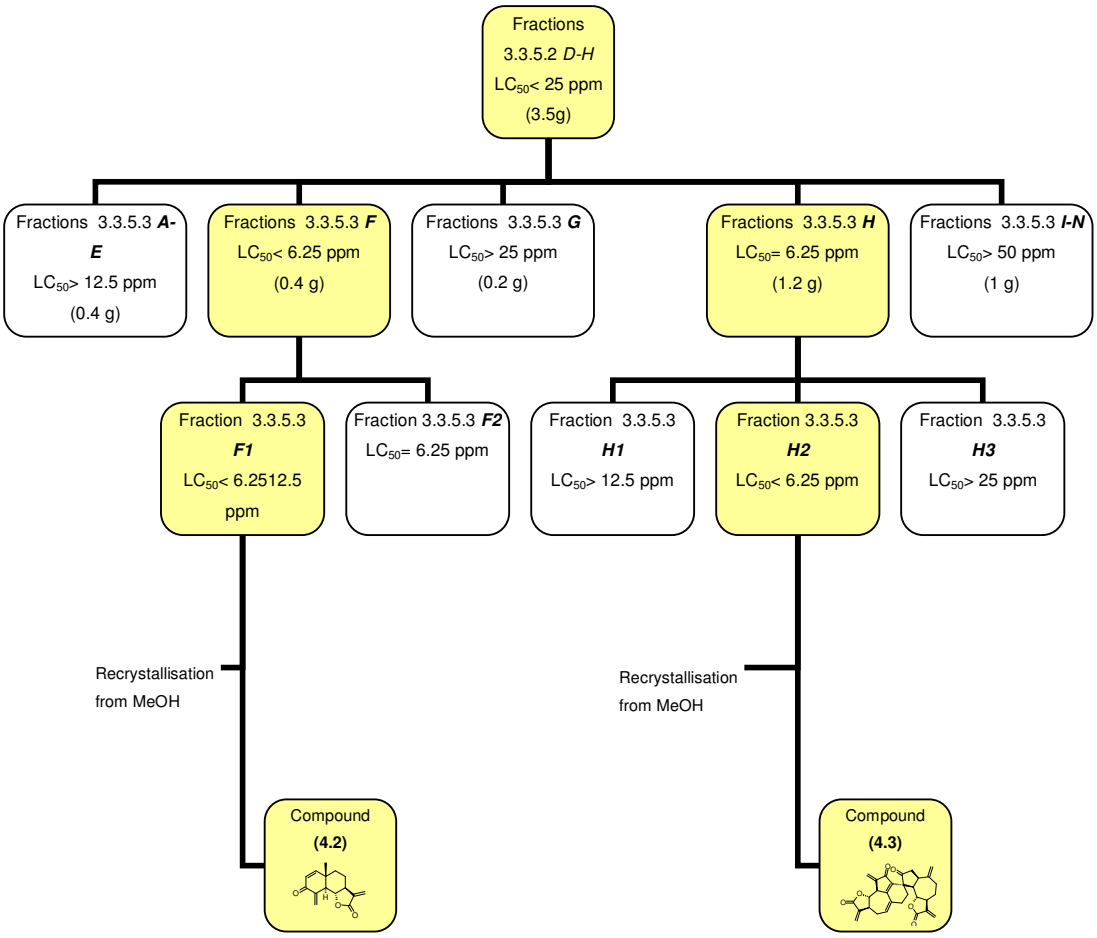


**Figure 3.3. Bioassay-guided isolation of compounds from extract of *D. anomala***

*3.3.5.4 Data of compound **4.2***

IUPAC: (3a*S*,5a*S*,9a*R*,9b*S*)-5a-methyl-3,9-dimethylidene-4,5,9a,9b-tetrahydro-3aH-naphtho[7,8-d]furan-2,8-dione

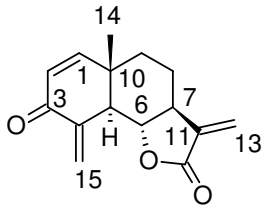


| | |
|---|---|
| Common name: | Dehydrobrachylaenolide |
| Yield: | 400 mg (0.013% w/w of dry plant material) |
| Molecular formula: | $C_{15}H_{16}O_3$ |
| ESI-MS, m/z: | 245.2 $[M+H]^+$ |
| Melting point: | 223-224 °C (lit.[52] mp 225 °C) |
| Optical rotation: | $[\alpha]^{24}_D$ +68 °(*c*= 0.50, $CHCl_3$); (lit. [53] $[\alpha]^{24}_D$ +67.9 °, *c*= 0.16, $CHCl_3$) |
| UV, $\lambda_{max}$ (nm): | 209; 244 |
| $^1$H NMR (400 MHz, $CDCl_3$), $\delta_H$ : | 1.02 (3H, s, H-14); 1.67 (2H, m, Ha-8, Ha-9); 1.81 (1H, m, Hb-9); 2.1 (1H, m, Hb-8); 2.6 (1H, ddddd, J = 3.0; 3.0; 3.2; 10.8; 11.0 Hz, H-7); 2.98 (1H, ddd, J = 2.2; 2.3; 10.9 Hz, H-5); 4.07 (1H, t, J = 10.7; Hz, H-6); 5.43 (1H, d, J = 3.1 Hz, Ha-13); 5.68 (1H, ddd, J = 0.9; 1.0; 2.4 Hz, Ha-15), 5.99 (1H, d, J = 9.9 Hz, H-2); 6.1 (1H, d, J = 3.2 Hz, Hb-13); 6.24 (1H, dd, J = 1.0; 2.2 Hz, Hb-15); 6.76 (1H, d, J = 10.0 Hz, H-1). |
| $^{13}$C NMR : | Refer to Table 4.2 (Section *4.4.1.1*) |
| Antiplasmodial activity (D10); (K1), (µg/mL): | $IC_{50}$= 0.38; 0.06 |
| Anticancer activity (µg/mL): | $GI_{50}$= 0.67 |
| Cytotoxicity (CHO) (µg/mL): | $IC_{50}$= 4.2; SI (D10)= 11; SI (K1)= 70. |

[52] Bohlmann F., Zdero C. (1982). *Phytochemistry*, **21**, 647-651.
[53] Higuchi Y., Shimota F., Koyanagi R., Suda K., Mitsui T., Kataoka T., Nagai K., Ando M. (2003). *Journal of Natural Products*, **66**, 588-594.

*3.3.5.5 Data of compound **4.3***

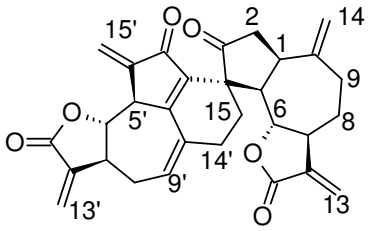


| | |
|---|---|
| Molecular formula: | $C_{30}H_{28}O_6$ |
| ESI-MS, m/z: | 485.2 $[M+H]^+$ |
| UV, $\lambda_{max}$ (nm): | 218; 312 |
| Melting point: | 170 °C melting followed by charring |
| Optical rotation: | $[\alpha]^{24}_D$ +56° (*c*= 0.50, $CHCl_3$) |
| $^1$H NMR (400 MHz, $CDCl_3$) $\delta_H$: | 1.48 (1H, m, Ha-8); 1.88 (1H, dt, J = 6.0; 10.6 Hz, Ha-15); 2.21 (1H, m, Ha-9); 2.24 (1H, m, Hb-15); 2.29 (1H, m, Ha-14'); 2.33 (1H, m, Hb-8); 2.58 (1H, m, Hb-9); 2.63 (1H, m, Hb-14'); 2.68 (1H, br d, J = 18.8 Hz, Ha-2); 2.27-2.82 (2H, m, H-8'); 3.01 (1H, m, H-7); 3.04 (1H, m, H-7'); 3.2 (1H, br d, J = 9.2 Hz, H-1); 3.28 (1H, dd, J = 9.2, 10.0 Hz, H-5); 3.36 (1H, dd, J = 3.1; 18.5 Hz, Hb-2); 3.73 (1H, br d, J = 10.9 Hz, H-5'); 4.03 (1H, dd, J = 9.5; 10.9 Hz, H-6'); 4.18 (1H, dd, J = 9.0, 10.0 Hz, H-6); 4.68 (1H, br s, Ha-14); 5.03 (1H, br s, Hb-14); 5.52 (1H, d, J = 3.0 Hz, Ha-13'); 5.53 (1H, d, J = 3.0 Hz, Ha-13); 5.98 (1H, m, H-9'); 6.06 (1H, d, J = 1.0 Hz, Hb-13); 6.11 (1H, t, J = 1.0, Ha-15'); 6.22 (1H, dd, J = 1.0; 1.7 Hz, Hb-15'); 6.24 (1H, d, J = 1.0 Hz, Hb-13'). |
| $^{13}$C NMR : | Refer to Table 4.3 (Section 4.4.2), |
| Antiplasmodial activity (D10); (µg/mL): | $IC_{50}$= 0.46. |
| Anticancer activity (µg/mL): | $GI_{50}$= 0.75. |
| Cytotoxicity (CHO) (µg/mL); SI | $IC_{50}$= 0.68, SI (D10) = 1.5. |

#### *3.3.5.6 Targeted isolation of compound **4.2** from the organic extract of Brachylaena transvaalensis*

The detannified MeOH:DCM extract of roots of *B. transvaalensis* was obtained from the CSIR's Bioprospecting extract repository. Presence of the compound **4.2** in the extract was established by means of HPLC-UV/MS analysis (method T3.1-3; $t_R$ = 25.4 min; UV $\lambda_{max}$ = 211, 242 nm; *m/z* 245.2 $[M+H]^+$). The sequence of solvent partitioning and chromatographic purifications (Section 3.3.6) was employed to purify DHB **(4.2)** from 1 g of the MeOH/DCM extract of *B. transvaalensis*. Compound **4.2,** isolated from *D. anomala* subsp. *gerrardii*, was used for the TLC analysis ($SiO_2$ $F_{254}$ plates, Merck) as a reference to guide the purification ($R_f$ = 0.38 in EtOAc/Hexane/DCM, 15:42.5:42.5 v/v; detection UV $\lambda_{max}$ = 352 nm). Recrystallisation of the fraction, equivalent to 3.3.5.3 ***F1*** from 2-propanol, produced 5 mg of pure compound **4.2** in 0.001% yield (w/w dry plant material). The authenticity of the structure was confirmed by $^1$H NMR analysis and the value of the optical rotation ($[\alpha]^{24}_D$ +67.9°; *c* = 0.2, $CHCl_3$).

#### *3.3.5.7 HPLC analysis of root extract of D. anomala subsp. anomala for the presence of DHB*

An ethyl acetate extract of *D. anomala* subsp. *anomala* collected from Mpumalanga was subjected to solvent partitioning. The dichloromethane soluble fraction (B) was analysed by LC-UV, using compound **4.2**, isolated from *D. anomala* subsp. *gerrardii,* as a standard (method: T3.1-2; $t_R$ **(4.2)** = 19.65 min; UV $\lambda_{max}$ = 211, 242 nm). The UV $\lambda_{max}$ chromatogram revealed that dehydrobrachylaenolide **(4.2)** was not present in the extract of *D. anomala* subsp. *anomala*

## 3.4 Preparation of sesquiterpene derivatives (Chapter 5)

### 3.4.1 Data for (6*β*)-3-oxoeudesm-1,4,11-trien-6,12-olide **(5.17)**

The compound was obtained from the Discovery Chemistry Group. Detection: TLC plates ($SiO_2$ $F_{254}$, Merck) were developed with EtOAc/hexane/DCM (15:42.5:42.5 v/v) as the mobile phase, then sprayed with 15% vanillin/$H_2SO_4$ reagent and baked in the oven for 5 min at 120 °C, $R_f$ **(5.17)** = 0.38; LC-UV (Method: T3.2-2), $t_R$ **(5.17)** = 23.67 min.

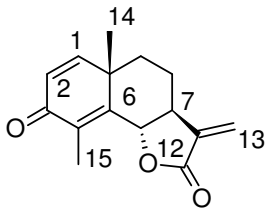


**(5.17)**

| | |
|---|---|
| Molecular formula: | $C_{15}H_{16}O_3$ |
| $^1$H NMR (400 MHz, $CDCl_3$), $\delta_H$: | 1.27 (3H, s, H-14); 1.55 (1H, m, Ha-9); 1.72 (1H, m, Ha-8); 1.9 (1H, m, Hb-9); 2.12 (3H, d, J = 0.5 Hz, H-15); 2.65 (1H, m, H-7); 4.72 (1H, dd, J = 0.5, 12.0 Hz, H-6); 5.5 (1H, d, J = 3.1 Hz, Ha-13); 6.19 (1H, d, J = 3.1 Hz, Hb-13); 6.2 (1H, d, J = 9.6 Hz, H-1); 6.66 (1H, d, J = 9.6 Hz, H-2). |
| $^{13}$C NMR: | Refer to Table 5.1 (Section 5.2) |
| Antiplasmodial activity (D10); (K1), (µg/mL): | $IC_{50}$ = 2.82; 2.21 |
| Anticancer activity (µg/mL): | $GI_{50}$ = 1.3 |
| Cytotoxicity (CHO) (µg/mL); SI(D10); SI(K1): | $IC_{50}$ = 1.71; SI (D10) = 0.6; SI(K1) = 0.78 |

### 3.4.2 General procedure for preparation of amino-acid adducts of compound **5.17**

Previously published methods were used for the preparation of the Michael-type adducts of sesquiterpene lactones (STLs) with amino-acids.[54,55] The corresponding sesquiterpene lactone (15 mg, 0.04 mmol) was dissolved in 5 drops of acetone and added to 1 mL of phosphate buffer of pH 7.4 (Sigma-Aldrich). The mixture was sonicated for 30 min to degas, and an equimolar amount of amino acid was added. The reaction was monitored by TLC for 24 h. The solvent was removed by azeotropic evaporation on the rotary evaporator using MeOH, alternatively, physical data were acquired on the supernatant of the reaction

[54] Heilmann J., Wasescha M. R., Schmidt T. J. (2001). *Bioorganic & Medicinal Chemistry*, **9**, 2189–2194.
[55] Schmidt T. J. (1997). *Bioorganic & Medicinal Chemistry*, **5**, 645–653.

mixture. Detection: TLC (cellulose $F_{254}$, Fluka); n-BuOH/$H_2O$/acetic acid (5:4:1 v/v) as the mobile phase; ninhydrin (0.25% ninhydrin in acetone) or anisaldehyde-spray reagent (10 mL acetic acid conc., 85% MeOH, 5 mL of $H_2SO_4$ conc., 0.5 mL anisaldehyde); the plate was sprayed and heated to 100 – 110 °C).

### *3.4.2.1 Reactivity of compound **5.17** towards L-cysteine at physiological pH*

The general method described in Section 3.4.2 was used to prepare an *L*-cystein adduct of compound **5.17**. Compound **5.17** and *L*-cysteine were used in equimolar amounts (0.04 mmol). The solvent was evaporated by letting the reaction mixture to stand open to air. Two major products were detected in the reaction mixture (NMR 400 MHz, $D_2O$). The structures were assigned on the bases of MS and NMR data. Detection: $R_f$ **(5.28b)** = 0.25; TLC (cellulose $F_{254}$, Fluka); n-BuOH/$H_2O$/acetic acid (5:4:1 v/v) as the mobile phase; ninhydrin spray reagent. The second product was not detected by the TLC analysis of the reaction mixture, as it is probably an artefact.

### *3.4.2.2 Data of compound **5.28a***

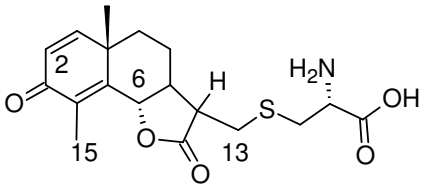


| | |
|---|---|
| Molecular formula | $C_{18}H_{23}NO_5S$ |
| UV, $\lambda_{max}$ (nm): | 243.9 |
| ESI-MS, m/z: | 366.3 $[M+H]^+$ |
| $^1H$ NMR (400 MHz, $D_2O$), $\delta_H$: | 1.33 (1H, m, Ha-9); 1.43 (3H, s, H-14); 1.57 (1H, m, Hb-9); 1.97 (1H, m, Ha-8); 2.13 (3H, d, J = 0.5 Hz, H-15); 2.26 (1H, m, Hb-8); 2.37 (1H, m, H-7); 2.8 (1H, m, Ha-13); 3.28-3.46 (2H, m, Cys-$\beta CH_2$); 3.37 (1H, m, H-11); 3.1 (1H, m, |

Hb-13); 4.2 (1H, dd, J = 3.9; 8.3 Hz, Cys-αCH); 5.26 (1H, d, J = 11.2 Hz, H-6); 6.36 (1H, H-2)[56]; 7.14 (1H, H-1).[56]

$^{13}$C NMR: Refer to Table 5.3 (Section 5.3.2)

### *3.4.2.3 Data of compound **5.28b***

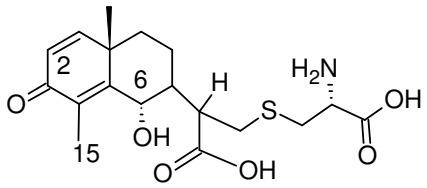


Molecular formula: $C_{18}H_{25}NO_6S$

Calculated mass: 368.4247

$^1$H NMR (400 MHz, $D_2O$), $\delta_H$: 1.36 (1H, m, Ha-8); 1.43 (3H, s, H-14); 2.13 (3H, d, J = 0.5 Hz, H-15); 1.97 (2H, m, Hb-8, Ha-9); 2.11 (1H, m, Hb-9); 2.26 (3H, d, Hz, H-15); 2.36 (1H, m, H-7); 2.8-2.82 (2H, m, H-13); 3.1 (1H, m, Hb-13); 3.28-3.46 (2H, m, Cys-$\beta CH_2$); 3.53 (1H, m, H-11); 4.2 (1H, dd, J = 3.9; 8.3 Hz, Cys-$\alpha$C-H); 4.74 (1H, H-6)[56]; 6.4 (1H, H-1)[56]; 7.15 (1H, H-1).[56]

$^{13}$C NMR: Refer to Table 5.4 (Section 5.3.2)

### *3.4.2.4 Addition of N-acetyl-L-cysteine to compound **5.17** at physiological pH*

The general method described in Section 3.4.2 was used to prepare an *N*-acetyl-*L*-cysteine adduct of compound **5.17**. Compound **5.17** and *N*-acetyl-*L*-cysteine were used in equimolar amounts (0.04 mmol). The solvent was evaporated by letting the reaction mixture to stand open to air. Physical data were acquired on the supernatant of the reaction mixture suspended in the deuterium oxide. Two products were identified in the reaction mixture (NMR, 400 MHz, $D_2O$). The structural assignments were deduced only for the major product **(5.29)**, and a structure of the probable minor product was proposed in Section 5.3.3. The

[56] $\delta$ determined from HSQC

structure was deduced from the MS and the NMR data (Table 5.5). Detection: TLC plates (cellulose $F_{254}$, Fluka), developed with n-BuOH/$H_2O$/acetic acid (5:4:1 v/v) as the mobile phase, and then sprayed with anisaldehyde reagent and baked in the oven for 5 min at 120 °C, $R_f$ **(5.32)** = 0.30; $t_R$ = 20.92 min, LC-UV (Method: T3.2-2). The second product was not detected by the TLC analysis of the reaction mixture, as it is probably an artefact.

### *3.4.2.5 Data of NAC adduct **5.32***

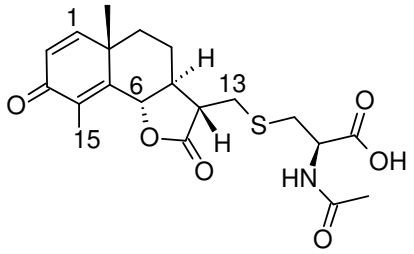


| | |
|---|---|
| Yield: | 56.5% (by HPLC-UV) |
| Molecular formula | $C_{22}H_{29}NO_5S$ |
| UV, $\lambda_{max}$ (nm): | 242.9 |
| EI-MS | m/z 408.2 $[M+H]^+$ |
| $^1$H NMR (400 MHz, $D_2O$), $\delta_H$: | 1.2 (3H, s, H-14); 1.38 (1H, m, Ha-8); 1.88 (2H, m, Ha-9, Hb-8); 1.92 (3H, s, CO-$CH_3$); 1.93 (3H, s, H-15); 1.95 (1H, m, H*α*-7); 2.1 (1H, m, Ha-9); 2.58 (1H, td, J = 3.1; 8.2; 10.1 Hz, H*β*-11); 2.75 (1H, dd, J =8.2; 13.6 Hz, Hb-13); 2.85 (1H, dd, J = 9.0; 14.0 Hz, Cys-*β*C-Hb); 2.95 (1H, dd, J = 3.1; 13.6 Hz, Ha-13); 3.14 (1H, dd, Cys-*β*C-Ha), 4.37 (1H, dd, J = 4.3; 9.0 Hz, Cys-*α*H); 5.05 (1H, dd, J = 1.2; 11.3 Hz, H*β*-6); 6.2 (1H, d, J = 9.7 Hz, H-2); 6.9 (1H, d, J = 9.7 Hz, H-1). |
| $^{13}$C NMR: | Refer to Table 5.5, Section 5.3.3 |

### *3.4.2.6 Addition of glutathione to compound **5.17** at physiological pH*

The general method described in Section 3.4.2 was used to prepare a glutathione adduct of compound **5.17**. Compound **5.17** and glutathione were used in equimolar amounts (0.04 mmol). The solvent was evaporated by letting the

reaction mixture to stand open to air. Physical data were acquired on the supernatant of the reaction mixture suspended in the deuterium oxide. Two products were identified in the reaction mixture (NMR, 400 MHz, in $D_2O$). The structural assignments were deduced only for the major product **(5.33)**, and a structure of the probable minor product was proposed in Section 5.3.4. The structure was deduced on the basis of the $^1H$ NMR data (Table 5.6). Detection: TLC plates (cellulose $F_{254}$, Fluka) were developed with n-BuOH/$H_2O$/acetic acid (5:4:1 v/v) as the mobile phase, then sprayed with ninhydrin reagent and baked in the oven for 5 min at 120 °C, $R_f$ **(5.33)** = 0.49; LC-UV (Method: 3.1.5), $t_R$ **(5.33)** = 21.07 min.

### *3.4.2.7 Data of glutathione adduct **5.33***

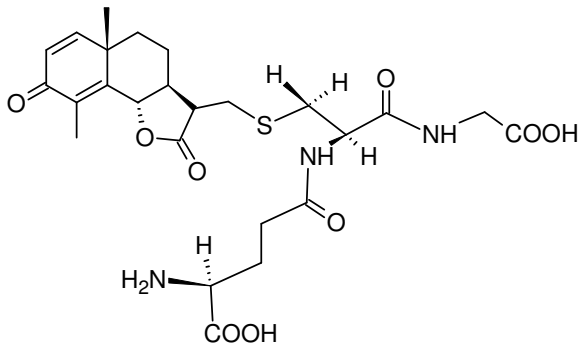


| | |
|---|---|
| Yield: | 44% (HPLC-UV: Method 3.1.5) |
| Molecular formula | $C_{25}H_{33}N_3O_9S$ |
| $^1H$ NMR (400 MHz, $D_2O$), $\delta_H$: | 1.2 (3H, s, H-14); 1.38 (1H, m, Ha-8); 1.88 (2H, m, Hb-8, Ha-9); 1.93 (3H, d, J = 1.2 Hz, H-15); 1.95 (1H, m, H-7); 2.04 (2H, m, Glu-$\beta CH_2$); 2.1 (1H, m, Ha-9); 2.42 (2H, m, Glu-$\gamma CH_2$); 2.62 (1H, td, J = 3.1; 8.2; 10.1 Hz, H$\beta$-11); 2.79 (1H, q, J = 9.0; 14.0 Hz, Cys-$\beta$C-Hb); 2.89 (2H, ddd, J = 3.1; 8.2; 13.6 Hz, H-13); 3.18 (1H, q, J = 5.1; 14.0 Hz, Cys-$\beta$C-Ha); 3.64 (1H, m, Gly-$\alpha$C-Hb); 3.76 (1H, m, Glu-$\alpha$C-H); 3.88 (1H, m, Hz, Gly-$\alpha$C-Ha); 4.45 (1H, dd, J = 5.1; 9.0 Hz, Cys-$\alpha$C-H); 5.02 (1H, dd, J = 1.2; 11.3 Hz, H$\beta$-6); 6.18 (1H, d, J = 10.1 Hz, H-2); 6.95 (1H, d, J = 10.1 Hz, H-1). |

### 3.4.3 Reactivity of compound **4.2** towards *L*-cysteine using basic conditions

Compound 4.2 (5 mg, 13 µmol) was suspended in $D_2O$ and sonicated for 30 min. Cysteine (5 mg, 41 µmol) and $EtN_3$ (0.2 mL) were added, and the reaction was left stirring for 48 h at RT. The solvent was reduced by azeotropic evaporation *via* the addition of methanol. The product was purified on the preparative Agilent 1200 HPLC system, $t_R$ = 15.2 min (Method T3.3). The structure was deduced on the basis of $^1$H NMR and $^{13}$C NMR data. Detection: LC-UV (Method: 3.1.3), $t_R$ **(5.27)** = 14.62 min.

#### *3.4.3.1 Data of compound **5.27***

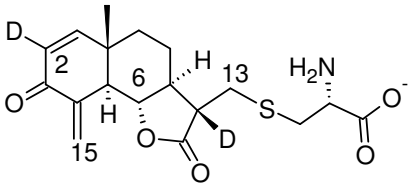


| | |
|---|---|
| Yield: | 6.5 mg (88.5% after prep. HPLC) |
| Molecular formula: | $C_{18}D_2H_{23}NO_6S$ |
| ESI-MS, m/z: | 384.3 $[M+H]^+$ |
| UV, $\lambda_{max}$ (nm): | 258.9 |
| $^1$H NMR (400 Hz, $D_2O$), $\delta_H$: | 0.93 (3H, s, H-14); 1.6 (2H, m, Ha-8, Hb-9); 1.45 (1H, m, Ha-9); 1.74 (1H, m, H-7); 2.52 (1H, br td, J = 1.0; 2.0; 10.3 Hz, H-5); 2.74 (1H, d, J = 12.0 Hz, Ha-13); 2.86 (1H, d, J = 12.0 Hz, Hb-13); 2.95 (1H, dd, J = 8.3; 15.2 Hz, Cys-*β*C-Ha); 3.09 (1H, dd, J = 3.9; 15.2 Hz, Cys-*β*C-Hb); 3.8 (1H, dd, J = 4.4; 8.3 Hz, Cys-*α*C-H); 3.84 (1H, dd, J = 10.3; 10.3 Hz, H*β*-6); 5.5 (1H, d, J = 2.0 Hz, Ha-15); 5.99 (1H, d, J = 1.0 Hz, Hb-15); 7.0 (1H, s, H-1) |
| $^{13}$C NMR: | Refer to Table 5.2 (Section 5.3.1) |

### 3.4.4 General procedure for reduction of sesquiterpene lactones with $NaBH_4$

The previously described method for $NaBH_4$ reduction of STLs was employed.[57] 15 mg (0.06 mmol) of a sesquiterpene lactone was dissolved in anhydrous ethanol (10 mL). The solution was cooled to 0 ºC, and $NaBH_4$ (78 mg, 2 mmol) was added. The mixture was stirred at 0 ºC for 10 min, after which 20% acetic acid (10 mL) was added to quench the reaction. The solution was diluted further with water (20 mL) and extracted twice with $CHCl_3$ (2 x 50 mL). The organic layers were combined, dried over anhydrous $Na_2SO_4$ and concentrated under vacuum on a rotary evaporator to afford brown gum.

#### *3.4.4.1 Stereoselective reduction of compound **5.17***

The reduction of compound **5.17** was performed by using the general method described in Section 3.4.3. The main product was purified by flash silica gel chromatography using EtOAc/Hexane (3:7 v/v), to afford 13.5 mg of a pale yellow solid (total yield = 90%). The structure was identified as *α*-santonin, on the basis of the EI-MS data (NIST 2005 Mass spectral database search, ThermaBeam TMD system, Waters) and NMR data and comparison with the published data.[58] Detection: TLC plates ($SiO_2$ $F_{254}$, Merck) were developed using EtOAc/Hexane/DCM (15:42.5:42.5 v/v) as the mobile phase, then sprayed with vanillin reagent and baked in the oven for 5 min at 120 ºC, $R_f$ **(5.36)** = 0.35.

#### *3.4.4.2 Data of reduction product **5.36***

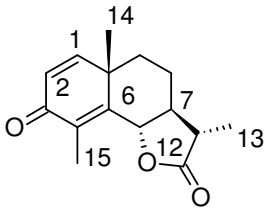


| | |
|---|---|
| Common name: | α-Santonin |
| Yield: | 13.5 mg (90% after CC) |
| Molecular formula: | $C_{15}H_{18}O_3$ |
| ESI-MS, m/z: | 246.2; 264.1 |

[57] Irwin M. A., Lee K. H., Simpson R. F., Geissman T. A. (1969). *Phytochemistry*, **8**, 2009–2012.
[58] Colomobo M. I., Testero S. A., Pellegrinet S. C., Bohn M. L., Rúveda E. A. (2001). *The Chemical Educator*, **6**, 350–352.

| | |
|---|---|
| UV, $\lambda_{max}$ (nm): | 246.4 |
| $^{1}$H NMR (400 Hz, $CDCl_3$), $\delta_H$: | 1.23 (3H, d, J = 6.9 Hz, H-13); 1.28 (3H, s, H-14); 1.44-2.07 (5H, m, H-7, H*α*-8, H*β*-8, H*α*-9, H*β*-9); 2.1 (3H, d, J = 1.3 Hz, H-15); 2.38 (1H, dq, J = 6.9, 11.7 Hz, H-11); 4.77 (1H, dq, J= 1.3, 10.9 Hz, H-6); 6.21 (1H, d, J = 9.9 Hz, H-2); 6.62 (1H, d, J = 9.9 Hz, H-1). |
| $^{13}$C NMR: | Table 5.7 (Section 5.4.1) |
| Antiplasmodial activity (D10); (K1), (µg/mL) | $IC_{50}$ = 8.34; 42.76 |
| Cytotoxicity (CHO) (µg/mL); SI(D10); SI(K1): | $IC_{50}$ = 88.31; SI (D10) = 11; SI (K1) = 2.1 |

#### *3.4.4.3 Reduction of compound **4.2***

The compound **4.2** was reduced using the general method described in Section 3.4.3. The reaction mixture was analysed by TLC: purple spot $R_f$ = 0.68 and blue spot $R_f$ = 0.75, TLC ($SiO_2$ $F_{254}$, Merck); EtOAc/Hexane/DCM (15:42.5:42.5 v/v); 15% vanillin/$H_2SO_4$ spray reagent. The mixture of products was further analysed by LC-ESEI-MS and 5 peaks were observed in the UV chromatogram [$t_R$ = 21.438 (m/z 246.2); 21.717 (m/z 248.2); 22.017 (m/z 248.3); 22.296 (m/z 250.30); 23.020 min (m/z 244.2, 264.2)]. No additional physical data were obtained due to the difficulty of separating the components.

## 3.5 Preparation of pro-drugs (Chapter 6)

### 3.5.1 The OSIRIS Property Explorer

The OSIRIS Property Explorer was used to calculate “on-the-fly” drug-relevant properties for chemical structures. The results allow prediction of properties with high risks of undesired effects such as mutagenicity or poor intestinal absorption. Lipinski's Rule of Five is a “rule of thumb” to evaluate drug-likeness, or to determine whether a chemical compound with a certain pharmacological or biological activity has properties that would make it a likely orally active drug in

humans. The rule is based on the calculated parameters, which contribute to the overall score of drug-likeness.[59,60]

### 3.5.2 General procedure for preparation of Michael adducts of STLs with $Et_2NH$.[61]

A mixture of sesquiterpene lactone (15 mg, 60 μM) and diethylamine (30 mg) in anhydrous EtOH (9 mL) was treated with $Et_3N$ and refluxed at 150 °C overnight. The ethanol and volatile di- and triethyl amines were then evaporated under vacuum on a rotary evaporator. The resulting residue was chromatographed over silica gel, using a DCM/MeOH (97:3 v/v) solvent mixture as the mobile phase. The structures were determined on the basis of MS and NMR data. Detection: TLC plates ($SiO_2$ $F_{254}$, Merck) were developed with DCM/MeOH (24:1 v/v) as the mobile phase, then sprayed with vanillin spray-reagent and heated in the oven at 120 °C; LC-MS (Method T3.2-1). Retention factors and retention times for products **6.6**, **6.7**, **6.8**, **6.9** and **6.10** are discussed in Chapter 6.

#### *3.5.2.1 Data of diethylamine derivative of parthenolide **(6.6)***

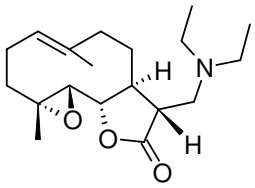


| | |
|---|---|
| Yield: | 10.9 mg (55% after CC) |
| Molecular formula: | $C_{19}H_{31}NO_3$ |
| $^1$H NMR (400 MHz, acetone-$d_6$), $\delta_H$: | 1.01 (6H, t, J =7.0 Hz, H-17); 1.16 (1H, m, Ha-3); 1.25 (3H, s, H-15); 1.75 (3H, s, H-14); 2.04 (1H, m, Hb-3); 2.12 (1H, m, Ha-2); 2.0-2.18 (2H, m, H-8); 2.19 (2H, m, H-9); 2.3-2.4 (1H, m, H-7); 2.42 (1H, m, Hb-2); 2.49 (1H, td, H-11); 2.42-2.52 (2H, m, $CH_3$-$CH_2$-N-); 2.73 (1H, dd, J = 5.5; |

[59] Lipinski C. A., Lombardo F., Dominy B. W., Feeney P. J. (1997). *Advanced Drug Delivery Reviews,* **23**, 3–25.
[60] http://www.organic-chemistry.org/prog/peo/. Accessed on 4 December 2008.
[61] Crooks P. A. Jordan C. T.; Wei X. (2007). Use of parthenolide derivatives as antileukemic and cytotoxic agents, US 7,312,242 B2.

| | |
|---|---|
| | 14.0 Hz, Ha-13); 2.74 (1H, d, J = 8.6 Hz, H-5); 2.78 (1H, dd, J = 4.7; 14.0, H-b-13); 3.89 (1H, t, J = 8.6; 9.2 Hz, H-6); 5.26 (1H, dd, J = 2.3; 12.1 Hz, H-1) |
| $^{13}$C NMR: | Refer to Table 6.2 (Section 6.3.1) |
| Antiplasmodial activity (D10), (K1), (µg/mL): | $IC_{50}$ = 4.27; 6.95 |
| Anticancer activity (µg/mL): | $GI_{50}$ = 1.11 |
| Cytotoxicity (CHO) (µg/mL): | $IC_{50}$ = 0.75, SI (D10) = 0.2 |

*3.5.2.2 Data of (11α)-diethylamine-3-oxoeudesma-1(2),4(15),11(13)-dien-12-olide **(6.7)***

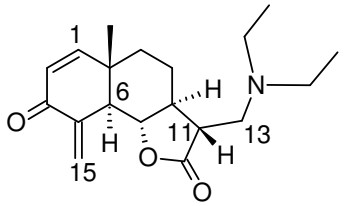


| | |
|---|---|
| Yield: | 5.2 mg (27% after CC) |
| EI-MS: | 318.0 $[M+H]^+$ |
| UV, $\lambda_{max}$ (nm): | 241.6 |
| Molecular formula | $C_{19}H_{27}NO_3$ |
| ESI-MS, m/z | 318.0 $[M+H]^+$ |
| $^1$H-NMR (400 MHz, acetone-$d_6$), $\delta_H$: | 1.04 (6H, t, J =7.0 Hz, *$CH_3$*-$CH_2$-N-); 1.05 (3H, s, H-14), 1.75-1.85 (2H, m, H-9); 1.98 (1H, m, H-7); 2.05-2.25 (2H, m, Ha,b-8); 2.48 (1H, dd, J = 8.2; 12.9 Hz, Ha-13); 2.4-2.67 (2H, m, J = 7.0; 14.0 Hz, -N-*$CH_2$*-$CH_3$); 2.68 (1H, ddd, J = 3.9; 8.2; 10.3 Hz, H-11); 2.83 (1H, dd, J = 3.9; 12.9 Hz, Hb-13); 2.96 (1H, dt, J = 2.4; 10.9 Hz, H-5); 4.40 (1H, t, J = 10.9 Hz, H-6); 5.51 (1H, ddd, J = 0.8; 1.6; 2.4 Hz, Ha-15); 5.95 (1H, dd, J = 0.8; 9.8 Hz, H-2); 6.04 (1H, dd, J = 1.5; 1.6 Hz, Hb-15); 6.97 (1H, d, J = 9.8 Hz, H-1). |
| $^{13}$C NMR | Refer to Table 6.3 (Section 6.3.2.1) |

| | |
|---|---|
| Antiplasmodial activity (D10); (K1), (µg/mL): | $IC_{50}$ = 1.29; 2.88 |
| Anticancer activity (µg/mL): | $GI_{50}$ = 1.3 |
| Cytotoxicity (CHO) (µg/mL): | $IC_{50}$ = 4.66, SI (D10)= 3.6 |

*3.5.2.3 Structure of ethyl (6α)-hydoxy-3-oxoeudesma-1(2),4(15),11(13)-trien-12-oate **(6.8)***

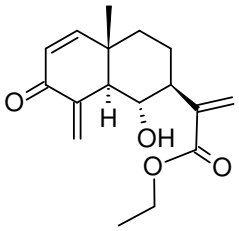


| | |
|---|---|
| Yield: | 3 mg (18% after CC) |
| Molecular formula: | $C_{17}H_{22}O_4$ |
| Calculated MW, (g/mol): | 290.3541 |
| $^1$H NMR (400 MHz, $CDCl_3$), $\delta_H$: | 1.06 (3H, s, H-14); 1.29 (3H, t, J = 7.4 Hz, *$CH_3$*-$CH_2$-O-); 1.59-1.90 (4H, m, 2H-8, 2H-9); 2.53 (1H, m, H-7); 4.07 (1H, dd, J = 1.2, 10.1 Hz, H-6); 4.21 (2H, q, J = 7.4 Hz, $CH_3$-*$CH_2$*-O-); 5.6 (1H, d, J = 1.2 Hz, Ha-15); 5.77 (1H, s, Hb-13); 5.96 (1H, d, J = 9.9 Hz, H-2); 6.1 (1H, d, J = 1.2 Hz, Hb-15); 6.29 (1H, d, J = 0.8 Hz, Hb-13); 6.73 (1H, d, J = 9.9 Hz, H-1). |

*3.5.2.4 Data of 11α-diethylamine-3-oxoeudesma-1(2),4(5),11(13)-dien-12-olide **(6.9)***

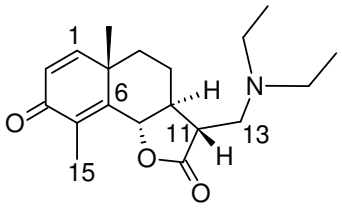


| | |
|---|---|
| Yield: | 5.6 mg (29% after CC) |
| ESI-MS, m/z: | 318.2 $[M+H]^+$ |
| UV, $\lambda_{max}$ (nm): | 241.2 |

| | |
|---|---|
| Molecular formula: | $C_{19}H_{27}NO_3$ |
| $^1$H NMR (400 MHz, acetone-$d_6$), $\delta_H$: | 0.96 (6H, t, J =7.0 Hz, *$CH_3$*-$CH_2$-N-); 1.25 (3H, s, H-14); 1.48 (1H, m, Ha-9); 1.66 (1H, m, Ha-8); 1.82 (1H, m, Hb-9); 1.95 (1H, m, H-7); 2.09 (3H, d, J =1.2 Hz, 3H-15); 2.4-2.54 (2H, m, J = 7.0; 13.7 Hz, $CH_3$-*$CH_2$*-N-); 2.53 (1H, ddd, J = 4.3; 8.6; J = 12.9 Hz, H-11); 2.59 (1H, dd, J = 4.3; 13.26 Hz, Ha-13); 2.89 (1H, dd, J = 8.6; 10.1 Hz, Hb-13); 4.73 (1H, dd, J = 1.2; 11.3 Hz, H-6); 6.21 (1H, d, J = 10.0 Hz, H-2); 6.64 (1H, d, J = 10.0 Hz, H-1) |
| $^{13}$C NMR: | Refer to Table 6.4a (Section 6.3.3.1) |
| Antiplasmodial activity (D10); (K1), (µg/mL): | $IC_{50}$ = 8.93; 19.91 |
| Anticancer activity (µg/mL): | $GI_{50}$ = 22.2 |
| Cytotoxicity (CHO) (µg/mL): | $IC_{50}$ = 28.31, SI (D10)= 3.2 |

### *3.5.2.5 Data of ethyl 6α-hydroxy-3-oxoeudesma-1(2),4(5),11(13)-trien-12-oate* ***(6.10)***

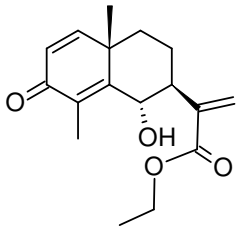


| | |
|---|---|
| Yield: | 2.0 mg (12% after CC) |
| Molecular formula: | $C_{17}H_{22}O_4$ |
| Calculated MW, (g/mol): | 290.3541 |
| $^1$H NMR (400 MHz, acetone-$d_6$), $\delta_H$: | 1.29 (3H, s, H-14); 1.3 (3H, t, J = 7.0 Hz, *$CH_3$*-$CH_2$-O-); 1.78 (1H, m, Ha-8); 2.05 (1H, m, Hb-8); 2.12 (1H, m, Hb-9); 2.21 (3H, d, J = 1.2 Hz, H-15); 2.68 (1H, td, J = 3.9, 11.0, 12.9 Hz, H-); 4.21 (2H, q, J = 7.0 Hz, $CH_3$-*$CH_2$*-O-); 4.77 (1H, dd, J = 1.2, 11.0 Hz, H-6); 5.77 (1H, s, Hb-13); 6.22 (1H, |

d, J = 10.0 Hz, H-2); 6.25 (1H, d, J = 0.8 Hz, Hb-13); 6.63 (1H, d, J = 10.0 Hz, H-1).

$^{13}$C NMR: Refer to Table 6.4b (Section 6.3.3.2)

### 3.5.3 Preparation of Michael adducts of STLs in an aprotic solvent

General procedure for preparation of Michael adducts with $Et_2NH$ was used. A mixture of sesquiterpene lactone **5.17** (15 mg, 60 µM) and an excess of $Et_2NH$ (100 µM) in dioxane (9 mL) was treated with $Et_3N$, refluxed at 150 ℃ overnight and analysed by TLC. Only the unreacted starting STL was detected in the reaction mixture.

# Chapter 4: Isolation, structural elucidation, bioactivity and biosynthesis of bioactive sesquiterpenoids from an extract of *Dicoma anomala* subsp. *gerrardii*.

## 4.1 Introduction

Plants have a long history of use in the treatment of cancer, and plant-derived anticancer agents constitute a significant part of the current arsenal of chemotherapeutic agents.[62] However, cancer as a specific disease entity is poorly recognised in terms of traditional medicine. Even though more than 3 000 plants species have been reported for this use, in many instances the "cancer" is undefined, and reference is made to conditions such as hard swellings, abscesses, calluses, corns, warts or tumours. Such symptoms would generally apply to the skin, and be tangible or visible conditions.[63] It is also reported, that from the high throughput screening programme of National Cancer Institute (NCI, USA), a large percentage of the actives, from randomly selected extracts, were those of plants with reported medicinal use. Furthermore, the discovery of the *Vinca* alkaloids, discussed in Chapter 1, was indirectly attributed to the observation of an unrelated medicinal use of the source plant.[64]

In the search for novel chemotherapeutics from plants, the CSIR began high-throughput screening of plant extracts in 1999 using *in vitro* screening technology transferred from the NCI. Two approaches were used to select the extracts from the 25 000-extract repository: random and ethnobotanical. The results of random screening are reported elsewhere.[65] From a total of 410 extracts tested through the ethnobotanical selection process, an extract of *Dicoma*

---

[62] Hartwell J. L. (1982). *Plants Used Against Cancer*. A survey. Lawrence, MA. Quarterman Publications.
[63] Cragg G. M., Newmann D. J. (2005). *Journal of Ethnopharmacology*, **100**, 72–79.
[64] Cragg G. M., Boyd M. R., Cardellina J. H., Newman D. J., Snader K. M., Mc. Cloud T. G. (1994). In: Ethnobotany and the Search for New Drugs. Ciba Foundation Symposium, Wiley: Chichester, UK, **185**, 178–196.
[65] Fouche G., Khorombi E., Kolesnikova N., Maharaj V. J., Nthambeleni R., van der Merwe M. (2006). *Pharmacologyonline*, **3**, 494–500.

*anomala* Sond. exhibited activity at micromolar concentrations, and was selected for further evaluation.

Previous phytochemical investigations of the *Dicoma* genus, which were discussed in detail in Section 2.4 (Chapter 2), revealed that the presence of costunolide **(4.1)** derivatives (Figure 2.2) with oxygen functions at C-14 and C-15 is characteristic of the genus.[9,10] The roots of various Dicoma species yielded several common compounds such as *β*-sitoterol, lupeol, phytol and *α*-humulene **(2.4)**.

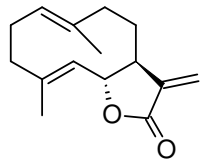


(+)-Costunolide **(4.1)**

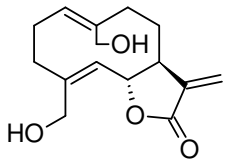


Albicolide **(2.19)**

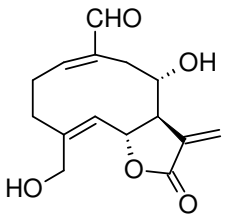


Urospermal A **(2.15)**

Extracts of various parts of *D. anomala* yielded several eudesmanolides **(2.39-2.44)**, germacranolides (albicolide **(2.19)** and urospermal A **(2.15)**) and guaianolide **2.33**.

However, *D. anomala* subsp. *gerrardii* has not been previously investigated. This chapter covers the bioactivity-guided isolation and structure elucidation of active compounds, and further biological screening of these compounds against *Plasmodium falciparum* (*in vitro* and *in vivo)*.

## 4.2 Plant recollection and processing

### 4.2.1 *D. anomala* subsp. *gerrardii*

The original specimen delivered to the CSIR in December of 1999 was identified as *D. anomala* Sensu (SANBI Batch No 99111). However, the latest taxonomic interpretation of *D. anomala* in Southern Africa (Chapter 2) enabled us to revise the original classification of the herbarium specimen. Based on the distinct morphological features (erect habit; ~12-mm-long involucra comprising few bracts), the specimen could be sub-classified as *D. anomala* Sond. subsp. *gerrardii* (Harv. ex F. C. Wilson) S. Ortíz & Rodr. Oubiña.

### 4.2.2 Bulk recollection and processing

Bulk recollection of rhizomes was carried out in the Brits region of North West Province in February of 2006. On average, the fresh rhizomes varied in size from 3 to 12 cm (Figure 4.2). The plants were air dried to remove excess moisture and stored prior to processing for 48 h. The rhizomes were oven dried and ground to a coarse powder (~40% mass loss on drying).

**Figure 4.2. Size distribution of the rhizomes in a batch**

### 4.2.3 Optimisation of the extraction method using anticancer 3-cell lines bioassay

The optimisation strategy was based on the initial anticancer screening results of the ethnobotanical extracts, using 5 g quantities of dried and ground plant material, and a range of organic solvents (Table 4.1). All extracts were screened against the preliminary 3-lines panel of cancer cells.

Whilst all the prepared extracts showed a considerable degree of activity, an ethyl acetate extract exhibited superior activity to that of the other extracts. The remainder of the bulk plant material was exhaustively extracted with ethyl acetate.

**Table 4.1. Cytotoxicity of crude extracts against CHO and cancer cell line panels**

| Extract description, CSIR/NCI ID number | CHO: $IC_{50}$ (ppm) | 3-cell line pre-screen (CSIR), potency, value (ppm) | | | 60-cell line panel (NCI), ppm (*selectivity*) |
|---|---|---|---|---|---|
| | | $GI_{50}$ | TGI | $LC_{50}$ | $GI_{50}$ |
| Hexane extract, SM01084A | - | Inactive | Inactive | Inactive | - |
| Crude MeOH:DCM extract (SM01084B) | - | 12.5 | 25 | 40 | 12.8 (*weak leukaemia*) |
| Hot infusion (SM01084C) | - | Inactive | Inactive | Inactive | - |
| EtOAc extract | 7.8 | <<6.25 | <<6.25 | <<6.25 | 1.86 (*strong leukaemia*) |
| DCM extract | - | 6.25 | <<6.25 | <<6.25 | - |

## 4.3 Bioassay-guided fractionation and isolation of active compounds from extract of *D. anomala*

The crude dry ethyl acetate extract was subjected to solvent partitioning (described in detail in Section 3.3.5.1 of Chapter 3) to produce four fractions: hexane-soluble fraction **(A)**; dichloromethane fraction **(B),** the aqueous fraction **(C)** and the insoluble residue fraction **(D).** Fraction **(B)** showed increased activity ($GI_{50}$ <<6.25 ppm), the insoluble fraction **(D)** yielded activity much lower than that of the crude extract ($GI_{50}$ = 25 ppm), whilst the hexane and aqueous fractions were completely devoid of activity. Further bioassay-directed fractionation of the dichloromethane fraction by vacuum liquid chromatography (VLC) on silica gel, followed by successive flash silica gel purifications, resulted in the isolation of two bioactive compounds **4.2** and **4.3**, with $GI_{50}$ values of 0.67 ppm and 1.0 ppm respectively against the 3-cancer cell lines panel.

## 4.4 Structure elucidation of compounds 4.2 and 4.3

The structural assignments of compounds **4.2** and **4.3** were based on detailed studies of the high-field $^{1}H$ and $^{13}C$ NMR spectra, two-dimensional (2D) NMR

techniques and comparison of the spectral data with that of compounds previously isolated from *Dicoma* sp.[66,67]

### 4.4.1 Structure of compound **4.2**

#### *4.4.1.1 Structure elucidation of compound **4.2** using spectroscopic techniques*

Compound **4.2** was isolated as a colourless powder with a total yield (w/w) from dry plant material of 0.013%. LC-ESI-MS analysis of compound **4.2** revealed a positive ion peak of m/z 245.2 $[M + H]^+$.

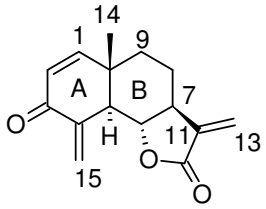


**(4.2)**

The $^1H$ NMR spectrum exhibited 13 signals which integrated as approximately 16 protons. The $^{13}C$ NMR data gave a total count of 15 non-equivalent carbon atoms. From the $^1H$ and $^{13}C$ NMR analyses, hydrogen and carbon counts allowed an estimation of a probable molecular composition of $C_{15}H_{16}O_3$ with eight sites of unsaturation. The $^1H$, $^{13}C$, gHSQC, gHMBC, COSY and NOESY data of compound **4.2** are summarised in Table 4.2.

The $^1H$ NMR spectral data clearly showed the presence of one tertiary methyl group at $\delta_H$ 1.02. Furthermore, it revealed the presence of a pair of olefinic hydrogens ($\delta_H$ 5.99 and $\delta_H$ 6.76) which had vicinal coupling of 10.0 Hz indicative of Z-geometry. The $^1H$ NMR spectrum also showed a pair of sharp doublets (J = 3.1 Hz) at $\delta_H$ 5.43 (J = 3.2 Hz) and at $\delta_H$ 6.10, which were assigned to geminal exomethylene protons. A further set of signals in the low-field region which corresponded to a doublet of doublet of doublets at $\delta_H$ 5.68 (J = 2.4; 1.0; 0.9 Hz)

---

[66] Croasmun W. R., Carlson R. M. K. (1987). Two-dimensional NMR Spectroscopy: Applications for Chemists and Biochemists. New York: VCH Publishers.

[67] Saunders J. M., Hunter B. K. (1987). *Modern NMR Spectroscopy. A Guide for Chemists*. Oxford: Oxford University Press.

was caused by the geminal and allylic coupling, and was assigned to a second exomethylene group. Another distinct proton signal, which appeared at $\delta_H$ 4.07 as a triplet (J = 10.7 Hz), corresponded to one oxymethine proton. The chemical shift values for a multiplet, resonating at $\delta_H$ 2.6, and a doublet of doublet of doublets (J = 2.2; 2.3; 10.9 Hz) at $\delta_H$ 2.98, suggested that both protons were deshielded by the neighbouring group/s. In addition, three aliphatic protons (by integration) were observed in the region $\delta_H$ 1.28 – 1.84.

The $^{13}C$ NMR spectra showed 15 signals, with 5 quaternary and 10 proton-bearing carbons, as was evident from the DEPT spectra. Of the five methine groups, there were two aliphatic CH groups. One was a deshielded oxymethine signal at $\delta_C$ 79.2, assignable to C-6 ($\delta_H$ 4.07), and the remaining two were assigned to the olefinic carbons C-1 ($\delta_C$ 158.4) and C-2 ($\delta_C$ 127.5), corresponding to proton signals as $\delta_H$ 5.99 and $\delta_H$ 6.76. Of the four $CH_2$ groups, two corresponded to the two sets of exomethylene protons ($\delta_H$ 5.43 and $\delta_H$ 6.1) and the remaining two to the aliphatic groups. Of the five quaternary carbons, two were carbonyl signals at $\delta_C$ 187.6 and $\delta_C$ 170.0, two were olefinic and one was an aliphatic carbon atoms. Two carbonyl groups and three double bonds (eight $sp^2$ carbons) accounted for five of the eight degrees of unsaturation. The three remaining degrees of unsaturation were assumed to ring structures. Based on this evidence, it was strongly suspected that the unknown compound may be a sesquiterpene lactone (STL), similar to those previously isolated from the *Dicoma* species. Structural assignments were deduced as follows.

Unambiguous $^{13}C\leftrightarrow^{1}H$ correlations were obtained from the gHSQC spectrum *via* one-bond $^{13}C\leftrightarrow^{1}H$ coupling. Examination of the COSY spectrum revealed a strong vicinal coupling (J = 10.8 Hz) between the H-6 and H-7 protons, while the H-7 proton showed strong coupling to C-8 ($\delta_H$ 1.67 and $\delta_H$ 2.1) and H-13 protons ($\delta_H$ 5.43 and $\delta_H$ 6.1). Further couplings of the Hb-8 proton to C-9 protons ($\delta_H$ 1.67 and $\delta_H$ 1.81) were also observed. HMBC correlations between C-1 with a proton signal at $\delta_H$ 1.67 of C-9 proton along with the long-range coupling between carbon C-9 at $\delta_C$ 36.1 and the H-14 protons, allowed the methyl group to be placed at C-10 ($\delta_C$ 39.6). Further long-range correlations in the HMBC spectrum were observed

between C-13 ($\delta_C$ 117.6) protons and the carbon C-7 ($\delta_C$ 49.5), the tertiary carbon C-11 ($\delta_C$ 138.2) and the carbonyl carbon C-12 ($\delta_C$ 170.0). HMBC correlation of the C-11 carbon to the oxymethine C-6 ($\delta_C$ 79.2) proton at $\delta_H$ 4.07 allowed a fragment **4.2-i** to be established, containing *α*,*β*-unsaturated ester or a lactone moiety.

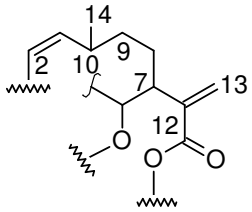


**(4.2-i)**

The location of the doubly conjugated keto-group, subsequently identified as C-3 ($\delta_C$ 187.6), followed from the HMBC correlations of the carbon signal C-3 to the geminal protons H-15, and a long-range correlation of carbon C-2 to proton signals for H-15. Further HMBC correlation between the C-6 proton and carbon C-5 ($\delta_C$ 138.2) and carbon C-10, and the correlation of the methyl proton H-5 to the tertiary carbon C-10 pointed to the existence of two fused cyclohexane rings forming a skeleton of the eudesmanolide-type sesquiterpenoid molecule. The last site of unsaturation was attributed to a lactone ring, and together with the above substantiation data, the structure of compound **4.2** was deduced.

The structure was further confirmed by comparison of its $^{1}$H NMR data, $^{13}$C NMR data and physical constants with published values.[52,68] Thus compound **4.2** was identified as 3-oxoeudesma-1,4(15),11(13)-triene-12,6*α*-lide, which was identical to the structure of dehydrobrachylaenolide **(2.42)**, previously isolated from various *Dicoma* species (Chapter 2).[10]

[68] Barrera J. B., Breton J. L., Fajardo M., Gonzalez A. G. (1967). *Tetrahedron Letters*, **36**, 3475–3476.

**Table 4.2. $^{1}H$ and $^{13}C$ NMR data for compound 4.2 in $CDCl_3$**

| Atom number | DEPT | $\delta_C$ | $\delta_H$, (multiplicity); J (Hz) | HMBC $^{13}C \leftrightarrow {}^{1}H$ | COSY $^{1}H \leftrightarrow {}^{1}H$ | NOESY $^{1}H \leftrightarrow {}^{1}H$ |
|---|---|---|---|---|---|---|
| 1 | CH | 158.4 | 6.76 (d); J = 10.0 | H-2, H-15 | H-2 | H-2, Hb-9 |
| 2 | CH | 127.5 | 5.99 (dd); J = 10.0; 1.0 | H-1 | H-1 | H-1 |
| 3 | C | 187.6 | - | H-1, Ha-15, Hb-15 | - | - |
| 4 | C | 140.5 | - | H-2, H-5, Hb-15 | - | - |
| 5 | CH | 52.6 | 2.98 (ddd); J = 2.2; 2.3; 10.9 | H-1, H-14, Ha-15, Hb-15 | H-6, Ha-15, Hb-15 | H-7 |
| 6 | CH | 79.2 | 4.07 (t); J = 10.7 | H-1,H-5, Hb-8 | H-5, H-7 | H-14, Ha-15 |
| 7 | CH | 49.5 | 2.6 (ddddd); J = 3.0; 3.0; 3.2; 10.8; 11.0 | Ha-8, Hb-8, Hb-9, Ha-13, Hb-13 | H-6, Hb-8, Hb-9, Ha-3, Hb -13 | H-5 |
| 8 | $CH_2$ | 21.1 | Ha 1.67 (m)<br>Hb 2.1 (m) | H-6 | H-7, Hb -8, H-9 | Ha-8↔H-14<br>Hb -8↔Ha-9 |
| 9 | $CH_2$ | 36.1 | Ha 1.67 (m)<br>Hb 1.81 (m) | H-1, Ha-8, H-14 | Hb-9↔Ha-8, Hb-8, Ha-9, H-14 | Ha -9↔Hb-8<br>Hb-9↔H-14 |
| 10 | C | 39.6 | - | H-1, H-2, H-5, Hb-8, Ha-9, Hb-9, H-14 | - | - |
| 11 | C | 138.2 | - | H-6, H-13 | - | - |
| 12 | C | 170.0 | - | Hb-13 | - | - |
| 13 | $CH_2$ | 117.6 | Ha 5.43 (d); $J_{13b}$ = 3.1<br>Hb 6.10 (d); $J_{13a}$ = 3.2 | - | H-7 | Ha-13↔Hb-13 |
| 14 | $CH_3$ | 19.6 | 1.02 (s) | H-1, H-5, Ha-9, Hb-9 | H-9 | H-6, Ha-8, Hb-9 |
| 15 | $CH_2$ | 122.2 | Ha 5.68 (ddd) $J_{15b}$ = 0.9; 1.0; 2.4<br>Hb 6.24 (dd); $J_{15a}$ = 1.0; 2.2 | H-5 | H-5 | Ha-15↔H-6, Hb-15 |

Assuming that H-7 is *α*-oriented, as in all sesquiterpene lactones from higher plants without exception, the relative stereochemistry of the asymmetric centres at

C-5, C-6, C-7 of compound **4.2** could be derived from the size of the observed $^{1}$H NMR couplings ($J_{5,6}$~$J_{6,7}$~10.8 Hz) and NOE correlations to be anti-periplanar, suggesting H*α*-5, H*β*-6 and H*α*-7 have a relative spatial orientation.[69]

This was in good agreement with previously reported stereochemistry for dehydrobrachylaenolide and irazunolide, and was subsequently confirmed by X-ray data (Section 4.4.1.2).[10,70]

### *4.4.1.2 X-ray crystallographic study of compound **4.2***

Compound **4.2** was recrystallised from 2-propanol to yield white orthorhombic crystals (mp 223-224 ℃). The crystal system and space group for compound **4.2** were identified from diffraction symmetry and systematic absences as orthorhombic, P $2_12_12_1$, with four equivalent molecules in the asymmetric unit (Figures 4.3 and 4.4). The X-ray crystal structure of compound **4.2** revealed the presence of the three-ring eudesmanolide system with endo-exo cross-conjugated methylenecyclohexenone moiety *trans*-fused with cyclohexane C-1 - C-5 and *trans*-annelated with the *α*-methylene-*γ*-lactone (at C-6 - C-7), and therefore confirmed the proposed structure for the compound **4.2**.

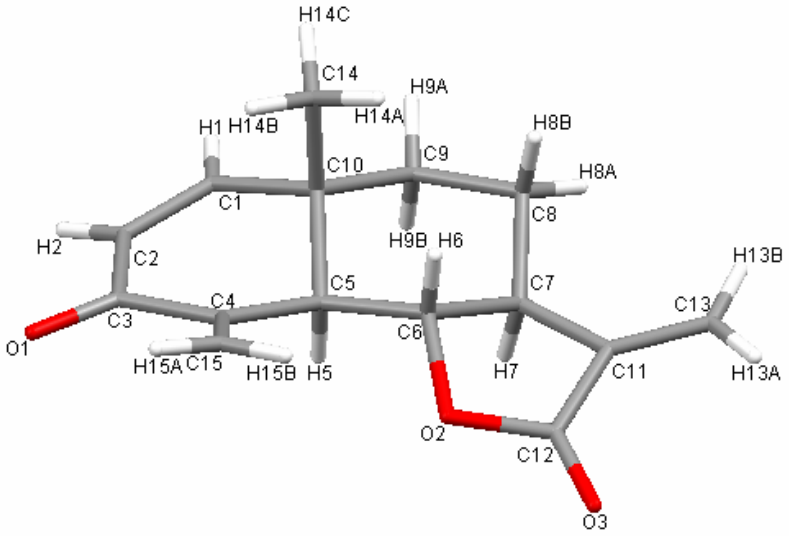


**Figure 4.3. X-ray structure of compound 4.2**

---

[69] Fischer N. H., Olivier E. J., Fischer H. D., (1979). In: *Progress in the Chemistry of Organic Natural Products*. New York: Verlag Wien, Vol. **38**, p. 47.

[70] Hasbun C., Calvo M. A., Poveda L. J., Malcolm A., Delord T. J., Watkins S. F., Fronczek F. R., Fischer N. H. (1982). *Journal of Natural Products*, **45**, 749–753.

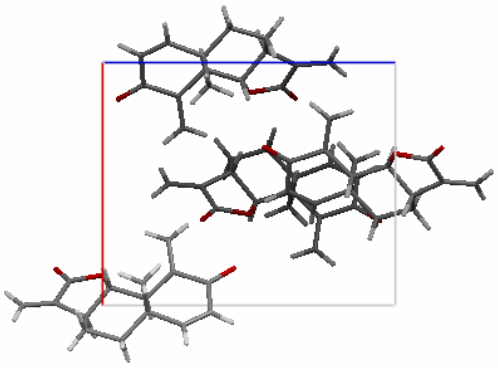

**Figure 4.4. Packing of the molecules in the crystal of compound 4.2**

The relative stereochemistry, initially deduced from the size of the coupling constants, whereby the anti-periplanar arrangements of the protons at C-5 to C-9 suggested H-5*α*, H-6*β* and H-7*α* spatial orientations, was also confirmed. While ring B exists in a classic chair conformation, the presence of four $sp^2$-hybidrised carbon atoms in ring A of compound **4.2** leads to a flattening of the chair due to their planar geometry with the four carbons lying in one plane (Figure 4.5).

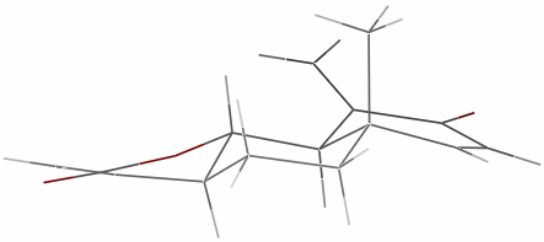

**Figure 4.5. Edge-on projection illustrating ring conformation of compound 4.2**

The structure shows that C-15 is placed in the pseudo-equatorial position while C-14 is in the axial position above the plane of the ring. Detailed crystallographic data for compound **4.2** are presented in Appendix 2.

The unambiguous assignment of absolute stereochemistry of compound **4.2** was made on the basis of the value of the optical rotation ($[\alpha]^{24}_{D}$+68° (c 0.50, $CHCl_3$)) which is identical to that of the synthetic compound ($[\alpha]^{24}_{D}$+67.9° (c 0.16, $CHCl_3$)), in which the stereochemistry followed from the precursors,[53] and is very close to the value for the natural isolate ($[\alpha]^{24}_{D}$+67° (c 0.16, $CHCl_3$)) with postulated absolute stereochemistry.[52]

### 4.4.2 Structure elucidation of compound **4.3**

The second active compound **4.3** was purified by flash silica gel chromatography and further re-crystallisation from cold MeOH to yield yellow needles with a total yield of 0.004% (w/w) of dry plant material. The optical rotation was measured to give $[\alpha]^{24}_{D}$ +56° (*c* = 0.5, $CHCl_3$). The structure of compound **4.3** was determined to be an asymmetrical guaianolide-type sesquiterpene lactone dimer.

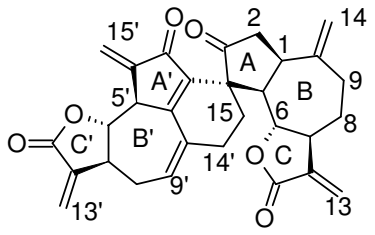


**(4.3)**

The melting point was not determined as the $C_{30}$ compound started melting at 170 °C and as soon as any liquid was generated, a lot of charring was observed. No further melting was observed below 270 °C (limit of apparatus). The low-resolution FAB of compound **4.3** showed a molecular peak at m/z 485.2 $[M + H]^+$ and UV $\lambda_{max}$ 218 and 312 nm. The monoisotopic exact mass of m/z 484.18511 was established by positive high-resolution EI-MS, which was consistent with the molecular formula $C_{30}H_{28}O_6$ and calculated mass of 484.1885. Seventeen sites of unsaturation were calculated from the molecular formula. The $^1H$, $^{13}C$, DEPT,

HSQC, HMBC, COSY and NOESY data for compound **4.3** are summarised in Table 4.3.

In the $^{13}C$ NMR spectra 30 intense signals were observed. There were 6 aliphatic and 4 olefinic methylenes, 7 methines, with 2 methines bearing an oxygen function ($\delta_C$ 83.1 and 84.1), as followed from the DEPT analysis. All proton-carbon relationships were determined from the HSQC analysis, and 11 carbon signals were assigned to quaternary carbons, 4 of which were carbonyl groups ($\delta_C$ 169.2, 169.6, 193.2 and 220.2). Detailed examination of HSQC also revealed the presence of a minor impurity.

Connectivity between the atoms was derived from COSY and HMBC experiments. The sub-structure of a 7-membered ring in fragment **4.3i** was derived from COSY cross-peaks between H-1 and H-5 and H-9, and the HMBC correlations of carbons C-9 and C-1 to H-14a,b. Further HMBC correlations of the carbon signal of C-10 with H-14 and of C-10 with H-2 were used to derive the connectivity C-14-C-10-C-1-C-2.

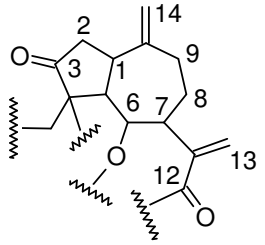


**(4.3i)**

The carbonyl keto-group C-3 ($\delta_C$ 220.2) was placed following positive cross-peaks between C-3 and protons H-1 and H-2, and between protons H-1 and H-5, and carbon C-4. Further long-range correlations in the HMBC spectrum were observed between C-13 geminal protons ($\delta_H$ 5.53 and $\delta_H$ 6.06) and the carbons C-7 ($\delta_C$ 43.52), C-11 ($\delta_C$ 138.2) and the carbonyl carbon C-12 ($\delta_C$ 169.6). HMBC correlation of the C-11 carbon to the oxymethine C-6 ($\delta_C$ 84.1) proton at H-6 ($\delta_H$ 4.18), and between carbon C-15 and protons H-5 ($\delta_H$ 3.28), H-6 and another proton resonating at $\delta_H$ 2.29 ppm, allowed a fragment **4.3i** to be established containing *α,β*-unsaturated ester or a lactone moiety. The expected coupling

between geminal protons Ha,b-14 of 0.5-3.0 Hz was not observed and the two proton signals ($\delta_H$ 4.68 and $\delta_H$ 5.03) appeared as broad singlets. In total, 6 sites of unsaturation were accounted for from the total of 17 sites.

**Table 4.3. $^{1}H$ and $^{13}C$ NMR data for compound 4.3 in $CDCl_3$**

| Atom number | DEPT | $\delta_C$ | $\delta_H$, (multiplicity); J (Hz) | HMBC $^{13}C\leftrightarrow{}^{1}H$ | COSY $^{1}H\leftrightarrow{}^{1}H$ | NOESY $^{1}H\leftrightarrow{}^{1}H$ |
|---|---|---|---|---|---|---|
| 1 | CH | 40.0 | 3.2 (br ddd); $J_{1,5,\text{-cis}}$ = 9.2 | H-5, H-9, H-14 | H-11 | H-7, Ha-9 |
| 2 | $CH_2$ | 45.1 | Ha 2.68 (ddd); $J_1$ =3.1 Hb 3.36 (dd); $J_{2a}$ = ~18.5 | C-10 | H-2a↔H-2b | Ha-2↔Ha-9, Ha-14 |
| 3 | C | 220.2 | - | H-1, H-2 | - | - |
| 4 | C | 51.7 | - | H-1, H-5, H-6 | - | - |
| 5 | CH | 50.0 | 3.28 (dd); $J_{1,5}$ = 9.2, $J_{5,6}$ = 10.0 | H-1, Hb-2, H-6 | H-6 | H-7 |
| 6 | CH | 84.1 | 4.18 (dd); $J_5$ = 10.0, $J_7$ = 9.0 | Ha-8 | H-5,H-7 | Hb-15 |
| 7 | CH | 43.5 | 3.01 (m) | H-8, Hb-13 | H-6, H-13a | H-1, H-5 |
| 8 | $CH_2$ | 32.2 | Ha 1.48 (m) Hb 2.33 (m) | H-6, H-9 | *β*H-8↔ *β*H-9 | Ha-8↔Hb-9, H-6, Ha-13 Hb-8↔H-7 |
| 9 | $CH_2$ | 39.5 | Ha 2.21 (m) Hb 2.58 (m) | H-1, Ha,b-14 | Ha-9↔Hb-8, Ha,b-14 | Ha-9↔H-1, H-7 |
| 10 | C | 150.5 | - | H-1, H-2, H-5, H-9, H-14 | - | - |
| 11 | C | 138.2 | - | H-7 | - | - |
| 12 | C | 169.6 | - | H-13 | - | - |
| 13 | $CH_2$ | 121.6 | Ha 5.53 (d); $J_7$ = 3.0 Hb 6.06 (d); $J_7$ = 1.0 | H-7 | H-5’ | Ha-13↔H-7, Ha-8 |

| | | | | | | |
|---|---|---|---|---|---|---|
| 14 | $CH_2$ | 114.1 | Ha 4.68 (br s)<br>Hb 5.03 (br s) | H-1, H-2, H-9’ | Hb-14 ↔ H-1, H-9’ | Ha-14↔Ha-2, Hb-14<br>Hb-14↔Hb-9, Ha-14 |
| 15 | $CH_2$ | 31.7 | Ha 1.88 (m)<br>Hb 2.24 (m) | H-5, H-6, H-14’ | Ha-15 ↔ Ha-14’ | Hb-15↔H-6 |
| 1’ | C | 158.5 | - | H-5’, H-9’ | - | - |
| 2’ | C | 144.6 | - | H-5’, H-9 | - | - |
| 3’ | C | 193.2 | - | Ha,b-15’ | - | - |
| 4’ | C | 141.2 | - | H-5’ | - | - |
| 5’ | CH | 49.1 | 3.73 (br d);<br>$J_{6'}$= 10.9 | H-15’ | H-6’, H-15’ | H-7’ |
| 6’ | CH | 83.1 | 4.03 (dd); $J_{5'}$ = 10.9, $J_{7'}$ = 9.5 | H-5’ | H-5’, H-7’ | |
| 7’ | CH | 46.8 | 3.04 (m) | H-8’, H-9’, Ha,b-13’ | H-1’, H-6’ | H-5’ |
| 8’ | $CH_2$ | 28.9 | Ha 2.28 (m)<br>Hb 2.82 (m) | H-9’ | H-6’, H-9’ | Ha-8’↔H-9’, Hb-8’↔H-13’a |
| 9’ | CH | 130.8 | 5.98 (m) | Ha-14’ | Hb-8’, Ha,b-14’ | Hb-8’, Ha-14’ |
| 10’ | C | 134.2 | - | H-8’ | - | - |
| 11’ | C | 138.6 | - | H-7’ | - | - |
| 12’ | C | 169.2 | - | H-5’, H-13’ | - | - |
| 13’ | $CH_2$ | 120.2 | Ha 5.52 (d);<br>$J_{7'}$ = 3.0<br>Hb 6.24 (d); $J_{7'}$ = 1.0 | H-7’ | Ha,b-13’↔H-7’ | Hb-8’ |
| 14’ | $CH_2$ | 33.0 | Ha 2.29 (m)<br>Hb 2.63 (m) | H-9’ | Ha-14’↔Ha-15, | Hb-14’↔H-6 |
| 15’ | $CH_2$ | 121.7 | Ha 6.11 (t); $J_{15'b}$ = 1.0<br>Hb 6.22 (dd); $J_{15'a}$ = 1.0, $J_{5'}$ = 1.7 | H-5’ | Ha-15’↔H-5’ | - |

The substructure **(4.3i)** appeared similar to a structure of sesquiterpene guaianolide dehydrozalluzanin C **(2.33)**, which is characteristic of this genus.[Error! Bookmark not defined.,71]

Following the above argument, protons H-13' ($\delta_H$ 5.52 and $\delta_H$ 6.64) showed cross peaks to C-7' ($\delta_C$ 46.8); Ha,b-13' ↔C-11' ($\delta_C$ 138.2), Ha,b-13 ↔C-12' ($\delta_C$ 169.6) and C-11'↔H-6 ($\delta_H$ 4.18)], another structural element, containing *α,β*-unsaturated ester or a lactone moiety, was deduced (part of fragment **4.3ii**). Further examination of the COSY spectrum allowed to establish the sequence from C-5' to C-9' in the fragment **4.3ii**. HMBC correlations of carbon C-1' to the olefinic proton H-9 ($\delta_H$ 5.97) and between carbon C-14' and the H-9' proton, and of carbon C-2' to the H-5' proton were also observed. The conjugated carbonyl C-3' ($\delta_C$ 193.2) was placed on the basis of cross-peaks between carbon C-3' and the C-15' protons ($\delta_H$ 6.11 and $\delta_H$ 6.22), the H-5' proton with carbon C-4' ($\delta_C$ 141.2), and the COSY correlation between the Ha,b -15' protons and the H-5' ($\delta_H$ 3.73) proton. The HMBC correlation of carbon C-1' to H-5', together with the above arguments, furnished fragment **(4.3ii)**, which is linked to fragment **(4.3i)** *via* carbon C-14'.

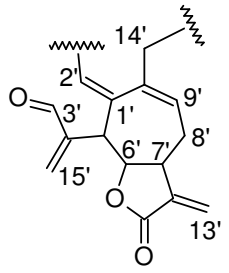


**(4.3ii)**

Along with the fragment **4.3i**, 13 of the 17 degrees of unsaturation were assigned. Of the remaining four, three degrees of unsaturation could be assigned to further ring elements, such as two lactone moieties (C-6-O-C-12 and C-6' -O- C-12') and a cyclopentanone ring through C-3' - C-2' closure (**4.3ii** ring A').

[71] Romo de Vivar A., Cabrera A., Ortega A., Romo J. (1967). *Tetrahedron*, **23**, 3903–3907.

The last unaccounted site of unsaturation could be that of the cyclohexene ring fused between rings A' and B' of substructure **4.3ii** thus connecting the two substructures **4.3i** and **4.3ii** via a spiro centre. The spatial orientation of the carbon C-14 at position C-4 is likely to be derived from steric approach control during the dimerisation process, the least hindered isomer being generated with C-15 above or below the plane of the molecule **(4.3iii** and **4.3iv)**.

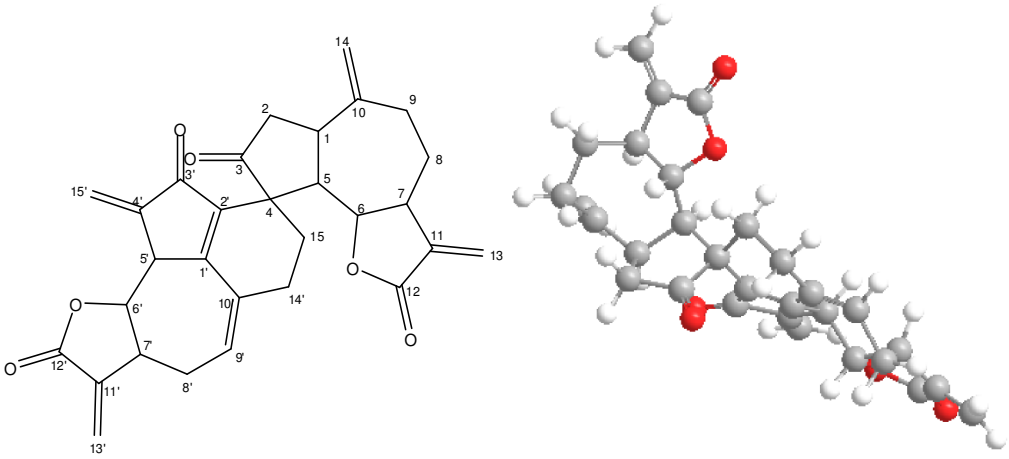

**(4.3iii)**

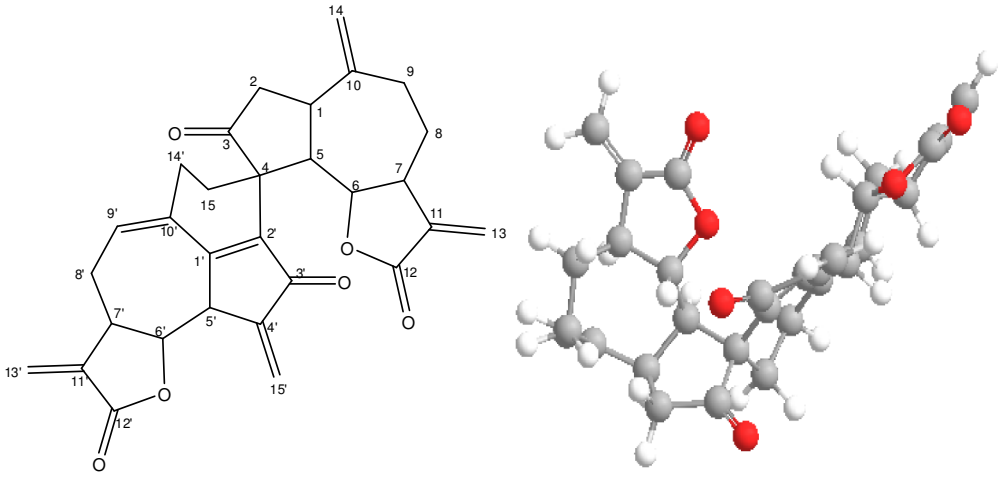

**(4.3iv)**

Analysis of the literature shows that dimeric guaiane lactones are, in the main, formed from A/B-*cis*, B/C-*trans* linked monomers. In monoguaianolides, the five-membered rings A and C usually assume envelope conformation, but sometimes

they adopt planar forms.[72] In compound **4.3** ring A was deduced to assume 1*α*-H and 5*α*-H envelope conformation, and the ring A' should be planar due to the presence of 4 $sp^2$ carbons. The size of the coupling constant (J = 9.2 Hz) further substantiated the *cis* relationship between the protons at the C-1 - C-5 ring junction. In case of 1*β*,5*α*–*trans*-guaianolide, a value of 10.0 Hz or greater is expected according to the literature.[73,74] Both lactone ring junctions were proposed to assume *trans*-(6*β*,7*α*)-H configuration from the size of the couplings ($J_{6,7}$ = 10.8 Hz and $J_{6'7'}$ = 9.4 Hz), and also from the observed long-range coupling (J = 3.0 Hz) between pairs of the Ha-13 methylene proton and the proton H-7, and the Ha-13' proton with the H-7' proton.[71]

From the previous X-ray structural results, and by means of empirical calculation by the methods of molecular mechanics, in the monomeric *cis*-, *trans*-guaianolides the 7-membered ring B exists mainly in the *twist*-chair conformations with approximate two-fold axis passing through C-5 and the midpoint of the C-8 - C-9 bond ($TC_5$ form) or $TC_8$ form, and rarely, in the chair conformation. The $TC_5$ form was found in 3-oxograndolide **(4.4)**,[75] while the $TC_8$ conformation was present in dehydrocostus lactone **(4.5a)**,[76] which is considered the most elementary exomethylenecycloheptane *trans*-fused guaian-6,12-olide. For an isolated methylenecycloheptane $TC_5$ and $TC_8$ are indistinguishable and represent one of the calculated minima for this species.[77]

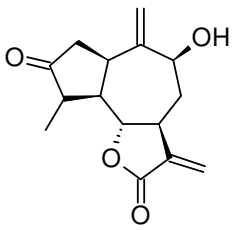


3-Oxograndolide **(4.4)**

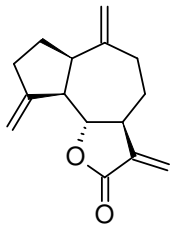


Dehydrocostus lactone **(4.5a)**

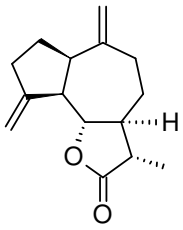


Mokko lactone **(4.5b)**

[72] Tashkhodzhaev B., Karimov Z. (1994). *Chemistry of Natural Compounds*, **30**, 186–192.
[73] Merfort I., Willuhn G., Wendisch D., Gondol D. (1996). *Phytochemistry*, **42**, 1093-1095.
[74] Zdero C., Bohlmann F., King R. M., Robinson H. (1987). *Phytochemistry*, **26**, 1207-1209.
[75] Rychlewska U. (1985). *Acta Crystallographica*, **41**, 540–542.
[76] Fronczek F. R., Vargas D., Parodi F. J., Fisher N. H. (1989). *Acta Crystallographica*, **45**, 1829-1831.
[77] Rychlewska U., Szczepanska B., Daniewski M., Nowak G. (1992). *Journal of Crystallographic and Spectroscopic Research*, **22**, 659–663.

The conformation of a 7-membered ring in dimeric guaianolides would be determined by the degree of the steric stress arising as the result of dimerisation and may differ from the traditional forms existing for the monoguaianolides. The chemical shift overlap precluded a detailed study of the conformations of the 7-membered ring of compound **4.3** *via* deduction of geminal coupling constants ($J_{7,8}$ and $J_{8,9}$). Due to the similarity of the chemical shifts of exomethylene protons in fragment **4.3i** to that of dehydrocostus lactone **(4.5a)**, it was assumed that the *twist*-chair conformation of the 7-membered ring should be the most probable conformation.[76,78]

The conclusion about the geometry at carbon C-4 (structure **4.3iv**) was based on the NOE correlation observed between H-6 ($\delta_H$ 4.18) and H-15b ($\delta_H$ 2.24), which would not be likely with carbon C-14 lying below the plane. This was in good agreement with the recently published relative stereochemistry of this dimer.[28]

## 4.5 Summary of the literature study of compounds 4.2 and 4.3

In summary, the literature review revealed that compound **4.2** was originally isolated from the roots of *Brachylaena transvaalensis* and that is where its name dehydrobrachylaenolide was derived from.[52] However, the compound was not detected in the roots of *D. anomala* subsp. a*nomala* in two previous investigations.[9,10] Several biological activities were reported for dehydrobrachylaenolide **(4.2)**. These included the inhibitory activity toward induction of intracellular adhesion molecule–1 (ICAM-1) with $IC_{50}$ value of 3.0 µM and antibacterial properties.[79] Compound **4.3** was reported only once in a recent patent application on its activity against *P. falciparum*.[28] However, the NMR structural data for this compound has not been published.

[78] Milosavljević S., Juranić I., Bulatović V., Macura S., Juranić N., Limbach H. H., Weisz K., Vajs V., Todorović N. (2004). *Structural Chemistry*, **15**, 237–245.
[79] Afolayan A. J., Sultana N. (2003). *South African Journal of Botany*, **69**, 158–160.

## 4.6 Targeted isolation of compound 4.2 from the organic extract of *B. transvaalensis*

*B. transvaalensis* E. Phillips & Schweick was investigated as potential source of dehydrobrachylaenolide **(4.2)**. The wood of this invasive tree, also known as Forest Silver Oak, is used for kraal construction.[80] The root system is large, and is widely spread around the stem. The presence of dehydrobrachylaenolide **(4.2)** in the extract of roots of *B. transvaalensis* was confirmed by LC-ESI-MS analysis (Method T3.1-3; $t_R$ = 25.4 min; UV $\lambda_{max}$ = 211, 242 nm; m/z 245.2 $[M+H]^+$). Subsequently, dehydrobrachylaenolide **(4.2)** was isolated from the extract of the roots of *B. transvaalensis* following the same sequence of solvent partitioning and chromatographic conditions as for the extract of *D. anomala* subsp. *gerrardii* (Section 3.3.5). Compound **4.2** isolated from *D. anomala* subsp. *gerrardii* was used as a TLC standard to guide the purification ($R_f$ = 0.38 in EtOAc/DCM/Hexane; 15:42.5:42.5 v/v). The compound was isolated as a white powder (0.001% yield w/w of dry plant material). The structure was confirmed by the $^1$H NMR analysis and the value of optical rotation.

## 4.7 HPLC analysis of root extract of *D. anomala* subsp. *anomala* for the presence of dehydrobrachylaenolide (4.2)

An ethyl acetate extract of *D. anomala* subsp. *anomala* collected in Gauteng was subjected to solvent partitioning (described in the experimental section) to produce a dichloromethane soluble fraction (B), which was analysed by HPLC, using compound **4.2**, isolated from *D. anomala* subsp. *gerrardii* as a standard (Method: T3.1-2; $t_R$ = 19.65 min; UV $\lambda_{max}$ = 211, 242 nm). The UV $\lambda_{max}$ chromatogram revealed that dehydrobrachylaenolide **(4.2)** was not present in the extract. This finding was in good agreement with the results of previous investigations of this subspecies of *Dicoma*.[9,10]

[80] Loffler L., Loffler P. (2005). *Swaziland Tree Atlas: SABONET Report No. 38.* Pretoria: Capture Press, p. 37..

## 4.8 *In vitro* evaluation of compounds 4.2 and 4.3 in the cancer and malaria models

### 4.8.1 *In vitro* anticancer activity

Compounds **4.2** and **4.3** were tested for their cytotoxicity towards cancer cell lines in the 3-cell line pre-screen to confirm their activity, and towards the Chinese hamster ovarian cell line (CHO) for general indication of their cytotoxicity.

Compound **4.2** was further evaluated against the 60-cell line panel at the NCI. Parthenolide was used as a positive standard. The results are summarised in Table 4.4.

**Table 4.4. Evaluation of the *in vitro* activity against cancer cell line panels and CHO**

| Sample description | CHO: $IC_{50}$ (µg/mL) | 3-cell line pre-screen (CSIR), (µg/mL) | | | 60-cell line panel, average over all cell lines (µM[a]/ µg/mL[b]) | | |
|---|---|---|---|---|---|---|---|
| | | $GI_{50}$ | TGI | $LC_{50}$ | $GI_{50}$ | TGI | $LC_{50}$ |
| EtOAc extract of *D. anomala* subsp. *gerrardii* | 7.8 | <<6.25 | <<6.25 | <<6.25 | 1.86[b] (strong leukaemia) | - | - |
| 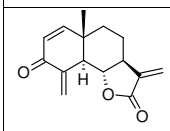 **(4.2)**/(NSC720795)[81] | 4.2 | 0.67 | 1.57 | 2.48 | 1.91[a] | 8.03[a] | 34.2[a] |
| 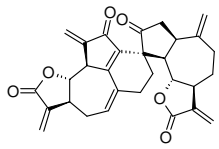 **(4.3)** | 0.68 | 0.75 | 4.89 | 12.23 | - | - | - |
| Parthenolide (NSC157035) | 0.75 | 1.11 | 2.35 | 3.58 | 17.9[a] | 46.6[a] | 153[a] |

[81] NCI compound identification number.

### 4.8.2 *In vitro* antimalarial activity

The pure compounds **4.2** and **4.3**, isolated from the roots of *D. anomala* subsp. *gerrardii*, and the crude ethyl acetate extract were tested for potential activity against *P. falciparum* in the high-throughput assay.

The relative $IC_{50}$ values were determined as a mean value for the two replicates and are not statistically significant. Chloroquine was used as positive control in each run. The results are summarised in Table 4.5 and some selected dose response curves are presented in Appendix 3. The selectivity index was also determined and used as an indicator of the toxicity of the test compound towards mammalian cells (CHO) when compared to the activity against the parasite.

**Table 4.5. *In vitro* activity against *P. falciparum***

| Sample description | *P. falciparum* D10 strain $IC_{50}$ (µg/ml) | *P. falciparum* K1 strain $IC_{50}$ (µg/ml) | CHO $IC_{50}$ (µg/ml); n = 2 | SI for D10 | SI for K1 |
|---|---|---|---|---|---|
| EtOAc extract of *D. anomala* subsp. *gerrardii* | 1.4 | - | 7.8 | 3.7 | - |
| 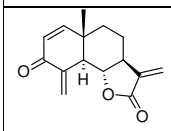 **(4.2)** | 0.38 | 0.06 | 4.2 | 11 | 70 |
| 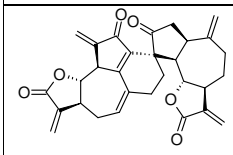 **(4.3)** | 0.46 | NT | 0.68 | 1.5 | - |
| Crude (DCM:MeOH) extract of *B. transvaalensis* | 2.1 | - | - | - | - |
| Chloroquine | 0.02 | 0.103 | | ~906 | ~179 |

*SI (selectivity index) = cytotoxicity* CHO $IC_{50}$/antiplasmodial $IC_{50}$
D10 = *P. falciparum* – chloroquine-sensitive strain
K1 = *P. falciparum* – chloroquine-resistant strain
CHO = Cytotoxicity against Chinese hamster ovarian cells
*n = number of data sets averaged*

Both pure compounds were regarded as potent against the two strains of the parasite, when compared to the standard compound chloroquine (CQ). Compound **4.2** showed significant activity towards the CQ-sensitive strain and superior activity against the CQ-resistant strain when compared to CQ with SI of 11 and 70, respectively. Compound **4.3** was found to exhibit a similar degree of cytotoxicity towards CHO cells as for *P. falciparum* infected erythrocytes, resulting in a selectivity index (SI) of 1.5. The crude extract of *D. anomala* subsp. *gerrardii* exhibited a 50% inhibitory concentration of 1.4 µg/mL.

### 4.9 *In vivo* evaluation of compound 4.2 in the rodent malaria model

Advancement of a potential antimalarial candidate from discovery to pre-clinical development requires a demonstration of *in vivo* efficacy in one or more animal models of malaria.[82] The *in vivo* antiplasmodial activity of compound **4.2** was evaluated using the murine *in vivo* model, where C57 Black6 mice were infected with chloroquine-sensitive *P. bergei* ANKA parasite strain. The compound and controls were all administered by subcutaneous injection. The results for the pure compound, tested at a once-off dose of 100 mg/kg in the *in vivo* assay (Figure 4.6) showed that 60% of the treated mice survived 9 days longer than the control group, indicating some beneficial properties.

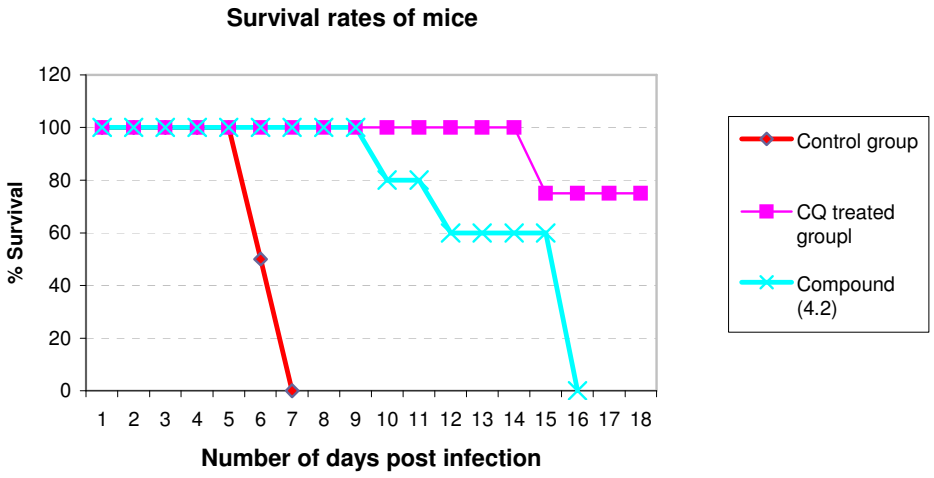


**Figure 4.6. Survival rates of mice following infection with *P. bergei***

[82] FDA Draft Guidance for Industry. Malaria: Developing drug and non-vaccine biological products for treatment and prophylaxis. (2007). CDER: http://www.fda.gov/Cder/guidance/7631dft.pdf. Accessed on 10 October 2008.

The level of parasitaemia in the *P. berghei* infected mice treated with compound **4.2** was exceptionally high, yet survival continued up to day 9 with 60% parasitaemia. All controls with parasitaemia levels of 28% died after day 6. These data have provided the first evidence of the *in vivo* efficacy of compound **4.2**, at least regarding short-term survival of parasitic infection – although evidence of parasitic clearance was not obvious. One can only assume that there may be some suppression of immune response associated with this effect. In the control group, two of the four mice died on day 6 and the remaining animals all perished on day 7.

## 4.10 Discussion

### 4.10.1 Isolation of bioactive compounds and their anticancer activity

Bioassay-guided fractionation of the ethyl acetate extract of *D. anomala* subsp. *gerrardii* using *in vitro* anticancer bioassay (3-cell line panel) resulted in the isolation of two potent sesquiterpenoids **4.2** and **4.3**, which showed approximately 3-fold higher activity than the crude extract. Compound **4.2** also showed the same selectivity trend towards the leukaemia sub-panel in the 60-cell line panel anticancer assay as the crude extract. The *in vitro* activity of compound (dehydrobrachylaenolide) **4.2** in the 60-cell line panel compares well with that of sesquiterpene lactone parthenolide ($GI_{50}$ = 17.9 μM) – a compound currently in clinical development in the form of an amino derivative. The lack of significant *in vivo* activity, revealed through extensive screening of this class of compounds by the NCI, precluded compounds **4.2** and **4.3** from being evaluated further. The poor *in vivo* activity trend of sesquiterpene lactones was attributed mostly to solubility problems.[83]

The solubility of a drug is often found by octanol-water partitioning and determination of the Log *P* value. For any given drug, for uptake to occur through a membrane, it should possess some lipophilic character, but should also possess limited aqueous solubility to allow distribution of the molecule (Log $P < 5$).[59] The octanol-water partition coefficient (measured Log *P*) could not be determined due to the insufficient quantity of the dehydrobrachylaenolide. The calculated Log *P*

[83] Cragg G. M. (2006). Personal communication.

value for compound **4.2** (Log *P* = 1.5) could be used to direct preliminary solubility optimisation studies aimed at improving its drug-like properties. [84]

### 4.10.2 Evaluation of compounds **4.2** and **4.3** for antimalarial activity

Due to the nature of the active compounds isolated from *D. anomala*, the compounds **4.2, 4.3** and the crude ethyl acetate extract were evaluated for a possible antiplasmodial activity *in vitro.* The crude extract, compounds **4.2** and **4.3** were found to exhibit potent activity against the QC-sensitive strain of the parasites (D10) with an SI of 3.7, 11 and 1.5 respectively [SI (chloroquine) > 1 500].[85,86] Based on the yields of the isolated active compounds **4.2** and **4.3** (0.8% and 0.25% w/w crude extract, respectively), the antimalarial activity of the crude extract ($IC_{50}$ = 1.4 ppm) could probably be attributed to these constituents [$IC_{50}$**(4.2)** = 0.38 ppm and $IC_{50}$**(4.3)** = 0.46 ppm]. It is possible that there are other bioactive constituents present in the extract, which may contribute to the overall activity. Furthermore, the activity of the compounds against the QC-sensitive strain (0.38 ppm and 0.46 ppm) is within an order of magnitude of that of the standard agents [$IC_{50}$(chloroquine) = 0.020 ppm; $IC_{50}$(quinine) = 0.063 ppm and $IC_{50}$(artemisinin) = 0.039 ppm].[87] The compound **4.2** was also potent against the K1 (CQ-resistant) strain, showing superior activity against the QC-resistant strain (K1) with an SI of 70, therefore falling well above the acceptable value of 10 for potential development.[86] Compound **4.3** is excluded from further consideration because of the high toxicity, irrespective of a provisional patent on its use, as a very poor selectivity index (SI = 1.5) makes it hardly an attractive candidate as an antimalarial drug. For dehydrobrachylaenolide **(4.2)**, this is a first report of its *in vitro* antiplasmodial activity. The *in vitro* data were sufficient to advance this compound into the *in vivo* model.

---

[84] XLog*P*: A partition coefficient or distribution coefficient that is a measure of differential solubility of a compound in two solvents. PubChem uses version 2 of the algorithm of the reference [Wang R., Gao Y., Lai L. (2000). *Perspectives in Drug Discovery and Design*. **19**, 47–66.] to generate the Xlog*P* value.

[85] Rasoanaivo P, Ratsimamanga-Urverg S., Amanitrahasimbola D., Rafrato H., Rakoto R. -A. (1999). *Journal of Ethnopharmacology*, **64**, 117–126.

[86] Pink R., Hudson A., Mouries M., Bendig M. (2005). *Natural Reviews in Drug Discovery*, **4**, 727–740.

[87] Francois G., Passreiter C. M. (2004). *Phytotherapy Research*, **18**, 184–186.

The efficacy of dehydrobrachylaenolide **(4.2)** was further demonstrated in the *in vivo* murine malaria model. The level of parasitaemia in the *P. berghei* infected mice treated with dehydrobrachylaenolide **(4.2)** was exceptionally high, yet the survival continued up to day 9 with 60% parasitaemia. All controls with parasitaemia levels of 28% died after day 6. This is, however, the first report of the *in vivo* efficacy of dehydrobrachylaenolide.

The clinical efficacy of artemisinin **(5.1)** and derivatives are characterised by an almost immediate effect and a rapid reduction of parasitaemia.[88] This suggests that the mode of action of dehydrobrachylaenolide **(4.2)** is rather different to that of artemisinins. Even though its antiparasitic activity was evident from the *in vitro* studies, the survival of animals with such high parasitaemea levels could be due to the suppression of immune response of a host, which normaly leads to septic shock and death.

Sesquiterpene lactones are well known for their ability to inhibit NF-κB DNA binding, and there is also the published activity of dehydrobrachylaenolide **(4.2)** to inhibit interlukin-1b induced expression of ICAM-1 in the A549 cell line *in vitro*.[53] It was also established that there is an increased expression of ICAM-1 on the endothelial surface of the brain at the ring and trophozoite blood stages of the parasite cycle in the host. Since ICAM-1 is one of the major receptors for sequestration of *P. falciparum*-infected erythrocytes in the brain endothelium, it may be reasonable to hypothesise that dehydrobrachylaenolide **(4.2)** could prevent adhesion of infected erythrocytes to the brain endothelium by inhibiting expression of ICAM-1.[89] Furthermore, in light of the specific mechanism involved, several models for studying malaria *in vivo* were reviewed, and it was found that in the current model with *P. bergei* infected C57BL/b mice, the sequestration of parasitised red blood cells could not be observed.[90] This suggests that the *P. bergei* model, used for evaluation of *in vivo* activity of compound **4.2**, may not be suitable. The fact that parasitaemia at day 9 reached 60% at 100% survival could imply a higher affinity of the drug towards the inhibition of induction of ICAM-1 than

---

[88] Kayser O., Kiderlen A. F., Croft S. L. (2003). *Parasitology Research*, **90**, 55–62.
[89] Tripathi A. K., Sullivan D. J., Stins M. F. (2006). *Infection and Immunity*, **74**, 3262–3270.
[90] Syarifah H. P., Masashi H., Somei K. (2003). *International Immunology*, **15**, 633–640.

towards a parasite-related target. The importance of this possibility warrants seeking a model in which the effect of a drug on the adhesion and sequestration of *P. falciparum*-infected erythrocytes can be observed.

### 4.10.3 Structure-activity relationship considerations for dehydrobrachylaenolide **(4.2)** and other eudesmanolides

Until recently, there was a common perception that STLs are poor drug candidates. One of the early publications by Schmidt stated that STLs as a class, although structurally diverse and with many associated therapeutic uses, do possess unspecific toxicity as alkylating agents, and presumably this precludes any useful application.[40,91] The reactivity of STLs towards sulfhydryl groups is mediated chemically by an *α,β*-unsaturated carbonyl moiety (e.g. *α*-methylene-*γ*-lactone). These functional groups react with biological nucleophiles, such as sulfhydryl groups of cysteine and GSH, by Michael-type addition, thereby inhibiting a variety of cellular functions which directs the cells into apoptosis.[55,91,92,93,94] In the series of eudesmanolides, the principle active centre (against cancer 3-cell lines) was attributed to an *α,β*-unsaturated ketone with an exocyclic methylene grouping, since this can act in the same way as *α*-methylene-*γ*-lactone.[97] This identifies the $O{=}C\text{-}C{=}CH_2$ system as being the necessary component of the structure. This was further supported by the findings of the qualitative structure-activity relationship (QSAR) studies, which indicated that the *α,β*-unsaturated carbonyl groups and an acyl moiety near an exocyclic methylene group correlate with the SAR requirements for cytotoxicity, and therefore it is unlikely to separate the desired therapeutic effect from undesired side effects such as cytotoxicity and allergenicity.[95]

In contrast, a recent study of the dehydrocostus – mokko lactones pair **(4.5a** - **4.5b)** showed that *α*-methylene-*γ*-butyrolactone moiety in dehydrocostus lactone is

---

[91] Schmidt T. J. (1999). *Current Organic Chemistry*, **3**, 577–608.
[92] Picman A. (1986). *Biochemical Systematic Ecology*, **14**, 255–281.
[93] Kupchan S. M., Fessler D. C., Eakin M. A., Giacobbe T. J. (1970). *Science*, **168**, 376–378.
[94] Dirsch V. M., Stuppner H., Ellmerer-Muller E. P., Vollmar A. M. (2000). *Bioorganic & Medicinal Chemistry*, **8**, 2747–2753.
[95] Siedle B., Garcia-Pineres A. J., Murillo R., Schulte-Monting J., Castro V., Rungeler P., Klaas C. A., DaCosta F. B., Kisiel W., Merfort I. (2004). *Journal of Medicinal Chemistry*, **47**, 6042–6054.

responsible for the cytoprotective effect in HepG2 cells.[96] There are other examples of STLs exhibiting high selectivity towards cancer cell lines *in vitro,* such as ludovicins (A, B, C) and parthenolide.[97,98] The above arguments suggested that each compound within the sesquiterpene lactone structural class should be treated individually since compounds with similar structural elements may exhibit vastly different activity profiles.

Enzyme alkylation is the most accepted mode of action reported in the antitumour, antiplasmodial and cytotoxic activities of STLs. It is postulated that for an effective alkylating agent should contain two or more functional groups.[99,100] Some studies showed a correlation between the number of alkylating structural elements and bioactivity.[101] The determination of the structural requirements for malaria/cancer activity was therefore guided by initial studies of the reactivity of dehydrobrachylaenolide **(4.2)** containing three potential alkylating sites (Figure 4.7) towards several essential amino acids such as cysteine, GSH and *N*-acetyl-*L*-cysteine.

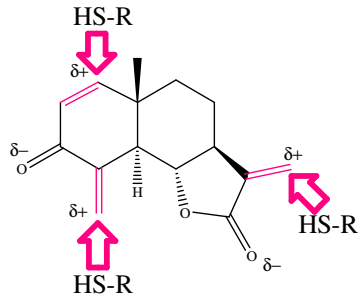


**Figure 4.7. Potential alkylation sites of compound 4.2**

[96] Jeong G. S., Pae H. O., Jeong S. O., Kim Y. C., Kwon T. O., Lee H. S., Kim N. S., Park S. D., Chung H. T. (2007). *European Journal of Pharmacology*, **565**, 37–44.
[97] Lee J. H., Mar T. H., Starnes E. C., El Gebaly S. A., Waddell T. G., Hadgraft R. I., Ruffner C. G., Weidner I. (1977). *Science*, **196**, 533–536.
[98] Guzman M. L., Rossi R. M., Karnischky L., Li X., Peterson D. R., Howard D. S., Jordan C. T. (2005). *Blood*, **105**, 4163–4169.
[99] Stock J. A. (1970). *Chemistry in Britain*, **6**, 11–16.
[100] Warwick G. P. (1968). *Reviews of Pure Applied Chemistry*, **18**, 245–252.
[101] Scotti M. T., Fernandes M. B., Ferreira M. J., Emerenciano V. P. (2007). *Bioorganic & Medicinal Chemistry*, **15**, 2927–2934.

The established reactivity pattern towards amino acids was used to further determine the strategy for our SAR evaluation. Work related to the preparation of amino acid adducts of model STLs and the SAR of some *α*-santonin derivatives is presented in Chapter 5.

### 4.10.4 Drug-likeness and the pro-drugs of STLs

In their natural form, sesquiterpene lactones may be regarded as having low therapeutic potential, especially when applied systemically.[102] This is due to their broad spectrum of biological effects and the lack of predictive selectivity, as well as the multitude of undesired side effects. However, some recent examples of so-called pro-drugs of STLs, namely ambrosin, arglabin, parthenin and parthenolide, reinforce the view of several authors that sesquiterpene lactones could serve as lead compounds for the development of pharmaceuticals.[103,104,105,106,107] Remarkably, the same strategy was involved in the pro-drug preparation for all three drugs and proved effective in the application of anticancer (arglabin and parthenolide) and antimalarial drug-development.

Other than the reactivity and kinetics of binding to biological nucleophiles, some physico-chemical and steric factors also proved important for their biological activity. The lipophilicity, molecular geometry and the chemical environment of the drug and/or a target sulfhydryl may also affect the end result.[108,109] However, the reports relating to the effect of aqueous solubility of STLs on toxicity are inconclusive. For instance, an increase in neurotoxicity accompanies increased lipophilicity in artemisinin derivatives with solubility of less than 50 mg/L (Log *P* > 3), whilst several compounds with a cyclopentanone ring, which varied significantly

---

[102] Willuhn G. (1998). In: L. D. Lawson, R. Bauer (eds), *Phytomedicines of Europe*. American Chemical Society: Washington, DC, ACS Symposium Series, **691,** pp. 118–132.
[103] Hejchman E., Haugwitz R. D., Cushman M. (1995). *Journal of Medicinal Chemistry*, **38**, 3407–3410.
[104] Shaikenov T. E., Adekenov S. M., Williams R. M., Prashad N., Baker F. L., Madden T. L., Newman R. (2001). *Oncology Reports*, **8**, 173–179
[105] Bhonsle J. B., Kamath H. V., Nagasampagi B. A., Ravindrananthan T. (1994). *Indian Journal of Chemistry*, **33**, 391–392.
[106] Hwang D. R., Wu Y. S., Chang C. W., Lien T. W., Chen W. C., Tan U. K., Hsu J. T. A., Hsieh H. P. (2006). *Bioorganic & Medicinal Chemistry*, **14**, 83–91.
[107] Willuhn, G. (1981). *Pharmazie in unserer Zeit*, **10**, 1–7.
[108] Gören N., Woerdenbag H. J., Bozok-Johansson C. (1996). *Planta Medica*, **62**, 419–422.
[109] Hartewell J. L. (1976). *Cancer Treatment Reports*, **60**, 1031–1067.

in lipophilicity, elicited the same cytotoxicity.[92] Therefore an optimum lipophilicity range (Log *P*) should be established for the best systemic activity.

Dehydrobrachylaenolide **(4.2)** could be used as a model to generate more water-soluble pro-drug candidates with possible enhanced bioavailability, which could favourably affect the toxicity-to-bioactivity ratio. This could be achieved by using a known approach similar to the one used in the preparation of water-soluble derivatives of parthenolide. The aim would be to investigate the effect of the addition of secondary amines to the C-11 - C-13 exocyclic double bond of some model STLs on biological activity and toxicity.[106] The solubility will also allow a more accurate assessment of the potency of the compound. Work related to the preparation of water-soluble pro-drug derivatives is presented in Chapter 6.

### 4.10.5 Biosynthesis

Sesquiterpene lactones are plant secondary metabolites that are mainly found in the Asteraceae but also occur infrequently in other higher plant families and lower plants.[110] Sesquiterpene lactones isolated from *Dicoma* species belong to the germacrane framework, and are further divided into to the guaianolide, eudesmanolide, or germacranolide types. It is generally accepted that most known lactones of these three types of sesquiterpene lactones have a common origin in synthesis in the plants, particularly those that co-occur or that are found in plants of close botanical affinity. It is considered plausible to derive some insight into the nature of the reactions involved in the transformation of biosynthetic precursors to complex compounds *via* established pathways, and subsequently by known secondary metabolic alterations. As previously proposed, all STLs from plants are derived from a single acyclic precursor, an activated form of farnesol-farnesyl diphosphate FPP **(4.6a)** *via* the mevalonate-FPP-germacradiene pathway.[111,112,113]

---

[110] Seigler, D. S. (1998). *Plant Secondary Metabolism.* Norwell, MA: Kluwer Academic Publishers, pp. 367–398.

[111] Geissman T. A. (1973). In: V. C. Runeckles, T. J. Mabry (eds), *Recent Advances in Phytochemistry..* California: University of California Press, Vol. **6**, pp. 65–95.

[112] Cane, D. E. (1999). In: D. Barton, K. Nakanishi, P. Meth-Cohn (eds), *Comprehensive Natural Products Chemistry*. Oxford: Pergamon Press, Elsevier, Vol. **2**, pp. 155–215.

[113] Herz W. (1977). In: V. H. Haywood, J. B. Harborne, B. L. Turner (eds), *The Biology and Chemistry of the Compositae.* London: Academic Press, Vol. **1**, pp. 337–357.

The results of a more recent study by Cane suggest that FPP undergoes ionisation followed by electrophilic attack of the resultant allylic cation on the distal double bond to form a 10-membered ring intermediate **4.7a** (Scheme 4.1)**.**[112] The derived cationic intermediate can itself undergo further cyclisations and rearrangements with the reaction being terminated by quenching of the positive charge, either by removal of a proton or capture of an external nucleophile, usually water. Recognising that there is a geometric barrier to direct cyclisation of trans, trans-FPP to 10-membered rings containing a *cis* double bond, it was subsequently proposed that FPP would in such cases undergo an initial isomerisation to the corresponding geometric form.[114]

With regard to further transformations, it was postulated that the majority of STLs are derived from a single germacranolide precursor, (+)-costunolide **(4.1)**,[113,115] the simplest of the sesquiterpene lactones in its relationship to farnesol. The reported biochemical pathway for (+)-costunolide in chicory roots involving various enzymes is shown in Scheme (4.1).[116] Cyclisation of farnesyl diphosphate (FPP) to (+)-germacrene A **(4.8)** is followed by hydroxylation of the isopropenyl side chain, and the oxidation of germacra-1(10),4,11(13)-trien-12-ol **(4.9)** *via* germacra-1(10),4,11(13)-trien-12-al **(4.10)** to form germacra-1(10),4,11(13)-trien-12-oic acid **(4.11)**. The postulated hydroxylation at the C-6 position of germacratrien-12-oic acid **(4.12)** and subsequent lactonisation yield (+)-costunolide **(4.1)**. The primarily formed cation **4.7a** could also be deprotonated to yield germacrene D **(2.5)**, previously isolated from *D. anomala,* after hydride migration to cation **(4.14)** and subsequent conformational change from cisoid structure **(4.15)** to transoid **(2.5)**.[9,117] According to currently accepted hypotheses, in addition to *trans*-FPP **(4.6a)** and *cis*-FPP, nerolidyl diphosphate (NDP) may also be a precursor in the enzymatically catalysed formation of sesquiterpenes in order to allow adequate alignment of p-orbitals for the formation of products with *cis*-double bonds.[118] However, there is not enough evidence to imply a mevalonate pathway to the

---

[114] Andersen N. H., Ohta Y. (1978). *Bioorganic Chemistry*, **2**, 1–37.
[115] Fischer, N. H. (1990), In: G. Towers, H. Towers (eds), *Biochemistry of the Mevalonic Acid Pathway to Terpenoids*. New York: Plenum Press, pp. 161–201.
[116] De Kraker J. -W., Franssen M. C., Dalm M. C., De Groot A., Bouwmeester H. J. (2001). *Plant Physiology*, **125**, 1930–1940.
[117] Bülow N., König W. A. (2000). *Phytochemistry*, **55**, 141–168.
[118] Cane D. E. (1985). *Accounts of Chemical Research*, **18**, 220–226.

formation of germacrene D **(2.5)** in *D. anomala* as it is also known to be formed *via* the methylerythritol phosphate pathway (mevalonate-independent pathway).[119]

Based on the previous study of a large number of stereospecific biomimetic transformations of germacranolides and their derivatives into eudesmanolides and guaianolides, it has been postulated that this second cyclisation, leading to eudesmanolides and guaianolides, is directed by C-1 - C-10 and C-3 - C-4 epoxidations respectively.[115]

*4.10.5.1 Biosynthesis of dehydrobrachylaenolide **(4.2)***

Eudesmanolides may be derived from germacranolides containing C(1)-C(10)-epoxide moiety.[115] Epoxidation, followed by acid-catalysed opening of the oxirane, allows either an $E_1$ elimination generating the allylic alcohol artemorin **(4.18a)** or its epimer **(4.18b)**. Alternatively, the intermediate cation **(4.17a)** and **(4.17b)** may be trapped resulting in the formation of a fused 6,6-ring system characteristic of the eudesmanolides. The resultant tertiary cation loses a proton to generate a tri-substituted double bond leading to douglanin **(4.19a)** or santamarine **(4.19b)** with the biosynthetic difference between the two considered to be in the initial epoxidation. The douglanin **(4.19a)** could be derived directly from artemorin **(4.18a)** *via* an acid-catalysed process.[111] The regiochemistry of double bond formation avoids the ring strain of introducing a $sp^2$ centre at a ring junction and the thermodynamically less stable exocyclic double bond. These species can then undergo epoxidation generating ludovicin A **(4.20a)** and its epimer **(4.20b)**. Reynosin **(4.19c)** and ridentin B **(4.20c)** are thought to be derived from known allylic alcohol species **4.18b**. The introduction of a 3-hydroxy group as in 3*α*-hydroxyreynosin **(4.21b)**, or the 3-keto group of ludovicin C **(4.22a)** can be accomplished by ring opening of a 3,4-epoxide.[111]

[119] Steliopoulos P., Wüst M., Adam K. P., Mosandl A. (2002). *Phytochemistry*, **60**, 13-20.

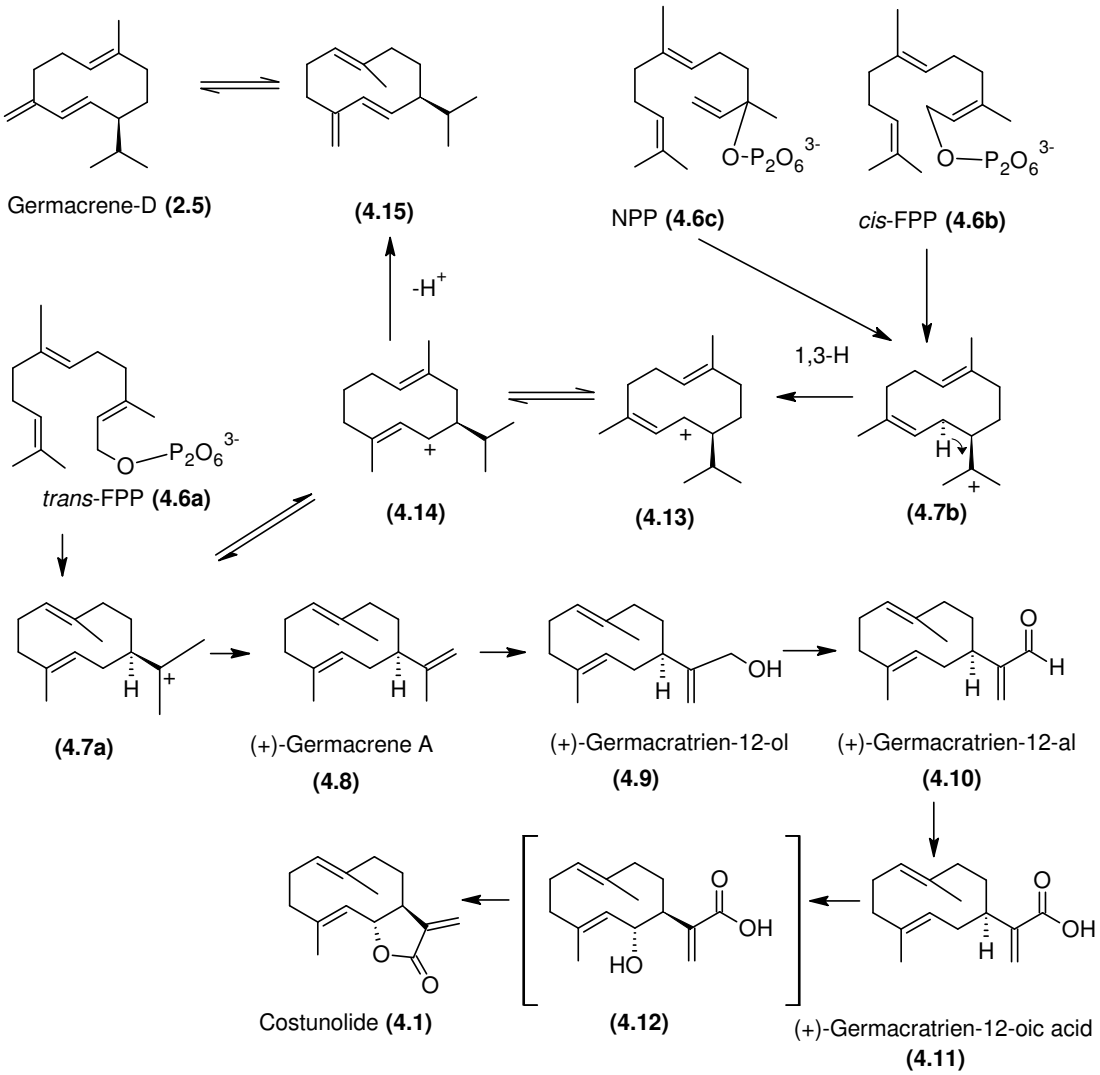


**Scheme 4.1. Reported pathway for biosynthesis of STLs in chicory[120]**

Rearrangement of the epoxides can also generate ludovicin B **(4.21a)** or 3*α*-hydroxyreynosin **(4.21b)** if we implicate the more spatially available methyl group (kinetic process). These can undergo dehydration, generating brachylaenolide **(2.43)** and tuberiferin **(2.41)** respectively, or oxidation resulting in ludovicin C **(4.22a)**, with the *β*-hydroxyketone functional group, which is susceptible to acid-catalysed elimination, generating the sesquiterpene lactone dehydrobrachylaenolide **(4.2)**, the subject of the current body of work. Dehydration of ludovicin A **(4.20a)** before rearrangement of the epoxide cannot be excluded in the generation of brachylaenolide **(2.43)**. Introduction of the 3*β*-hydroxy group in

[120] De Kraker J. W., Franssen C. R., De Groot A., König W. A., and Bouwmeester H. J. (1998). *Plant Physiology*, **117**, 1381–1392.

ridentin **(4.20c)** *via* an alternative process followed by oxidation to β-hydroxyketone resulting in artecalin **(4.22b)** could also lead to dehydrobrachylaenolide **(4.2)**.

Taking into account that costunolide was never isolated from *Dicoma* sp., and that the 14,15-hydroxy compounds are characteristic of the genus, it is possible that enzymatic hydroxylation occurs prior to any further transformation of costunolide. An alternative biosynthetic path is proposed in Scheme 4.3. The hydroxylation at C-1 occurs through 1,3-allylic rearrangement of the primary alcohol at C-14, yielding compounds **4.24a** or **4.24b**, followed by the protonation of the exocyclic double bond, which in turn leads to 6,6-cyclisation *via* proton transfer (most likely the C-3 proton) to yield 15-hydroxydouglanin **(4.26a)** or 15-hydroxysantamarine **(4.26b)**, which can undergo a second 1,3-allylic rearrangement to yield dihydroxy-dienes **(4.21a-c)**.

Even though any of these routes is chemically possible, only albicolide **(2.19)** of the most likely intermediates has been previously isolated from the *Dicoma* species. Since several compound pairs in Scheme 4.2 were isolated from a single plant species *Tanacetum praeteritum* subsp. *praeteritum*[108] (e.g. douglanin – santamarin; reynosin - 3*α*-hydroxyreynosin), it is possible that all the proposed synthetic routes co-exist in the same plant. Further phytochemical studies are required to establish the biogenesis of *Dicoma* sesquiterpene lactones.

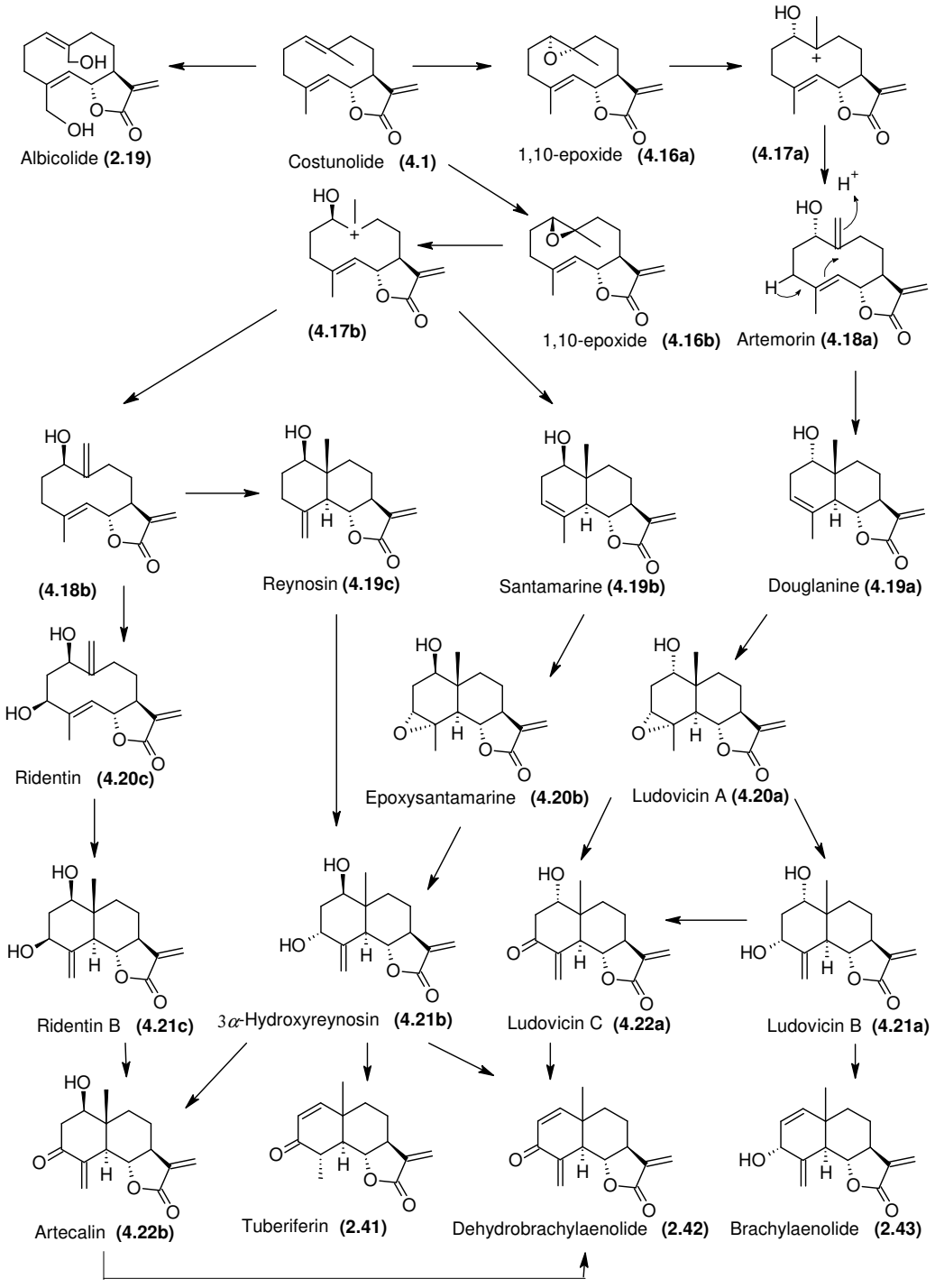


**Scheme 4.2. Proposed biosynthetic pathways to the eudesmanolides from (+)-costunolide**

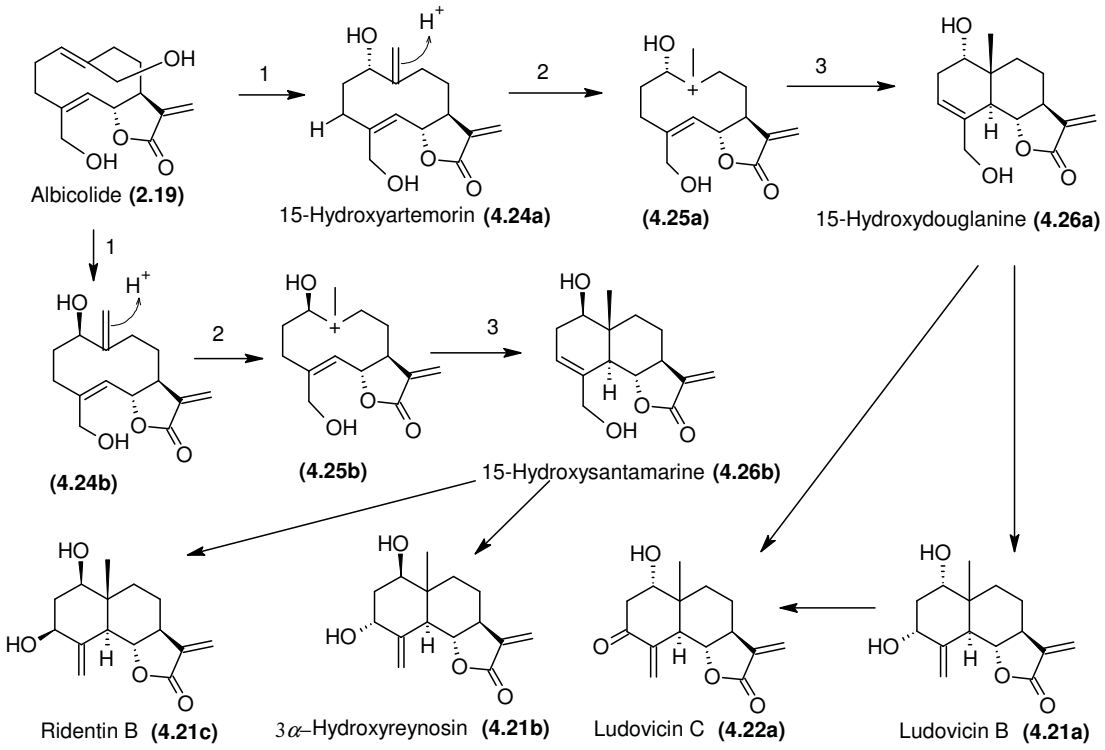


**Scheme 4.3. Proposed biosynthetic pathways to the eudesmanolides from costunolide *via* albicolide**

*4.10.5.2 Biosynthesis of the guaianolide dimer **4.3***

The structure of the bissesquiterpenoids, the carbon skeleton of which consists of 30 atoms, was considered as the product of the Diels-Alder [4+2] cyclo-addition of two sesquiterpenoid molecules with subsequent dehydration (Scheme 4.3). It may be assumed that in the plant it is formed as the result of the diene synthesis between dehydrozaluzanin C **(2.33)** corresponding to **fragment 1**, and another guaianolide **(4.38)** corresponding to **fragment 2.** This hypothesis is partially confirmed by the reported isolation of dehydrozaluzanin C from another subspecies of *D. anomala*, but it has not yet been possible to isolate the guaianolide corresponding to **fragment 2**.

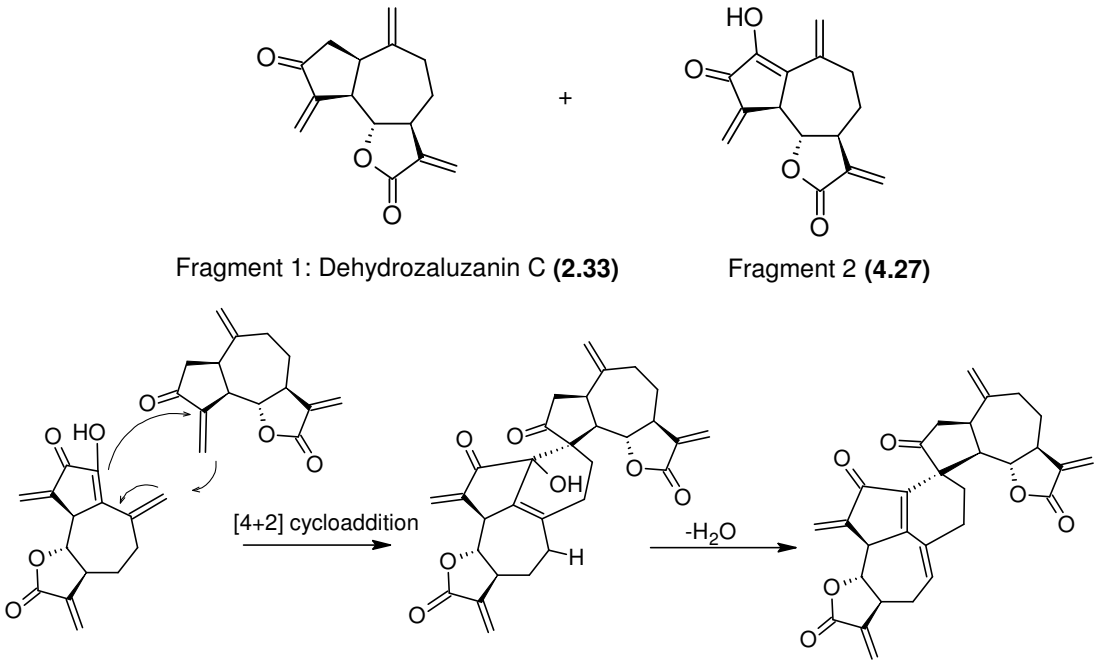


Fragment 1: Dehydrozaluzanin C **(2.33)** Fragment 2 **(4.27)**

**Scheme 4.4. Proposed precursors of guaianolide dimer 4.3**

Following the argument as for biosynthesis of eudesmanolides, the C-4 - C-5 epoxide of the germacradienolide **4.16c** would be cyclised into the guaianolide skeleton (Scheme 4.4). After several biosynthetic steps following the second cyclisation, cumambrin B **(4.28)** or 8-desoxycumambrin B **(4.29)** could probably serve as a precursor of this group of guaianolides.[111,121] The cumambrin B **(4.28)** appears to have arisen by stereospecific oxidative closure of the costunolide-like ring, or it could also be derived directly from the dehydrocostus lactone. Its presence in *D. anomala* subsp. *gerrardii* is yet to be established to support this hypothesis.

[121] Bohlmann F., Ang W., Trinks C., Jakupovic J., Huneck S. (1985). *Phytochemistry*, **24**, 1009–1015.

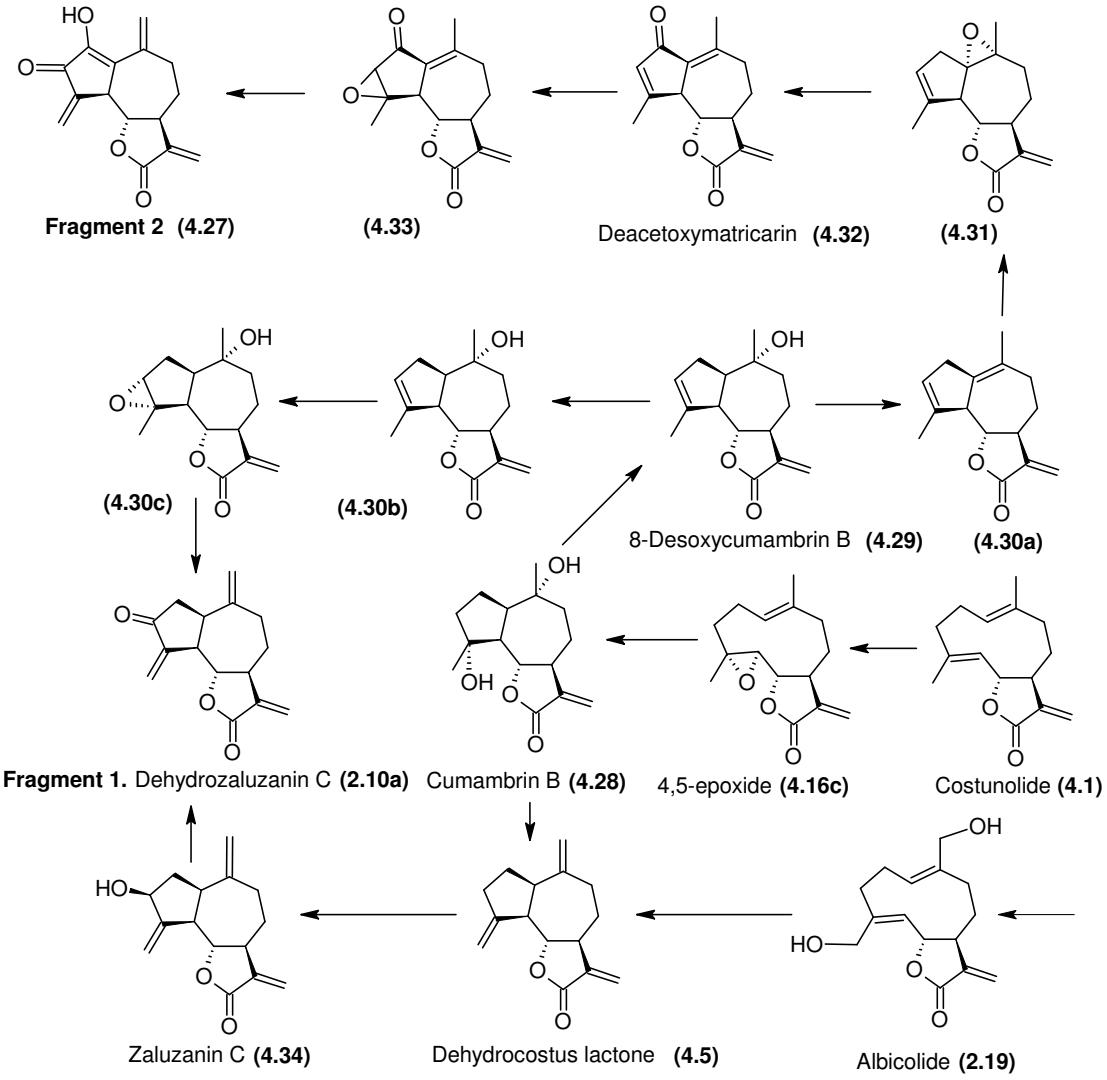


**Scheme 4.5. Proposed biosynthetic pathways to the guaianolide fragments from (+)-costunolide**

Consequently, it appears likely that the required biosynthetic machinery to produce the required precursors for the C-30 compound **4.3** is present in the *Dicoma* spp. of interest. The postulated Diels-Alder type cycloaddition could then proceed either in the presence or absence of a controlling enzyme – the electron densities of the coupling partners being favourably matched. It is possible that the plant may utilise this dimerisation process to detoxify the compounds by removal of some conjugating capability in times of over-accumulation or over-expression.

# Chapter 5: Reactivity of sesquiterpene lactones towards biological nucleophiles – structure-activity relationships of some natural and synthetic eudesmanolides

## 5.1 Literature overview of the biological activities of eudesmanolides

The dehydrobrachylaenolide **(4.2)**, isolated from the extract of roots of *D. anomala* subsp. *gerrardii*, has shown potent *in vitro* activity against cancer cell lines and against *P. falciparum*. The compound has also shown an unusual activity profile in the *in vivo* murine malaria model.

There is a common perception that the structural requirements of sesquiterpene lactones (STLs), necessary for bioactivity, are the same as for cytotoxicity, tagging the entire class with limited pharmacological applicability. Even though a large number of STLs lack selectivity *in vitro*, recently several STLs have made it to the market. The best examples, as seen from the literature review, are the registered drugs artemisinin **(5.1)** for treatment of malaria and arglabin **(5.2)** for treatment of cancer. Another plant-derived STL, parthenolide **(5.3)**, has been recently advanced into the Rapid Development Programme (RADP) by the NCI as an antileukaemic drug candidate due to its unique mode of action.[122]

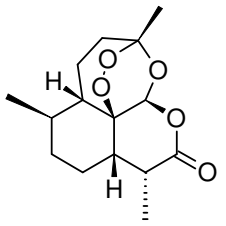

Artemisinin **(5.1)**

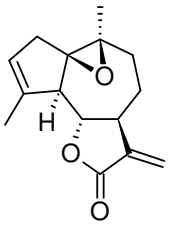

Arglabin **(5.2)**

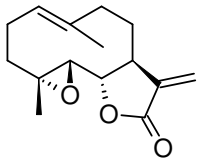

Parthenolide **(5.3)**

Generally, most of the observed biological effects of STLs have been attributed to their capability to deactivate enzymes and other essential proteins by the formation of covalent bonds with free sulfhydryl groups, such as cysteine (CYS) residues in such polypeptides, resulting in alkylation of these groups. In general,

[122] Guzman M. (2005). Blood. online edition (www.webmd.com/content/Article/101/106103.htm).

STLs have been demonstrated to inhibit a variety of important sulfhydryl-bearing enzymes (phosphofructokinase, glycogen synthase, inosine monophosphate dehydrogenase and others), leading to cellular dysfunction or death.[55] The mechanism is believed to be based on Michael-type addition of the free thiol groups of proteins to *α,β*-unsaturated carbonyl structures of STLs.[91] The dehydrobrachylaenolide **(4.2)** possesses an endo-exo cross-conjugated cyclohexadienone structure in the A ring, in addition to the *α*-methylene-*γ*-lactone, thus altogether containing three electrophilic sites which qualify as Michael reaction acceptors (MRAs).[53]

MRAs can undergo nucleophyllic addition to thiol groups of biomolecules such as glutathione (gly-cys-γ-glu or GSH). The bioactivities of STLs are known to be neutralised by cellular GSH, which is able to bind to *α*-methylene-*γ*-lactones and thereby inactivate their biological activity.[123,124] However, substantial depletion of intracellular GSH by STLs did not lead to loss of cell viability and to a significant deactivation of such drugs, as reported in another study.[95] It was also shown that cellular GSH depletion by STLs can chemosensitise tumour cells to oxidative damage. This sensitisation was shown to correlate to the rate of GSH resynthesis in the cells.[125] Furthermore, GSH-STL conjugates were found to be capable of deactivating vital cellular proteins, as it appears, by an entirely different mechanism to that of free STL.[126]

Michael receptor acceptors are also able to act as inducers of phase II enzymes, thus having a potential for cytoprotection. In turn, the potency of Michael reaction acceptors as inducers of phase II enzymes depends on their reactivity towards sulfhydryl groups.[127] Several studies have clearly demonstrated that reaction of STLs with sulfhydryl reagents such as cysteine and GSH can be reversible, and that the reaction kinetics depends on the number and type of the *α,β*-unsaturated

---

[123] Kawai S., Kataoka T., Sugimoto H., Nakamura A., Kobayashi T., Arao K., Higuchi Y., Ando M., Nagai K. (2000). *Immunopharmacology*, **48**, 129–135.
[124] Taniguchi M., Kataoka T., Suzuki H., Uramoto M., Ando M., Arao K., Magae J., Nishimura T., Otake N., Nagai K. (1995). *Biosciences, Biotechnology and Biochemistry*, **59**, 2064–2067.
[125] Arrick B. A., Nathan C. F., Cohn Z. A. (1983). *The Journal of Clinical Investigation*, **71**, 258–267.
[126] Schmidt T. J. (2000). *Planta Medica*, **66**,106–109.
[127] Dinkova-Kostova A. T., Massiah M. A., Bozak R. E., Hicks R. J. (2001). *Proceedings of the National Academy of Sciences of the United States of America,* **98**, 3404–3409.

carbonyl sites, the pH of the medium, the concentration of thiol and the character of sulfhydril target structures.[128] For instance, at physiological pH, the rate of GSH and CYS addition to the exocyclic methylene group of helenalin is much higher than addition to the endocyclic cyclopentanone double bond, with the latter reaction being completely reversible at physiological pH.

It was also noticed that another antioxidant sulfhydryl-containing amino acid, which increases intracellular GSH levels, *N*-acetyl-*L*-cystein (NAC) can neutralise the bioactivity of STLs. NAC is a generically available nutritional supplement which has been demonstrated to increase intracellular-reduced and total glutathione by 92% and 58% respectively.[129] For instance, costunolide-induced apoptosis in human leukaemia U937 cells was almost completely blocked by the addition of NAC.[130] Furthermore, parthenolide-mediated apoptosis, correlated with reactive oxygen species (ROS) generation, was completely inhibited by NAC.[131]

Multiple studies into structure-activity relationships (SAR) of STLs are reported. Some are significant to the present discussion. As it was realised that the effect of a given STL on the cell may vary from cytoprotection to induction of apoptosis and that this variation is determined by actual STL, the cell type and the environment, the SAR was reviewed within a narrow group of structurally related STLs of eudesmanolide skeleton in the selected bioassays. *In vitro* growth inhibition of cancer cells and of *P. falciparum* was examined. The inhibition of induction of ICAM-1 was also considered because of its relevance to dehydrobrachylaenolide **4.2**, and because of its implication in pathologies associated with cancer and malaria.

---

[128] Heilmann J., Wasescha M. R., Schmidt T.J. (2001). *Bioorganic & Medicinal Chemistry*, **9**, 2189-2194.
[129] Yim C. Y., Hibbs Jr J. B., McGregor J. R., Galinsky R. E., Samlowski W. E. (1994). *The Journal of Immunology*, **152**, 5796-5805.
[130] Choi J. -H., Ha J., Park J. -H., Lee J.Y., Lee Y. S., Park H. -J., Choi J. -W., Masuda Y., Nakaya K., Lee K. -T. (2002). *Japanese Journal of Cancer Research*, **93**, 1327-1333.
[131] Wang W., Adachi M., Kawamura R., Sakamoto H., Hayashi T., Ishida T., Imai K., Shinomura Y., (2006). *Apoptosis*, **11**, 2225-2235.

### 5.1.1 Anticancer activity of eudesmane STLs

Although various modes of action have been suggested to account for some biological activities of STLs, the exact mechanism of their anticancer activity has not been sufficiently explained.[132] Several eudesmane compounds isolated from *Tanaceum praeterium* subsp. *praeterium* were tested against the human lung carcinoma cell line $GLC_4$ and the colorectal cancer cell line COLO 320.[108]

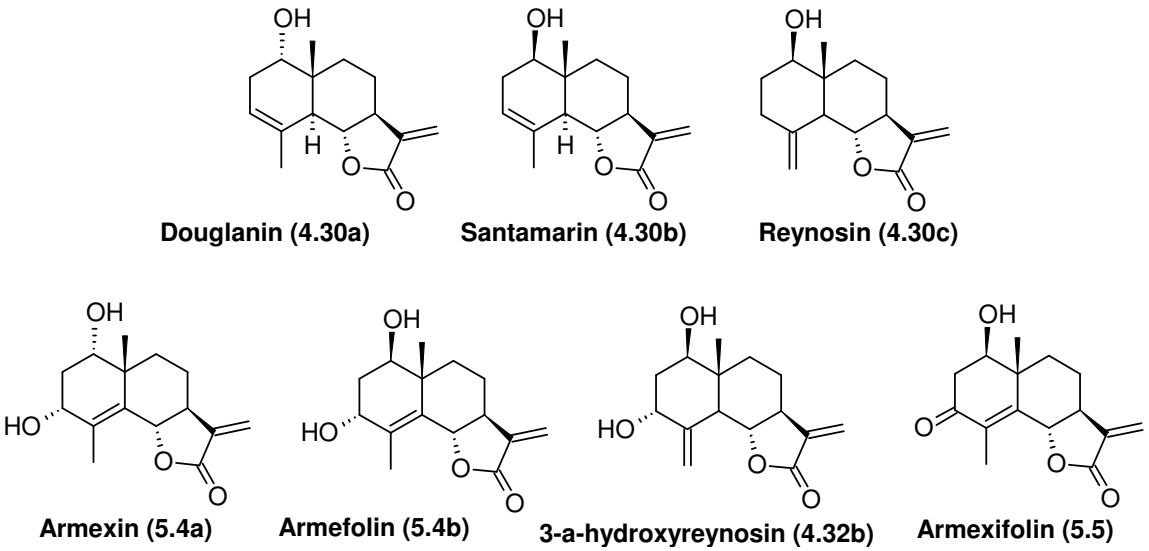


**Figure 5.1. STLs evaluated for activity against $GLC_4$ and COLO320 cell lines**

The SAR for this series of compounds can be summarised as follows: in the mono-hydroxy eudesmanolides (**4.30a**, **4.30b**, **4.30c** and **5.5**) the spatial orientation of the C-1-OH group does not effect the activity [$IC_{50}$ **(5.4a)** = 7.8 µM ($GLC_4$), 8.1 µM (COLO 320); $IC_{50}$ **(4.30b)** = 8.1 µM (GLc4), 7.4 µM (COLO320); $IC_{50}$ **(4.30c)** = 10.7 µM ($GLC_4$); 8.9 µM (COLO320)], but the presence of a conjugated enone element in compound **5.5** causes a 2 - 4 times increase in growth inhibitory concentration [$IC_{50}$ **(5.5)** = 2.5 µM ($GLC_4$); 4.3 µM (COLO 320)]. The difference in spatial orientation of the C-1-OH group in the dihydroxy compounds caused some activity variation (50%), with *α*H-1 and *α*H-3 showing superior activity. The shift of a double bond [exo-endo: C-4 - C-15 to C-4 - C-5],

[132] Ma G., Khan S. I., Benavides G., Schühly W., Fischer N. H., Khan I. A., Pasco D. S. (2007). *Cancer Chemotherapy and Pharmacology,* **60**, 35–43.

however, had no significant effect on activity in pairs of isomers **4.30b** – **4.30c** and **5.4b** – **4.32b** [$IC_{50}$ **(5.4)** = 15.2 μM (GLc4), 8.1 μM (COLO320); $IC_{50}$ **(4.32b)** 16 μM (GLc4), 18.2 μM (COLO320)]. It is noteworthy that a vastly different bioactivity relationship exists for the santamarin **(4.30b)** - douglanin **(4.30a)** pair evaluated in the NF-κB DNA binding assay, with santamarin showing 3-fold stronger activity [$IC_{100}$ **(4.30b)** = 100 μM; $IC_{50}$ **(4.30a)** = 300 μM].[95]

The results of *in vitro* evaluation of a range of synthetic eudesmane compounds (Figure 5.2) against murine lymphocytic leukaemia P388 are also reported.[133,134]

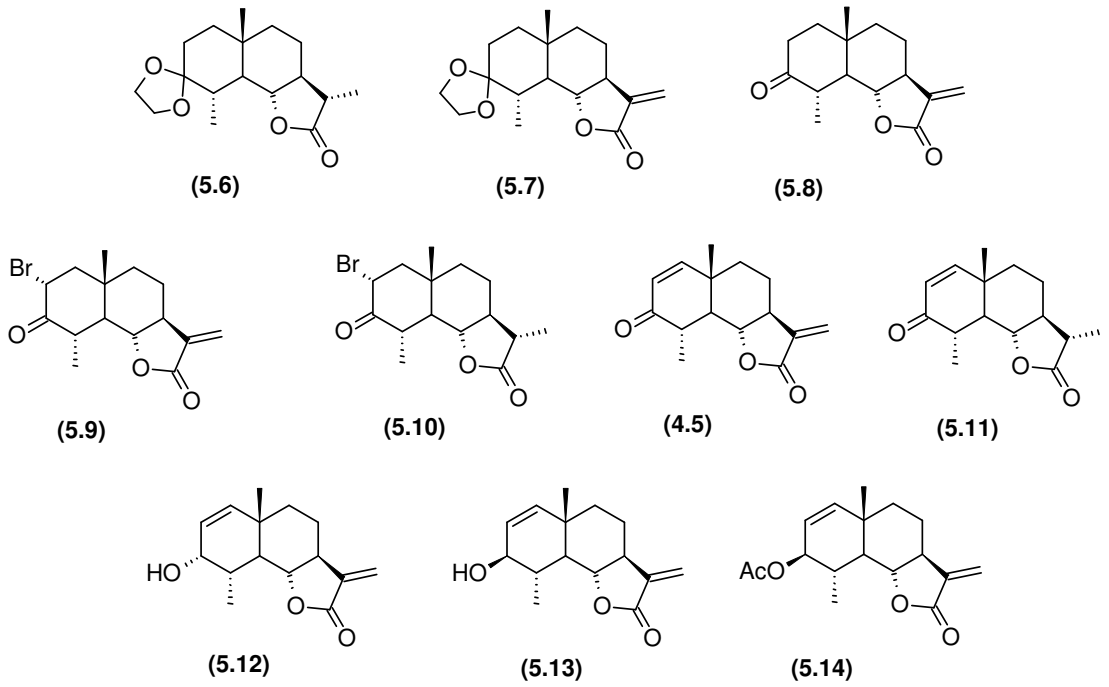


**Figure 5.2. STLs evaluated for activity against P388 lymphocytic leukaemia**

Overall, the *α*-methylene-*γ*-lactones showed stronger activity than the corresponding saturated *α*-methyl-*γ*-lactones. The C-3 acetal **(5.7)** exhibited a 4-fold stronger activity [$GI_{50}$**(5.7)** ~ 0.5 ppm] than its keto precursor [$GI_{50}$**(5.8)** ~ 2 ppm]. The *α*-bromo ketone **(5.9)** was the most active compound in the series,

[133] Ando M., Wada T., Kusaka H., Takase K., Hirata N., Yanagi Y. (1987). *Journal of Organic Chemistry*, **52**, 4792-4796.
[134] Ando M., Isogai K., Azami H., Hirata N., Yanagi Y. (1991). *Journal of Natural Products*, **54**, 1017–1024.

followed by tuberiferine **(2.41)**, and a 20-fold decrease in activity was observed in compound **(5.11)** due to the saturation of α-methylene of the lactone [$IC_{50}$**(5.11)** < 0.1 ppm; $IC_{50}$**(2.41)** ~ 0.3 ppm]. Interestingly, the *α*-bromo ketone **5.10**, possessing a saturated α-methyl-γ-lactones moiety, showed significant growth inhibitory activity when compared to compounds **5.9** and **5.11** [$IC_{50}$**(5.10)** ~ 0.5 ppm]. The spatial orientation of the C-3-hydroxy group in compounds **5.12** and **5.13** had a 10-fold activity difference, with the *α*-hydroxy compound being more active than its epimer [$GI_{50}$**(5.12)** ~ 0.1 ppm; $GI_{50}$**(5.13)** ~ 1 ppm]. However, the acetate of the β-hydroxy compound showed activity of the same order of magnitude as the α-hydroxy compound **5.12**.

In addition, several synthetic eudesmane compounds were tested for activity against human epidermoid nasopharynx carcinoma (KB) cells *in vitro.*[135]

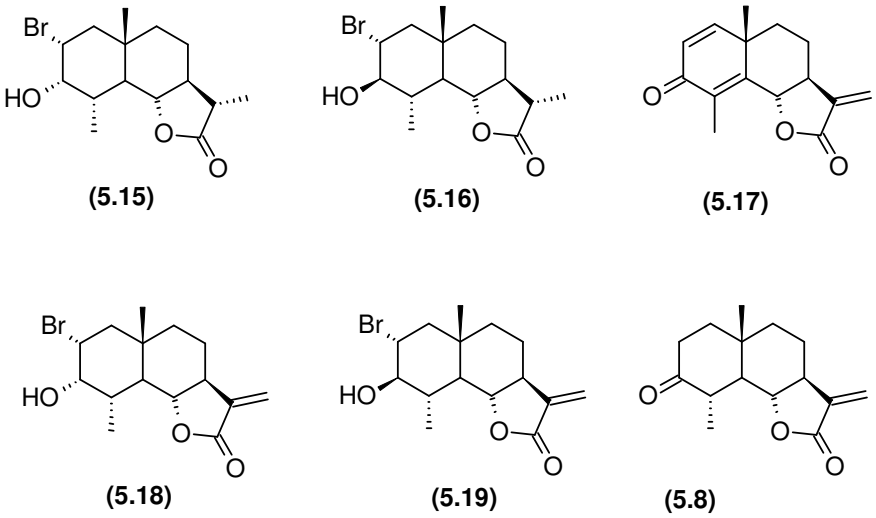


**Figure 5.3. STLs evaluated for activity against KB tumour cells**

In the 2-bromo-3-hydroxy-compounds **5.15** - **5.16** with saturated C-11 - C-13 bond, the orientation of the hydroxy group markedly influenced the bioactivity. For 2*α*-bromo-3*α*-hydroxy-*α*-methyl-*γ*-lactone **(5.16)** the activity was almost as high [$GI_{50}$ = 0.56 ppm] as that of a doubly conjugated C-3-keto compound **5.17** with an *α*-methylene-*γ*-lactone moiety [$GI_{50}$ = 0.48 ppm], whilst its 3-*β*OH epimer was

[135] Rossi C., Ambrogi V., Grandolini G., Scarcia V., Furlani A. (1986). *Journal of Pharmaceutical Sciences*, **75**, 784–786.

found to be completely inactive.[133,135] In the unsaturated 2-bromo-3-hydroxy-*α*-methylene-*γ*-lactones **5.18** - **5.19**, the orientation of the 1-OH group was to a less significant extent (10-fold). In 2*α*-bromo-3*α*-hydroxy-*α*-methyl and 2*α*-bromo-3*α*-hydroxy-*α*-methylene-*γ*-lactones, the bromine and hydroxy groups are located on the same face of the molecule. Thus the hydroxy group assumes an axial position while the bromine remains equatorial. Such an antiperiplanar arrangement between *β*H-2 and the hydroxy group makes the structure highly susceptible to elimination. In the 2-bromo-*α*-methyl-*γ*-lactone range of eudesmanolides, *α*-bromo and -*β*OH are on opposite faces and both assume equatorial positions. This conformation is considered more stable, which may adequately account for the drop in bioactivity.

### 5.1.2 SAR against *P. falciparum*

In the series of STLs isolated from *Eupatorium semialatum* Benth. (Figure 5.4) the configuration of the cyclohexane ring system was found to have an effect on their antiplasmodial activity against a chloroquine-sensitive strain (CQS) of the parasite (pLDH-assay).[47,136] All the active compounds within the series contained structural elements that assumed a full chair conformation. The activity of the compounds with different geometry of the A ring fell into a much lower range. A shift of the C-4 - C-5 endocyclic methylene group to a C-4 - C-15 exocyclic position led to decreased activity [$IC_{50}$**(5.20)** = 27 µM; $IC_{50}$**(5.21)** = 16.3 µM; $IC_{50}$**(5.22)** = 13.3 µM; $IC_{50}$ (CQ) = 0.18 µM].

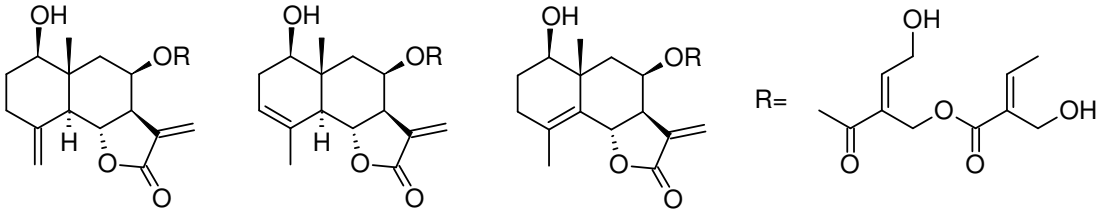


**(5.20)** **(5.21)** **(5.22)**

**Figure 5.4. Eudesmanolides evaluated for activity against *P. falciparum***

[136] Lang G., Passreiter C. M., Wright C. W., Filipowicz N. H., Addae-Kyereme J., Medinilla B. E., Castillo J. J. (2002). *Zeitschrift für Naturforschung*, C, **57**, 282-286.

The overall activity of these compounds was by two orders of magnitude less potent than CQ itself.

### 5.1.3 SAR of eudesmane STLs as inhibitors of induction of the intracellular adhesion molecule-1

The eudesmane STLs were screened for their inhibitory activity on the induction of intracellular adhesion molecule-1 (ICAM-1) through an *in vitro* model of human endothelial cells A549 (lung carcinoma) by a group of Japanese researchers.[53,123]

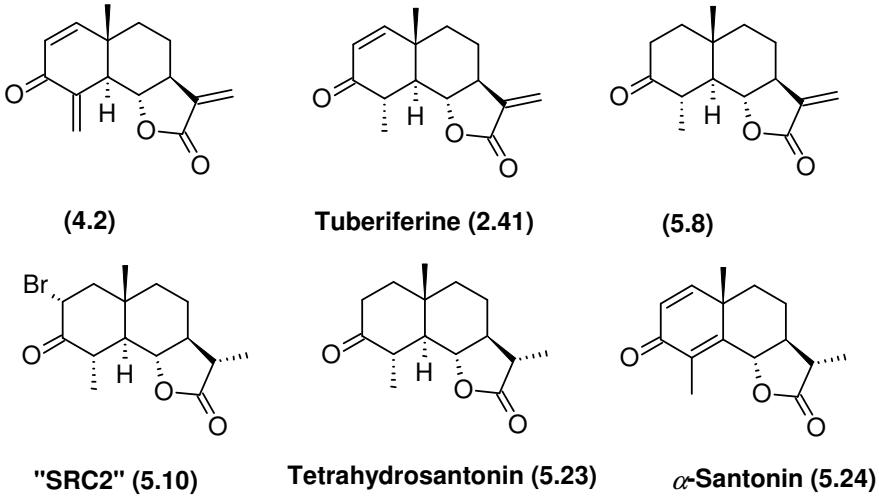


**Figure 5.5. Structures evaluated for inhibitory activity of ICAM-1 induction**

The activity within the series ranged from $IC_{50}$ = 3-1000 µM, with DHB **(4.2)** being the most active, and tetrahydrosantonin **(5.23)** the least active compound [$IC_{50}$ > 1000 µM]. In another study by Dirsch, a compound coded "SRC2" **(5.10)** [$IC_{50}$ = 5.6 µM], with toxic concentration to normal A459 cells [$IC_{50}$ > 100 µM], was almost as active as DHB **(4.2)**, whilst *α*-santonin **(5.24)** showed no activity [$IC_{50}$> 100 µM].[94,123] The toxicity of DHB **(4.2)** was more than double that of "SRC2" [$IC_{50}$ (A459) = 55 µM], but their selectivity index (SI) was very similar [SI~20]. Compounds which lacked an *α*-methylene-*γ*-lactone moiety, appeared to inhibit the signalling pathway that triggered nuclear translocation of NF-κB. However, STLs containing an α-methylene-γ-lactone moiety, seemed to control the same pathway by a different mechanism, which is apparently upstream from the nuclear translocation.

### 5.1.4 SAR summary

Although the structural requirements for the antitumour and antiplasmodial activity of some STLs have been postulated, the overall impression from the literature studies is that these compounds cannot be generalised even within their class (e.g. eudesmanolides). Different bioactivities have different structural requirements.[94] The SAR is highly dependent on the spatial and physicochemical characteristics of a candidate compound in relation to the target/targets. Different alkylating sites within a given molecule may have entirely different effects on targets, thus certain selectivity can be assumed. The number of potential alkylating centres, however, is well correlated with the activity trend in non-halogen containing compounds. Structures containing an *α*-methylene-*γ*-lactone moiety should be treated separately from their *α*-methyl-*γ*-lactone containing counter-structures when the SAR is reviewed.

Briefly it can be said that bioactivities of STLs depend on a specific mechanism and often show considerable selectivity towards the target, thus leaving a "therapeutic window" between activity and toxicity. Even though some direction of the SAR can be derived from the literature studies in Chapter 3 and the present background study, further work is required to derive the SAR for compound **4.2** and its congeners.

## 5.2 Objectives

The reactivity and selectivity of the three potential alkylating structural elements in DHB towards biological thiols was not previously studied. One of the main objectives of the work presented in the following sections was to establish a correlation of alkylatable functionality of compound **(4.2)** and its biological activities. Preparation of amino acid adducts of some STLs, and the detection and characterisation of the reaction products constitutes the first part of this chapter. Due to the limited quantity of compound **(4.2)**, only preparation of *L*-cysteine adduct was attempted. Further reactivity towards amino acids was studied using the readily available, structurally related synthetic compound **5.17**. The literature

review revealed that compound **5.17** is patented for its use as an antileukaemic agent,[137] but no reports related to *P. falciparum* have been found to date.

A second objective was to establish structure-reactivity relationships of the two sesquiterpene lactones **4.2** and **5.17**. Several target structures were identified (Figure 5.6) for the study of the SAR. Due to the low yields and limited quantity of compound **4.2**, *α*-santonin **(5.24)** was identified as an alternative scaffold for structural manipulation.[133,138]

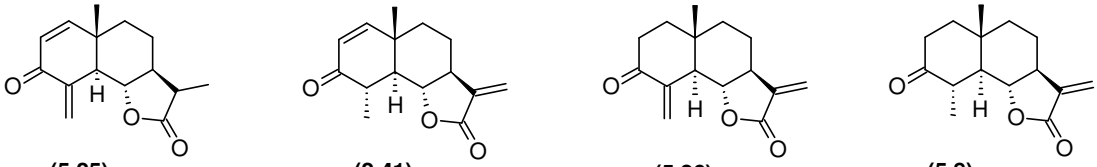

**(5.25)** **(2.41)** **(5.26)** **(5.8)**

**Figure 5.6. STLs selected for SAR**

Furthermore, reduction of compounds **4.2** and **5.17** was attempted in order to obtain some of the targeted compounds for the SAR study. The final selection of STLs used in the SAR study was based mainly on the availability of the compounds.

## 5.3 NMR assignments for (6*β*)- 3-oxoeudesm-1,4,11-trien-6,12-olide (5.17)

The Discovery Chemistry group of the CSIR provided compound **5.17** in ample quantities. The compound resulted from an attempted synthesis of dehydrobrachylaenolide **(4.2)**, as a thermodynamically more stable isomer.

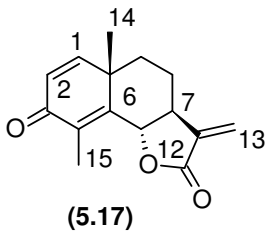


**(5.17)**

[137] Adenkov S. M. (2000). Arglabin compounds and therapeutic uses thereof. US Patent 6,020,365.
[138] Yamakawa K., Nishitani K., Tominaga T. (1975). *Tetrahedron Letters*, **33**, 2829–2832.

**Table 5.1. $^{1}H$ and $^{13}C$ NMR data for compound 5.17 in $CDCl_3$**

| Atom number | Assigned multiplicity | $\delta_C$ | $\delta_H$ (multiplicity), J (Hz) | Published data[135] | |
|---|---|---|---|---|---|
| | | | | $\delta_C$ | $\delta_H$ (multiplicity), J (Hz) |
| 1 | CH | 154.6 | 6.2 (d), J = 9.6 | 154.0 | 6.20 (d), J = 9.6 |
| 2 | CH | 126.2 | 6.66 (d), J = 9.6 | 124.6 | 6.67 (d), J = 9.6 |
| 3 | C | 186.4 | - | 184.9 | - |
| 4 | C | 129.2 | - | 127.3 | - |
| 5 | C | 150.9 | - | 150.0 | - |
| 6 | CH | 81.6 | 4.72 (dd), J = 12.0; 0.5 | 80.3 | 4.70 (dd), J =12.0; J = 0.5 |
| 7 | CH | 50.5 | 2.65 | 49.1 | Not reported |
| 8 | $CH_2$ | 21.9 | Ha 1.72 (m); Hb 2.18 (m) | 20.4 | Not reported |
| 9 | $CH_2$ | 37.9 | Ha 1.55 (m); Hb 1.9 (m) | 36.5 | Not reported |
| 10 | C | 41.5 | - | 40.3 | - |
| 11 | C | 137.9 | - | 136.4 | - |
| 12 | C | 169.2 | - | 169.4 | - |
| 13 | $CH_2$ | 119.8 | Ha 5.5 (d); Hb 6.19 (d), J =3.12 | 118.4 | 5.52 (d), J = 3.0 6.15 (d), J = 3.0 |
| 14 | $CH_3$ | 11.0 | 1.27 (s) | 9.6 | 1.30 |
| 15 | $CH_3$ | 25.4 | 2.12 (d), J =0.5 | 24.0 | 2.13 (d), J = 0.5 |

* Varian EM-390 (90 MHz); $CDCl_3$ solution, using TMS as an internal standard.

The $^{1}H$ NMR and $^{13}C$ NMR signals (Table 5.1) were assigned based on previously published data.[135]

## 5.4 Reactivity towards amino acids

As determined in previous studies by Schmidt (1999), the reaction of STLs with free amino acids is pH dependant (Scheme 5.1).[55] At higher pH values (in the physiological range), the course of the reaction is determined by the ratio of acidity of the thiol group of amino acid (forward reaction) to the adduct's enol tautomer (reverse reaction). At low pH values the speed of addition of amino acids is said to be very low. The equilibrium lies on the product side since protonation at the

thioether-sulfur (initiating a reverse reaction) is less favourable compared with protonation of the conjugated carbonyl oxygen (forward reaction).

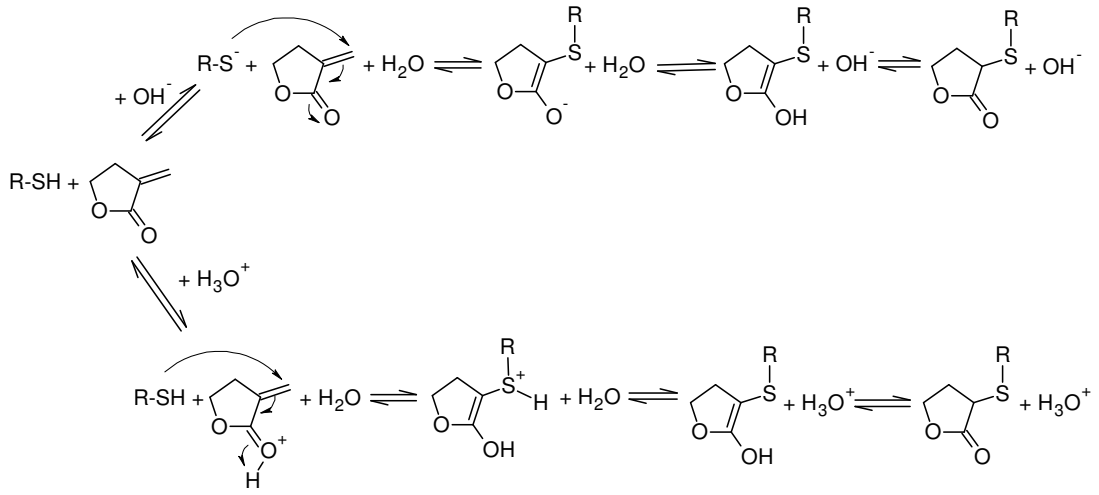

**Scheme 5.1. Mechanism of Michael addition of amino acids to STLs under basic and acidic conditions (adopted from Schmidt, 1999)[55]**

The addition of amino acids to STLs was studied in the basic environment as well at the physiological pH, using available methods. Progress of the reactions with amino acids was monitored by TLC using cellulose plates and specific spraying agents: anisaldehyde/sulfuric acid reagent (detection of STLs) and ninhydrin reagent (detection of amino acids). The appearance of a coloured band upon detection with ninhydrin requires a direct reaction of this compound's *α*-amino and the carboxyl groups of the amino acids. If reaction takes place through an *α*-amino group of amino acids, anisaldehyde can be used for detection of the product.

### 5.4.1 Reactivity of dehydrobrachylaenolide **(4.2)** towards *L*-cysteine using basic conditions

The adduct of dehydrobrachylaenolide **(4.2)** and cysteine was prepared under basic conditions in deuterated water (24 h, RT). Two coloured spots were observed on the TLC plate upon detection with ninhydrin, of which the lower one corresponded to the free amino acid. The reaction mixture was separated using the preparative HPLC reversed phase column (UV $\lambda_{max}$ = 258.9; $t_R$ = 10.335 min), employing an isocratic method described in Section 3.4.2.8 (Chapter 3). This yielded pure DHB-CYS adduct **5.27** in 37% yield. The structure was determined by $^{1}$H NMR and $^{13}$C NMR analysis (Table 5.2).

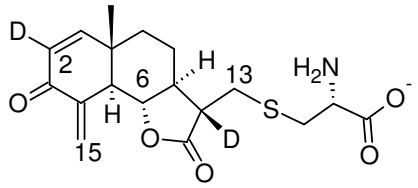


**(5.27)**

Examination of the $^{1}H$ NMR and $^{13}C$ NMR spectra revealed the presence of an amino acid moiety with characteristic carbon chemical shifts at Cys-C*β* $\delta_C$ 33.5 ($\delta_H$ 2.95 and $\delta_H$ 3.09 ) and Cys-*α*C $\delta_C$ 53.9 ($\delta_H$ 3.8 ).[97,139] The disappearance of the olefinic signals corresponding to C-13 protons in the $^{1}H$ NMR spectrum, and the signals corresponding to C-11 and C-13 in the $^{13}C$ NMR spectrum, were suggestive of addition of cysteine to C-13 rather than to C-1 or C-15. The lactone ring and the exocyclic double bond between C-4 and C-15 remained intact. The deuterium was incorporated at C-11, but the expected triplet was not observed in the $^{13}C$ NMR spectrum probably due to the low intensity. This was further supported by the observed COSY correlation of the Cys-*β*C protons with $H_{a,b}$-13 and the splitting pattern of the $H_{a,b}$-13, which appeared as doublets and not as a double doublet as would be expected in the case of hydrogen incorporation at C-11. Furthermore, an additional deuterium was incorporated at C-2 which gave no resonance in the $^{13}C$ NMR spectrum.

The distinct doublet for H-1 in the parent structure resonating at $\delta_H$ 6.76 collapsed into a sharp singlet at $\delta_H$ 7.0 due to deuteration of C-2. This could be a result of the addition reaction of the second cysteine to C-1 which was reversible, and the rapid elimination of cysteine from C-1 resulted in the product **5.26**.[93]

[139]Yoshikawa M., Hatakeyama S., Inoue Y., Yamahara J. (1993). *Chemical Pharmaceutical. Bulletin*, **41**, 214–216.

**Table 5.2. $^{1}H$ and $^{13}C$ NMR data for compound 5.27 in $D_2O$**

| Atom number | Mult. (DEPT) | $\delta_C$ | $\delta_H$ (multiplicity); J (Hz) | HMBC $^{13}C \leftrightarrow {}^{1}H$ | COSY $^{1}H \leftrightarrow {}^{1}H$ |
|---|---|---|---|---|---|
| 1 | CH | 165.5 | 7.0 (s) | H-3, H-9, H-10 | - |
| 2 | CD | Not observed | - | - | - |
| 3 | C | 194.8 | - | H-1, H-15 | - |
| 4 | C | 143.2 | - | H-1, H-5 | - |
| 5 | CH | 54.4 | 2.52 (dt); J = 10.3 | H(14) | H-6, Ha,b-15 |
| 6 | CH | 67.1 | 3.84 (dd); J = 10.3 | - | H-5 |
| 7 | CH | 47.6 | 1.74 (m) | H-13 | H-8 |
| 8 | $CH_2$ | 21.0 | Ha 1.48 (m); Hb 1.49.(m) | H-7 | H-7 |
| 9 | $CH_2$ | 35.3 | Ha 1.48 (m); Hb 1.6 (m) | H-14 | H-8 |
| 10 | C | 39.7 | - | H-14 | - |
| 11 | CD | Not observed | - | - | - |
| 12 | C | 170.4 | - | | - |
| 13 | $CH_2$ | 29.5 | Ha 2.74 (d); J = 12.0<br>Hb 2.86 (d); J= 12.0 | H-7, Cys-$\beta$CHa,b, H-12 | H-1, H-5 |
| 14 | $CH_3$ | 17.2 | 0.93 (s) | H-1 | - |
| 15 | $CH_3$ | 121.8 | Ha 5.5 (d); J = 2.0<br>Hb 5.99 (d); J = 1.0 | H-3 | H-5 |
| Cys-$\beta$C | $\beta CH_2$ | 33.5 | Ha ~2.95 (dd); J = 8.3; 15.2<br>Hb~3.09 (dd); J = 3.9; 15.2 | H-13 | Cys-$\alpha$CH |
| Cys-$\alpha$C | $\alpha$CH | 53.9 | ~3.8 (dd); J = 8.3; J = 4.4 | Cys-$\beta$CH | |
| COO- | - | 180.7 (from HMBC) | - | Cys-$\beta$CHa,b | - |

The stereochemistry at C-11 could not be deduced due to the incorporation of deuterium at C-11. However, the expected absence of Nuclear Overhauser effects between H-6 and $H_{a,b}$ -13 in the NOESY spectrum, which would occur if the side chain was $\beta$-orientated, was suggestive of deuterium assuming the $\beta$-

position.[139,140] Strong resonances of formic acid, originating from the HPLC buffered solvent used for purification, were present in the spectra ($\delta_c$ 170.4 and $\delta_H$ 8.2).

### 5.4.2 Reactivity of compound **5.17** towards *L*-cysteine at physiological pH

The addition of cysteine was carried out in a phosphate buffer (pH 7.4) to mimic intracellular pH conditions using a published method.[141] Progress of the reaction was monitored by TLC over 24 h (Figure 5.7 (left): cellulose $F_{254}$; n-Bu-OH/$H_2O$/AcOH 5:4:1 v/v; ninhydrin spray reagent, 120 °C).

The solvent from the reaction mixture was evaporated by adding MeOH for azeotropic effect, resuspended in a MeOH/$H_2O$ (1:1 v/v) solvent mixture, and then analysed by LC-ESI-MS/UV. A mixture of products was obtained as indicated by the UV analysis. The positive ESI-MS showed two major molecular peaks ($t_R$ = 12.22 and 12.39 min). Structures of C-13 - cysteinyl adducts **5.28a** and **5.28b** were identified by using $^1H$, $^{13}C$, gHSQC and gCOSY NMR analysis. The NMR data are summarised in Tables 5.3 and 5.4 respectively.

Two sets of intense signals corresponding to STL-cysteinyl adducts **5.28a** and **5.28b** were distinguished using gHMQC (Figure 5.8) and gCOSY (Figure 5.9) pulse sequences.

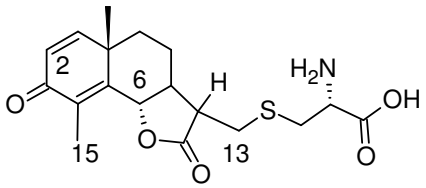


**(5.28a)**

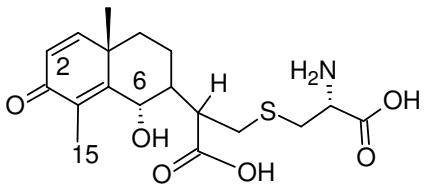


**(5.28b)**

[140]Yoshikawa M., Shimoda H., Uemura T., Morikawa T., Kawahara Y., Matsuda H. (2000). *Bioorganic & Medicinal Chemistry*, **8**, 2071–2077.

[141]Lastra A. L., Ramirez T. O., Salazar L., Martinez M., Trujillo-Ferrara J. (2004). *Journal of Ethnopharmacology*, **95**, 221–227.

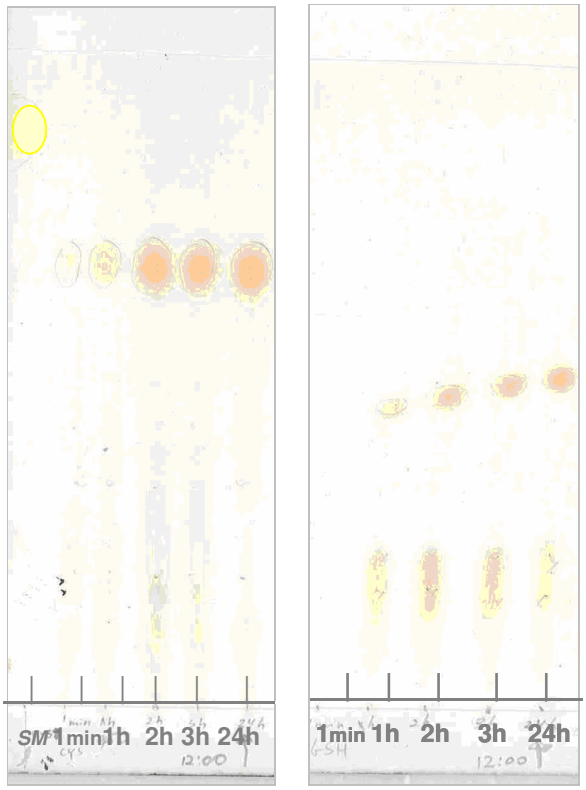


**Figure 5.7. TLC of the addition of cysteine (left) and glutathione (right)**

The carbon proton assignments were deduced from the gHMQC spectrum. Characteristic disappearance of proton resonances corresponding to the olefinic H-13 protons indicated that the products present in the supernatant of the reaction mixture lacked C-11 - C-13 double bond, and that the nucleophyllic addition took place at position C-13 of the STL. The C-1 - C-2 and C-4 - C-5 double bonds remained in place and their proton chemical shifts were extracted from the gHSQC cross peaks, and were almost indistinguishable in the two products (**5.28 a**/**b**; $\delta_C$ 158.8, C-1; $\delta_C$ 124.3, C-2; $\delta_C$ 154.8/154.9, C-4; $\delta_C$ 128.9/127.3, C-5).

The presence of olefinic signals corresponding to H-1 and H-2 in the proton and carbon spectra indicated that the C-1 - C-2 double bond was unaffected in both major reaction products. The proton chemical shifts could not be differentiated due to the overlapping of the resonances and were approximated to the value of the centre of the COSY cross-peaks corresponding to H-1 and H-2.

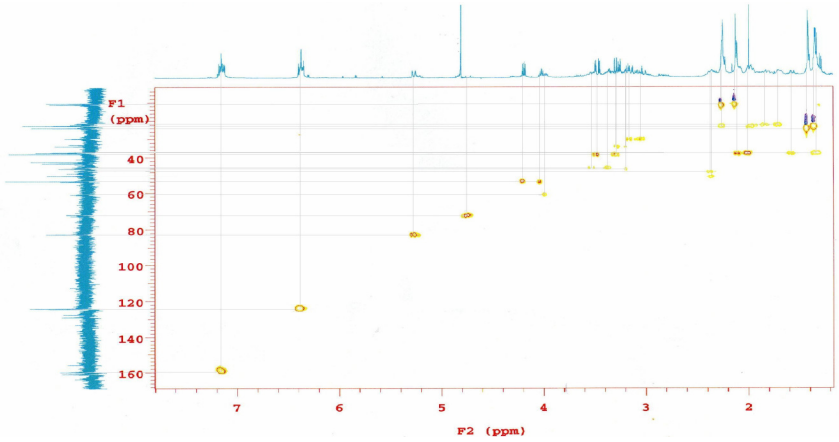


**Figure 5.8. gHSQC spectrum of the supernatant of the reaction mixture of compound 5.17 and *L*-cysteine**

Similarities in the values of the chemical shifts and the sizes of the proton couplings, and the equal ratio of the two major products also precluded a definite assignment of the proton sets of C-13 and C-11 to the corresponding structures. Therefore some of the assignments are interchangeable, since it was not possible to obtain a quality HMBC spectrum and to establish long-range proton carbon correlations.

The two cross-peaks of the same size and intensity at $\delta_H$ 5.26 and $\delta_H$ 4.74 and the chemical shifts of the corresponding carbons C-6 and C-6' and in the $^{13}C$ spectrum indicated that the lactone ring was intact in the one product **5.28a** ($\delta_C$ 82.0) but was opened in the other **5.28b** ($\delta_C$ 72.9). Further examination of the $^{13}C$ spectrum revealed that there were three sets of signals assignable to the cysteine moieties, which were differentiated by analysis of HSQC and COSY positive cross-peaks. The first set was at $\delta_C$ 33.7 ($\delta_H$ 4.2) and $\delta_C$ 53.9 ($\delta_H$ 3.28 and $\delta_H$ 3.46) and was assigned to the product **5.28a** on the basis of the similarity of coupling constants J to that of the DHB-CYS adduct **5.27**.

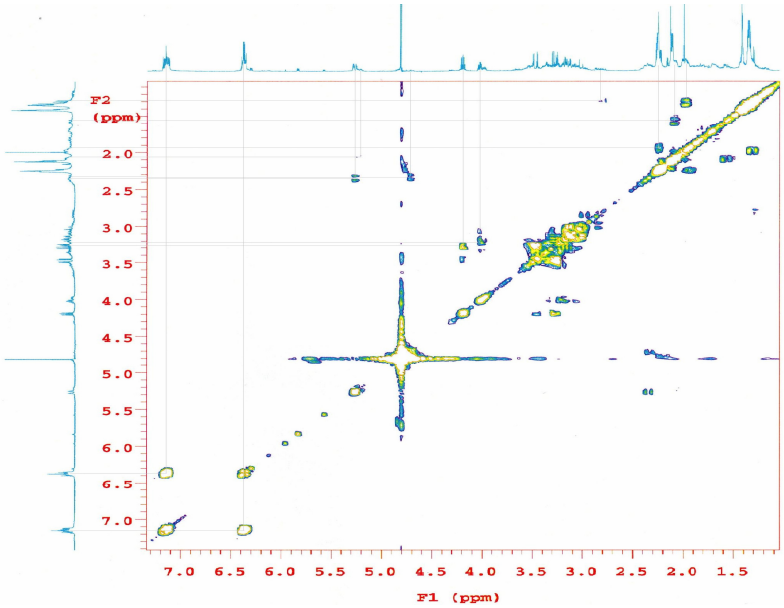


**Figure 5.9. gCOSY spectrum of the supernatant of the reaction mixture of compound 5.17 and cysteine**

The second set also followed from the gCOSY spectrum, $\delta_H$ 4.02 , $\delta_H$ 3.16 and $\delta_H$ 3.07, with the corresponding carbons resonating at $\delta_C$ 53.9 and $\delta_C$ 34.0, which was deduced from the HMQC spectrum, and was assigned to Cys-*α*H of the second product **5.28b** (Table 5.3). The size of the integration was equivalent to that of the proton resonating at $\delta_H$ 4.2, thus the earlier estimated ratio of the major products could be confirmed as 1:1.

The peak at 12.22 min, m/z 382.2 $[M - H]^-$ and m/z 384.3 $[M + H]^+$, UV $\lambda_{max}$ = 243.9 nm is consistent with the molecular formula $C_{18}H_{25}NO_6S$ with a calculated mass of 383.4518. This corresponded to a second product **5.28b**, which was not observed on the TLC of the reaction mixture, but was present in the supernatant of the reaction mixture at a slightly lower concentration. The structure was also determined to be a mono-adduct of cysteine at position C-13 but with the lactone ring being opened as a result of hydrolysis. As a result of the ring opening, the resonance corresponding to H-6 shifted upfield by 0.5 ppm ($\delta_H$ 4.74) (Table 5.4).

**Table 5.3. $^{1}H$ and $^{13}C$ NMR data for compound 5.28b in $D_2O$**

| Atom number | Assigned multiplicity | $\delta_C$ | $^{1}H$ $\delta_H$ (multiplicity); J (Hz) | COSY $^{1}H \leftrightarrow {}^{1}H$ |
|---|---|---|---|---|
| 1 | CH | 158.8 | ~7.1* | H-2 |
| 2 | CH | 124.3 | ~6.4* | H-1 |
| 3 | C | 189.7 | - | - |
| 4 | C | 154.8 | - | - |
| 5 | C | 128.9 | - | - |
| 6 | CH | 82.0 | 5.26 (br d); J = 2.0; 11.2 | H-7 |
| 7 | CH | 49.0 | 2.37 (m) | |
| 8 | $CH_2$ | 24.0 | Ha 1.36 (m); Hb 1.97 (m) | |
| 9 | $CH_2$ | 37.7 | Ha 1.97 (m); Hb 2.11 (m) | |
| 10 | C | 40.8 | - | - |
| 11 | CH | 46.0 | 3.53 (m) | H-13 |
| 12 | C | 163.3 | - | - |
| 13 | $CH_2$ | 29.97 | 3.05* ; 3.17* | |
| 14 | $CH_3$ | 22.64 | 1.43 (s) | |
| 15 | $CH_3$ | 10.73 | 2.13 (d); $J_6$ = 1.2 | |
| Cys-$\alpha$CH | CH | 53.9 | 4.2 (dd); J = 3.9; 8.3 | Cys-$\beta H_2$ |
| Cys-$\beta CH_2$ | $CH_2$ | 36.98 | Ha 3.27 (dd); J = 8.3; 14.7<br>Hb 3.46 (dd); J = 3.9; 14.7 | Cys-$\alpha$H |
| COO- | C | 180.87 | - | - |

*Multiplicity and coupling constants were not determined due to the overlap with other signals

This resonance was not observed in the $^{1}H$ NMR spectrum due to suppression by the solvent, and was deduced from the gHSQC and COSY positive cross-peaks of the H-6 and H-7 ($\delta_H$ 2.36) protons. The typical resonance up-field shift by 0.5 ppm from the closed lactone ring is characteristic for these compounds. The stereochemistry at the newly formed stereogenic centre C-11 could not be determined. The signal of lower intensity at $\delta_H$ 3.9 was assigned to another cysteinyl derivative (from gHSQC correlations), which is probably a less favourable stereoisomer of compound **5.28a** at C-11. However, a full structure could not be proposed due to the low concentration of the compound in the mixture and the complexity of the spectrum.

**Table 5.4. $^{1}H$ and $^{13}C$ NMR data for compound 5.28a in $D_2O$**

| Atom number | Assigned multiplicity | $\delta_C$ | $\delta_H$ (multiplicity); J (Hz) | COSY $^{1}H \leftrightarrow {}^{1}H$ |
|---|---|---|---|---|
| 1' | CH | 160.0 | ~7.1 | |
| 2' | CH | 124.4 | ~6.4 | |
| 3' | C | 188.5 | - | |
| 4' | C | 154.9 | - | |
| 5' | C | 127.3 | - | |
| 6' | CH | 72.91 | 4.74** | H-7 |
| 7' | CH | 50.93 | 2.36 (m) | H-6 |
| 8' | $CH_2$ | 22.64 | Ha 1.97(m); Hb 2.26 (m) | |
| 9' | $CH_2$ | 37.61 | Ha 1.33 (m); Hb 1.57 (m) | |
| 10' | C | 42.08 | - | |
| 11' | CH | 46.0 | 3.39 (m) | |
| 12' | COO | 178.2 | - | - |
| 13' | $CH_2$ | 28.5 | Ha 3.05 (m)*<br>Hb 3.16 (m)* | |
| 14' | $CH_3$ | 24.0 | 1.43 (s) | |
| 15' | $CH_3$ | 10.1 | 2.26 (d); J = 2.0 | |
| Cys- $\alpha$CH | CH | 53.9 | 4.02 (dd); J = 4.4; 7.3 | |
| Cys-$\beta CH_2$ | $CH_2$ | 34.0 | Ha 3.2 (m)*; Hb 3.29 (m)* | Cys-Ha |
| COO- | COO- | 180.9 | - | - |

* Multiplicity and coupling constants were not determined due to the overlap with other signals
**Chemical shift was determined from COSY positive cross peaks

### 5.4.3 Addition of *N*-acetyl-*L*-cysteine to compound **5.17** at physiological pH

Reaction at physiological pH, using the same method as in Section 5.4.2, resulted in one major product (LCMS-UV). Since the $\alpha$-amino group of NAC is acylated, no reaction with ninhydrin was observed. The positive ESI-MS of the reaction mixture showed a molecular peak at m/z 408.2 $[M + H]^+$ and the negative ESI-MS showed a peak at m/z 406.1 $[M - H]^-$, UV $\lambda_{max}$ 242.9 nm, which is consistent with the molecular formula $C_{22}H_{29}NO_5S$ with a calculated mass of 407.4806. The total yield of 56% was estimated on the basis of the total area of the UV $\lambda_{max}$ peaks resolved by HPLC. The major reaction product **5.29** was identified as an *N*-acetyl-*L*-cysteinyl adduct to C-13 of the sesquiterpene lactone by means of $^{1}H$ NMR spectroscopy, which was acquired on the supernatant of the reaction mixture to

avoid interference from the sesquiterpene starting material. The coupling constants, chemical shifts and proton assignments are presented in Table 5.4.

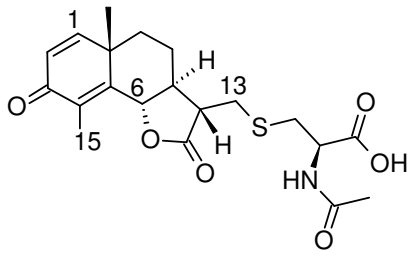


**(5.29)**

The structural assignment of the $^1$H NMR signals of the 13(11)-*N*-acetyl-cysteinyl adduct was possible by detailed examination of the proton spectrum, coupling constants and comparison to the $^1$H NMR data of the cumanin-13(11*β*)-*N*-acetyl-cysteinyl adduct.[141] Complete disappearance of the proton peaks corresponding to germinal protons of the C-11 – C-13 exocyclic double bond at $\delta_H$ 5.5 and $\delta_H$ 6.19 indicated that unreacted starting material was not present in the supernatant. The addition reaction took place between C-13 of the exocyclic double bond of the starting material and the sulfhydryl group of NAC. This is a first report of the structure of compound **5.29**.

One equivalent of unreacted NAC was present as a disulfide in the $^1$H NMR spectrum at $\delta_H$ 4.2 (Cys-*α*H); $\delta_H$ 3.3 and $\delta_H$ 3.1; and $\delta_H$ 1.9. The assignment of stereochemistry at C-11 was based on the detailed comparisions of $^1$H NMR chemical shifts and coupling constants to that of the eudesmanolides saussureamine D and E **(5.30** and **5.31)**, where the thermodynamically favoured addition product with *β*H-11 was formed.[139,140] The coupling constant $J_{7,11}$ of 10.1 Hz is characteristic of the pseudo-axial position of *β*H-11 in trans-lactones. In the case of *α*H-11 the size of coupling constant H-11 - H-7 would be in the region of 6.4 – 8.0 Hz.[142]

[142] Narayanan C. R., Venkatasubramanian N. K. (1968). *The Journal of Organic Chemistry*, **33**, 3156–3162.

**Table 5.5. $^{13}C$ and $^{1}H$ NMR data for compound 5.29 in $D_2O$**

| Atom number | Assigned multiplicity | $\delta_H$, (multiplicity) | J (Hz) |
|---|---|---|---|
| 1 | CH | 6.90 (d) | $J_{1,2}$ = 9.7 |
| 2 | CH | 6.20 (d) | $J_{2,1}$ = 9.7 |
| 3 | C | - | - |
| 4 | C | - | - |
| 5 | C | - | - |
| 6 | CH | 5.05 (dd) | $J_{6,7}$ = 11.3; $J_{6,15}$ = 1.2 |
| 7 | CH | 1.95 (m) | |
| 8 | $CH_2$ | Ha 1.38 (m); Hb 1.88 (m) | |
| 9 | $CH_2$ | Ha 1.88 (m); Hb 2.1 (m) | |
| 10 | C | - | - |
| 11 | CH | 2.58 (td); J = 3.1; J = 8.2; J= 10.1 | $J_{7\alpha}$ = 10.1; $J_{13b}$ = 8.2; $J_{13a}$ = 3.1 |
| 12 | C | - | - |
| 13 | $CH_2$ | Ha 2.95 (dd)<br>Hb 2.75 (dd) | $J_{13b}$ = 13.6; $J_{11\beta}$ = 3.1<br>$J_{13a}$ = 13.6; $J_{11\beta}$ = 8.2 |
| 14 | $CH_3$ | 1.20 (s) | - |
| 15 | $CH_3$ | 1.93 (s) | - |
| Cys-$\beta CH_2$ | $CH_2$ | Ha 3.14 (dd) J = 8.2; J = 13.6<br>Hb 2.85 (dd) J = 3.1; J = 13.6 | $J_{Hb\text{-}Cys\text{-}\beta}$ = 14.0; $J_{H\text{-}Cys\text{-}\alpha}$ = 4.3<br>$J_{Ha\text{-}Cys\text{-}\beta}$ = 14.0; $J_{H\text{-}Cys\text{-}\alpha}$ = 9.0 |
| Cys-αCH | CH | 4.37 (dd) | $J_{Hb\text{-}Cys\text{-}\beta}$ = 4.3; $J_{Ha\text{-}Cys\text{-}\beta}$ = 9.0 |
| CO-N | C | - | - |
| COO- | C | - | - |
| CO-$CH_3$ | $CH_3$ | 1.92 (s) | - |

The second set of signals, next to resonances of H-1 and H-2, with much lower absolute intensity at $\delta_H$ 6.15 (J = 9.7 Hz) and $\delta_H$ 6.93 (J = 9.7 Hz) was attributed to olefinic protons H-1 and H-2 of a minor reaction product.

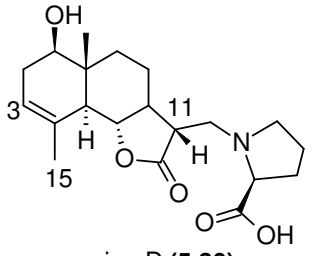


Saussureamine D **(5.30)**

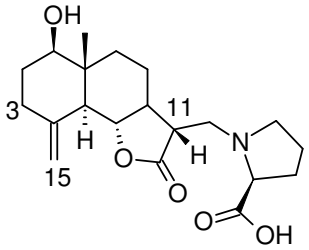


Saussureamine E **(5.31)**

The upfield signal at $\delta_H$ 1.93 of the shielded methyl group of C-15 was present, thus indicating that both internal conjugated double bonds on the A ring of the sesquiterpene lactone remained intact. Integration of the $^1$H NMR spectrum indicated that the products were in the ratio of 2.5:1. The minor compound was of too low a concentration to enable full structure assignment. However, close examination of the lower intensity signals allowed a structure to be proposed for the minor product **5.32** as the *α*H-11- stereoisomer of the major product **5.29** at position C-11.

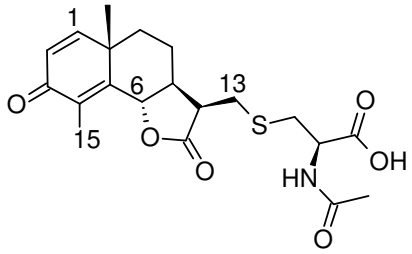


**(5.32)**

The unassigned set of signals at $\delta_H$ 4.0, which appeared of equal value of the integral to that of the assigned resonance at $\delta_H$ 4.2, was subsequently assigned to the two protons of the Cys-*α*H of the NAC disulfide as a by-product of the reaction. This followed from the size of the integration and the splitting pattern of this resonance, which appeared as a set of overlapping triplets indicating a small difference in the chemical environment of the two protons, but the equivalence of the neighbouring Cys-$\beta H_2$ protons, as opposed to the NAC moiety of the STL adduct, where Cys-$\beta H_2$ protons are diastereotopic.

5.4.4 Addition of glutathione to compound **5.17** at physiological pH

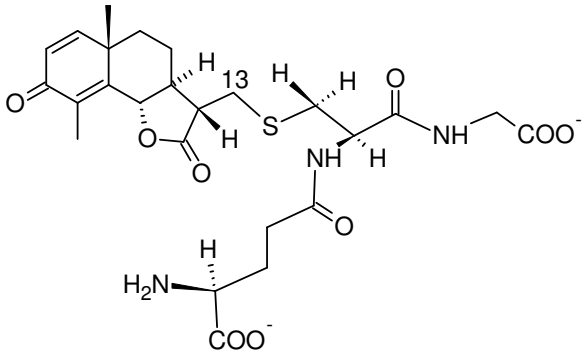

**(5.33)**

The reaction at physiological pH, using the same method as in Section 5.4.2 resulted in the formation of one major product ($R_f$ = 0.49; TLC: cellulose $F_{254}$; n-BuOH/$H_2O$/AcOH, 5:4:1 v/v; ninhydrin spray reagent, 100 °C). This was further supported by the LC-UV/MS analysis of the reaction mixture. The addition product eluted at $t_R$ 21.07 min (UV $\lambda_{max}$ = 241.9 nm) and was followed by the starting STL at $t_R$ 23.65 min (UV $\lambda_{max}$ = 243 nm). The yield of the glutathionyl adduct was estimated to be 42% on the basis of the total area of the UV $\lambda_{max}$ peaks resolved by HPLC. The negative ESI-MS showed a molecular ion peak at m/z 550.2 [M - H], and the m/z 552.4 $[M + H]^+$ was observed in the positive ESI-MS. These data were consistent with the molecular formula $C_{25}H_{33}N_3O_9S$ and the calculated molecular weight of 551.6092 corresponding to STL glutathionyl adduct. The structural assignments were based on the $^1H$ NMR analysis of the $D_2O$ soluble components of the dried reaction mixture. The chemical shifts and coupling constants are summarised in Table 5.6.

Complete disappearance of the proton peaks corresponding to germinal protons of the C-11 - C-13 exocyclic double bond was indicative of the absence of the starting material in the supernatant. The addition reaction took place at the expected position C-13. In addition, the appearance of the double sets of signals with different absolute intensity at $\delta_H$ 6.18 and $\delta_H$ 6.15 (J = 10.1 Hz); and $\delta_H$ 6.95 and $\delta_H$ 6.93 (J = 10.1 Hz) revealed the presence of a second minor product in the reaction mixture. Integration of the $^1H$ NMR spectrum indicated that the products were in a ratio of 2.5:1.

**Table 5.6. $^1$H NMR data for compound 5.33 in $D_2O$**

| Atom number | Assigned multiplicity | $\delta_H$ (multiplicity) | J (Hz) |
|---|---|---|---|
| 1 | CH | 6.95 (d) | J = 10.1 |
| 2 | CH | 6.18 (d) | J = 10.1 |
| 3 | C | - | - |
| 4 | C | - | - |
| 5 | C | - | - |
| 6 | CH | 5.02 (dd) | $J_7$ = 11.3; $J_{15}$ = 1.2 |
| 7 | CH | 1.95 (m) | |
| 8 | $CH_2$ | Ha 1.38(m); Hb 1.88 (m) | |
| 9 | $CH_2$ | Ha 1.88 (m); Hb 2.1 (m) | |
| 10 | C | - | - |
| 11 | CH | 2.62 (td) | $J_7$ = 10.1; $J_{13b}$ = 8.2; $J_{H13a}$ = 3.1 |
| 12 | C | - | - |
| 13 | $CH_2$ | Ha 2.89 (dd)<br>Hb 2.89 (dd) | $J_{13b}$ = 13.6; $J_{11}$ = 3.1<br>$J_{13a}$ = 13.6; $J_{11}$ = 8.2 |
| 14 | $CH_3$ | 1.2 (s) | - |
| 15 | $CH_3$ | 1.93 (d) | $J_6$ = 1.2 |
| Cys-*α*CH | CH | 4.45 (dd) | $J_{Hb\text{-}Cys\text{-}\beta}$ = 5.1; $J_{Ha\text{-}Cys\text{-}\beta}$ = 9.0 |
| Cys-*β*$CH_2$ | *β*$CH_2$ | Ha-Cys-β 3.18 (dd)<br>Hb-Cys-β 2.79 (dd) | $J_{Hb\text{-}Cys\text{-}\beta}$ = 14.0; $J_{H\text{-}Cys\text{-}\alpha}$ = 5.1<br>$J_{Ha\text{-}Cys\text{-}\beta}$ = 14.0; $J_{H\text{-}Cys\text{-}\alpha}$ = 9.0 |
| Cys-*α*CONH | C | - | - |
| Gly-*α*$CH_2$ | $CH_2$ | Ha 3.88 (dd); Hb 3.64 (dd) | - |
| Gly-*α*COOH | C | - | - |
| Glu- *α*CH | CH | ~3.76 | |
| Glu- *β*$CH_2$ | $CH_2$ | 2.04 | - |
| Glu-*γ*$CH_2$ | $CH_2$ | 2.42[b] | |
| Glu-*α*COOH | C | - | - |
| Glu-*γ*CONH | C | - | - |

[a] The chemical shifts for Gly-*α*$CH_2$-Ha and Hb were taken as the centre of the multiplet as the ABX splitting pattern could not be analysed directly from the spectrum due to overlapping of several frequencies.

[b] The chemical shifts for Glu-*γ*$CH_2$-Ha and Hb were taken as the centre of the multiplet as the $ABM_2X$ splitting pattern could not be analysed directly from the spectrum.

In the $^1H$ spectrum of the reaction mixture, a number of GSH peaks were identifiable.[143] An ABX splitting pattern was observed for the methylene protons of the cysteine residue (Cys-$\beta CH_2$). These protons are diastereotopic and have different chemical shifts ($\delta_H$ 3.18 and $\delta_H$ 2.79). The two protons of Gly-$CH_2$ are also not equivalent. Two ABX quartets overlap with Glu-$\alpha$CH with a chemical shift of $\delta_H$ 3.76. All the chemical shifts and coupling constants were in good agreement with the literature values for GSH.[144,145] Based on these deductions, the major reaction product was identified as STL-13(11)-glutathionyl adduct **5.33**. The stereochemistry at C-11 was deduced from the size of coupling constant $J_{7,11}$ of 10.1 Hz, which is identical to that of the NAC adduct **(5.29)** and is characteristic of the pseudo-axial position of $\beta$H-11 in *trans*-lactones.[142] This is a first report of this structure.

The unaccounted high absolute intensity of the resonances at $\delta_H$ 3.76 and $\delta_H$ 2.04 was explained by following the same argument as was used to deduce the presence of NAC-disulfide. Based on the values of the corresponding integrals and the yield of the product determined from the HPLC, it was plausible to assume that the unreacted GSH was present as a disulfide rather than as a free amino acid.

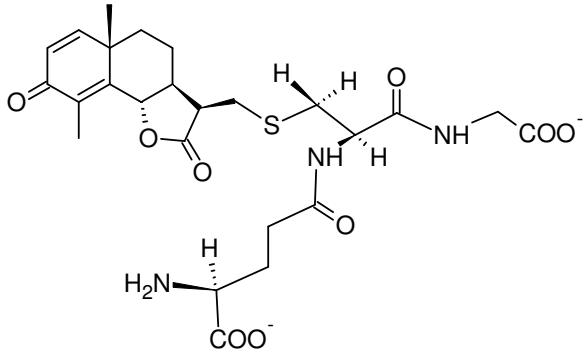


**(5.35)**

The minor compound was present in a too low concentration to enable full assignment of the structure. However, the positions of the minor peaks suggested

[143] Brown F. F., Campbell I. D., Kuchel P. W., Rabenstein D. C. (1977). *FEBS Letters*, **82**, 12–16.
[144] Keire D. A., Rabenstein D. L. (1989). *Bioorganic Chemistry*, **17**, 256–267.
[145] Kennett E. C. (2005). University of Sydney. *PhD thesis*, 217 p. http://hdl.handle.net/2123/620. Accessed on 10 October 2008.

that possibly the by-product is an *α*H-11-stereoisomer of the major product at C-11. The following structure is proposed as **5.35**. Instances of the formation of both isomers in various ratios during the addition reaction of the cysteine and glutathione to STLs have been previously reported.[54,93]

## 5.5 Reduction of compounds 4.2 and 5.17 with $NaBH_4$

Since the biological activity of most sesquiterpene lactones often depends on the *α*-methylene-*γ*-lactone moiety, an attempt was made to determine what effect the reduction of the C-11 - C-13 exocyclic double bond would have on the antiplasmodial activity and cytotoxicity of compounds **5.17** and **4.2**. The STLs were reduced with $NaBH_4$ in ethanol using a previously published method.[57]

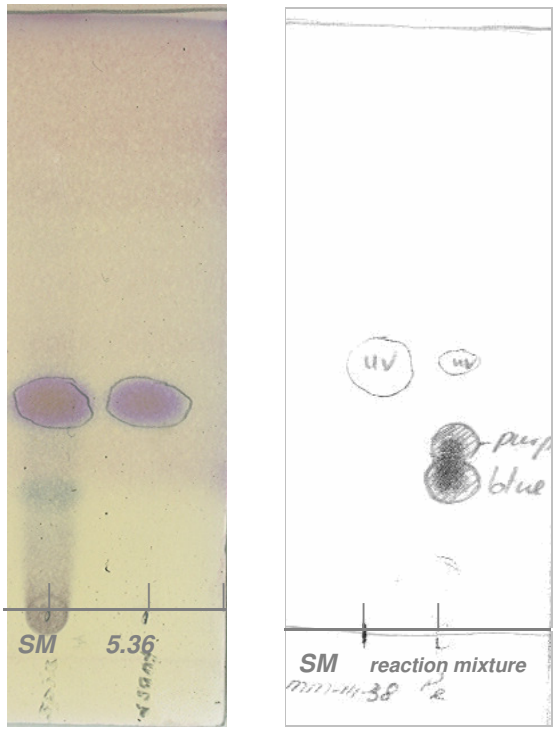


**Figure 5.11. TLC plates: reduction of compounds 5.17 (left) and 4.2 (right)**

### 5.5.1 Stereoselective reduction of compound **5.17**

The reduction of compound **5.17** led to a single product, obtained in 90% yield. The positive ESI-MS of the product showed a molecular ion peak at m/z 246. 2 $[M + H]^+$, UV $\lambda_{max}$ 241.6 nm, which is consistent with the molecular formula $C_{15}H_{18}O_3$.

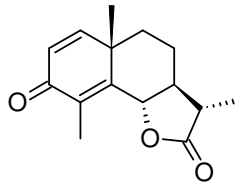

**(5.36)**

The reaction product was isolated as a yellow gum. The TLC analysis (Figure 5.9, left) revealed that the $R_f$ value of the reaction product was identical to that of *α*-santonin **(5.24)** standard (EtOAc/Hexane 30:70 v/v). The presence of a single product (UV $\lambda_{max}$ = 246.4 nm; TIC EI m/z = 246.2) was confirmed by LC-ESEI-MS analysis of the reaction mixture (Section 3.1.3.3, Chapter 3). The molecular ion at 264.0 was assigned to $M+H_2O$. The structure was fully assigned on the basis of $^1H$ and $^{13}C$ NMR data, which was almost identical to that of the synthetic *α*-santonin, with the exception of a small solvent impurity resonating at $\delta_H$ 0.15 and $\delta_C$ 29.9. The $^1H$ and $^{13}C$ NMR data are summarised in Table 5.7. The $^1H$ NMR data clearly indicated that the *α*-methylene function was reduced to give the 11,13-dihydro derivative. The pair of doublets corresponding to the C-13 methylene group in the starting material were absent from the $^1H$ NMR spectrum of the product due to replacement by a methyl group signal resonating at $\delta_H$ 1.23 (d, J = 6.9 Hz). An additional proton signal resonating at $\delta_H$ 2.38 was subsequently assigned to H-11. This was further supported by the observed multiplicity of this resonance which appeared as a dq due to vicinal coupling with H-7 (J = 11.7 Hz) and to both of the methyl protons, H-13 (J = 6.9 Hz).

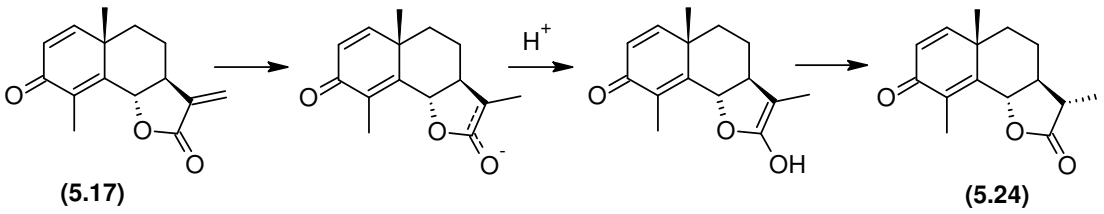


**(5.17)** **(5.24)**

**Figure 5.12. Mechanism of $NaBH_4$ reduction of compound 5.17**

**Table 5.7. $^{1}H$ and $^{13}C$ NMR data for compound 5.36 in $CDCl_3$**

| Atom number | Experimental data | | Lit.[58] NMR data for α-santonin (5.24) | |
|---|---|---|---|---|
| | $\delta_C$ | $\delta_H$ (multiplicity); J (Hz) | $\delta_C$ | $\delta_H$ (multiplicity); J (Hz) |
| 1 | 154.9 | 6.62 (d); J = 9.9 | 155.0 | 6.7 (d); J = 9.9 |
| 2 | 126.1 | 6.21 (d); J = 9.9 | 125.5 | 6.25 (d); J = 9.9 |
| 3 | 186.5 | - | 186.1 | - |
| 4 | 129.1 | - | 128.2 | - |
| 5 | 151.1 | - | 151.1 | - |
| 6 | 81.6 | 4.77 (dq); J = 1.3; J = 10.9 | 81.1 | 4.81 (dq); J = 1.3; J = 10.9 |
| 7 | 53.7 | 1.44-2.07 (m, 5H) | 53.3 | 1.44-2.07 (m, 5H) |
| 8 | 23.3 | | 22.7 | |
| 9 | 38.1 | | 37.6 | |
| 10 | 41.5 | - | 41.2 | - |
| 11 | 41.2 | 2.38 (dq); J = 6.9, J = 11.7 | 40.7 | 2.43 (dq); J = 6.9, J = 11.7 |
| 12 | 177.7 | - | 177.5 | - |
| 13 | 12.67 | 1.23 (d); J = 6.9 | 12.3 | 1.28 (d); J = 6.9 |
| 14 | 25.4 | 1.28 (s) | 25.3 | 1.34 (s) |
| 15 | 11.1 | 2.1 (d); J = 1.3 | 10.7 | 2.14 (d); J = 1.3 |

The stereochemistry at C-11 followed from the magnitude of the coupling constant between H-7 and H-11 (J = 11.7 Hz), which suggested an antiperiplanar relationship. The anion is protonated from the less-hindered side of the enolate double bond to form the thermodynamically more stable stereoisomer, where the new methyl group is less hindered. These results thus confirmed the previously described stereoselectivity of reduction of STLs with $NaBH_4$.[57] The orientation of the methyl group was confirmed by measuring the specific optical rotation of the product in chloroform ($\alpha^{25}_D$ = -100 °, c = 4%) and for the synthetic 95% pure (-)-α-santonin ($\alpha^{25}_D$ = -125°, c = 0.4).

### 5.5.2 $NaBH_4$ reduction of dehydrobrachylaenolide **(4.2)**

The dehydrobrachylaenolide **(4.2)** was reduced with $NaBH_4$ using a published method.[57] The reaction resulted in a mixture of starting material and two products by TLC (Figure 5.9, right). The reaction mixture was further analysed using LC-EI-MS. The Maxplot chromatogram produced a cluster of five peaks with retention times between 21.23 and 23.37 minutes. The TIC EI chromatogram displayed six peaks with common mass ions observed between m/z 230 and 250 (230, 233, 246, 248 and 250). Based on the published data of $NaBH_4$ reduction of dehydrocostus lactone **4.5a** and the general mechanism of $NaBH_4$ reduction, two conceivable reduction products **5.39** and **5.23** were assigned to the major peaks with masses of m/z 248.3 ($t_R$ = 21.816 min) and m/z 250.3 ($t_R$ = 22.100 min).[140] One of the minor peaks at $t_R$ 21.816 min with a mass of m/z 246.3 could be ascribed to structure **5.25**.

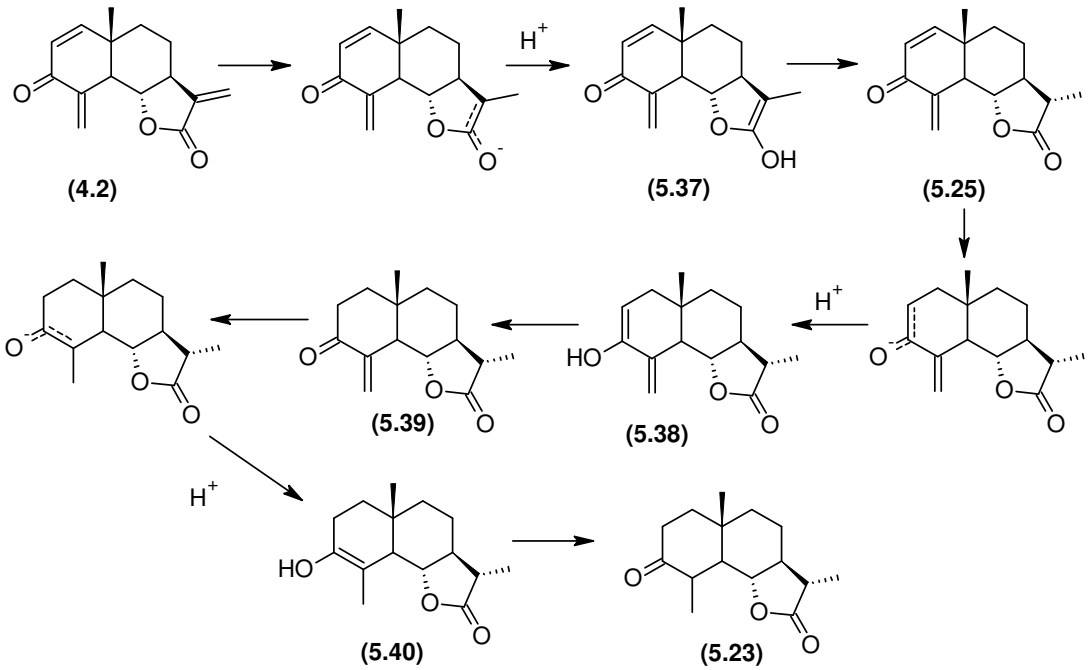


**Figure 5.13. Conceivable mechanism of reduction of dehydrobrachylaenolide (4.2)**

The formation of the proposed C-4 - C-15 over the C-1 – C-2 reduction product can be substantiated by a strong possibility of a solvent cross-coordination of the

carbonyl oxygen and exocyclic methylene group as depicted below (structure **(5.41)**).

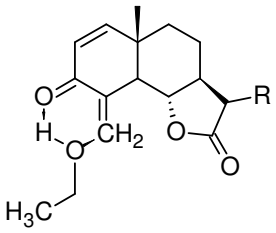

**(5.41)**

The possibility of the presence of trapped intermediates **5.37** with MW 248.3 and MW 250.3 - **5.38** cannot be ruled out. No additional physical data could be obtained for these products due to low yield and difficulty of separation.

## 5.6 SAR

To study the SAR, five structurally modified STLs were generated as intermediates in an attempted synthesis of dehydrobrachylaenolide **(4.2)** by the Discovery Chemistry Programme of the CSIR, and were tested for growth inhibitory properties *in vitro*.

### 5.6.1 *In vitro* anticancer activity

The SAR study was carried out in the 3-cell line anticancer assay at the CSIR. All the compounds were tested across a concentration range of 6.25-100 ppm. The effect of the test compounds on growth inhibition of CHO cells was also evaluated. The results are summarised in Table 5.8.

Although *α*-santonin **(5.24)** was completely devoid of activity, dehydrobrachylaenolide **(4.2)** was found to exhibit the highest activity within the series. Furthermore, its activity was found to be at least 10-fold stronger than the activity of its isomer compound **(5.17)** and of parthenolide **(5.2)**. A mixture of compounds **(5.42)** showed a 50-fold drop in activity and a 3-fold decrease in cytotoxicity towards CHO cells. A similar activity drop was observed for compound **(5.43)** which contains a saturated *α*-methyl-*γ*-lactone moiety, whilst its cytotoxicity towards CHO cells decreased by 50-fold. Finally, the growth inhibitory concentration of the currently developed drug parthenolide **(5.2)** towards cancer

and CHO cells was almost identical, suggesting that CHO cells are of limited use for measuring the selectivity of this type of compound as an anti-cancer lead.

**Table 5.8. *In vitro* cytotoxicity of STLs towards CHO and cancer cell lines**

| Structure | Code | CHO: $IC_{50}$ (µg/mL) | 3-cell line pre-screen (CSIR), µM | | |
|---|---|---|---|---|---|
| | | | $GI_{50}$ | TGI | $LC_{50}$ |
| 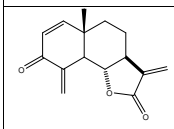 | **(4.2)** | 17.2 | 0.67 | 1.57 | 2.48 |
| 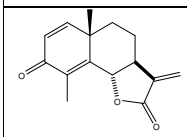 | **(5.17)** | 7.0 | 11.7 | 31.9 | 78.7 |
| Mixture (2:1) 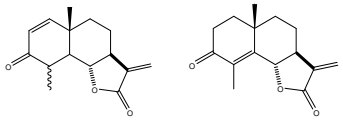 | **(5.42)** | 42.1 | 46.1 | 85 | >100 |
| 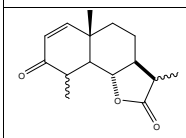 | **(5.43)** | 55.3 | 55.6 | 93.2 | >100 |
| 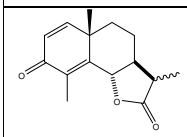 | **(5.24)** | >100 | >100 | >100 | >100 |
| 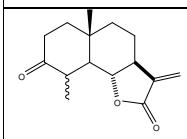 | **(5.8)** | 91.7 | 54.2 | 81 | >100 |
| Parthenolide | **(5.2)** | 7.6 | 5.32 | 18.1 | 46.1 |

### 5.6.2 *In vitro* antimalarial activity

The test compounds were assayed in duplicate against chloroquine-sensitive (CQS) and chloroquine-resistant (CQR) strains of *P. falciparum* (D10 and K1). The quantitative assessment of antiplasmodial activity *in vitro* was determined *via* the LDH assay described in detail in the experimental section (Chapter 3). The results are summarised in Table 5.9.

**Table 5.9. *In vitro* antiplasmodial activity against *P. falciparum***

| Compound/s | Compound code | CQS, D10: $IC_{50}$ (µg/mL) | CQR, K1 or Dd2: $IC_{50}$ (µg/mL) | CHO: $IC_{50}$ (µg/mL) | SI, D10* |
|---|---|---|---|---|---|
| 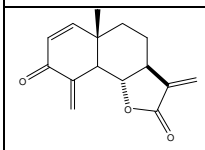 | **(4.2)** | 0.38 | 0.06 | 4.2 | 11 |
| 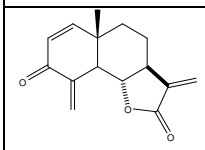 | (4.2) | 0.27 | 0.22 | NT | ND |
| Mixture (2:1) 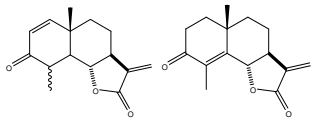 | **(5.42)** | 4.2 | NT | 10.35 | 2 |
| 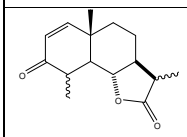 | **(5.43)** | 4.55 | NT | 13.61 | 3 |
| 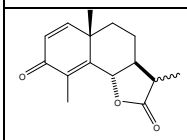 | **(5.24)** | >100 | NT | >100 | ND |
| 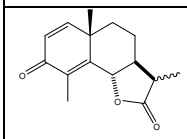 | **(5.36)** | 8.34 | 42.76 | 88.31 | 11 |
| 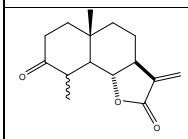 | **(5.8)** | 7.0 | NT | 22.75 | 3 |
| 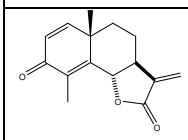 | **(5.17)** | 2.82 | 2.21 | 1.71 | 0.6 |
| Chloroquine (CQ) | - | 0.012 | 0.122 (K1)<br>0.152<br>(Dd2) | | |

It could be clearly seen that the presence of the *α*-exomethylene double bond C-11 - C-13 is not sufficient for the antimalarial activity observed in our parent compound. With removal of the endocyclic and exocyclic double bonds in the A ring, an almost 20-fold drop in the activity was observed, with a reduced SI of 3.

The mixture of isomers **5.42** showed only a 10-fold drop in activity compared to DHB **(4.2)**, and a 3-fold decrease in toxicity followed by the drop in the SI. The activity of compound **5.17** was inferior when compared to DHB **(4.2)** with the poorest cytotoxicity index of the samples examined. This is likely to be attributable to the effect of the migration of the C-4 - C-15 double bond to carbons C-4 - C-5 and the the resultant change in the geometry of the A ring. Interestingly, commercial *α*-santonin **(5.24)** was considered completely inactive, whilst its toxicity was reduced only 3-fold.

The activity of *α*-santonin **(5.36)**, obtained by the reduction of compound **5.17**, showed an almost 10-fold higher activity than commercial *α*-santonin **(5.24)** with very low cytotoxicity towards CHO cells. This activity could possibly be due to the hydrocarbon solvent impurity present in the reduction product. The possibility of an experimental error in the bioassay cannot be ruled out. The dehydrobrachylaenolide **(4.2)** showed superior antimalarial activity against both strains of the parasite and is discussed in detail in Chapter 4.

## 5.7 Discussion

### 5.7.1 Reactivity towards amino acids and product characterisation

The monocysteine adduct at C-13 of dehydrobrachylaenolide **(4.2)** was obtained *via* a reaction of equimolar quantities of sesquiterpene lactone and free amino acid in the basic environment. The reaction proceeded regioselectively. Incorporation of deuterium at C-2 suggested transient addition of the second molecule of cysteine to C-1 of STL followed by a rapid elimination reaction. This finding led to the conclusion that in addition to the *α*-methylene-*γ*-lactone moiety, the *α*,*β*-unsaturated endocyclic methylene also has a strong alkylating potential. From the stereochemical considerations, the preferred site for the addition of the second cysteine would be C-15 carbon of the exocyclic double bond due to its *cis*-orientation in relation to the carbonyl oxygen. With such geometry, a simultaneous interaction of the carbonyl oxygen of the STL with the protonated amino group of the amino acid and its thiol group with exocyclic methylene carbon could take place. This would likely lead to electron withdrawal from the conjugated system and subsequent activation of *β*-carbonyl. This situation could be simulated by

coordination of the solvent. This could partly explain the selectivity towards the C-1 site. It is also highly probable that in a situation where there is close proximity of a number of donor species, e.g. surface or pocket of polypeptides,[102] all three potential binding sites in dehydrobrachylaenolide **(4.2)** could form covalent bonds with protein residues.

The reaction of compound **5.17** with equimolar amounts of GSH and NAC at physiological pH resulted in the formation of C-13 amino-acid mono-adduct in both cases. Low yields of the products could equally be due to the formation of a by-product and possibly to slow rates or reversibility of the reaction. The reaction proceeded stereospecifically to yield the expected product with *S*-configuration of the newly formed stereogenic centre, as was deduced from the size of the coupling constants H-7 – H-11. The Michael-type addition of STLs to amino acids and amines is said to occur from the exo-face of the convex-shaped molecule. This is in good agreement with the data published for the STLs of other structural types.[146,147] The additional potentially alkylating structural element of compound **5.17** did not show reactivity towards amino acids in the physiological buffer. Formation of a by-product **5.29** in the addition reaction with GSH and NAC implicated potential reactivity of compound **5.17** towards the OH-nucleophiles. It is evident from previous studies that reactivity with the OH-nucleophiles does not correlate with the bioactivity of STLs.[148]

### 5.7.2 Reduction with $NaBH_4$

The reduction of compound **5.17** proceeded as expected, regioselectively and stereospecifically, to yield α-santonin as a single product. Such selectivity and specificity is in good agreement with the previously reported data for other structural types of STLs.[57] Reduction of compound **4.2** afforded a mixture of products. No further work to deduce the exact structures of the reductants was completed due to the limited quantities of dehydrobrachylaenolide **(4.2)**.

---

[146] Matsuda H., Kagerura T., Toguchida I., Ueda H., Morikawa T. (2000). *Life Sciences*, **66**, 2151–2157.
[147] Lawrence N., McGown A. T., Nduka J., Hadfield J. A., Pritchard R. G. (2001*). Bioorganic Medicinal Chemistry Letters*, **11**, 429–431.
[148] Schmidt T. J. (2006). *Studies in Natural Products Chemistry*, **33**, 309–392.

### 5.7.3 SAR

As became apparent from the literature review, there is an overall inclination to reinforce a relationship between the presence of alkylating elements in STLs and bioactivity. This was confirmed to hold for the series of compounds evaluated in the present study. DHB, with three potential alkylating sites, exhibited the strongest activity profile in the *in vitro* cancer and malaria models within the series of tested compounds. It inhibited the growth of cancer cell lines at 0.68 (µg/mL) and showed potent activity against *P. falciparum* at $IC_{50}$ equal to 0.38 (µg/mL) for the D10 strain and equal to 0.06 (µg/mL) for the K1 strain, which fall within the activity range of the standard drug chloroquine [$IC_{50}$(K1) = 0.122 (K1); $IC_{50}$(Dd2) = 0.152 µg/mL]. It was also found to inhibit growth of a CHO cell line at a 10 to 70-fold higher concentration ($IC_{50}$ = 4.2 µg/mL). Although it showed some selectivity towards the targets *in vitro* (cancer cells and *P. falciparum* infected cells), there is a potential threat of generic toxicity, which can manifest *in vivo*. As it appeared in this SAR study, the presence of 1,2-*cis and* 4,15-*trans* double bonds cross-conjugated with the keto group as well as the presence of the *α*-methylene-*γ*-lactone moiety is essential for bioactivity. Removal of any of the potentially alkylating elements from the eudesmane skeleton resulted in a dramatic loss of activity (10 to 50-fold), whilst the cytotoxicity was reduced by a single digit number at the most. The *α*,*β*-unsaturated ketone, with the exocyclic methylene group, was reported to act just as *α*-methylene-*γ*-lactone.[149] In contrast, the most drastic activity drop was found to be due to the saturation of *α*-methylene of the lactone and not due to saturation of the ketone-conjugated olefinic elements.

Furthermore, in another SAR study of the series of eudesmanolides, the importance of the conformation of the A-ring was emphasised, where a full chair arrangement was required for activity against *P. falciparum.*[136] This requirement, however, did not hold for DHB **(4.2)**, as its A-ring is completely flattened by the four $sp^2$ carbon atoms, as was evident from the X-ray structure of DHB **(4.2)** (Section 4.4.1.2). In the same study it was observed that stronger activity against *P. falciparum* occurred in eudesmanolides containing endocyclic C-4 - C-5 or C-3 - C-4 rather than exocyclic C-4 - C-5 double bond. This requirement did not hold

[149] Konaklieva M. I., Plotkin B. J. (2005). *Mini-Reviews in Medicinal Chemistry*, **5**, 73–95.

either for the compounds in which the double bond was conjugated with the *α*,*β*-unsaturated ketone function. The compound **(4.2)** was found to be at least 10-fold more active than its isomer **5.17** with the C-4 - C-5 unsaturation in both *in vitro* models. It showed a similar activity advantage over parthenolide **(5.2)**.

From the SAR work presented in this chapter, it can be concluded that DHB could play a valuable role as a drug candidate. Further mechanistic studies and an *in vivo* dose response toxicity study would be necessary to gain in-depth knowledge of the structural requirements for *selectivity* with respect to the desired biological activity and systemic toxicity.

# Chapter 6: Preparation, structures and bioactivity of pro-drugs of sesquiterpene lactones

## 6.1 Background and objectives

Further development of many STL-based drugs with antitumour and antimalarial properties has been limited by their aqueous insolubility and lack of selectivity, especially for oral intake.[103,150] STLs are highly reactive compounds and can hypothetically alkylate any thiol, amino and hydroxy group containing molecules of suitable geometry. Such reactivity profile can lead to non-beneficial and toxic effects. Detailed investigations of the sesquiterpene lactones helenalin, parthenin and ambrosin provided evidence of the formation of *mono*- and *bis*- Michael-type adducts with secondary amines **(6.1-6.3)**, which were later proposed to act as pro-drugs of these potent STLs.[103,105,151] The reversibility rate is said to be controlled by the physicochemical factors of the environment and half-life of a pro-drug, and it is a function of time. Just by a variation of the added amine, the end result induced by a pro-drug, can vary not only in potency towards a specific target, but by the target protein, or may even affect an entirely different pathway.

These secondary and tertiary amino Michael-adduct products of STLs are further converted to water-soluble hydrochlorides and quaternary ammonium salts which are considered to serve as pro-drugs, and are converted back to parent STLs after administration by a retro-Michael mechanism. The conversion of tertiary amino Michael adducts back to STL could possibly be activated through metabolic N-oxidation of the amines to the N-oxides followed by Cope elimination.[103,152]

---

[150] García-Piñeres A. J. (2003). ***Doctoral Ph D*** *dissertation*, Albert-Ludwigs Universität, Germany.
[151] Lee K. -H., Furukawa H., Huang E. -S. (1972). *Journal of Medicinal Chemistry*, **15**, 609–611.
[152] Low L. L., Castagnoli N., (1980). In: M. E. Wolff (ed); *Burger's Medicinal Chemistry*. John Wiley and Son: New York, pp. 107-226.

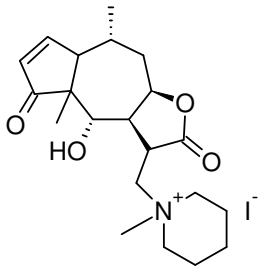

**(6.1)**

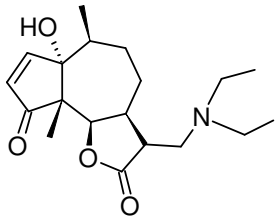

**(6.2)**

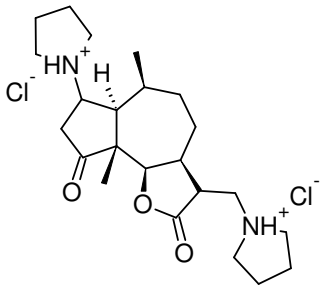

**(6.3)**

At least two reassuring examples of the success of this approach are known. The first is the registered drug, arglabin, for treatment of leukaemia, which is used in the form of dimethylamino hydrochloride **(6.4)**.[153] Another good example is the hydrochloride of the dimethylamino adduct of parthenolide (DMAP; **(6.5)**), which at present is in the Rapid Development Program of the NCI, having shown up to a 70% increase in oral bioavailability through such modification.[61]

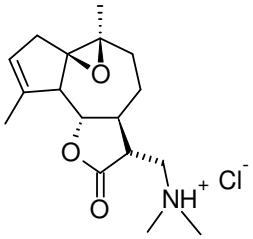

**(6.4)**

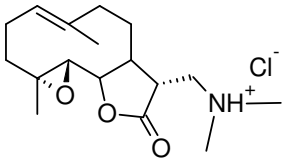

**(6.5)**

This approach was selected as a starting point in an attempt to improve the *in vivo* activity of dehydrobrachylaenolide (DHB) through preparation of secondary amino derivatives that might retain bioactivity *via* a pro-drug mechanism. The present chapter deals with the preparation and *in vitro* bioactivity evaluation of Michael-type secondary amino adducts of dehydrobrachylaenolide **(4.2),** 6*β*-3-oxoeudesma-1(2),4(5),11(13)-trien-6,12-olide **(5.17),** and parthenolide **(5.3)** as a reference compound.

[153] Adenkov S. M. (2004). Therapeutic uses of Arglabin in combination with other chemotherapy agents, US 6,770,673 B1.

## 6.2 Selection of the amino side chain based on prediction of OSIRIS molecular properties

Molecular properties were calculated with the OSIRIS Property Explorer.[154] The following calculated properties contributing to the overall drug-likeness score are included in the computing (the explanation below is cited directly from the website):

- Molecular weight
- Log S calculation
- Log *P* value

"Optimizing compounds for high activity towards a biological target often goes along with increased molecular weights. However, compounds with higher weights are less likely to be absorbed. More than 80% of all traded drugs have a molecular weight below 450. The aqueous solubility of a compound significantly affects its absorption and distribution characteristics. Typically, a low solubility goes along with a bad absorption and therefore the general aim is to avoid poorly soluble compounds. The estimated log S values are given as a unit stripped logarithm (base 10) of the solubility measured in mol/L. It is said that more than 80% of drugs on the market have an estimated log S value greater than -4. The value of Log *P* of a compound, which is the logarithm of its partition coefficient between n-octanol and water log ($c_{octanol}/c_{water}$), is a well established measure of the compound's hydrophilicity. Low hydrophilicities and therefore high Log *P* values cause poor absorption or permeation. It has been shown that for compounds to have a reasonable probability of being well absorbed, their Log *P* value must not be greater than 5.0. The distribution of calculated Log *P* values of more than 3 000 drugs on the market underlines this fact".[154]

Parthenolide and DMAP were used as examples. The following set of molecular properties was shown for parthenolide and DMAP, respectively: cLog *P* of 2.77 and 1.99; solubility of (-2.97) and (-2.19); drug-likeness 0.33 and 1.98 and drug scores of 0.16 and 0.55 respectively.

---

[154] http://www.organic-chemistry.org/prog/peo/. Accessed on 12 October 2008.

For parthenolide **(5.1)**, some undesired effects were predicted, such as high risk of mutagenicity and high risk of irritatant effects, with a very low drug score. In contrast, the calculated properties for PDMA were suggestive of drug-conformance behaviour. The results of the calculations for DHB side chain compounds are summarised in Table 6.1.

**Table 6.1. Predicted molecular properties for hypothetic DHB derivatives**

| Molecule/side chain | Log*P* | Solubility | Drug likeness | Drug score | Risks of undesired effects |
|---|---|---|---|---|---|
| 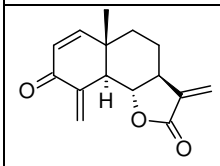 | 2.16 | -2.99 | -6.55 | 0.21 | Medium risk of mutagenicity and high risk of irritant effects |
| | 1.1 | -2.03 | -0.47 | 0.31 | Potential mutagenicity; irritant |
| 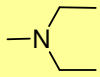 | 1.97 | -2.63 | 1.26 | 0.38 | Drug-conformance behaviour; with medium risk of mutagenicity and irritant effects |
| 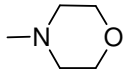 | 1.02 | -2.1 | -1.07 | 0.27 | High risk of mutagenicity and irritant effects |
| 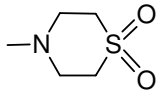 | 0.47 | -2.23 | -3.21 | 0.22 | High risk of irritant effects |
| 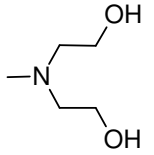 | 0.06 | -1.62 | -2.43 | 0.24 | High risk of mutagenicity and irritant effects |

Based on the empirical calculations of molecular properties, a diethylamino side chain was selected for the preparation of the Michael adducts of STLs.

## 6.3 Preparation of Michael adducts with diethylamine

The general synthetic method shown in Scheme 6.1 was employed for the preparation of the corresponding Michael adducts **(6.6, 6.7 and 6.9)** utilising diethylamine (DEA).

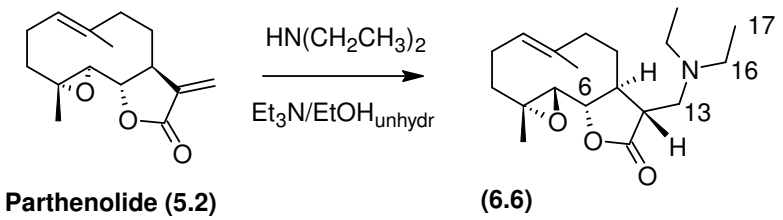


**Parthenolide (5.2)** **(6.6)**

**Scheme 6.1. Synthesis of the diethylamino adduct of parthenolide**

### 6.3.1 Preparation of diethylamino-parthenolide **(6.6)**

The diethylamino-parthenolide **(6.6)** was prepared on the 60 µM scale. Following a single purification by column chromatography on silica gel (EtOAc/n-Hexane 1:1 v/v) of the pure diethylamino-parthenolide adduct **6.6** was recovered (55% yield). The structure of the product **6.6** was confirmed by analysis of the $^{1}H$ NMR and $^{13}C$ NMR data, which was compared to the published data of DEA-parthenolide. The $^{1}H$ and $^{13}C$ NMR values for diethylamino-parthenolide **(6.6)** are summarised in Table 6.2.

The $^{13}C$ NMR spectrum exhibited the 17 resonance signals. The presence of the two oversized N-ethyl resonances at $\delta_C$ 47.3 and $\delta_C$ 11.54, and the disappearance of the signal for the exocyclic methylene C-13 at $\delta_C$ 121.3 ppm were observed. These findings were further substantiated by $^{1}H$ NMR data, where signals corresponding to the pair of exomethylene geminal protons have disappeared, indicating that addition took place across the C-11 - C-13 exomethylene double bond.

Further examination of the $^{1}H$ NMR spectrum revealed a typical triplet corresponding to six methyl protons of the diethylamine.

**Table 6.2. $^{1}H$ and $^{13}C$ NMR data for diethylamino -parthenolide in Acetone-$d_6$ (6.6)**

| Atom number | Multiplicity (DEPT) | $\delta_C$ | $\delta_H$ (multiplicity); J (Hz) | Lit.[106] $^{1}H$ NMR $\delta_H$ (mult.); J (Hz) |
|---|---|---|---|---|
| 1 | CH | 124.7 | 5.26 (dd); J = 2.3; J = 12.1 | 5.15 (dd); J = 2.4; J = 12.0 |
| 2 | $CH_2$ | 24.0 | Ha 2.12 (m); Hb 2.42 (m) | |
| 3 | $CH_2$ | 36.7 | Ha 1.16 (m); Hb 2.04 (m) | |
| 4 | C | 60.9 | - | - |
| 5 | CH | 66.6 | 2.74 (d); J = 9.0 | 2.72 (d); J = 9.0 |
| 6 | CH | 82.1 | 3.89 (t); J = 9.0; J = 9.2 | 3.81 (t); J = 9.0 |
| 7 | CH | 48.4 | 2.3 - 2.4 (m) | |
| 8 | $CH_2$ | 29.8 | Ha 2.0 (m); Hb 2.18 (m) | |
| 9 | $CH_2$ | 41.1 | 2.19 (m) | |
| 10 | C | 135.0 | - | - |
| 11 | CH | 46.5 | 2.49 (m) | |
| 12 | C | 176.7 | - | - |
| 13 | $CH_2$ | 52.8 | Ha 2.73 (dd); $J_{11}$ = 5.5; $J_{13b}$ = 14.0 Hb 2.78 (dd); $J_{11}$ = 4.7; $J_{13a}$ = 14.0 | 2.8 (ddd); J = 4.9; J = 14.1; J = 29.8 |
| 14 | $CH_3$ | 16.5 | 1.75 (s) | |
| 15 | $CH_3$ | 16.8 | 1.25 (s) | |
| $N\boldsymbol{CH_2}CH_3$ | $CH_2$ | 47.3 | Ha 2.42 (m); Hb 2.52 (m) | |
| $NCH_2\boldsymbol{CH_3}$ | $CH_3$ | 11.6 | 1.01 (t); J = 7.0 | 1.01 (t) |

However, instead of the expected quartet for the four $-CH_2$ protons of the ethyl group of amino side chain, two multiplets were observed, which were assigned to two sets of geminal diastereotopic protons ($\delta_H$ 2.42 and $\delta_H$ 2.52). The resonance at $\delta_H$ 2.49 was assigned to H-11. The protons of C-13 appeared to be diastereotopic ($\delta_H$ 2.73 and $\delta_H$ 2.78) as the rotation around the C-11 - C-13 was restricted for steric hindrance.

An upfield shift of 0.4 in the $^{1}H$ NMR spectrum was observed for H-7 which was no longer allylic. The connectivity of the diethylamino was evident from the HMBC

correlations between C-13 ($\delta_C$ 52.8) to the $-CH_2$ protons of the ethyl group of amino side chain ($\delta_H$ 2.42 and $\delta_H$ 2.52) and from the strong COSY cross-peaks between the H-13 and $-CH_2$ protons of the ethyl group of amino side chain The stereochemistry of the newly formed stereogenic centre C-11 has previously been determined by means of X-ray crystallography as an *S*-configuration.[106]

### 6.3.2 Preparation of diethylamino-dehydrobrachylaenolide **(6.7)**

The DEA-dehydrobrachylaenolide was prepared using the general method depicted in Scheme 6.1. The reaction on the micromolar scale of compound **4.2** resulted in a mixture of the two major products (Figure 6.1) and some unreacted starting material ($R_f$ = 0.92; MeOH/DCM 1:24 v/v). The reaction products were purified using column chromatography (MeOH/DCM/hexane 3:97 v/v) to afford starting material **4.2**, DHB-ethyl ester **6.8** ($R_f$ = 0.68; MeOH/DCM 1:24 v/v) and diethylamino-adduct **6.7** ($R_f$ = 0.36; MeOH/DCM 1:24 v/v), with a total yield after chromatography of 27% of the desired product **6.7** and 18% yield of the by-product **6.8**.

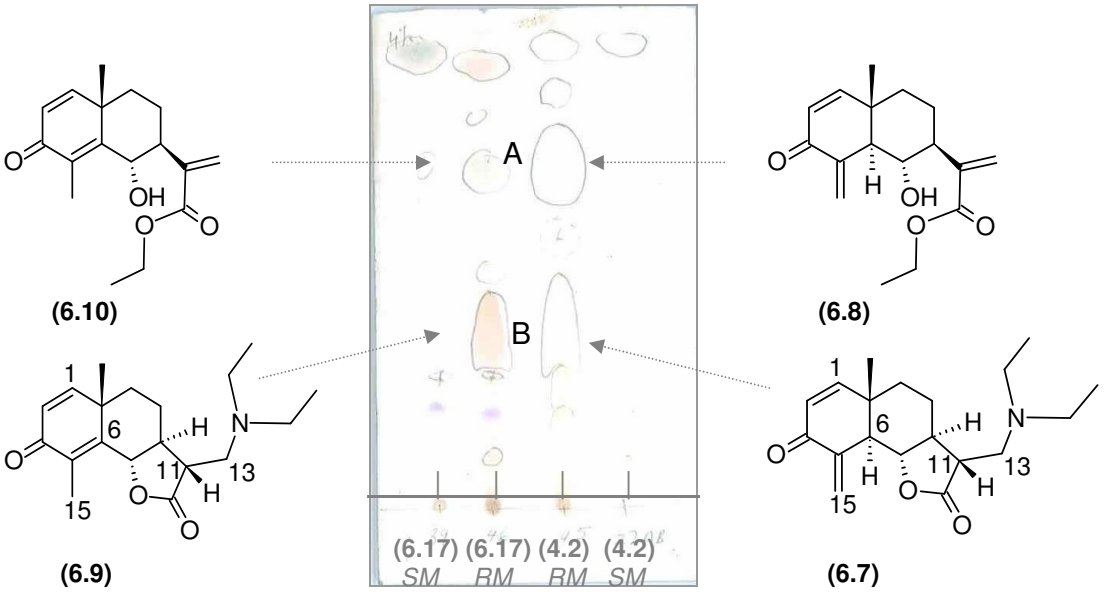


**Figure 6.1. TLC of the reaction of STLs with $Et_2NH$ and structures of the products**

#### *6.3.2.1 Structure of (5α,6β,7α,10β,11β)-13-diethylamino-3-oxoeudesma-1(2),4(15)-dien-12-olide **(6.7)***

LC-ESI-MS analysis of the fraction B (Figure 6.1) containing mostly the diethylamino-DHB adduct ($t_R$ = 9.45 min; Method T3.2-1) showed a molecular peak (UV $\lambda_{max}$ = 241.6 nm) at m/z 318.0 $[M + H]^+$ in a positive mode, which is consistent with the molecular formula $C_{19}H_{27}NO_3$ and the calculated molecular mass of 317.1990. The details of the method are described in the experimental Section 3.1.1.4 (Chapter 3). The $^1$H NMR and $^{13}$C NMR data are summarised in Table 6.3.

A total of 17 carbon signals were observed in the $^{13}$C NMR spectrum. The multiplicity of carbon resonances were derived from DEPT spectra. Following the same argument as for diethylamino-parthenolide, it could be concluded that the addition of the diethylamine proceeded a C-13 of the STL, as anticipated.

Furthermore, the upfield shift of the H-7 resonance by 0.6 in the $^1$H NMR spectrum is ascribed to the allylic disposition of this proton, and it is characteristic for the C-13-regioselective addition. The absolute alignment of protons H-2 and Ha-15 was not affected by the change in hybridisation of the C-11 and C-13 carbons, since the $^5$J coupling of 0.7-0.8 Hz as it in the parent STL, between the aforementioned protons, was also evident in the product. The doublet of doublets for the germinal Hb-15 appeared as a triplet due to a similar size of coupling constants $^1J_{Hb\text{-}15}$ and $^4J_{\alpha H\text{-}5}$ of 1.5 Hz. In turn, the proton H-5 at the AB ring junction appeared as a set of double triplets, and not as the triplet of doublets, since the coupling of 1.5 Hz had collapsed due to the resolution restriction of the instrument. The stereochemistry at the newly formed stereogenic centre C-11 followed from the size of coupling constant (J = 10.3 Hz) between *α*H-7 and H-11, which is characteristic of the pseudo-axial position of *β*H-11 in *trans*-lactones.[142]

**Table 6.3. $^{1}H$ and $^{13}C$ NMR data for compound 6.7 in acetone-$d_6$**

| Atom number | Multiplicity (DEPT) | $\delta_C$ | $\delta_H$ (multiplicity) | J (Hz) |
|---|---|---|---|---|
| 1 | CH | 160.7 | 6.97 (d) | $J_2$ = 9.8 |
| 2 | CH | 127.5 | 5.95 (dd) | $J_1$ = 9.8; $J_{15a}$ = 0.8 |
| 3 | C | 188.2 | - | |
| 4 | C | 143.5 | - | |
| 5 | CH | 53.3 | 2.96 (dt) | $J_{15a}$ = 2.4; $J_6$ = 10.9 |
| 6 | CH | 79.2 | 4.40 (t) | $J_5$ = 10.9 |
| 7 | CH | 51.5 | 1.98 (m) | |
| 8 | $CH_2$ | 24.3 | Ha 2.05 (m)<br>Hb 2.25 (m) | |
| 9 | $CH_2$ | 37.2 | Ha 1.75 (m)<br>Hb1.85 (m) | |
| 10 | C | 40.4 | - | |
| 11 | CH | 45.1 | 2.68 (ddd) | $J_7$ = 10.3; $J_{13a}$ = 8.2; $J_{13b}$ = 3.9 |
| 12 | C | 178.1 | - | - |
| 13 | $CH_2$ | 53.8 | Ha 2.48 (dd)<br>Hb 2.83 (dd) | $J_{13b}$ = 12.9; $J_{11}$ = 8.2<br>$J_{11}$ = 3.9; $J_{13a}$ = 12.9 |
| 14 | $CH_3$ | 12.3 | 1.05 (s) | |
| 15 | $CH_2$ | 120.5 | Ha 5.51 (ddd)<br>Hb 6.04 (dd) | $J_2$ = 0.8; $J_{15b}$ = 1.6; $J_5$ = 2.4<br>$J_{15a}$ = 1.6; $J_5$ = 1.5 |
| $N\boldsymbol{CH_2}CH_3$ | $CH_2$ | 47.9 | Ha 2.4 (m);<br>Hb 2.67 (m) | J = 14.0; J = 7.0 |
| $NCH_2\boldsymbol{CH_3}$ | $CH_3$ | 19.9 | 1.04 (t) | J = 7.0 |

A total of 17 carbon signals were observed in the $^{13}C$ NMR spectrum. The multiplicity of carbon resonances were derived from DEPT spectra. Following the same argument as for diethylamino-parthenolide, it could be concluded that the addition of the diethylamine proceeded a C-13 of the STL, as anticipated. Furthermore, the upfield shift of the H-7 resonance by 0.6 in the $^{1}H$ NMR spectrum is ascribed to the allylic disposition of this proton, and it is characteristic for the C-13-regioselective addition. The absolute alignment of protons H-2 and Ha-15 was not affected by the change in hybridisation of the C-11 and C-13 carbons, since

the $^{5}J$ coupling of 0.7-0.8 Hz as it in the parent STL, between the aforementioned protons, was also evident in the product. The doublet of doublets for the germinal Hb-15 appeared as a triplet due to a similar size of coupling constants $^{1}J_{Hb\text{-}15}$ and $^{4}J_{\alpha H\text{-}5}$ of 1.5 Hz. In turn, the proton H-5 at the AB ring junction appeared as a set of double triplets, and not as the triplet of doublets, since the coupling of 1.5 Hz had collapsed due to the resolution restriction of the instrument.

The stereochemistry at the newly formed stereogenic centre C-11 followed from the size of coupling constant (J = 10.3 Hz) between *α*H-7 and H-11, which is characteristic of the pseudo-axial position of *β*H-11 in *trans*-lactones.[150] In the case of αH-11, the size of coupling constant H-11 - H-7 would be in the region of 6.4-8 Hz. This is also consistent with the previously deduced spatial orientation of the natural amino adducts of eudesmanolides **5.30** and **5.31** with *L*-proline side chain, where the thermodynamically favoured addition product with *β*H-11 is formed.[139]

#### *6.3.2.2 Structure of ethyl (6α)-hydroxy-3-oxoeudesma-1(2),4(15),11(13)-trien-12-oate **(6.8)***

The structure of the minor product **6.8** was determined from $^{1}H$ NMR analysis, which is summarised in the experimental part (Chapter 3). The resonances of all olefinic protons remained unchanged as compared to the parent STL. The position of a resonance corresponding to the allylic proton H-7 was also unaffected. Two additional resonances with characteristic splitting patterns, the quartet at $\delta_H$ 4.2 and the triplet at $\delta_H$ 1.3, which integrated for 2- and 3-protons respectively, were assigned to an ethyl group as part of an ester function of the ring-opened lactone carbonyl. The oxymethine proton H-6 also shifted by 0.4 ppm downfield. This is due to a minor conformational change of the cyclohexane ring, which is a result of the released ring strain caused by the opening of the lactone. The data were consistent with the published $^{1}H$ NMR data for methyl (6*α*)-hydroxy-3-oxoeudesma-1(2),4(15),11(13)-trien-12-oate (or methyl ester of DHB).[155]

[155] Grass S., Zidorn C., Ellmerer E. P., Stuppner H. (2004). *Chemistry & Biodiversity*, **1**, 353–360.

### 6.3.3 Michael adducts of compound **5.17**

The reaction was performed on the µM scale, and resulted in a mixture of the two major products (Figure 6.1) and some unreacted starting material as was detected by TLC analysis ($R_f$ = 0.92; MeOH/DCM 1:24 v/v). The reaction products were purified using silica gel column chromatography (MeOH/DCM/hexane 3:97 v/v) to afford starting STL **(5.17)**, the STL-ethyl ester **6.10** ($R_f$ = 0.68; MeOH/DCM 1:24 v/v) and diethylamino-adduct **6.9** ($R_f$ = 0.36; MeOH/DCM 1:24 v/v), with a total yield of the DEA adduct of 29%.

#### *6.3.3.1 Structure of (6β,7α,10β,11β)-13-diethyamino-3-oxoeudesma-1(2),4(5),-dien-12-olide **(6.9)***

The positive ESI-MS of the fraction B (Figure 6.1) showed one major product ($t_R$ = 9.52 min; Method T3.2-1; m/z 318 $[M + H]^+$), in the positive mode. This was consistent with the molecular formula for the adduct $C_{19}H_{27}NO_3$ and the calculated mass of 317.1990. The details of the method are described in the experimental Section 3.1.1.4 (Chapter 3). The $^1H$ and $^{13}C$ NMR data are summarised in Table 6.4.

A total of 19 carbon signals was observed in the $^{13}C$ NMR spectrum. Two low-intensity signals at $\delta_C$ 0.1 and $\delta_C$ 29.9 were assigned to a common NMR solvent impurity, which was also observed in the spectra of compounds **5.31** and **6.8**. The multiplicity of the remaining 17 carbon resonances were derived from DEPT analysis. The addition of the diethylamine took place at position C-13 of the STL as two of the previous products **6.6** and **6.7**. This was evident from the disappearance of the resonance of the olefinic carbon C-13 at $\delta_C$ 119.8 from the $^{13}C$ NMR spectrum with corresponding signals of its geminal protons in the $^1H$-NMR spectrum at $\delta_H$ 5.5 and $\delta_H$ 6.19, which appeared in the olifatic region of the spectra. The observed upfield resonance shift of 0.6 ppm, which is due to the allylic disposition of the H-7 proton, is characteristic of C-11 - C-13 addition. Due to restricted rotation in the N-C bonds, the -N*CH*$_2$*C*H$_3$ protons appeared as a diastereotopic set with a chemical shift difference of 0.14 ppm.

**Table 6.4. $^{1}H$ and $^{13}C$ NMR data for compound 6.9 in $CDCl_3$**

| Atom number | Multiplicity (DEPT) | $\delta_C$ | $\delta_H$ (multiplicity) | J (Hz) |
|---|---|---|---|---|
| 1 | CH | 155.1 | 6.64 (d) | J = 9.8 |
| 2 | CH | 126.7 | 6.21 (d) | J = 9.8 |
| 3 | C | 186.5 | - | |
| 4 | C | 151.3 | - | |
| 5 | C | 128.9 | - | |
| 6 | CH | 81.7 | 4.73 (dd) | $J_{15}$ = 1.2; $J_7$ = 11.3 |
| 7 | CH | 51.9 | 1.95 (m) | |
| 8 | $CH_2$ | 24.3 | Ha 1.66 (m); Hb 2.25 (m) | |
| 9 | $CH_2$ | 38.4 | Ha 1.48 (m); Hb 1.82 (m) | |
| 10 | C | 41.4 | - | |
| 11 | CH | 44.8 | 2.53 (dd) | J = 4.3; J = 8.6; J = ~10.1* |
| 12 | C | 176.7 | - | |
| 13 | $CH_2$ | 52.9 | Ha 2.59 (dd)<br>Hb 2.89 (dd) | $J_{13b}$ = 13.3; $J_{11}$ = 4.3 $J_{11}$ = 8.6; $J_{13a}$ = 13.3 |
| 14 | $CH_3$ | 11.1 | 1.25 (s) | - |
| 15 | $CH_3$ | 25.3 | 2.09 (d) | $J_6$ = 1.2 |
| -N*$CH_2$*$CH_3$ | T | 47.2 | Ha 2.4 (dd)<br>Hb 2.54 (dd) | J =7.0; J = 13.7<br>$J_{17}$ =7.0; J = 13.7 |
| -$NCH_2$*$CH_3$* | Q | 11.8 | 0.96 (q) | J = 7.0 |

* The multiplicity and coupling constants estimated due to overlapping with another resonance.

The stereochemistry at the newly formed stereogenic centre C-11 could not be deduced from the size of the coupling constant between *α*H-7 and H-11 due to the overlapping of the H-11 proton with the diastereotopic $-CH_2$ protons of the ethyl group on the amine. Based on the similarity of the chemical shifts and some key coupling constants to those of compound **6.7**, it is reasonable to assume that the proton H-11 assumes a *β*-spatial orientation. This hypothesis is consistent with the previously deduced spatial orientation of H-11 in the Saussureamines (Section 5.4.3), which are natural amino adducts of eudesmanolides, where the thermodynamically favoured addition product with *β*H-11 is formed.[139]

### *6.3.3.2 Structure of (6α)-hydroxy-3-oxoeudesma-1(2),4(5),11(13)-trien-12-oate* ***(6.10)***

The structure of the minor product **6.10** was determined from $^{1}H$ and $^{13}C$ NMR analysis, which is summarised in Table 6.5. The resonances of all the olefinic protons remained unchanged from the parent STL. The position of a resonance corresponding to allylic proton H-7 was also unaffected by the opening of the lactone ring. The release of the steric strain of the lactone ring junction did not have an effect on the chemical shift of the oxymethine proton H-6, which appeared at $\delta_H$ 4.77, but affected the size of the coupling constant by 0.4 Hz. Two additional resonances with characteristic splitting pattern, the quartet at $\delta_H$ 4.21 and the triplet at $\delta_H$ 1.3, which integrated for 2- and 3-protons, respectively, were assigned to the ethyl group connected to the STL through an ester function at C-12.

**Table 6.5. $^{1}H$ and $^{13}C$ NMR data for compound 6.10 in $CDCl_3$**

| Atom number | $\delta_C$ | $\delta_H$ (multiplicity) | J (Hz) |
|---|---|---|---|
| 1 | 156.1 | 6.63 (d) | J = 9.9 |
| 2 | 126.0 | 6.22 (d) | J = 9.9 |
| 3 | 187.5 | - | - |
| 4 | 130.1 | - | - |
| 5 | 157.7 | - | - |
| 6 | 74.9 | 4.77 (d) | $J_{15}$ = 1.2; $J_7$ = 10.9 |
| 7 | 50.9 | 2.68 (td) | $J_8$ = 3.9; $J_6$ = 10.9; $J_8$ = 12.9 |
| 8 | 26.2 | Ha 1.78 (m); Hb 2.05 (m) | |
| 9 | 38.1 | Ha 1.66 (m); Hb 2.12 (m) | |
| 10 | 42.3 | - | - |
| 11 | 141.5 | - | - |
| 12 | 167.9 | - | - |
| 13 | 126.6 | Hb 5.77 (s); Ha 6.25 (d) | J = 0.8 |
| 14 | 11.4 | 1.3 (s) | - |
| 15 | 23.9 | 2.21 (d) | J = 1.2 |
| O-*$CH_2$*-$CH_3$ | 61.4 | 4.21 (q) | J = 7.0 |
| O-$CH_2$-*$CH_3$* | 14.3 | 1.3 (t) | J = 7.0 |

Two low-intensity carbon signals at $\delta_C$ 0.1 and 29.9 were assigned to the common NMR solvent impurity.

## 6.4 Attempted preparation of Michael adducts of STLs in an aprotic solvent

In order to minimise the formation of the by-product, a reaction of compound **5.17** in the aprotic solvent dioxane for over 48 hours was attempted, but proved unsuccessful. Only starting STL was found in the reaction mixture (by TLC).

## 6.5 Biological screening of Michael adducts of STLs

The diethylamino derivatives (DEA) prepared in this study were evaluated for their growth inhibitory properties on cultured cancer cells. The $IC_{50}/GI_{50}$ values were compared to those of their parent STLs.

### 6.5.1 *In vitro* anticancer activity

The DEA derivatives were tested against a preliminary 3-cancer cell line panel at the CSIR. All the compounds were tested across a concentration range of 6.25 – 100 ppm as described in the experimental Section 3.2.4 (Chapter 3). The effect of the test compounds on growth inhibition of CHO cells was also evaluated. The results are summarised in Table 6.6.

To summarise the results from Table 6.6, with the exception of the *parthenolide: DEA-parthenolide* pair, a general trend was observed. Whereas for the *DHB: DEA derivative* the toxicity towards mammalian cells has not changed with derivatisation, the desired decrease in cytotoxicity was observed for the DEA derivative of compound **5.17**. For the *parthenolide: parthenolide DEA* pair, both the activity against cancer cells and the cytotoxicity values towards mammalian cells increased 5- and 20-fold respectively.

**Table 6.6. *In vitro* activity against a 3-cancer cell line panel and CHO**

| Structure | Code | 3-cell line cancer screen (CSIR), µM | | | $IC_{50}$(CHO), µg/mL |
|---|---|---|---|---|---|
| | | $GI_{50}$ | TGI | $LC_{50}$ | |
| 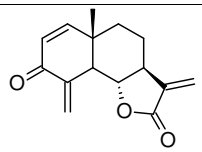 | **(4.2)** | 0.67 | 1.57 | 2.48 | 4.2 |
| 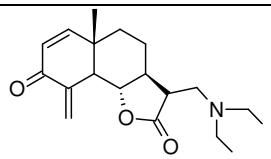 | **(6.7)** | 1.3 | 2.6 | 3.98 | 4.66 |
| 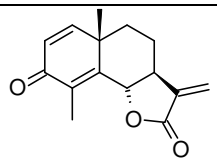 | **(5.17)** | 7.79 | 18.29 | 28.8 | 1.71 |
| 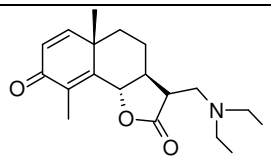 | **(6.9)** | 22.2 | 51.1 | 80.1 | 28.31 |
| 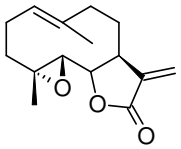 | **(5.3)** | 5.32 | 10.8 | 16.3 | 1.89 |
| 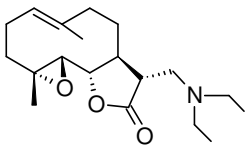 | **(6.6)** | 1.11 | 2.35 | 3.58 | 0.75 |

### 6.5.2 *In vitro* antimalarial screening

All compounds were tested in duplicate against *P. falciparum* CQS (D10) and CRS (K1), with CQ used as a reference compound in all experiments. The results of the cytotoxicity were measured as 50% inhibitory concentration obtained from the dose response curves (fitting analysis Graph Pad Prism v4 software). The SI index was calculated as the ratio of the $IC_{50}$ values of the toxicity towards mammalian cells (CHO) to the toxicity towards *P. falciparum*. The results are summarised in Table 6.7.

As is evident from Table 6.7, there is no general activity or cytotoxicity trend between the three pairs of *STL and DEA-STL*.

**Table 6.7. *In vitro* antiplasmodial activity against *P. falciparum***

| Structure | Code | $IC_{50}$ (µg/mL) | | | |
|---|---|---|---|---|---|
| | | CQS (D10) | CRS (K1) | CHO | SI (D10) |
| 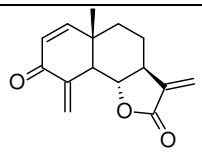 | **(4.2)** | 0.38 | 0.06 | 4.2 | 11 |
| 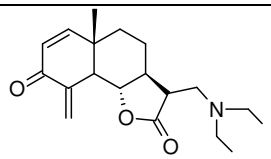 | **(6.7)** | 1.29 | 2.88 | 4.66 | 3.6 |
| 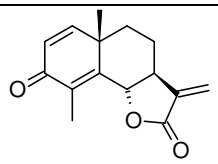 | **(5.17)** | 2.82 | 2.21 | 1.71 | 0.6 |
| 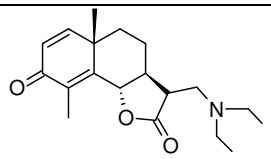 | **(6.9)** | 8.93 | 19.91 | 28.31 | 3.2 |
| 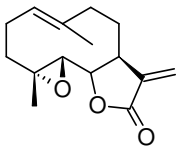 | **(5.3)** | 1.97 | 2.46 | 1.89 | 1 |
| 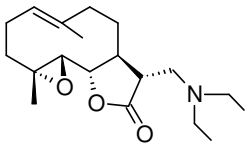 | **(6.6)** | 4.27 | 6.95 | 0.75 | 0.2 |
| Chloroquine | **CQ** | 0.012 | 0.122 (K1)<br>0.152 (Dd2) | | |

*SI (selectivity index) = cytotoxicity* CHO $IC_{50}$/antiplasmodial $IC_{50}$
D10 = *P. falciparum* – chloroquine-sensitive strain
KI = *P. falciparum* – chloroquine-resistant strain
CHO = Chinese hamster ovarian cells

In the case of DHB and its DEA derivative, a 4-fold drop in activity was observed against the D10 strain with a subsequent drop in SI value, with no change in cytotoxicity towards mammalian cells. In the case of compound **5.17**, its *DEA-*

derivative exhibited a 3-fold lower activity, whilst the cytotoxicity value improved by 14-fold, with subsequent improvement in SI (3.2). The least active compound, *parthenolide* [$IC_{50}$(D10) = 1.97 µg/mL], showed the smallest drop in activity (2-fold), whilst its cytotoxicity value increased with a 5-fold drop in SI.

## 6.6 Discussion

Three Michael-type secondary amino adducts of the selected STLs were prepared and characterised. The addition of secondary amines was regioselective and stereospecific to afford adducts with an *α*-orientated amino side chain. Attempts to minimise the lactolysis by using aprotic solvents in the reaction media proved to be unsuccessful.

Furthermore, all diethylamino derivatives and their parent STLs were screened for *in vitro* activity against a 3-cancer cell line panel and against *P. falciparum* as described in the previous chapters. The activity and cytotoxicity of the derivatives did not follow any general trend. The activity of all derivatives in the two test models used remained in the micromolar range. These results, however, cannot be extrapolated to *in vivo*. Several other Michael adducts of dehydrobrachylaenolide **(4.2)** should be prepared to find the ultimate side chain, which it is hoped will improve the solubility and activity of the compound.

# Chapter 7: Summary and Concluding Remarks

## 7.1 General

The South African medicinal plant *Dicoma anomala* subsp. *gerrardii,* the extract of which had previously been proved to possess selective *in vitro* anticancer activity against a 3-cell line panel ($GI_{50}$ = 12.5 µg/mL), was subject of this investigation. To our knowledge, this subspecies was not previously documented in the ethnobotanical literature. Several compounds, such as flavonoids, terpenoids and phytosterols, which were reported to occur in other *Dicoma* species, could be responsible for or contribute to the activity of the root extract. Because of the phytochemical variability amongst various members of the genus, the isolation of the compounds responsible for the activity through bioassay-guided fractionation was performed.

## 7.2 Confirmation of the taxonomic identity of the ethnobotanical sample

Since the original botanical specimen was only partially identified, the correct taxonomy had to be established prior to the recollection efforts. Based on the re-evaluation of the original botanical specimen, and by comparing the stated habit with the description of various subspecies in the recent revision of the genus, it was possible, with great certainty, to subclassify the plant as *D. anomala* subsp. *gerrardii*.

## 7.3 Bulk recollection and processing

The bulk recollection effort was then directed by the availability of the plant, which was harvested from a large population in the North West province, RSA. An extraction method was optimised for the small scale of the plant material and the selection of solvent was guided by its bioactivity. Five crude extracts were produced with solvents of different polarity, which were tested for *in vitro* anticancer activity. Ethyl acetate was found to afford an extract with superior activity ($GI_{50}$ << 6.25 ppm) and was used for the bulk extraction.

## 7.4 Bioassay-guided isolation of active compounds

Bioassay-guided fractionation of the ethyl acetate extract of the rhizomes of *D. anomala* subsp. *gerrardii* led to the isolation of two bioactive compounds: a sesquiterpene lactone and a dimeric sesquiterpene lactone. The structures were solved on the basis of MS, HR-MS, UV/VIS and NMR analysis ($^{1}$H-NMR, $^{13}$C-NMR, DEPT135, $^{1}$H↔$^{1}$H COSY, $^{1}$H↔$^{13}$C HMQC and HMBC) to afford two known compounds, (**4.2**; $GI_{50}$ = 0.67 µg/mL) and (**4.3**; $GI_{50}$ = 0.75 µg/mL). The compound **4.2** was identical to the previously isolated dehydrobrachylaenolide (DHB) **(2.42)** and its structure was further confirmed by comparing the assigned spectroscopic values with the published data. The DHB **(4.2)** was previously reported to possess antibacterial properties against the *Bacillus subtilis* gram-positive bacterium and an inhibitory activity regarding the induction of the intracellular adhesion molecule-1 (ICAM-1). The dimer **4.3** is a known compound which is patented for its antiplasmodial properties; however the NMR data and the structure assignment for this compound have not been published previously.

## 7.5 Structures and stereochemistry of the active compounds

Relative stereochemistry of compound **4.2** was established on the basis of $^{1}$H↔$^{1}$H coupling constants, where hydrogens at C-5, C-6 and C-7 were assumed in the anti-periplanar positions ($J_{5,6}$~$J_{6,7}$~10.8 Hz). This finding was further confirmed by determination of the crystal structure. The previously postulated absolute configuration of dehydrobrachylaenolide **(4.2)** was confirmed on the basis of the value of the measured optical rotation ($[\alpha]^{24}_{D}$+68°; c 0.50, $CHCl_3$), which was compared with that of synthetic dehydrobrachylaenolide ($[\alpha]^{24}_{D}$+67.9°; c 0.16, $CHCl_3$). Therefore the configuration of the stereogenic centres in DHB isolated from *D. anomala* subsp. *gerrardii* is as follows: 10*S*, 5*R*, 6*S*, 7*S*.

The relative and absolute configuration of the sesquiterpene dimer **4.3** could not be assigned with certainty. The relative orientation of the protons was deduced to be as follows: H-1/H-5 *cis* and H-4'/H-5', H-5/H-6' and H-4'/H5' all *trans*. This followed from the sizes of the coupling constants, which were then compared with the values reported for guaianolide-type sesquiterpenes. Both lactone moieties are *trans*-fused, with C-6, C-6', C-7 and C-7' assuming an *S*-configuration. This result

could not be confirmed by X-ray due to the difficulties with obtaining suitable crystals.

However, it should be possible to determine the absolute stereochemistry by employing electronic circular dichroism (ECD) or vibrational circular dichroism (VCD) techniques. For ECD technique a simple correlation between the sign of the Cotton effect (CE) and the stereochemistry of the chromophores can be deduced from the data.[156] With the VCD technique, the absolute configuration of the guaiane-type sesquiterpene lactones and the predominant solution-state conformation can be determined by comparing the experimental and calculated VCD spectral data.[157] Further experiments need to be conducted to determine the absolute stereochemistry of compound **4.3** using one or both of the abovementioned techniques.

### 7.6 Bioactivity of the compounds *vs* activity of the crude extract

The activity of the crude extract of *D. anomala* subsp. *gerrardii* could probably be attributed to the isolated compounds. The presence of other compounds with similar bioactivity profiles could not be ruled out. However, since the activity of the fractions containing dehydrobrachylaenolide **(4.2)** and the dimer **4.3** was superior amongst the resulting fractions, the overall effect observed for the crude extract *in vitro* could be due to the synergistic action of the various components.

### 7.7 Chemotaxonomic remarks

For chemotaxonomic and ethnobotanical purposes, a comparative HPLC study of another subspecies of *Dicoma* was embarked on to establish whether the chemistry of the two taxonomically recognised subspecies really differs. The results showed that the HPLC profiles were vastly different, and the presence of dehydrobrachylaenolide **(4.2)** and of the sesquiterpene dimer in the DCM-soluble fraction of the root extract of *D. anomala* subsp. *anomala* (collected in Gauteng) could not be confirmed. One publication reports that the dimer **4.3** was isolated

---

[156] Stöcklin W., Waddelland T. G., Geissman T. A. (1970). *Tetrahedron*, **26**, 2397–2409.
[157] Michalskia O., Kisielb W., Michalskab K., Setnickac V., Urbanovad M. (2007). *Journal of Molecular Structure*, **871**, 67–72.

from an unspecified subspecies of *D. anomala* harvested from the Free State and Lesotho.[28] In order to establish a correlation between the chemistry and the proposed classification, further investigations into subspecies and regional forms of *D. anomala* are required. Moreover, it is noteworthy that two vernacular names, *i.e.* Kloenya (Sotho) and Nyongwane (Zulu), were provided by the traditional healer for the plant with the specified habitat and life form (erect). A further ethnobotanical study should be considered to establish whether the use of vernacular names is specific to the plant or to its medicinal properties.

## 7.8 Identification of sustainable sources of compound 4.2

There are several possibilities for the bulk production of the reasonably pure dehydrobrachylaenolide **(4.2)**. The most obvious resource is the plants themselves, which could be harvested from the wild in a sustainable manner (high-impact harvesting). However, there are several reports pointing to the already existing threat of overutilisation of *D. anomala* in the RSA and Namibia. This is because of the widespread use of *D. anomala* in primary healthcare and because this species is propagated only by seed and is highly site-specific and sensitive. High-impact harvesting of rhizomes could wipe out the plant populations altogether.[158] The establishment of cultivation programmes could be an alternative to wild harvesting. Plant material of specific genetic make-up could be cultivated through tissue culture technique, and was successfully developed at the CSIR for *D. anomala* subsp. *gerrardii* (results are not reported in this dissertation).

Other plant species were investigated as potential sources of DHB. The roots of the invasive tree *Brachylaena transvaalensis* could serve an alternative, but are hardly an attractive source due to their very low content of the compound.

Another route dehydrobrachylaenolide is semisynthesis. A simple one-step oxidation of the conjugated unsaturated alcohol **2.43**, which was found in abundance in the aerial parts of *D. capensis* can be successfully achieved by using $MnO_2$. Cultivation or wild harvesting of *D. capensis* is also a possibility.

---

[158] Dzerefos C. M., Witkowski E. T. F. (2004). *Biomedical and Life Sciences*, **10**, 1875–1876.

Finally, there are several reported methods for the synthesis of DHB from commercially available *α*-santonin. Most of these, however, suffer from low yields and irreproducibility.[53] However, the attempted synthesis of compound **4.2**, using some of the reported methods, by Dr E. Mmutlane of the Discovery Chemistry group of the CSIR resulted in a thermodynamically favoured reaction product compound **5.17**. The optimisation of reaction conditions to achieve kinetically controlled and thus desired product should be investigated.

### 7.9 Antimalarial activity of dehydrobrachylaenolide (4.2)

In addition, the isolated compounds, dehydrobrachylaenolide **(4.2)** and the dimer **4.3**, were tested for *in vitro* inhibitory activity against *P. falciparum*. Based on the considerable antiplasmodial activity [$IC_{50}$(D10) = 0.38 µg/mL; $IC_{50}$(K1) = 0.06 µg/mL] and the selectivity index (70), dehydrobrachylaenolide **(4.2)** was advanced into the *in vivo* murine malaria model. A substantial survival rate of the animals treated subcutaneously with dehydrobrachylaenolide **(4.2)** was achieved (60% of the animals in the treated group lived 9 days longer than the control group), but the extreme levels of parasitaemia experienced could not be rationalised (60%).

One of the possible explanations for these *in vivo* data is that dehydrobrachylaenolide **(4.2)** may, in addition to its direct effect on the parasite observed *in vitro*, affect other pathways, leading to offset of the death in spite of the lethal parasitaemia levels. One of the clues was found in relation to the reported inhibitory activity of the induction of surface intracellular adhesion molecule-1 (ICAM-1) in the *in vitro* model of human endothelial cells. The expression of excess ICAM-1 (or “up-regulation”) on the surface of the endothelial cells of a blood vessel plays an important role in the progress of a wide range of inflammatory and immune reactions,[158] and is implied in certain stages of progression of tumorigenesis and cerebral malaria. It was previously established that there is an increased expression of ICAM-1 on the brain endothelial surface at the ring and trophozoite blood stages of the parasite cycle in the host. Since ICAM-1 is one of the major receptors for the sequestration of infected erythrocytes in the brain endothelium, it is reasonable to hypothesise that dehydrobrachylaenolide **(4.2)** could prevent the adhesion of infected erythrocytes

to the brain endothelium by inhibiting the expression of ICAM-1, thus offsetting the necrosis and death.

Furthermore, it was found that the nuclear factor-κB (NF-κB) pathway mediates the induction of ICAM-1 at the trophozoite stage. The transcription factor NF-κB is a DNA-binding complex regulator related to cellular inflammation, immune responses and carcinogenesis. In general, NF-κB promotes the transcription of pro-inflammatory genes such as ICAM-1, enzymes such as inducible nitric oxide synthase (iNOS) and cycloxygenase-2 (COX-2), cytokines and chemokines.[159] Various components of NF-κB-activating signalling pathways are frequent targets for antiinflammatory, anticancer and antimalarial agents such as STLs.[89,160] For instance, STLs are the only compounds for which a selective alkylation of p65/NF-κB has been proved to date.[161,162] Some results show that compounds with α-methylene-γ-lactone moiety control the signalling pathway upstream of the nuclear translocation of NF-κB.[163] The structural make-up of dehydrobrachylaenolide **(4.2)** has all of the elements known to be required for the potential inhibition of NF-κB-related components. It would be of great value to test dehydrobrachylaenolide **(4.2)** for the inhibitory activity of NF-κB DNA-binding activity, which can lead to the deactivation of NF-κB.

The possibility is suggested here that dehydrobrachylaenolide **(4.2)** has affinity for multiple targets; a dose-response study should be conducted since efficacy towards multiple drug targets may require a higher dose for *in vivo* study. In the light of the specific mechanism involved, several *in vivo* models were reviewed. It was found that in the current model with *P. bergei*-infected C57BL/b mice, the sequestration of parasitised red blood cells could not be observed.[90] However, the observed effects of DHB **(4.2)** *in vivo* could be partially due to the reduced adhesion of monocytes to brain endothelium (as a result of the inhibition of the

---

[159] Juurlink B. H. J. (2001). *Canadian Journal of Physiology and Pharmacology*, **79**, 266–282.
[160] Huang W. -C., Chan S. -T., Yang T. -L., Tzeng C. -C., Chen C. -C. (2004). *Carcinogenesis*, **25**, 1925–1934.
[161] Garcia-Pineres A. J., Lindenmeyer M. T., Merfort I. (2004). *Life Sciences*, **75**, 841–856.
[162] Lyß G. Knorre A., Schmidt T. J., Pahl H. L., Merfort I. (1998). *The Journal of Biological Chemistry*, **273**, 33508-33516.
[163] Yuuya S., Hagiwara H., Suzuki T., Ando M., Yamada A., Suda K., Nagai K. (1999). *Journal of Natural Products*, **62**, 22–30.

expression of ICAM-1), which subsequently may lead to a reduction of perivascular infiltration of mononuclear cells (observed in *P. bergei*-infected mice) and to the prolonged survival of the mice. The fact that on day 9 parasitaemia reached 60% at 100% survival could imply that the drug had a higher affinity towards inhibiting the induction of ICAM-1 than towards a parasite-related target. The importance of this possibility warranted seeking a model in which the effect of the drug on the adhesion and sequestration of *P. falciparum*-infected erythrocytes could be observed.

A model with *P. bergei*, in which young (BALB57XC57BL/b)F1 hybrid mice develop typical neurological symptoms (7 to 8 days post infection) in association with the sequestration of parasitised red blood cells, was identified.[164] The feasibility of using the hybrid strain for future *in vivo* experiments should be evaluated.

### 7.10 SAR

These results assumed certain specificity of the reaction of STLs with biological thyols. The addition of *N*-acetyl-*L*-cysteine to compound **5.17** proceeded stereospecifically to afford an adduct with an *α*-orientated side-chain. This finding is in good agreement with the previously reported orientation of the side-chain in synthetic and – most importantly – natural Michael adducts of STLs.[140]

The stereochemistry at C-11 was not determined for the cysteine or glutathione adducts due to the overcrowding of the $^{1}$H NMR spectra. The attempt to minimise the formation of the by-product by using less polar solvents proved unsuccessful. The by-product should be isolated and evaluated for efficacy in the *in vitro* models prior to the dose-response studies *in vivo*.

Several synthetic analogues were evaluated for bioactivity in an attempt to establish a correlation between the number of alkylating elements in dehydrobrachylaenolide **(4.2)** and the bioactivity, in both *in vitro* models (cancer

---

[164] Hearn J., Rayment N., Landon D. N., Katz D. R., De Souza J. B. (2000). *Infection and Immunity*, **68**, 5364–5376.

and malaria). Removal of any potentially alkylating elements resulted in significantly decreased bioactivity. These results were in good agreement with the previously suggested relationship in STLs.[55,91-94] The exocyclic double bond C-4 - C-15 did not participate in any Michael addition reaction, but probably potentiated the reactivity of the C-1 - C-2 alkylating effect, resulting in a 10-fold drop in bioactivity when compared with its isomer **5.17** with an endocyclic double bond C-4 - C-5. However, the overall requirement for the bioactivity of eudesmanolides cannot be stated with certainty.

### 7.11 Preparation of pro-dugs

If the *in vivo* efficacy of the compound proves to be convincing, there are a few possibilities for modifying the compound for oral administration with estimated oral bioavailability up to 70%. A study of the preparation of the so-called "pro-drugs" of dehydrobrachylaenolide **(4.2)** and its close isomer compound **5.17** showed that there was no general trend in the changes in the bioactivity-cytotoxicity ratio amongst the three drug – pro-drug pairs. However, a general drop in bioactivity and cytotoxicity was noted in both the *in vitro* bioassays (cancer and malaria). Further investigations of the kinetics and rate constants of the reverse reaction at physiological pH using $^{1}$H NMR analysis will be required in order to design a further *in vivo* study with the synthesised pro-drugs, which will be used for to select the best side-chain and for further evaluation of efficacy.

Additional studies into the mode of action of dehydrobrachylaenolide **(4.2)** against falciparum malaria have been initiated to elucidate the primary pathways and the target(s) underlying the antimalarial efficacy of dehydrobrachylaenolide **(4.2)** through systems biology approaches, by combining primarily proteomics and transcriptomics technologies (not reported in this dissertation). The preliminary results gave early indications that treatment with dehydrobrachylaenolide **(4.2)** resulted in significant changes in the proteome of *P. falciparum* in the ring stage of the parasite lifecycle.

# Appendix 1: NMR spectra of selected compounds (Chapters 4 to 6)

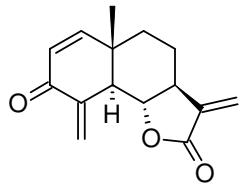


**Plate 1. $^{13}C$ NMR spectrum (400 MHz, $CDCl_3$) of compound 4.2 (assignments on p. 54)**

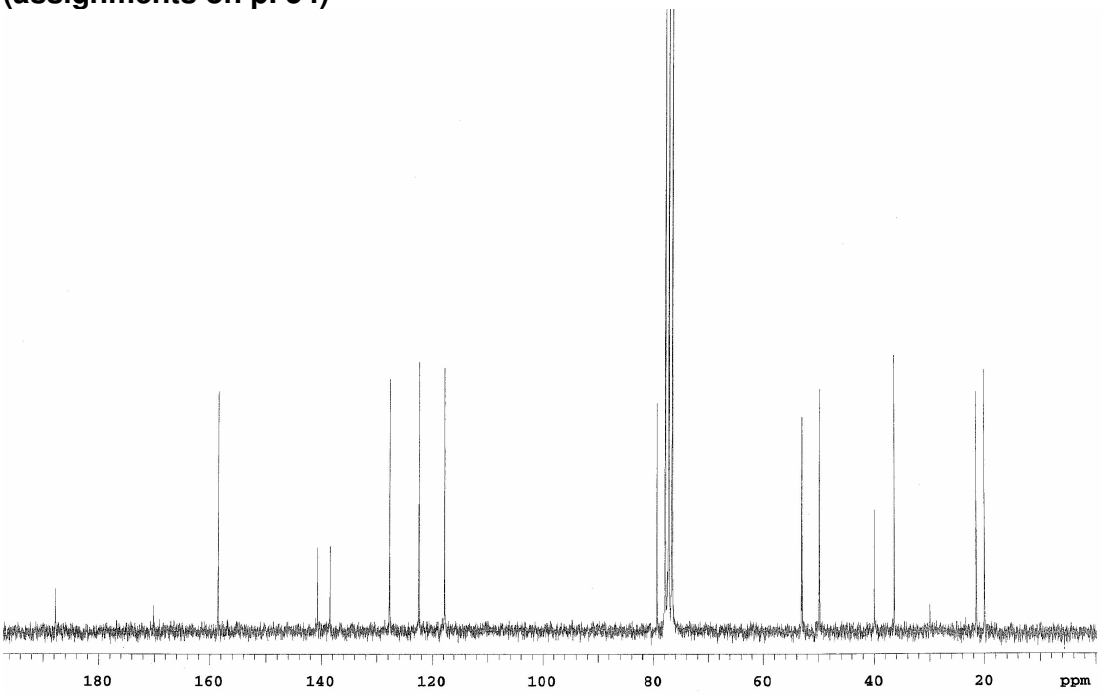


**Plate 2. $^{1}H$ NMR spectrum (400 MHz, $CDCl_3$) of compound 4.2 (assignments on p. 54)**

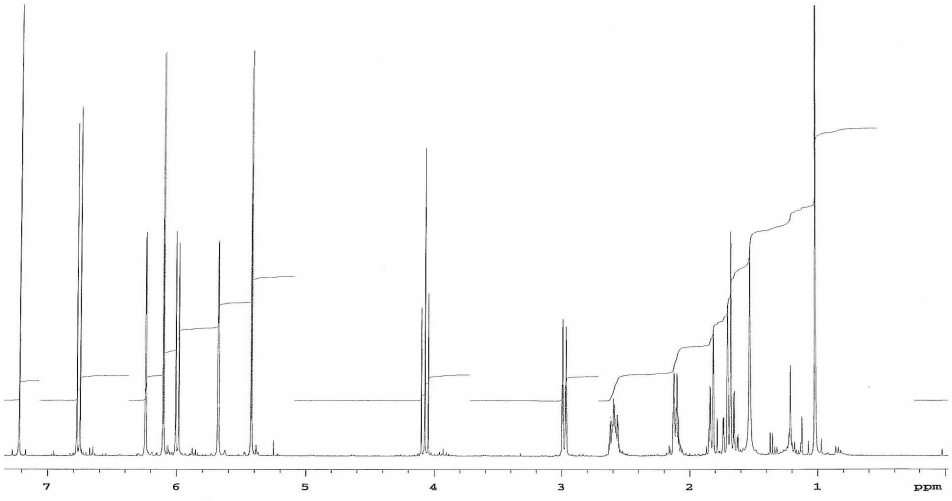

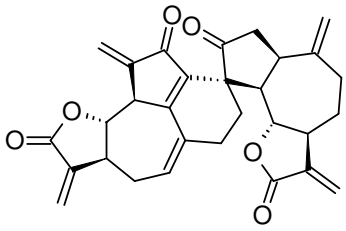

**Plate 3. $^{13}C$ NMR spectrum (400 MHz, $CDCl_3$) of compound 4.3 (assignments on p. 61)**

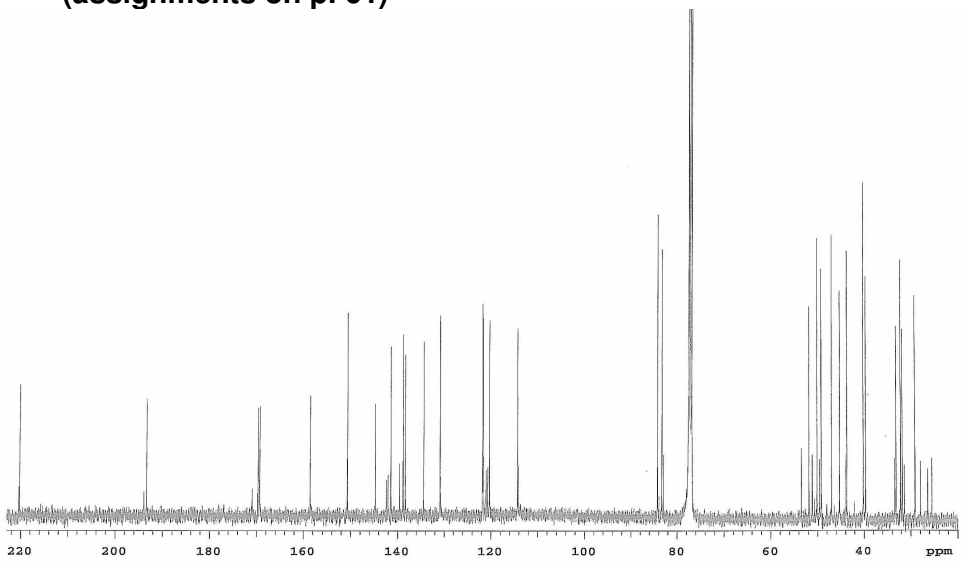


**Plate 4. $^{1}H$ NMR spectrum (400 MHz, $CDCl_3$) of compound 4.3 (assignments on p. 61)**

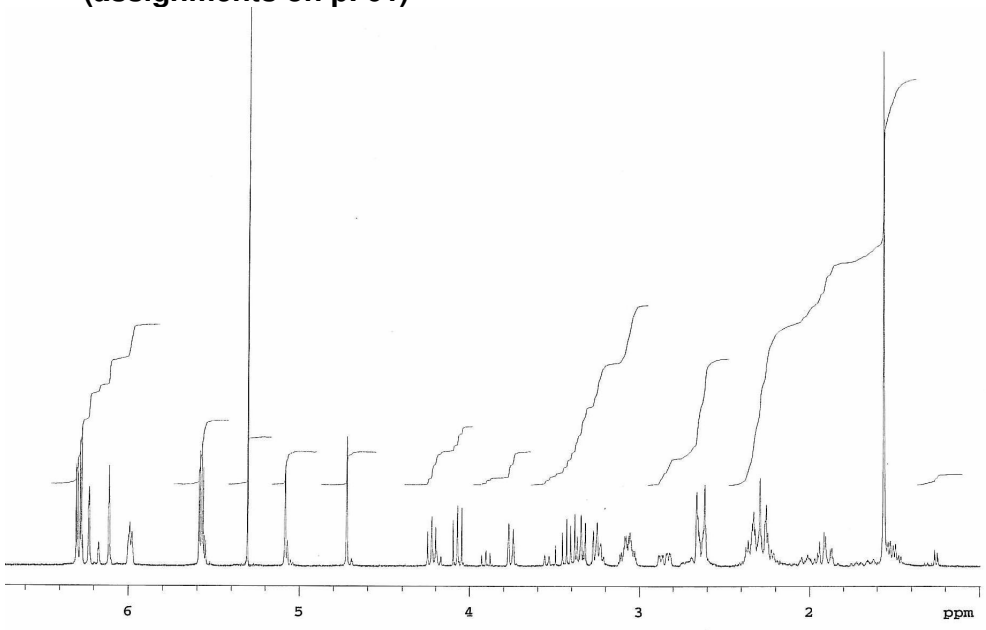

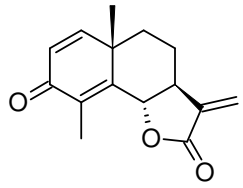


**Plate 5**. **$^{13}$C NMR spectrum (400 MHz, $CDCl_3$) of compound 5.17 (assignments on p. 96)**

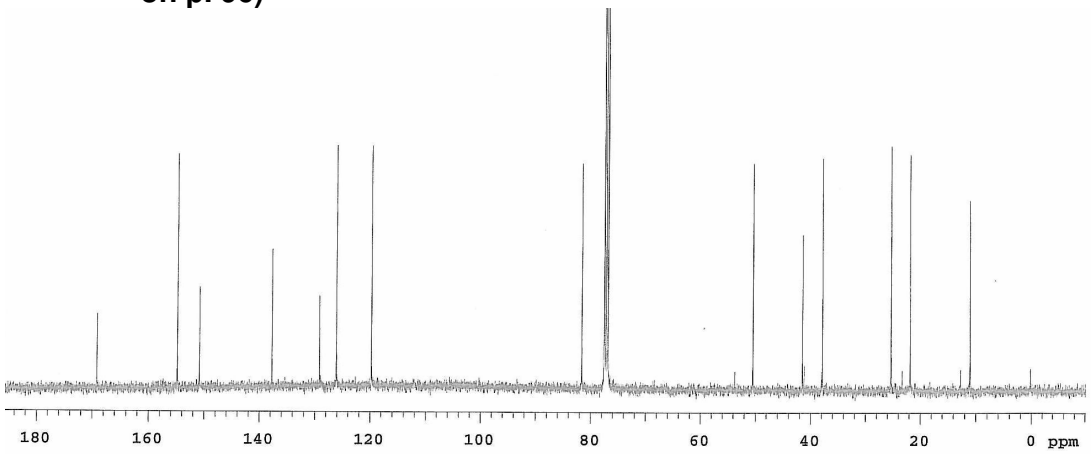


**Plate 6**. **$^{1}$H NMR spectrum (400 MHz, $CDCl_3$) of compound 5.17 (assignments on p. 96)**

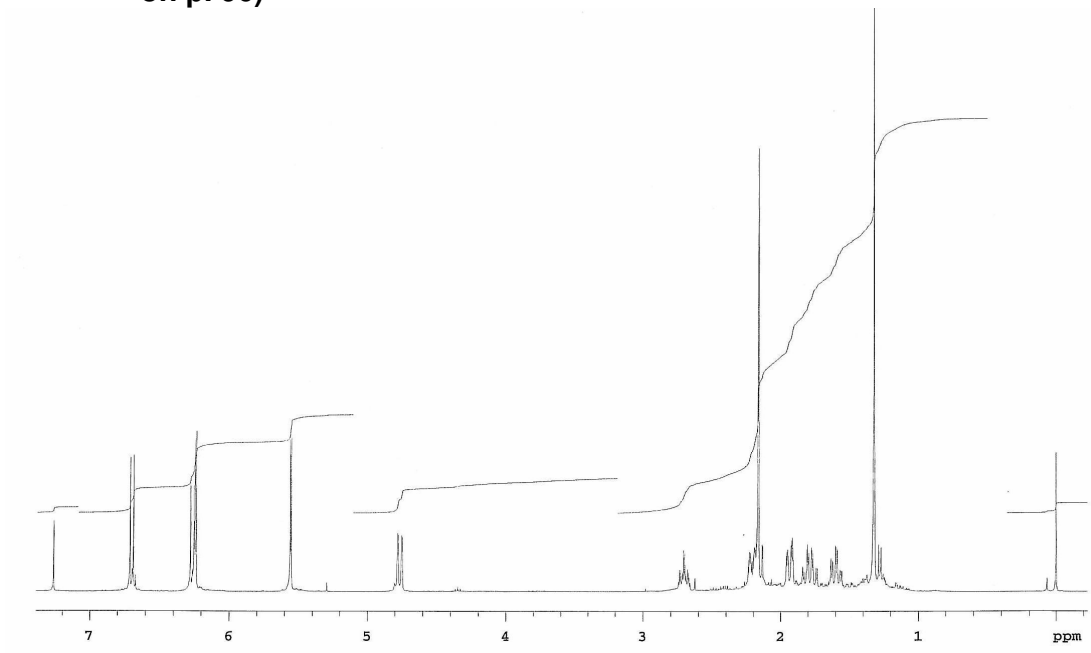

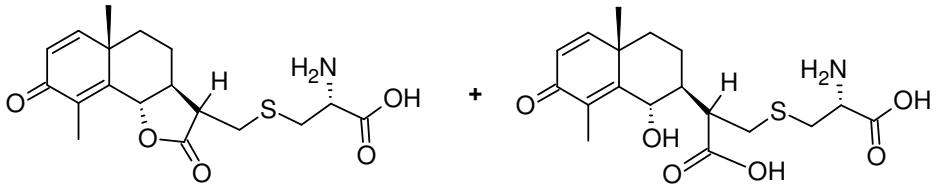

**Plate 7. $^{13}C$ NMR spectrum (400 MHz, $D_2O$) of compounds 5.28a and 5.28b (assignments on p. 101)**

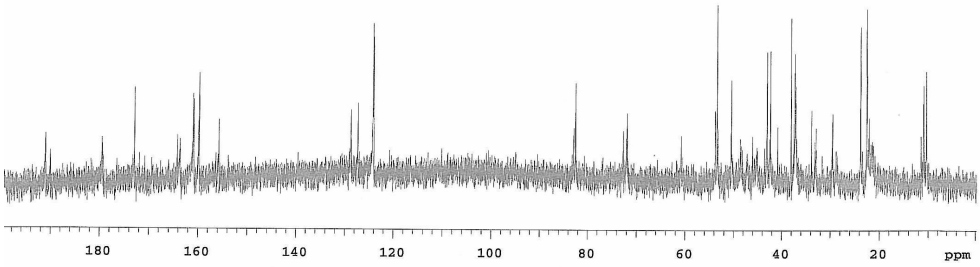


**Plate 8. $^{1}H$ NMR spectrum (400 MHz, $D_2O$) of compounds 5.28a and 5.28b (assignments on p. 101)**

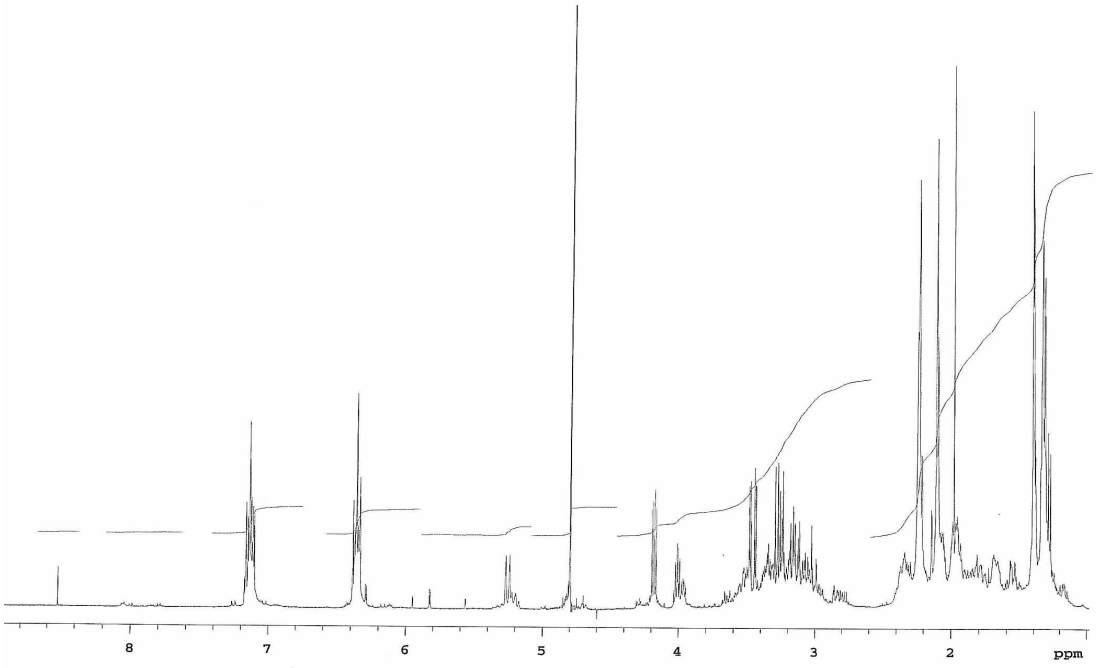

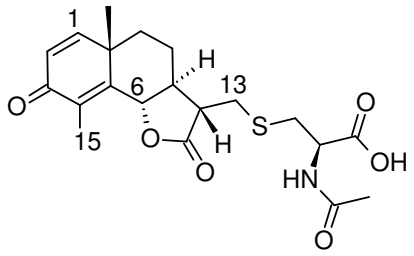


**Plate 9. $^{1}$H NMR spectrum (400 MHz, $D_2O$) of compound 5.29 (assignments on p. 106)**

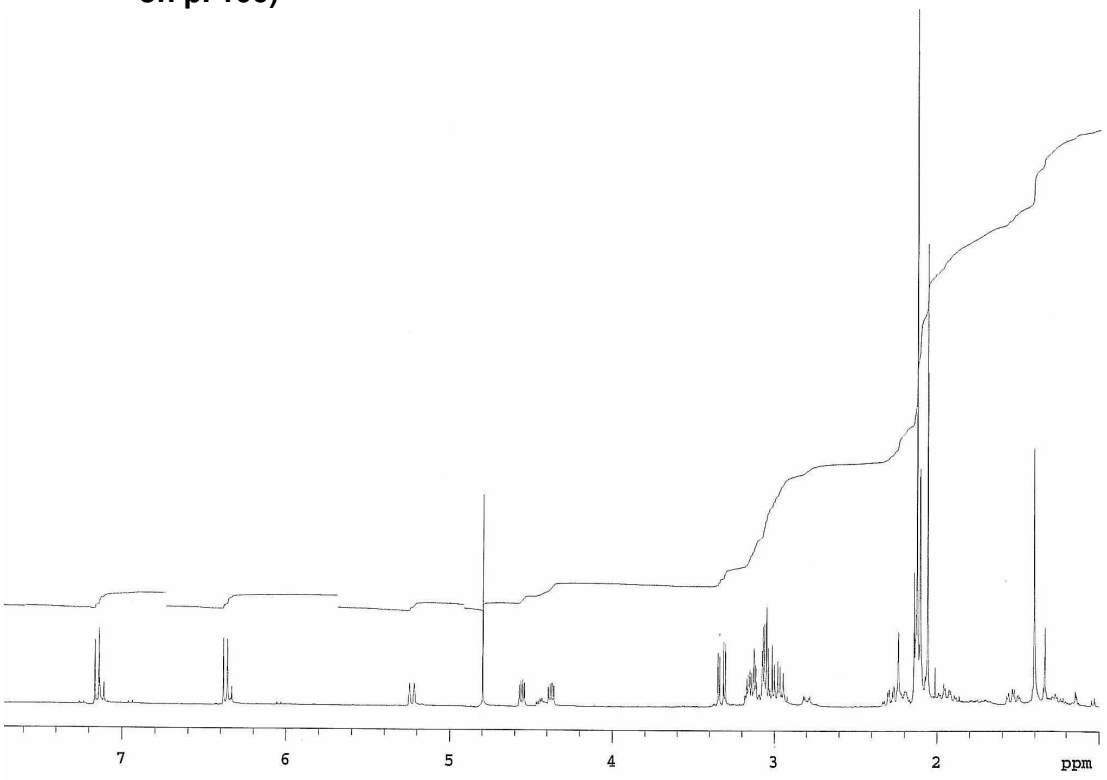

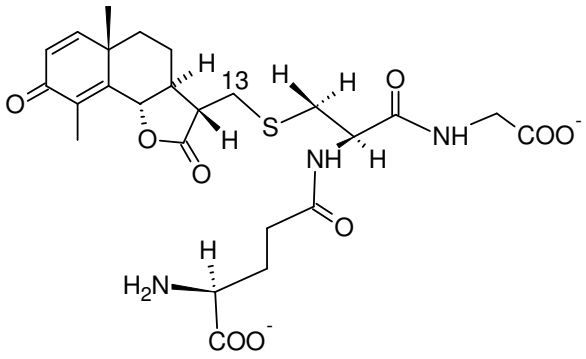


**Plate 10**. **$^1$H NMR spectrum (400 MHz, $D_2O$) of compound 5.33 (assignments on p. 109)**

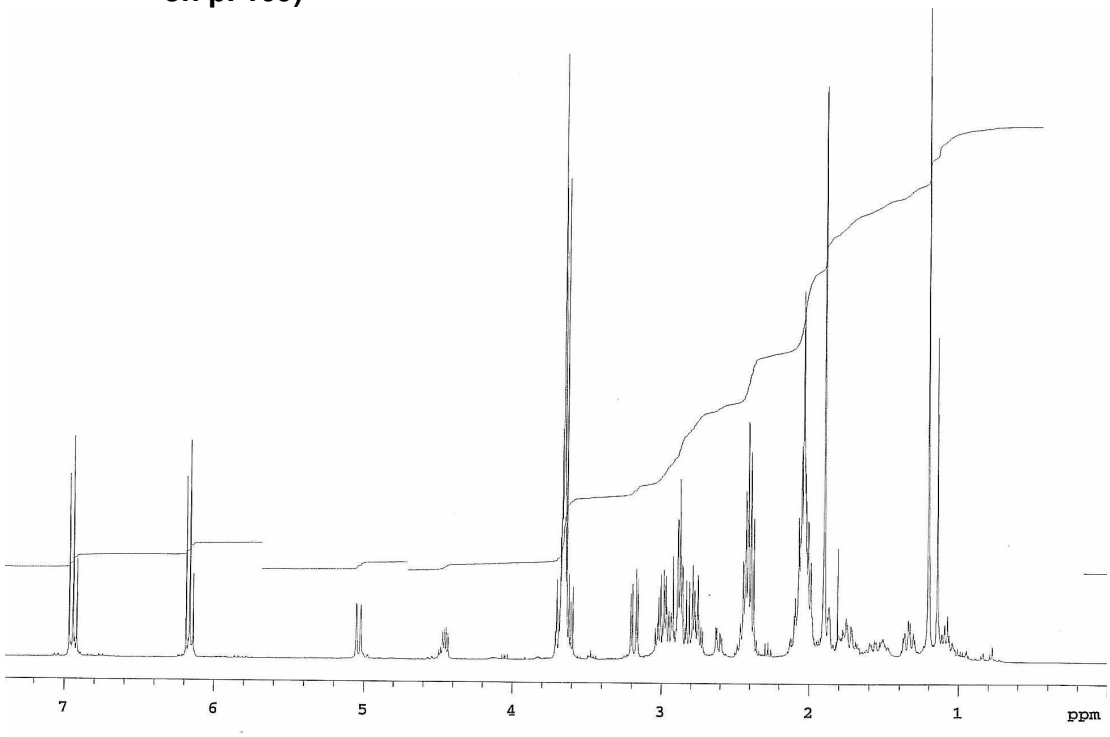

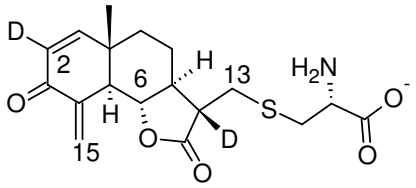


**Plate 11**. **$^{13}$C NMR spectrum (400 MHz, $D_2O$) of compound 5.27 (assignments on p. 98)**

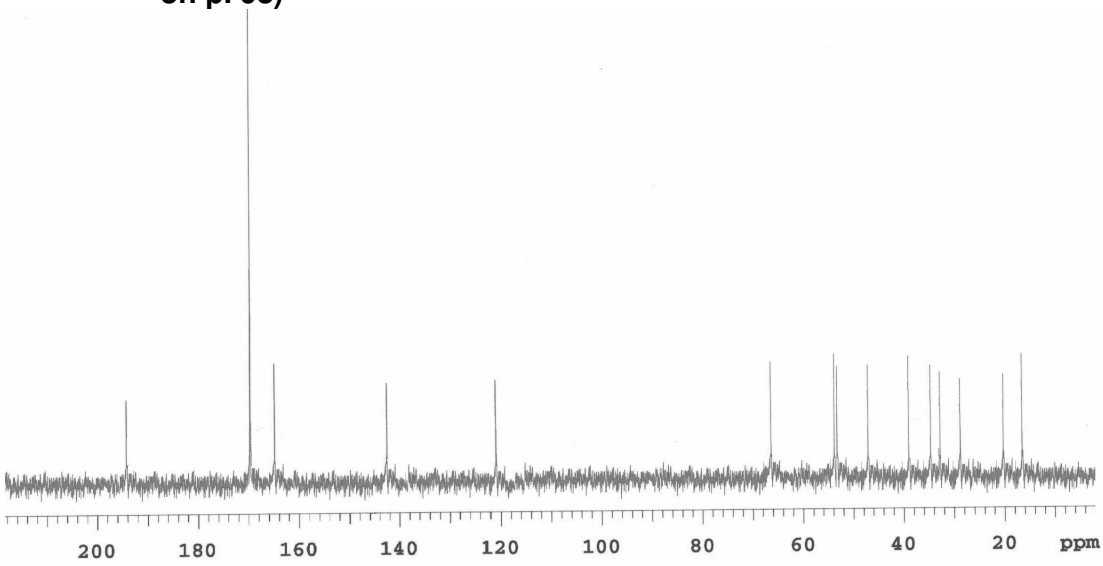


**Plate 12**. **$^{1}$H NMR spectrum (400 MHz, $D_2O$) of compound 5.27 (assignments on p. 98)**

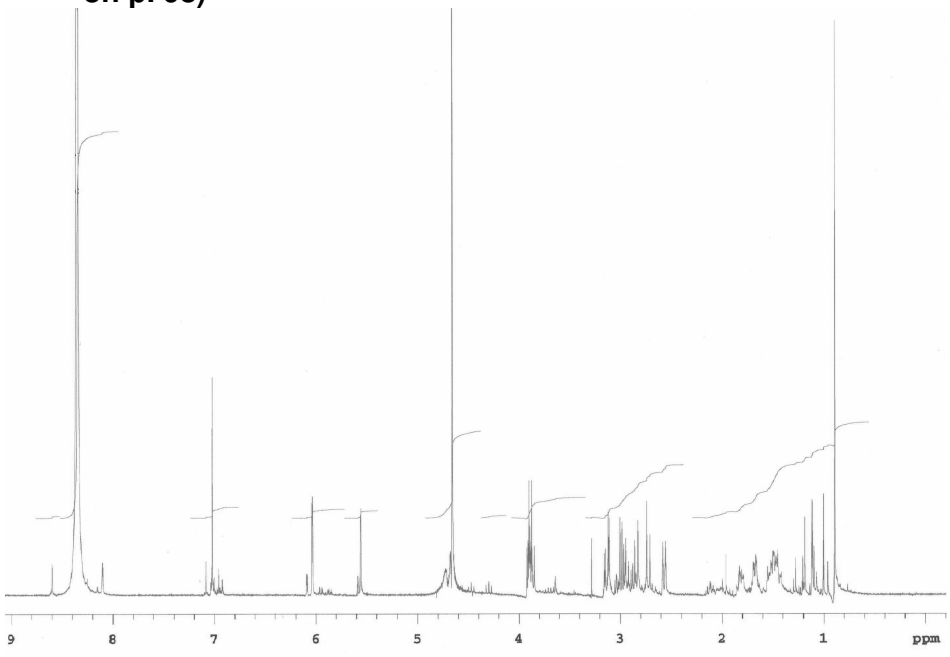

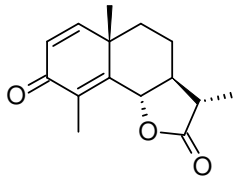


**Plate 13. $^{13}C$ NMR spectrum (400 MHz, $CDCl_3$) of compound 5.36 (assignments on p. 112)**

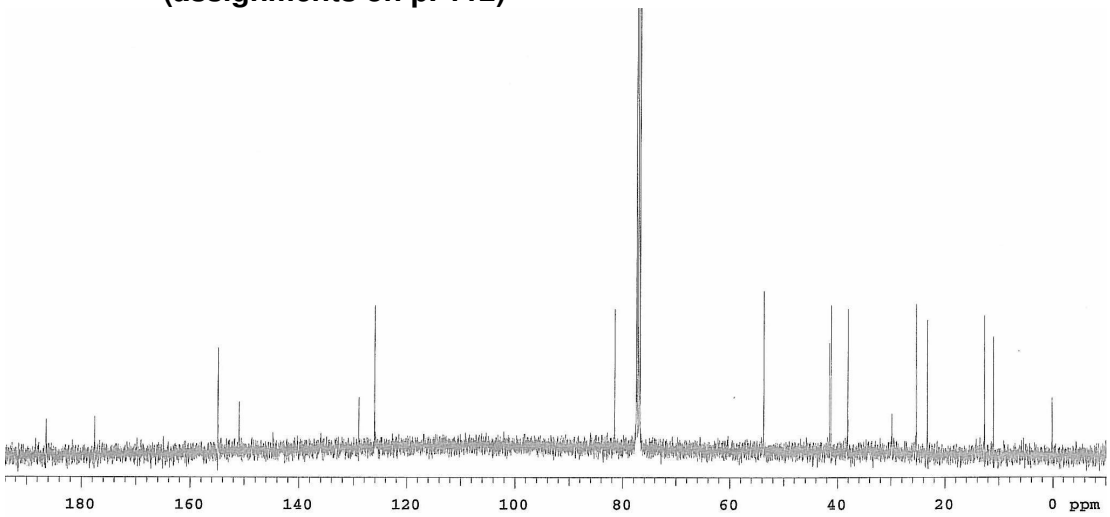


**Plate 14. $^{1}H$ NMR spectrum (400 MHz, $CDCl_3$) of compound 5.36 (assignments on p. 112)**

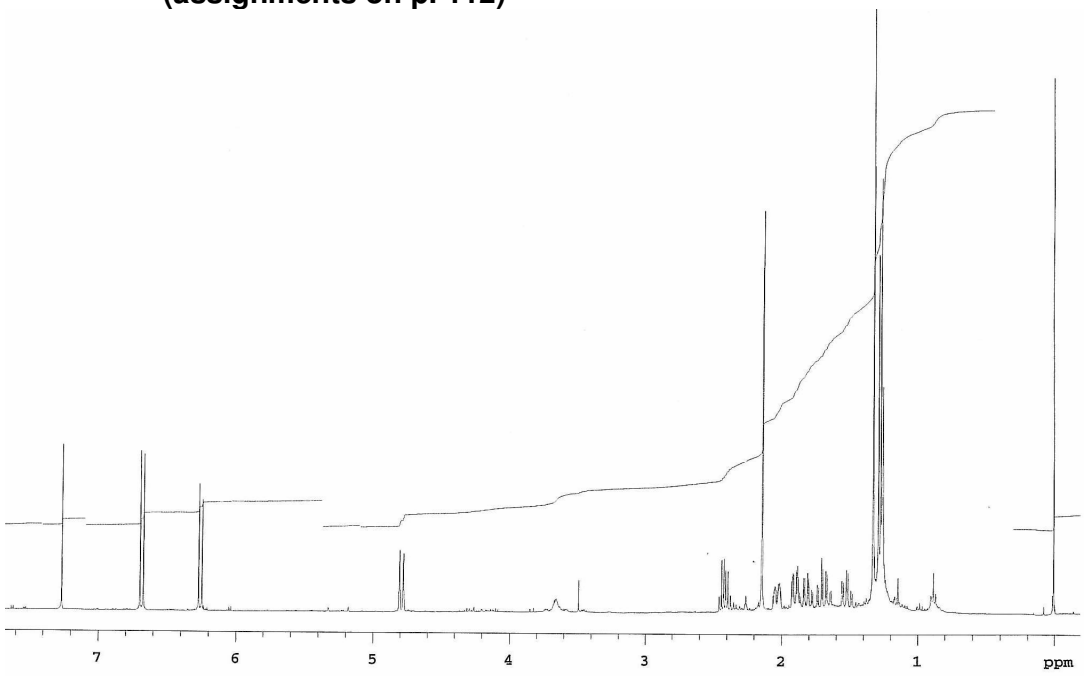

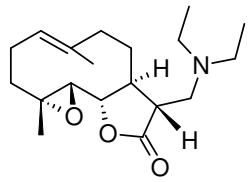


**Plate 15**. **$^{13}$C NMR spectrum (400 MHz, aceton-$d_6$) of compound 6.6 (assignments on p. 127)**

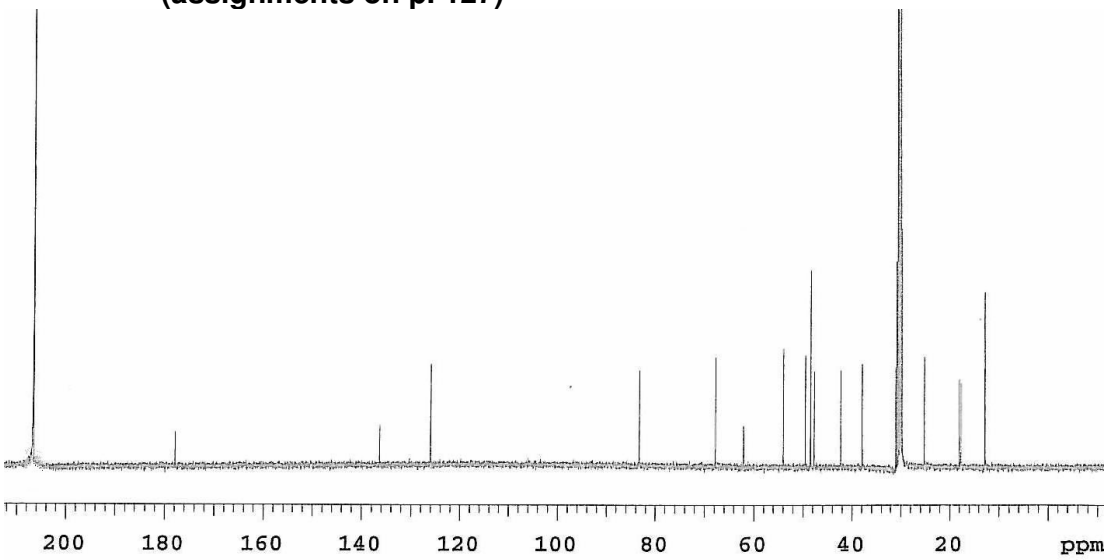


**Plate 16**. **$^{1}$H NMR spectrum (400 MHz, aceton-$d_6$) of compound 6.6 (assignments on p. 127)**

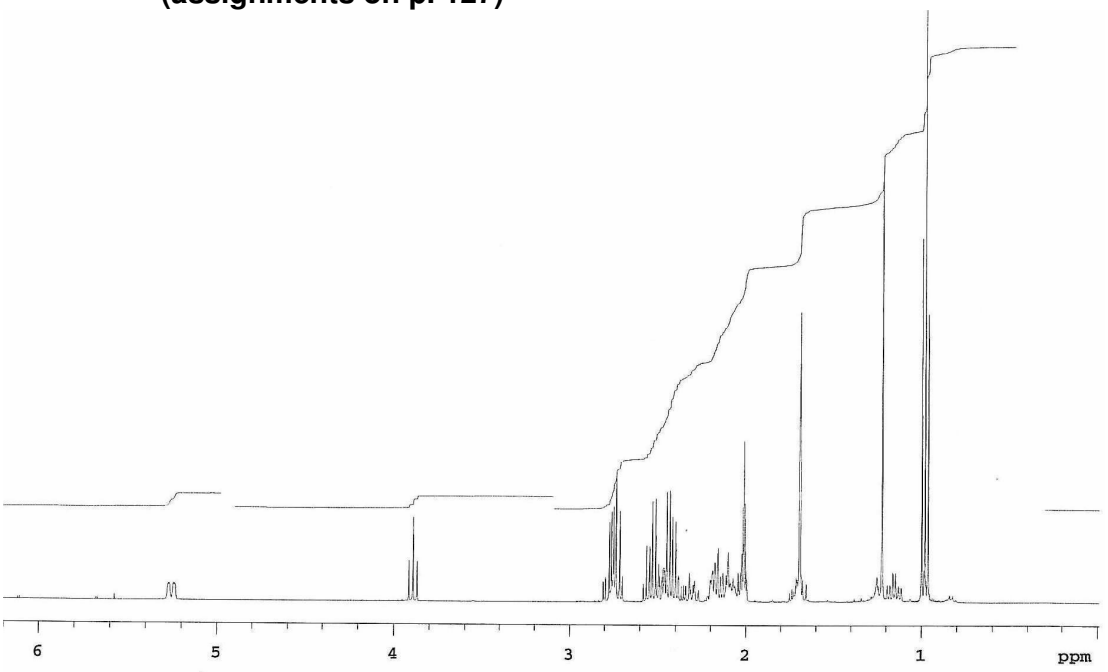

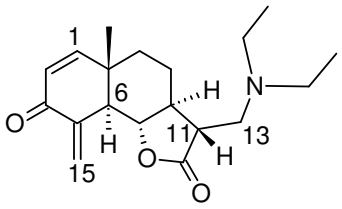


**Plate 17. $^{13}C$ NMR spectrum (400 MHz, aceton-$d_6$) of compound 6.7 (assignments on p. 129)**

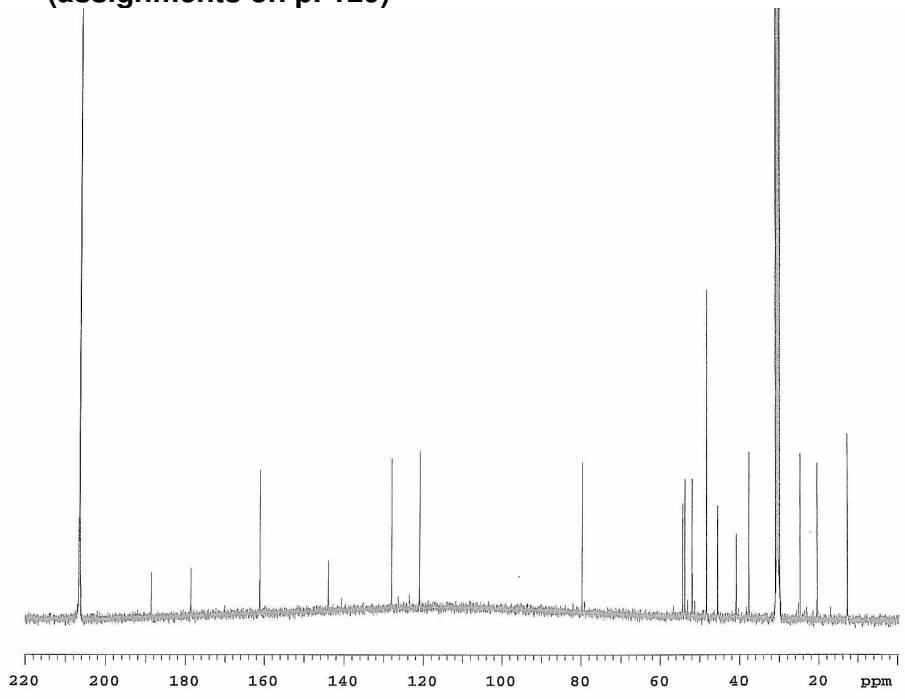


**Plate 18. $^{1}H$ NMR spectrum (400 MHz, aceton-$d_6$) of compound 6.7 (assignments on p. 129)**

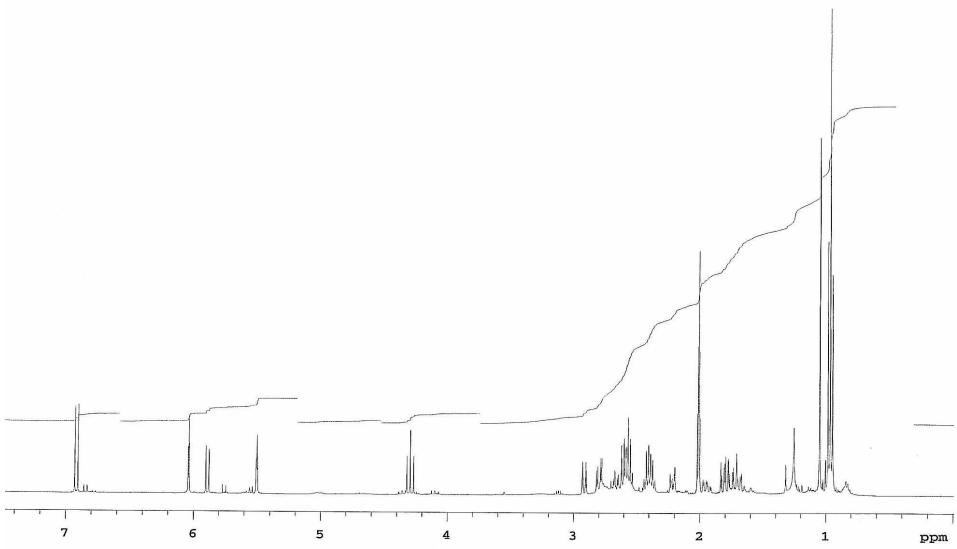

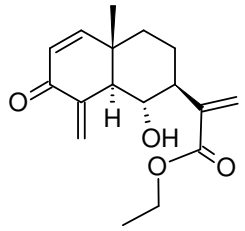


**Plate 19**: **$^1$H NMR spectrum (400 MHz, $CDCl_3$) of compound 6.8 (assignments on p. 129)**

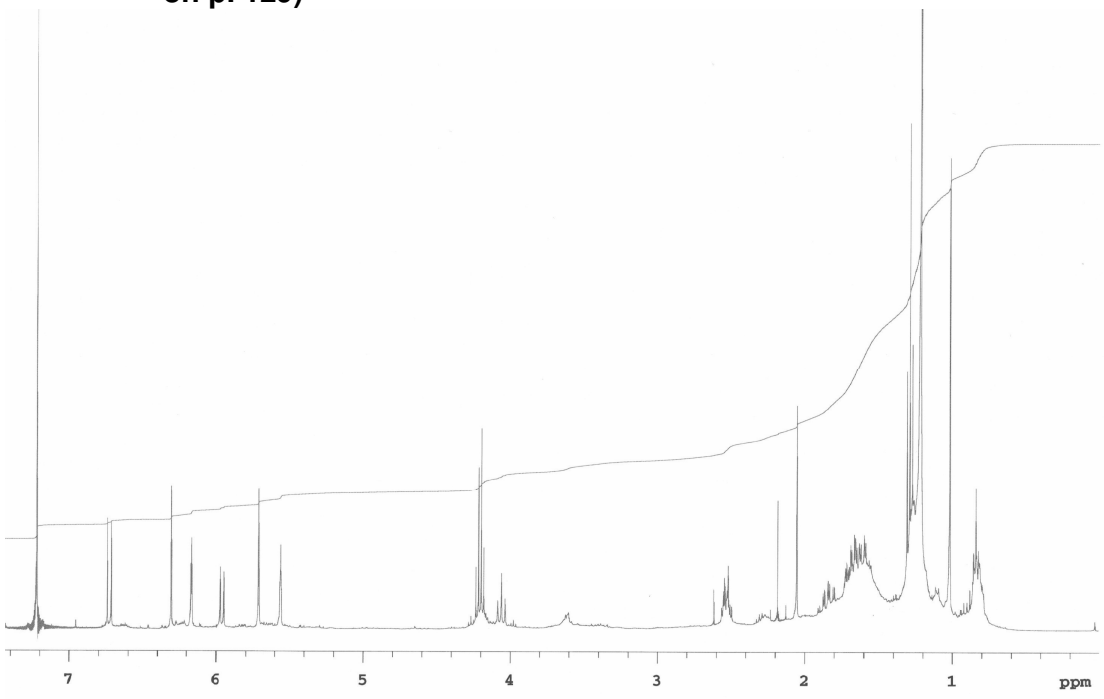

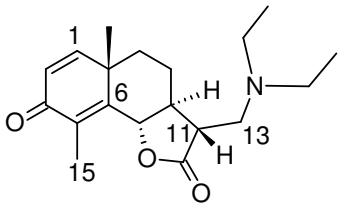


**Plate 20**. **$^{13}$C NMR spectrum (400 MHz, $CDCl_3$) of compound 6.9 (assignments on p. 132)**

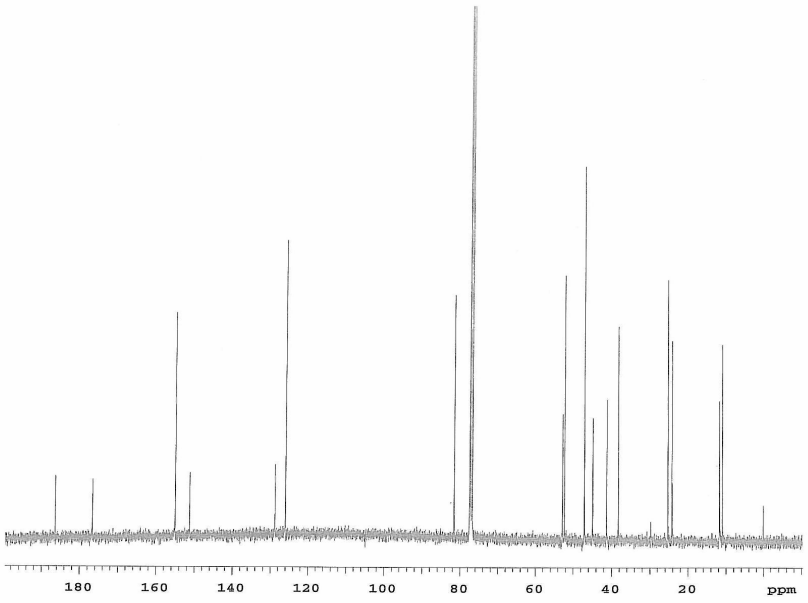


**Plate 21**. **$^{1}$H NMR spectrum (400 MHz, $CDCl_3$) of compound 6.9 (assignments on p. 132)**

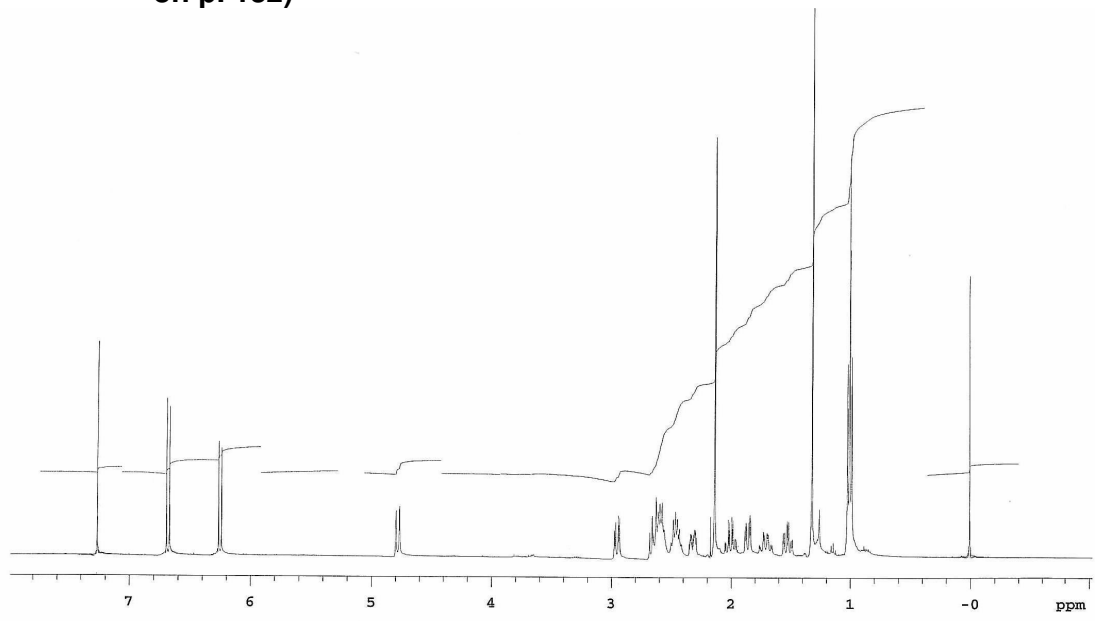

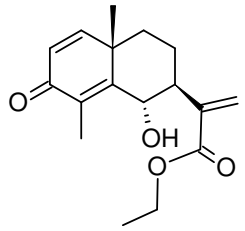


**Plate 22. $^{13}C$ NMR spectrum (400 MHz, $CDCl_3$) of compound 6.10 (assignments on p.134)**

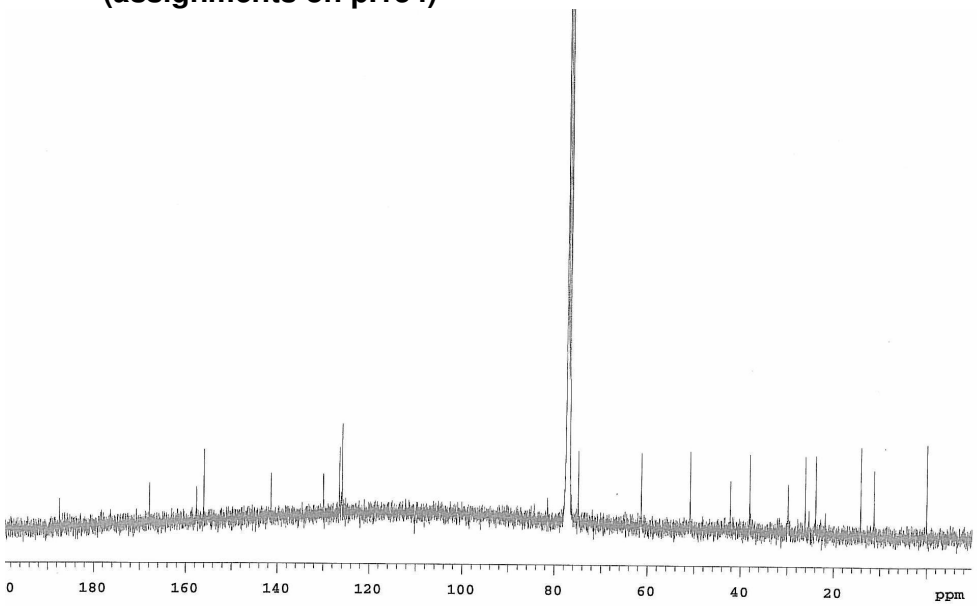


**Plate 23. $^{1}H$ NMR spectrum (400 MHz, $CDCl_3$) of compound 6.10 (assignments on p. 134)**

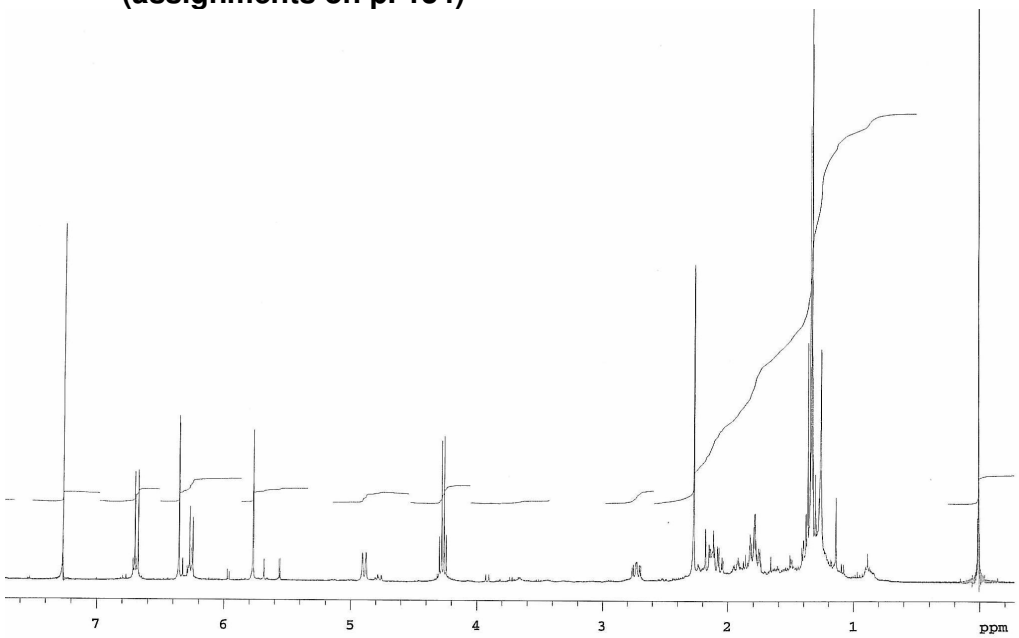

# Appendix 2: X-Ray crystallographic data for compound 4.2 (Chapter 4)

**Table A2.1. Crystal data, data collection and structure refinement parameters for compound 4.2**

| | |
|---|---|
| Empirical formula | $C_{15}H_{16}O_3$ |
| Formula weight | 244.28 |
| Temperature | 293(2) K |
| Wavelength | 0.71073 Å |
| Crystal system | Orthorhombic |
| Space group | P $2_1$ $2_1$ $2_1$ |
| Unit cell dimensions | a = 9.5648(6) Å α = 90º |
| | b = 11.1631(6) Å β = 90º |
| | c = 11.5542(6) Å γ = 90º |
| Volume | 1233.67Å$^3$ |
| Z | 4 |
| Z' | 0 |
| Density (calculated) | 1.315 mg/m$^3$ |
| Absorption coefficient | 0.091 mm$^{-1}$ |
| F(000) | 520 |
| Crystal size | 0.3 x 0.45 x 0.45 mm$^3$ |
| Crystal colour | Colourless |
| Crystal description | Block |
| Theta range for data collection | 3.97 to 31.87º |
| Index ranges | -13<=h<=13, -15<=k<=16, -16<=l<=17 |
| Reflections collected | 12 604 |
| Independent reflections | 2 294 [R(int) = 0.0160] |
| Completeness to theta = 25.00º | 95% |
| Absorption correction | Multi-scan[165] (semi-empirical from equivalents) |
| Max. and min. transmission | 0.909 and 0.963 |
| Refinement method | Full-matrix least-squares on $F^2$ |
| Data / restraints / parameters | 2 294 / 0 / 163 |

[165] Blessing R. H. (1995). *Acta Crystallographica*. **A51**, 33–38.

| | |
|---|---|
| Goodness-of-fit on $F^2$ | 1.054 |
| Final R indices [I>2sigma(I)] | R1 = 0.0328, wR2 = 0.0947 |
| R indices (all data) | R1 = 0.0397, wR2 = 0.0913 |
| Extinction coefficient | 0.091 |
| Highest peak | 0.31 at 0.0571 0.5786 0.4054 [ 0.70 A from C5 ] |
| Deepest hole | -0.21 at 0.0260 0.6593 0.5553 [ 1.21 A from C7 ] |

**Table A2.2. Atomic coordinates and equivalent isotropic displacement parameters (Ueq) for non-hydrogen atoms of compound 4.2**

| Atom label | X | Y | Z | U(eq) |
|---|---|---|---|---|
| O(1) | 0.15159(13) | 0.91471(10) | -0.44767(9) | 0.0385(3) |
| O2 | 0.12459(10) | 0.79267(7) | -0.00141(7) | 0.0245(2) |
| O3 | 0.14756(12) | 0.68047(9) | 0.15844(9) | 0.0372(3) |
| C1 | -0.08111(15) | 1.08813(12) | -0.27617(12) | 0.0279(3) |
| C2 | -0.02875(16) | 1.03277(13) | -0.36888(11) | 0.0304(3) |
| C3 | 0.09192(15) | 0.95122(12) | -0.36063(11) | 0.0274(3) |
| C4 | 0.13820(14) | 0.91816(11) | -0.24094(11) | 0.0237(2) |
| C5 | 0.02974(13) | 0.93776(10) | -0.14800(10) | 0.0197(2) |
| C6 | 0.07435(13) | 0.91479(10) | -0.02492(10) | 0.0197(2) |
| C7 | -0.04877(12) | 0.92856(11) | 0.05839(10) | 0.0210(2) |
| C8 | -0.10043(14) | 1.05781(12) | 0.05999(11) | 0.0246(3) |
| C9 | -0.14347(13) | 1.08979(11) | -0.06503(11) | 0.0245(2) |
| C10 | -0.02589(13) | 1.06955(10) | -0.15444(10) | 0.0213(2) |
| C11 | 0.01008(14) | 0.86585(11) | 0.16233(11) | 0.0234(2) |
| C12 | 0.10064(14) | 0.76895(11) | 0.11286(11) | 0.0263(3) |
| C13 | -0.00061(16) | 0.88888(13) | 0.27472(11) | 0.0303(3) |
| C14 | 0.09241(14) | 1.16252(11) | -0.13671(12) | 0.0270(3) |
| C15 | 0.26826(15) | 0.87920(12) | -0.22442(14) | 0.0321(3) |

## Table A2.3. Bond lengths for compound 4.2

| Bond | Bond distance [Å] | Bond | Bond distance [Å] |
|---|---|---|---|
| C(4)-C(15) | 1.332(2) | C(14)-H(14B) | 0.9600 |
| C(4)-C(3) | 1.4982(18) | C(14)-H(14C) | 0.9600 |
| C(4)-C(5) | 1.5090(16) | C(6)-C(5) | 1.5067(16) |
| O(2)-C(12) | 1.3659(15) | C(6)-H(6) | 0.9800 |
| O(2)-C(6) | 1.4708(14) | C(3)-O(1) | 1.2260(16) |
| C(7)-C(11) | 1.4997(17) | C(3)-C(2) | 1.473(2) |
| C(7)-C(8) | 1.5253(18) | C(11)-C(13) | 1.3278(18) |
| C(7)-C(6) | 1.5287(16) | C(11)-C(12) | 1.4991(18) |
| C(7)-H(7) | 0.9800 | C(1)-C(2) | 1.334(2) |
| C(8)-C(9) | 1.5439(18) | C(1)-C(10) | 1.5167(17) |
| C(8)-H(8A) | 0.9700 | C(1)-H(1) | 0.9300 |
| C(8)-H(8B) | 0.9700 | C(5)-C(10) | 1.5662(15) |
| C(9)-C(10) | 1.5437(17) | C(5)-H(5) | 0.9800 |
| C(9)-H(9A) | 0.9700 | C(15)-H(15A) | 0.9300 |
| C(9)-H(9B) | 0.9700 | C(15)-H(15B) | 0.9300 |
| O(3)-C(12) | 1.2059(16) | C(13)-H(13A) | 0.9300 |
| C(14)-C(10) | 1.5490(17) | C(13)-H(13B) | 0.9300 |
| C(14)-H(14A) | 0.9600 | C(2)-H(2) | 0.9300 |

## Table A2.4. Bond angles [º] for compound 4.2

| Atom site label | Bond angle [º] | Atom site label | Bond angle [º] |
|---|---|---|---|
| C(15)-C(4)-C(3) | 119.26(12) | C(2)-C(1)-H(1) | 118.3 |
| C(15)-C(4)-C(5) | 125.99(12) | C(10)-C(1)-H(1) | 118.3 |
| C(3)-C(4)-C(5) | 114.71(11) | C(6)-C(5)-C(4) | 116.89(10) |
| C(12)-O(2)-C(6) | 107.66(9) | C(6)-C(5)-C(10) | 107.51(9) |
| C(11)-C(7)-C(8) | 123.60(10) | C(4)-C(5)-C(10) | 109.63(9) |
| C(11)-C(7)-C(6) | 99.69(10) | C(6)-C(5)-H(5) | 107.5 |
| C(8)-C(7)-C(6) | 110.63(10) | C(4)-C(5)-H(5) | 107.5 |
| C(11)-C(7)-H(7) | 107.3 | C(10)-C(5)-H(5) | 107.5 |
| C(8)-C(7)-H(7) | 107.3 | C(1)-C(10)-C(9) | 110.29(10) |
| C(6)-C(7)-H(7) | 107.3 | C(1)-C(10)-C(14) | 106.58(10) |
| C(7)-C(8)-C(9) | 107.08(10) | C(9)-C(10)-C(14) | 110.22(10) |
| C(7)-C(8)-H(8A) | 110.3 | C(1)-C(10)-C(5) | 106.91(10) |
| C(9)-C(8)-H(8A) | 110.3 | C(9)-C(10)-C(5) | 110.69(9) |
| C(7)-C(8)-H(8B) | 110.3 | C(14)-C(10)-C(5) | 112.02(9) |
| C(9)-C(8)-H(8B) | 110.3 | C(4)-C(15)-H(15A) | 120.0 |
| H(8A)-C(8)-H(8B) | 108.6 | C(4)-C(15)-H(15B) | 120.0 |
| C(10)-C(9)-C(8) | 113.46(10) | H(15A)-C(15)-H(15B) | 120.0 |
| C(10)-C(9)-H(9A) | 108.9 | C(11)-C(13)-H(13A) | 120.0 |
| C(8)-C(9)-H(9A) | 108.9 | C(11)-C(13)-H(13B) | 120.0 |
| C(10)-C(9)-H(9B) | 108.9 | H(13A)-C(13)-H(13B) | 120.0 |
| C(8)-C(9)-H(9B) | 108.9 | O(3)-C(12)-O(2) | 121.23(12) |
| H(9A)-C(9)-H(9B) | 107.7 | O(3)-C(12)-C(11) | 129.75(13) |
| C(10)-C(14)-H(14A) | 109.5 | O(2)-C(12)-C(11) | 109.00(10) |
| C(10)-C(14)-H(14B) | 109.5 | C(1)-C(2)-C(3) | 121.90(12) |
| H(14A)-C(14)-H(14B) | 109.5 | C(1)-C(2)-H(2) | 119.1 |
| C(10)-C(14)-H(14C) | 109.5 | C(3)-C(2)-H(2) | 119.1 |
| H(14A)-C(14)-H(14C) | 109.5 | C(12)-C(11)-C(7) | 104.38(10) |
| H(14B)-C(14)-H(14C) | 109.5 | C(2)-C(1)-C(10) | 123.39(12) |

| | |
|---|---|
| O(2)-C(6)-C(5) | 115.13(9) |
| O(2)-C(6)-C(7) | 103.21(9) |
| C(5)-C(6)-C(7) | 111.05(10) |
| O(2)-C(6)-H(6) | 109.1 |
| C(5)-C(6)-H(6) | 109.1 |
| C(7)-C(6)-H(6) | 109.1 |
| O(1)-C(3)-C(2) | 121.14(13) |
| O(1)-C(3)-C(4) | 122.53(13) |
| C(2)-C(3)-C(4) | 116.32(11) |
| C(13)-C(11)-C(12) | 123.86(13) |
| C(13)-C(11)-C(7) | 131.60(13) |

**Table A2.5. Anisotropic displacement parameters for compound 4.2**

| Atom label | $U^{11}$ | $U^{22}$ | $U^{33}$ | $U^{23}$ | $U^{13}$ | $U^{12}$ |
|---|---|---|---|---|---|---|
| O(1) | 0.0493(6) | 0.0366(6) | 0.0297(5) | -0.0008(4) | 0.0165(5) | -0.0062(5) |
| O(2) | 0.0309(5) | 0.0174(4) | 0.0253(4) | 0.0023(3) | 0.0029(4) | 0.0031(3) |
| O(3) | 0.0499(7) | 0.0262(5) | 0.0356(5) | 0.0081(4) | 0.0000(5) | 0.0061(5) |
| C(1) | 0.0288(6) | 0.0252(6) | 0.0297(6) | 0.0036(5) | -0.0043(5) | 0.0015(5) |
| C(2) | 0.0358(7) | 0.0301(6) | 0.0253(6) | 0.0048(5) | -0.0011(5) | -0.0048(5) |
| C(3) | 0.0330(6) | 0.0233(6) | 0.0259(5) | 0.0017(5) | 0.0076(5) | -0.0079(5) |
| C(4) | 0.0291(6) | 0.0164(5) | 0.0257(5) | 0.0005(4) | 0.0069(5) | -0.0021(5) |
| C(5) | 0.0202(5) | 0.0171(5) | 0.0217(5) | -0.0002(4) | 0.0021(4) | -0.0007(4) |
| C(6) | 0.0195(5) | 0.0148(5) | 0.0248(5) | -0.0001(4) | 0.0012(4) | 0.0006(4) |
| C(7) | 0.0202(5) | 0.0206(5) | 0.0221(5) | -0.0030(4) | 0.0013(4) | -0.0010(4) |
| C(8) | 0.0239(6) | 0.0254(6) | 0.0244(5) | -0.0048(5) | 0.0003(5) | 0.0037(5) |
| C(9) | 0.0200(5) | 0.0245(6) | 0.0289(6) | -0.0027(4) | -0.0014(5) | 0.0036(5) |
| C(10) | 0.0212(5) | 0.0186(5) | 0.0241(5) | 0.0000(4) | -0.0022(4) | 0.0011(4) |
| C(11) | 0.0233(6) | 0.0207(5) | 0.0261(5) | 0.0001(4) | 0.0015(5) | -0.0040(4) |
| C(12) | 0.0303(6) | 0.0219(6) | 0.0266(6) | 0.0019(4) | -0.0002(5) | -0.0028(5) |
| C(13) | 0.0314(6) | 0.0337(7) | 0.0257(6) | 0.0006(5) | 0.0028(6) | -0.0050(6) |
| C(14) | 0.0277(6) | 0.0168(5) | 0.0366(6) | 0.0014(5) | -0.0027(5) | -0.0020(5) |
| C(15) | 0.0310(7) | 0.0263(6) | 0.0391(7) | 0.0040(6) | 0.0129(6) | 0.0033(5) |

**Table A2.6. Hydrogen coordinates and isotropic displacement parameters for compound (4.2)**

| Atom label | X | Y | Z | U(eq) |
|---|---|---|---|---|
| H(1) | -0.1553 | 1.1409 | -0.2867 | 0.033 |
| H(2) | -0.0696 | 1.0460 | -0.4408 | 0.036 |
| H(5) | -0.0491 | 0.8844 | -0.1647 | 0.024 |
| H(6) | 0.1475 | 0.9722 | -0.0037 | 0.024 |
| H(7) | -0.1253 | 0.8789 | 0.0286 | 0.025 |
| H(8A) | -0.0268 | 1.1109 | 0.0864 | 0.029 |
| H(8B) | -0.1798 | 1.0657 | 0.1117 | 0.029 |
| H(9A) | -0.1717 | 1.1732 | -0.0675 | 0.029 |
| H(9B) | -0.2238 | 1.0416 | -0.0866 | 0.029 |
| H(13A) | 0.0499 | 0.8436 | 0.3278 | 0.036 |
| H(13B) | -0.0586 | 0.9503 | 0.3004 | 0.036 |
| H(14A) | 0.1306 | 1.1540 | -0.0603 | 0.041 |
| H(14B) | 0.0553 | 1.2419 | -0.1458 | 0.041 |
| H(14C) | 0.1646 | 1.1493 | -0.1930 | 0.041 |
| H(15A) | 0.3292 | 0.8728 | -0.2868 | 0.039 |
| H(15B) | 0.2981 | 0.8584 | -0.1505 | 0.039 |

**Table A2.6. Torsion angles for compound 4.2**

| Atom site label | Torsion angles [º] | Atom site label | Torsion angles [º] |
|---|---|---|---|
| C(11)-C(7)C(8)-C(9) | -176.53(11) | C(2)-C(1)-C(10)-C(14) | -88.95(15) |
| C(6)-C(7)-C(8)-C(9) | -58.75(13) | C(2)-C(1)-C(10)-C(5) | 31.01(17) |
| C(7)-C(8)-C(9)-C(10) | 55.27(14) | C(8)-C(9)-C(10)-C(1) | -173.06(11) |
| C(12)-O(2)-C(6)-C(5) | 153.05(11) | C(8)-C(9)-C(10)-C(14) | 69.52(13) |
| C(12)-O(2)-C(6)-C(7) | 31.88(12) | C(8)-C(9)-C(10)-C(5) | -54.96(13) |
| C(11)-C(7)-C(6)-O(2) | -39.39(11) | C(6)-C(5)-C(10)-C(1) | 175.55(10) |
| C(8)-C(7)-C(6)-O(2) | -171.01(9) | C(4)-C(5)-C(10)-C(1) | -56.42(12) |
| C(11)-C(7)-C(6)-C(5) | -163.29(9) | C(6)-C(5)-C(10)-C(9) | 55.39(12) |
| C(8)-C(7)-C(6)-C(5) | 65.10(12) | C(4)-C(5)-C(10)-C(9) | -176.57(10) |
| C(15)-C(4)-C(3)-O(1) | -20.6(2) | C(6)-C(5)-C(10)-C(14) | -68.06(12) |
| C(5)-C(4)-C(3)-O(1) | 161.68(12) | C(4)-C(5)-C(10)-C(14) | 59.98(12) |
| C(15)-C(4)-C(3)-C(2) | 158.27(13) | C(6)-O(2)-C(12)-O(3) | 170.70(12) |
| C(5)-C(4)-C(3)-C(2) | -19.48(16) | C(6)-O(2)-C(12)-C(11) | -10.45(13) |
| C(8)-C(7)-C(11)-C(13) | -19.4(2) | C(13)-C(11)-C(12)-O(3) | -21.0(2) |
| C(6)-C(7)-C(11)-C(13) | -142.26(15) | C(7)-C(11)-C(12)-O(3) | 163.19(14) |
| C(8)-C(7)-C(11)-C(12) | 155.99(11) | C(13)-C(11)-C(12)-O(2) | 160.33(12) |
| C(6)-C(7)-C(11)-C(12) | 33.14(12) | C(7)-C(11)-C(12)-O(2) | -15.53(13) |
| O(2)-C(6)-C(5)-C(4) | 58.69(14) | C(10)-C(1)-C(2)-C(3) | 2.2(2) |
| C(7)-C(6)-C(5)-C(4) | 175.49(10) | O(1)-C(3)-C(2)-C(1) | 169.28(13) |
| O(2)-C(6)-C(5)-C(10) | -177.59(9) | C(4)-C(3)-C(2)-C(1) | -9.6(2) |
| C(7)-C(6)-C(5)-C(10) | -60.79(12) | | |
| C(15)-C(4)-C(5)-C(6) | -2.05(18) | | |
| C(3)-C(4)-C(5)-C(6) | 175.53(10) | | |
| C(15)-C(4)-C(5)-C(10) | -124.67(13) | | |
| C(3)-C(4)-C(5)-C(10) | 52.90(13) | | |
| C(2)-C(1)-C(10)-C(9) | 151.41(13) | | |

**Symmetry transformations used to generate equivalent atoms:**

1. x,y,z (identity) order1, type 1
2. ½-x, -y, ½+z (screw axis 2-fold), order 2, type 2
3. –x, ½+y, ½-z (screw axis 2-fold), order 2, type 2
4. ½+x, ½-y, -z (screw axis 2-fold), order 2, type 2

# Appendix 3: Selected dose response curves for *in vitro* antimalarial screen (Chapter 4)

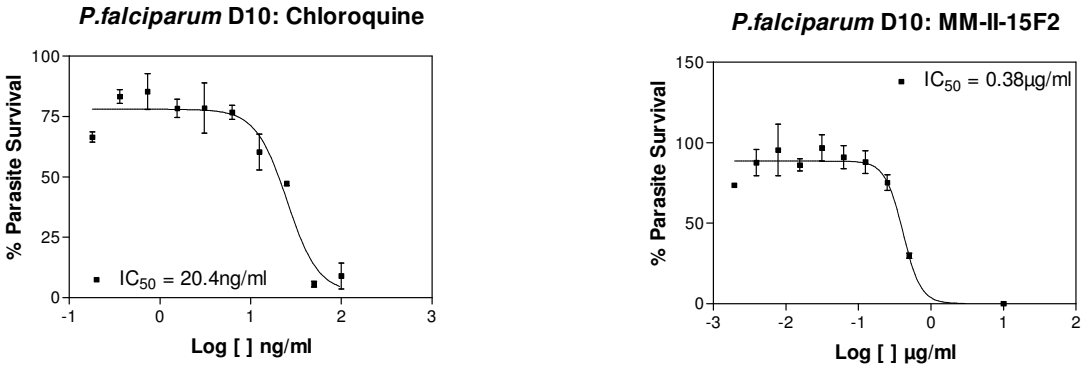


**Figure A3-1. Dose-response curves of compound 4.2 (MM-II-15F2) against *P. falciparum* (D10)**

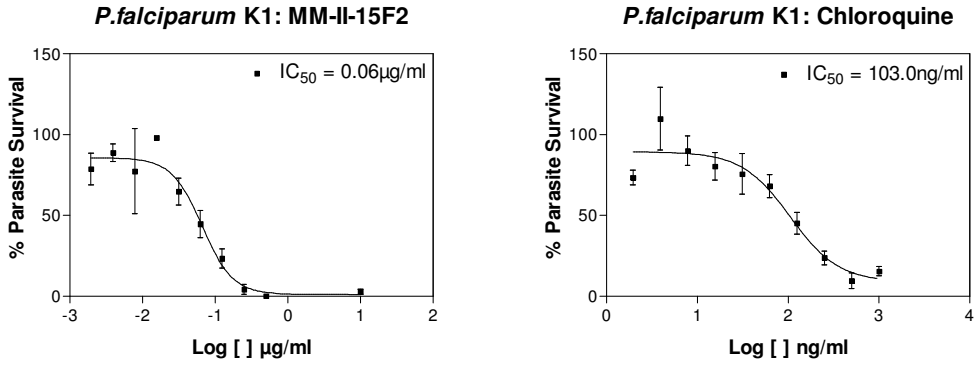


**Figure A3-2. Dose-response curves for compound 4.2 (MM-II-15F2) against *P. falciparum* (K1)**